Spurious Numerical Dissipation and Time Accuracy

by

Farjana Siddiqua

B.Sc. in Mathematics, University of Dhaka, 2013

M.Sc. in Applied Mathematics, University of Dhaka, 2014

M.Sc in Mathematical Science, Florida International University, 2017

Submitted to the Graduate Faculty of

the Kenneth P. Dietrich School of Arts and Sciences in partial fulfillment

of the requirements for the degree of

Doctor of Philosophy

University of Pittsburgh

2024

UNIVERSITY OF PITTSBURGH

KENNETH P. DIETRICH SCHOOL OF ARTS AND SCIENCES

This dissertation was presented

by

Farjana Siddiqua

It was defended on

June 23, 2024

and approved by

William J. Layton, Professor of Mathematics, University of Pittsburgh

Catalin Trenchea, Professor of Mathematics, University of Pittsburgh

Ming Chen, Associate Professor of Mathematics, University of Dhaka

Eleanor W. Jenkins, Professor of Mathematical and Statistical Sciences, Clemson University

Spurious Numerical Dissipation and Time Accuracy

Farjana Siddiqua, PhD

University of Pittsburgh, 2024

In this thesis, we do the numerical analysis of an advection-diffusion-reaction problem in bioseparation and a corrected Smagorinsky model for turbulence. Numerical dissipation due to time discretization schemes often contributes to or causes overdissipation. The goal of this dissertation is to control spurious numerical dissipation and to acquire long-time high-order accuracy.

In the first project, we analyze an advection-diffusion-reaction problem with the non-homogeneous boundary conditions (useful for practical settings) that model the chromatography process, a vital stage in bioseparation. We prove stability and error estimates using finite elements for spatial discretization and the midpoint method for time discretization. These yield a second-order convergence rate and better total mass conservation. The numerical tests validate the theoretical results.

In the second project, we develop a turbulence model named the Corrected Smagorinsky Model (CSM) and analyze it. When the ratio of dissipation of turbulent kinetic energy (TKE) and the production of TKE is equal to 1, we call it statistical equilibrium. We extend a classical model for turbulence at statistical equilibrium to non-equilibrium turbulence and propose and analyze algorithms for the solution of the extended model. The classical Smagorinsky model's solution is an approximation to a (resolved) mean velocity. Since it is an eddy viscosity model, it cannot represent a flow of energy from unresolved fluctuations to the (resolved) mean velocity. This classical Smagorinsky model was corrected to incorporate this flow and still be well-posed. The computational experiments verify the properties of the algorithms and show that the model captures the non-equilibrium effects.

In the third project, we analyze the one-leg, two-step variable time step methods of Dahlquist, Liniger, and Nevanlinna (DLN) for the time discretization in the Corrected Smagorinsky Model. Turbulent flows strain computational resources in terms of memory

usage and CPU (central processing unit) speed. The adaptive DLN methods are second-order accurate and allow large timesteps, hence requiring less memory and fewer FLOPS (floating point operations per second). We demonstrated the method's second-order accuracy, quantified its numerical dissipation, demonstrated error estimates in addition to proving the kinetic energy is bounded for various time steps and illustrated theoretical results by numerical tests.

Table of Contents

List of Tables

List of Figures

Preface

Dr. William Layton is an excellent advisor one could ever ask for. I am fortunate to start my PhD research journey with him and follow his guidelines to finish it. I am grateful for his constant guidance and availability, encouragement, expectations of excellence, enthusiastic support, and research ideas. I am forever grateful & I offer my deepest gratitude to my co-advisor, Dr. Catalin Trenchea who not only guided me in my PhD research but also always inspired me to stay positive amidst all the chaos I faced in life.

I would also like to thank Dr. Ming Chen and Dr. Eleanor W. Jenkins for their invaluable comments and helpful communications while serving on my dissertation committee. I want to show my acknowledgment to Dr. Ivan Yotov and Dr. Michael Neilan for their insightful classes which provided me with a strong foundation in Numerical Analysis and Scientific Computing. I thank my collaborators, Dr. Xihui Xie and Dr. Wenlong Pei. Their knowledge, direction, and spirit of cooperation have greatly enhanced the quality and depth of my research work. Moreover, I would like to thank faculties, staff members, and my friends in the math department whose warm behavior, and patience made the journey enjoyable.

I cannot thank my friends in the Bangladeshi community enough for always giving me breathing space without whom I could not survive the stresses during my PhD journey. I value their presence in my life and appreciate their love, friendship, and good humor immensely.

I cannot forget my teachers in Bangladesh who paved the way for my learning. I also want to thank Dr. Mohammad Ferdows from the University of Dhaka and Dr. Zhongming Wang from Florida International University with whom I first started doing research in numerical analysis and who inspired me to do more research which eventually led me to start PhD.

A heartfelt and special thanks to my parents, my awesome elder brothers, sister-in-laws, and my friends for their love, unending support, and memorable moments.

Finally, I thank my fiancé, Amit Sikder, whose unwavering love and support kept me motivated during this challenging journey. Whenever I felt like I was about to give up, he

patiently encouraged me to keep going. He is my greatest support and inspiration.

"I dedicate my PhD thesis to my beloved parents, Ayesha Siddiqua & Kutub Uddin Bhuiyan, who worked tirelessly and sacrificed a lot to ensure a prosperous life for me and my three siblings, Arif Mainuddin, Tareq Saifuddin, and Raihan Shorfuddin."

- Dr. Farjana Siddiqua

1.0 Introduction

Understanding the intricacies of fluid flow dynamics is essential for decision making, optimizing systems such as weather prediction, climate change, geophysical systems, engineering applications, waste disposal, and cooling etc. Manufacturers can cut expenses, increase productivity, and lessen their environmental effect by understanding these systems and modeling their behavior. Computational fluid dynamics (CFD) is of worldwide importance, as it underlies many different fields and innumerable pragmatic applications. For example, modeling and simulating flows of liquids and gases is important for understanding river flows, blood flow within the body, the dispersion of smoke, atmospheric streams, and vehicle aerodynamics. A broad variety of processes and industries rely on an understanding of fluid flows; as a result, accurate mathematical modeling of these processes is critical for increasing efficiency and safety in the industrial setting. Advanced mathematical models of CFD can become computationally expensive and complex quite quickly, so it is also important to ensure that CFD models are concise, simple, accurate, and effective. However, in computational fluid dynamics (CFD), minimizing numerical dissipation and attaining long-time temporal accuracy are essential elements. Computational simulations can represent complex fluid dynamics phenomena and small-scale flow features more accurately by decreasing numerical dissipation and improving time accuracy. In [127], a discussion of numerical dissipation is presented in the framework of characteristics-based techniques for solving the Euler equations of fluid dynamics and the difficulties associated with excessive dissipation and its consequences for accurately capturing shock waves and other discontinuities are emphasized. More discussion of the impact of numerical dissipation on the accuracy can be found in [5, 31, 34, 53, 70, 126, 132, 142, 144]. In [104, 156, 157], the importance of minimizing numerical dissipation in advection-dominated problems is discussed. In [83, 105], topics related to time integration and the importance of reducing dissipation for achieving accurate time-stepping solutions are covered. This thesis focuses on reduced

numerical dissipation while selecting time discretization schemes for two types of problems in three chapters. We analyzed the advection diffusion reaction problem in Chapter 2 and developed and analyzed a new turbulent model named the Corrected Smagorinsky Model in Chapter 3 and Chapter 4. The numerical simulations are performed by using FreeFEM++ and MATLAB.

Applications of advection-diffusion-reaction problem form a wide array of nationally funded research areas such as oil recovery, pollutant tracking/pollution abatement, chemical processing, and global climate studies. The work in the Chapter 2 builds upon the thesis work of Wilson [153] and we considered an advection-diffusion-reaction problem with non-homogeneous boundary conditions which is a simulation tool of chromatography process [18–20]. We proved the stability and error estimates using finite elements for spatial discretization and the midpoint method for the time discretization, improving results in [153]. Due to the absence of numerical dissipation, the accuracy comes in two ways, such as the rate of convergence is higher and the mass is better conserved when the midpoint method is used. Numerical tests validate the theoretical results. The nonlinearity of the problem makes the analysis challenging. We drop the following assumptions in our work that was used in [153]:

- *Liquid phase concentration* $C(x,t)$ *is nondecreasing in time at every* x.
- $C(x,t) = 0$ *on inflow boundary* $\Gamma_{in} = \{x \in \Gamma : \overrightarrow{n} \cdot \mathbf{u}(x) < 0\}$.
- $C(x,t)$ *is non-negative.*

Instead, we considered the non-homogeneous boundary condition at the inflow boundary and using a maximum principle argument, we proved that the continuous solution is positive and bounded above for all $(x,t) \in \Omega \times (0,T)$. Some results of this chapter is published in [136].

In Chapter 3 and Chapter 4, this PhD work improve the stability of viscosity models and the accuracy of turbulent flow simulation, while reducing computational costs. Turbulence is an essential phenomenon to understand, since it is fundamental to astrophysics, water flow, geophysics, and engineering. Although it is a significant multiscale phenomenon that affects our everyday life, turbulence is not well understood from a scientific standpoint.

Plane crashes, and climate changes, among other natural events, are sometimes caused by turbulent effects. The crucial question that arises is: how can we predict when, where, or how turbulent effects are determined in an application? This is a challenging subject, at the same time mathematically deep and physically important. Moreover, progress in this area is only possible through fundamental insights, since it requires bridging the physics of flow, mathematical theory, and carefully designed simulation. In our work, we sought to develop an accurate solution for including intermittent energy transfer from fluctuations to means. To accomplish this, we adapted an eddy viscosity model to nonequilibrium turbulence in Chapter 3. We developed a numerically efficient model for turbulent flow at statistical non-equilibrium. The new model does not add the problematic complexity of any additional fitting parameters, and it naturally extends the Smagorinsky model to nonequilibrium turbulence. Impressively, our model demonstrates the ability to incorporate statistical backscatter without using negative turbulent viscosities [35, 143, 148]. We validate the model with numerical experiments in Section 3.6 and confirm that the model captures the energy transfer from fluctuation to means. While comparing results of Backward Euler (BE) discretization and Linearlized Crank Nicolson (CNLE) discretization in this model, we observe backscatter in the latter case which indicates that added numerical dissipation in BE prevents us to see backscatter. The new model represents an important contribution to studies of turbulence, and CFD modeling. The results of this chapter is published in [137].

Due to the Corrected Smagorinsky Model's sensitivity to time discretization method, we do further investigation in Chapter 4 using a one-leg, two-step time discretization DLN method proposed by Dahlquist, Liniger, and Nevanlinna [47, 96–98]. The DLN method is a 1-parameter ($0 \leq \theta \leq 1$) family of A-stable, 2-step, G-stable methods. In Chapter 4, we focus on reducing the computational cost and memory usage while speeding up CPU. Since the adaptive DLN has second-order accuracy and allows for large timesteps, it results in decreased memory usage and fewer FLOPS. We analyze the DLN methods with variable timesteps applied to the Corrected Smagorinsky model. We prove the kinetic energy is bounded, show second-order accuracy, quantify its numerical dissipation, and provide er-

ror estimates. Several numerical experiments verify the theoretical results. DLN for the Corrected Smagorinksy has backscatter when $\theta = 1$, which is consistent with the purpose of this model. On the other hand, we observe that the constant step DLN for $\theta < 1$ has bigger numerical dissipation, which negatively impacts the backscatter from DLN. We prove that adapting the time step produces a significant difference in the solution. Some numerical experiments show that backscatter is visible even for $\theta < 1$ when variable timestep is considered. The results of this chapter is published in [135].

2.0 A second-order symplectic method for an advection-diffusion-reaction problem in Bioseparation

In this chapter, an advection-diffusion-reaction problem with non-homogeneous boundary conditions is considered that models the chromatography process, a vital stage in bioseparation. We do stability analysis and error estimates for constant and affine adsorptions using the midpoint method for time discretization and finite elements for spatial discretization. In addition, we did the stability analysis for nonlinear, explicit adsorption in the continuous, semi-discrete, and fully discreet cases. For nonlinear, explicit adsorption, we also have done an error analysis for the semi-discrete case and proved the existence of a solution for the fully discrete case. The numerical tests are performed that validate our theoretical results.

2.1 Introduction

The global market for biopharmaceuticals is expected to hit $856.1 billion by 2030 and 50% of top 100 drugs will most likely be derived from biotechnology [2, 41]. The high demand for biopharmaceuticals is due to their effectiveness in treating various illnesses such as diabetes, anemia, cancer, etc. [102]. For example, monoclonal antibodies [106, 123], general products from bioseparation are very useful medications to treat Covid-19 [1, 3, 4]. Other key factors driving the growth of the market are rising investments in the research and development of novel treatments, favorable government regulations, and increasing adoption of biopharmaceuticals by the global population [2]. To maximize production capacity while minimizing costs, manufacturers are constantly developing new methods. As an alternative to constructing new biomanufacturing facilities due to financial risk, integrating new technologies into existing facilities would be more economically viable. Upstream and downstream processes are typically part of a biomanufacturing facility. In the upstream

process, cells cultured by genetically engineered methods release the desired product into a solution and in the downstream process, the product is purified from the solution [39]. The capacity of production is often limited by downstream purification, usually including chromatography. In the protein chromatography process, when the solution is pushed through the column, the materials in columns separate the proteins [153]. Ideal media for chromatography columns used for bioseparation are resin beds, monoliths, and membranes [149]. Membrane chromatography [18–20] addresses the low efficiency of resin chromatography, and uses a porous, absorptive membrane as the packing medium instead of the small resin beads The protein binding capacity is crucial in membrane chromatography as it determines the volume of membrane required for purification. Most absorption mechanisms, such as ion-exchange membranes, lose the protein binding capacity at relatively low conductivity and often require additional processing stages, causing lower yield and higher production costs. Recent research in [19, 151] has focused on multimodal membrane-based chromatography. The development of a modeling framework capable of characterizing the chromatography process under continuous flow circumstances is critical. To model this process for creating a simulation tool for transport in a porous medium, the reactive transport problem (advection-diffusion-reaction problem) considered in [9, 43, 143, 145, 153] is given below.

Let Ω be a bounded domain in $\mathbf{R^d}$, $d = 1,\ 2,\ or\ 3$ with piecewise smooth boundary Γ. We partition the boundary into three non-overlapping segments $\Gamma = \Gamma_{\text{in}} \cup \Gamma_{\text{n}} \cup \Gamma_{\text{out}}$ where inflow boundary, $\Gamma_{\text{in}} = \{x \in \Gamma : \overrightarrow{n} \cdot \mathbf{u}(x) < 0\}$, outflow boundary, $\Gamma_{\text{out}} = \{x \in \Gamma : \overrightarrow{n} \cdot \mathbf{u}(x) > 0\}$ and boundaries comprising no-flow hydraulic zone(s), $\Gamma_{\text{n}} = \Gamma \backslash (\Gamma_{\text{in}} \cup \Gamma_{\text{out}})$. Let $\mathbf{u}$ be a fluid velocity through the membrane and $\overrightarrow{n}$ denote the unit outward normal to Ω. We consider $\mathbf{u}$ is given, which is computed by Darcy [43] satisfying $\boldsymbol{\nabla \cdot \mathbf{u}} = 0$ and $\mathbf{u} \cdot \overrightarrow{n}(x,t) = 0,\ \ x \in \Gamma_{\text{n}},\ t > 0$. Let ω be the total porosity of the membrane ($0 \leq \omega \leq 1$), ρ_s be the density of the membrane, D be the diffusion tensor that represents diffusivity of fluid through the membrane, C and $q(C)$ be the concentration in the liquid and absorbed phases respectively. For a forcing function $f \in L^2(0, T; L^2(\Omega))$, given velocity $\mathbf{u}$ and initial concentration $C_0 \in L^2(\Omega)$, we consider the

following initial boundary value problem of finding concentration $C(x,t)$:

$$\begin{cases} \omega\partial_t C + (1-\omega)\rho_s \partial_t q(C) + \boldsymbol{\nabla}\cdot(\mathbf{u}C) - \boldsymbol{\nabla}\cdot(D\boldsymbol{\nabla}C) = f,\ x\in\Omega,\ t>0, \\ C(x,t) = g,\ x\in\Gamma_{\text{in}},\ t>0, \\ (D\boldsymbol{\nabla}C)\cdot\overrightarrow{n}(x,t) = 0,\ x\in\Gamma_{\text{n}}\cup\Gamma_{\text{out}},\ t>0, \\ C(x,0) = C_0(x),\ x\in\Omega. \end{cases} \tag{1}$$

For the inflow boundary, we keep the fixed concentration [16, 43]. The illustration of the

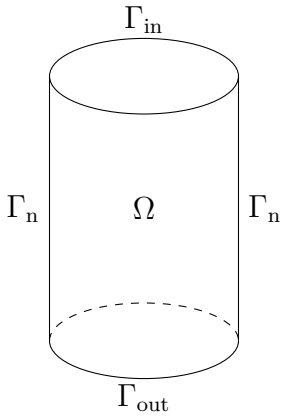

Figure 1: Domain Ω

domain is given in Figure 1.

In this chapter, we consider three cases of isotherms. They are constant isotherm, $q(C) = K$, affine isotherm, $q(C) = K_1 + K_2 C$ and nonlinear, explicit isotherm $q(C)$. A typical example of the nonlinear, explicit isotherm is Langmuir's isotherm [20,138], $q(C) = \frac{q_{max}K_{eq}C}{1+K_{eq}C}$, where K_{eq} is Langmuir equilibrium constant, q_{max} is the maximum binding capacity of the porous medium. New insights into adsorption processes have led to implicit representations of q as a function of C [111,112,114,150]. The main result of this chapter is gaining improved accuracy by using the midpoint method for time discretization at the same computational cost as the Backward Euler method. The accuracy comes in two ways, such as the rate of convergence is higher and the mass is better conserved when the midpoint method is

used. The fully discrete formulation of the considered problem is given in Section 2.3. The stability analysis and error analysis for constant and affine $q(C)$ are given in Section 2.4. We also show the stability analysis for the nonlinear, explicit $q(C)$ in the same section. Error analysis for nonlinear, explicit $q(C)$ is given in Section 2.4.5. The proof of the existence of the solution in a fully discrete case is given in Section 2.4.5.1. Numerical tests validating these estimates are given in Section 2.5.

2.1.1 Related work

The general advection-diffusion equation has been the subject of extensive mathematical study during the past decades [12, 21, 40, 69, 72, 82]. The analysis and numerical solution are typically more difficult in the presence of reaction terms, especially nonlinear ones [125]. In [153, 154], constant, linear, and nonlinear adsorptions are analyzed by using Backward Euler for time discretization and the upwind Petrov-Galerkin (SUPG) finite element for spatial discretization and numerical validation for each of the priori estimates are provided. Recently, a computational framework has been developed to model and optimize the capture chromatography for the purification of monoclonal antibodies [42, 129, 130].

2.2 Notation and Preliminaries

We denote the $L^2(\Omega)$ norm and inner product by $\|\cdot\|$ and, $(\cdot,\cdot)$ respectively. We denote the usual Sobolev spaces $W^{m,p}(\Omega)$ with the associated norms $\|\cdot\|_{W^{m,p}(\Omega)}$ and in the case when $p=2$, we denote $W^{m,2}(\Omega) = H^m(\Omega) = \{v \in L^2(\Omega) : \frac{\partial^\alpha v}{\partial x^\alpha} \in L^2(\Omega),\ |\alpha| \leq r\}$ where α is a multi-index, with norm $\|v\|_r = \left(\sum_{|\alpha|\leq r} \int_\Omega \left|\frac{\partial^\alpha v}{\partial x^\alpha}\right|^2 d\Omega\right)^{1/2}$. The function space for the liquid phase concentration is defined as:

$$H^1_{0,\Gamma_{\text{in}}}(\Omega) := \{v : v \in H^1(\Omega) \text{ with } v = 0 \text{ on } \Gamma_{\text{in}}\}.$$

We define the space $H^{1/2}(\Gamma_{\text{in}}) := \{g \in L^2(\Gamma_{\text{in}}) : \|g\|_{H^{1/2}(\Gamma_{\text{in}})} < \infty\}$ where

$$\|g\|_{H^{1/2}(\Gamma_{\text{in}})} = \inf_{\substack{G \in H^1(\Omega) \\ G\big|_{\Gamma_{\text{in}}} = g}} \|G\|_{H^1(\Omega)}.$$

The Bochner Space [6] norms are

$$\|C\|_{L^2(0,T;X)} = \left(\int_0^T \|C(\cdot,t)\|_X^2 dt \right)^{\frac{1}{2}}, \ \|C\|_{L^\infty(0,T;X)} = \operatorname{ess\,sup}_{0 \le t \le T} \|C(\cdot,t)\|_X.$$

We also define discrete L^p-norms with $p = 2$ or ∞

$$\|C\|_{L^2(0,T,X)} = \big(\Delta t \sum_{n=0}^{N} \|C^n\|_X^2\big), \ \|C\|_{L^\infty(0,T,X)} = \max_{0 \le n \le N} \|C^n\|_X.$$

For the Finite Element Approximation, we consider a regular triangulation of Ω, $\mathcal{T}_h = \{A\}$ with $\Omega = \bigcup_{A \in \mathcal{T}_h} A$. We choose a finite dimensional subspace $X^h \subset H^1(\Omega)$ and define

$$X^h_{0,\Gamma_{\text{in}}} = \{v_h \in X^h : \ v_h = 0 \text{ on } \Gamma_{\text{in}}\}$$

with Ω a polyhedron, $X^h_{0,\Gamma_{\text{in}}} \subset H^1_{0,\Gamma_{\text{in}}}(\Omega)$. Let X^* be the dual space of $X^h_{0,\Gamma_{\text{in}}}$, with norm $\|f\|_* = \sup_{v \in X^h_{0,\Gamma_{\text{in}}}} \frac{(f,v)}{\|\boldsymbol{\nabla} v\|}$. We denote $X^h_{\Gamma_{\text{in}}}$ as the restriction of functions in X^h to the boundary Γ_{in} and define $X^h_0 = \{v_h \in X^h : \ v_h = 0 \ on \ \partial\Omega\}$ with Ω a polyhedron, $X^h_0 \subset H^1_0(\Omega)$. Throughout, K will denote a constant taking different values in different instances. We assume that there exists a $k \ge 1$ such that X^h possesses the approximation property,

$$\inf_{C_h \in X^h} \|C - C_h\|_s \le K h^{r-s} \|C\|_r, \ \text{for} \ \ s = 0, 1 \ \ \text{and} \ \ 1 \le r \le k+1. \tag{2}$$

For example, (2) holds if X^h consists of piecewise polynomials of degree$\le k$. We assume that a similar approximation holds on X^h_0. In particular, if $C \in H^r(\Omega) \cap H^1_0(\Omega)$, we will use

$$\inf_{C_h \in X^h_0} \|C - C_h\|_1 \le K h^{r-1} \|C\|_r. \tag{3}$$

We further assume that the space $X^h_{\Gamma_{\text{in}}}$ possesses the approximation property

$$\inf_{C_h \in X^h_{\Gamma_{\text{in}}}} \|C - C_h\|_{0,\Gamma_{\text{in}}} \le K h^{r-1/2} \|C\|_{r-1/2,\Gamma_{\text{in}}}. \tag{4}$$

Lemma 1. *For all $v \in H^1_{0,\Gamma_{in}}(\Omega)$, there exists a constant $\tilde{K}_{PF}$ such that*

$$\|v\|_1 \leq \tilde{K}_{PF}\|\boldsymbol{\nabla} v\|.$$

Proof. This is the direct consequence of the Poincaré inequality that holds for $v \in H^1_{0,\Gamma_{\text{in}}}(\Omega)$ [58]. □

Lemma 2. *(See [94, p.154]) Let $\mathcal{P}$ and $\mathcal{P}^1$ be the orthogonal projections with respect to the L^2 inner product (u, v) and H^1 inner product $(\boldsymbol{\nabla} u, \boldsymbol{\nabla} v)$, respectively. Then, for any $w \in X$,*

$$\boldsymbol{\nabla}\mathcal{P}_{X^h} w = \mathcal{P}^1_{\boldsymbol{\nabla} X^h}\boldsymbol{\nabla} w.$$

Lemma 3. *Let $f, g : [0, \alpha] \to [0, \infty)$ be continuous and let C be a nonnegative number. If $f(t) \leq C + \int_0^t g(s)f(s)ds,\ 0 \leq t < \alpha$, then*

$$f(t) \leq C exp \int_0^t g(s)ds,\ 0 \leq t < \alpha.$$

Lemma 4. *Given $g \in H^{r-1/2}(\Gamma_{in})$ for $r \geq 1$, let $\Pi_h g$ denote the $X^h_{\Gamma_{in}}$-interpolant of g. Then, if X^h satisfies the approximation properties* (2)-(4)*,*

$$\inf_{\substack{\hat{C}_h \in X^h \\ \hat{C}_h|_{\Gamma_{in}} = \Pi_h g}} \|C - \hat{C}_h\|_1 \leq Kh^{r-1}\|C\|_r. \tag{5}$$

Proof. This proof follows the proof of [61, Lemma 4]. We give the proof for the reader's convenience. Let $\Pi_h C$ denote X^h-interpolant of C and $\Pi_h g$ denote $X^h_{\Gamma_{\text{in}}}$- interpolant of g. Then, for $\hat{C}_h|_{\Gamma_{\text{in}}} = \Pi_h g$, we write the triangle inequality

$$\|C - \hat{C}_h\|_1 \leq \|C - \Pi_h C\|_1 + \|\hat{C}_h - \Pi_h C\|_1. \tag{6}$$

From the interpolation theory [24], we get,

$$\|C - \Pi_h C\|_1 \leq Kh^{r-1}\|C\|_r. \tag{7}$$

We may choose $\hat{C}_h$ so that it has the same value at all interior nodes as does $\Pi_h C$. Since $\hat{C}_h|_{\Gamma_{\text{in}}} = \Pi_h g$ and $(\Pi_h C)\Big|_{\Gamma_{\text{in}}} = \Pi_h g$, we get $(\hat{C}_h - \Pi_h C) = 0$, which concludes the argument. □

2.2.1 Assumptions and Preliminary Results

We make the following assumptions [153]:

1. ω and ρ_s are constants in time and space [43].
2. $\mathbf{u}$ is nonzero and bounded in L^∞ norm [37, 133].
3. $D(x) = [d_{ij}]_{i,j=1,2,\cdots,n}$ is symmetric positive definite and $\|D\|_\infty \leq \beta_1$, $|\frac{\partial}{\partial x_i} d_{ij}| \leq \beta_2$, for all i, j [8, 37, 43, 133].
4. There exists a unique solution $C \in L^\infty(0, T, L^2(\Omega)) \cap L^2(0, T, H^1(\Omega))$ [133].
5. $q = q(C) \in C^1$ is an explicit, Lipschitz continuous function of C, $q(0) = 0$, $q(C) > 0$ for $C > 0$ and $q(C)$ is strictly increasing. Moreover, we assume that $q'(C) \geq \kappa_1 > 0 \; \forall C \geq 0$ [15, 43, 51, 124, 125, 133].
6. The rate of increase in adsorption is Lipschitz continuous and bounded above so that $\frac{dq}{dC} = q'(C) \leq \kappa_2$ [43].
7. The second derivative of the adsorption, $q''(C)$, is Lipschitz continuous and bounded.

Remark 5. *In our analysis, we drop the assumption "$C(x,t)$ is nondecreasing in time at every x and $C(x,t) = 0$ on Γ_{in}" stated in [153]. Instead, we considered the non-homogeneous boundary condition at the inflow boundary.*

In [15, 43, 51, 133, 153], another assumption on the continuous and the discrete solution was imposed, namely that "C is non-negative". Using a maximum principle argument, we prove that the continuous solution is positive and bounded above for all $(x, t) \in \Omega \times (0, T)$.

Proposition 6. *Assuming no forcing term $f = 0$ and positivity of the initial condition $0 < C_0(x)$, then we have*

$$0 < C(x,t) \leq \max_{x \in \Omega} \{C(x,0), g(x)\} \qquad \textit{for all } (x,t) \in \Omega \times [0,T).$$

Proof. Since $\mathbf{u}$ is incompressible, we rewrite the convective term as

$$\boldsymbol{\nabla} \cdot (uC) = (\boldsymbol{\nabla} \cdot u)C + \mathbf{u} \cdot \boldsymbol{\nabla} C = u \cdot \boldsymbol{\nabla} C.$$

Next, we rewrite the adsorption term as

$$\frac{\partial q}{\partial t} = \frac{\partial q}{\partial C}\frac{\partial C}{\partial t} = q'(C)\frac{\partial C}{\partial t}.$$

Then the equation (1) writes

$$(\omega + (1-\omega)\rho_s q'(C))\partial_t C + \mathbf{u}\cdot\boldsymbol{\nabla} C - \boldsymbol{\nabla}\cdot(D\boldsymbol{\nabla} C) = f,\ x\in\Omega,\ t>0. \tag{8}$$

Since $q'(C) > 0$ by assumption (F5), we can divide (8) by $(\omega + (1-\omega)\rho_s q'(C))$. Hence, assuming $f = 0$, (8) writes,

$$\begin{aligned} &-\partial_t C + \sum_{i,j=1}^{n}((\omega + (1-\omega)\rho_s q'(C))^{-1}D_{ij})\frac{\partial^2 C}{\partial x_i \partial x_j} \\ &+\sum_{j=1}^{n}\Big((\omega + (1-\omega)\rho_s q'(C))^{-1}\big(\frac{\partial D_{ij}}{\partial x_i} - u_j\big)\Big)\frac{\partial C}{\partial x_j} = 0. \end{aligned}$$

We assume that $C_0(x) > 0$. Suppose the claim in the proposition is false. Then there is a $y \in \bar{\Omega}$ and $T > 0$ such that $C(y,T) = 0$ and $C(x,t) > 0$ for $(x,t) \in \bar{\Omega} \times [0,T)$. Therefore, by Maximum Principle [120, pages 173-174], maximum of $C(x,t)$ is on the boundary and $(D\boldsymbol{\nabla} C)\cdot\overrightarrow{n}(x,t) < 0$. This contradicts the boundary condition we have in (1). Hence, we proved the claim. □

2.3 Variational Formulation

The standard Galerkin variational formulation for the transport problem (1) is: Find $C \in H^1(\Omega)$ such that $C\Big|_{\Gamma_{\text{in}}} = g$ and

$$(\frac{\partial}{\partial t}(\omega C + (1-\omega)\rho_s q(C)), v) + (u \cdot \boldsymbol{\nabla} C, v) + (D\boldsymbol{\nabla} C, \boldsymbol{\nabla} v) = (f, v),\ \forall\ v \in H^1_{0,\Gamma_{\text{in}}}(\Omega). \quad (9)$$

This variational formulation (9) is equivalent to following:

$$((\omega + (1-\omega)\rho_s q'(C))\frac{\partial C}{\partial t}, v) + (u \cdot \boldsymbol{\nabla} C, v) + (D\boldsymbol{\nabla} C, \boldsymbol{\nabla} v) = (f, v),\ \forall\ v \in H^1_{0,\Gamma_{\text{in}}}(\Omega), \quad (10)$$

where we used Green's Theorem to the diffusive term, the boundary condition $(D\boldsymbol{\nabla} C) \cdot n(x,t) = 0,\ x \in \Gamma_{\text{n}} \cup \Gamma_{\text{out}}$ and the fact that $v \in H^1_{0,\Gamma_{\text{in}}}$ to get

$$-(\boldsymbol{\nabla} \cdot (D\boldsymbol{\nabla} C), v) = -\int_{\Gamma} (D\boldsymbol{\nabla} C) \cdot \overrightarrow{n} v\ ds + (D\boldsymbol{\nabla} C, \boldsymbol{\nabla} v) = (D\boldsymbol{\nabla} C, \boldsymbol{\nabla} v).$$

Next, we write a finite element approximation of the variational formulation of the transport problem. We state both semi-discrete in space and fully discrete approximations.

2.3.1 Semi-Discrete in Space Approximation

We denote g_h as an interpolant of g. Then we obtain the following semi-discrete in-space formulation: Find $C_h \in X^h$ such that $C_h\Big|_{\Gamma_{\text{in}}} = g_h$ and $\forall\ v_h \in X^h_{0,\Gamma_{\text{in}}}(\Omega)$,

$$(\frac{\partial}{\partial t}(\omega C_h + (1-\omega)\rho_s q(C_h)), v_h) + (u \cdot \boldsymbol{\nabla} C_h, v_h) + (D\boldsymbol{\nabla} C_h, \boldsymbol{\nabla} v_h) = (f, v_h). \quad (11)$$

The semi-discrete in-space formulation (11) is equivalent to the following: $\forall\ v_h \in X^h_{0,\Gamma_{\text{in}}}(\Omega)$,

$$((\omega + (1-\omega)\rho_s q'(C_h))\frac{\partial C_h}{\partial t}, v_h) + (u \cdot \boldsymbol{\nabla} C_h, v_h) + (D\boldsymbol{\nabla} C_h, \boldsymbol{\nabla} v_h) = (f, v_h). \quad (12)$$

2.3.2 Fully-discrete approximation

We partition the time interval as $t_0 = 0 < t_1 < t_2 < \cdots < t_N = T$. Let $\Delta t = t_{n+1} - t_n$ be the time step size, $t_n = n\Delta t$ and $f^n(x) = f(x, t_n)$. Let $C_h^n(x)$ denote the Finite Element approximation to $C(x, t_n)$. We define $t_{n+1/2} = \frac{t_n + t_{n+1}}{2}$. First, we recall the first order Backward Euler time discretization scheme for Finite Element Approximation (12): Given $C_h^n \in X^h$, find $C_h^{n+1} \in X^h$ such that $C_h^{n+1}\Big|_{\Gamma_{\text{in}}} = g_h$ satisfying

$$\begin{aligned}&(\omega\frac{C_h^{n+1} - C_h^n}{\Delta t} + (1-\omega)\rho_s\frac{q(C_h^{n+1}) - q(C_h^n)}{\Delta t}, v_h) + (u \cdot \boldsymbol{\nabla} C_h^{n+1}, v_h) + (D\boldsymbol{\nabla} C_h^{n+1}, \boldsymbol{\nabla} v_h)\\ &= (f^{n+1}, v_h),\ \forall v_h \in X^h_{0,\Gamma_{\text{in}}}(\Omega).\end{aligned} \tag{13}$$

Equivalently,

$$\begin{aligned}&(\omega + (1-\omega)\rho_s q'(C_h^{n+1})\frac{C_h^{n+1} - C_h^n}{\Delta t}, v_h) + (u \cdot \boldsymbol{\nabla} C_h^{n+1}, v_h) + \quad (D\boldsymbol{\nabla} C_h^{n+1}, \boldsymbol{\nabla} v_h)\\ &= (f^{n+1}, v_h),\ \forall v_h \in X^h_{0,\Gamma_{\text{in}}}(\Omega).\end{aligned} \tag{14}$$

Next, we propose the midpoint method for time discretization in Finite Element Approximation (12): Given $C_h^n \in X^h$, find $C_h^{n+1} \in X^h$ such that $C_h^{n+1}\Big|_{\Gamma_{\text{in}}} = g_h$ satisfying

$$\begin{aligned}&(\omega\frac{C_h^{n+1} - C_h^n}{\Delta t} + (1-\omega)\rho_s\frac{q(C_h^{n+1}) - q(C_h^n)}{\Delta t}, v_h) + (u \cdot \boldsymbol{\nabla} C_h^{n+1/2}, v_h) + \quad (D\boldsymbol{\nabla} C_h^{n+1/2}, \boldsymbol{\nabla} v_h)\\ &= (f^{n+1/2}, v_h),\ \forall v_h \in X^h_{0,\Gamma_{\text{in}}}(\Omega),\end{aligned} \tag{15}$$

where $C_h^{n+\frac{1}{2}}$ denotes $\frac{C_h^n + C_h^{n+1}}{2}$.
Equivalently, $\forall v_h \in X^h_{0,\Gamma_{\text{in}}}(\Omega)$,

$$\begin{aligned}&((\omega + (1-\omega)\rho_s q'(C_h^{n+1/2}))\frac{C_h^{n+1} - C_h^n}{\Delta t}, v_h) + (u \cdot \boldsymbol{\nabla} C_h^{n+1/2}, v_h) + (D\boldsymbol{\nabla} C_h^{n+1/2}, \boldsymbol{\nabla} v_h)\\ &= (f^{n+1/2}, v_h).\end{aligned} \tag{16}$$

To simplify computation, we use the refactorization of the midpoint method [29] for time discretization. Hence, we get the following full discretization: Given $C_h^n \in X^h$, find $C_h^{n+1} \in$

X^h such that $C_h^{n+1}\Big|_{\Gamma_{\text{in}}} = g_h$ satisfying

Step 1: Backward Euler step at the half-integer time step $t_{n+1/2}$,

$$\begin{aligned}&(\omega\frac{C_h^{n+1/2}-C_h^n}{\Delta t/2}+(1-\omega)\rho_s\frac{q(C_h^{n+1/2})-q(C_h^n)}{\Delta t/2},v_h)+(u\cdot\boldsymbol{\nabla}C_h^{n+1/2},v_h)+(D\boldsymbol{\nabla}C_h^{n+1/2},\boldsymbol{\nabla}v_h)\\&=(f^{n+1/2},v_h),\ \forall v_h\in X^h_{0,\Gamma_{\text{in}}}(\Omega).\end{aligned}\tag{17}$$

Equivalently,

$$\begin{aligned}&((\omega+(1-\omega)\rho_s q'(C_h^{n+1/2}))\frac{C_h^{n+1/2}-C_h^n}{\Delta t/2},v_h)+(u\cdot\boldsymbol{\nabla}C_h^{n+1/2},v_h)+(D\boldsymbol{\nabla}C_h^{n+1/2},\boldsymbol{\nabla}v_h)\\&=(f^{n+1/2},v_h),\ \forall v_h\in X^h_{0,\Gamma_{\text{in}}}(\Omega).\end{aligned}\tag{18}$$

Step 2: Forward Euler step at t_{n+1},

$$\begin{aligned}&(\omega\frac{C_h^{n+1}-C_h^{n+1/2}}{\Delta t/2}+(1-\omega)\rho_s\frac{q(C_h^{n+1})-q(C_h^{n+1/2})}{\Delta t/2},v_h)+(u\cdot\boldsymbol{\nabla}C_h^{n+1/2},v_h)\\&+(D\boldsymbol{\nabla}C_h^{n+1/2},\boldsymbol{\nabla}v_h)=(f^{n+1/2},v_h),\ \forall v_h\in X^h_{0,\Gamma_{\text{in}}}(\Omega).\end{aligned}\tag{19}$$

Equivalently,

$$\begin{aligned}&((\omega+(1-\omega)\rho_s q'(C_h^{n+1/2}))\frac{C_h^{n+1}-C_h^{n+1/2}}{\Delta t/2},v_h)+(u\cdot\boldsymbol{\nabla}C_h^{n+1/2},v_h)+(D\boldsymbol{\nabla}C_h^{n+1/2},\boldsymbol{\nabla}v_h)\\&=(f^{n+1/2},v_h),\ \forall v_h\in X^h_{0,\Gamma_{\text{in}}}(\Omega).\end{aligned}\tag{20}$$

Remark 7. *Step 2 is equivalent to a linear extrapolation* $C_h^{n+1}=2C_h^{n+1/2}-C_h^n$.

2.3.3 Time-integrated finite element formulation

For the error analysis for the case of nonlinear, explicit adsorption, we formulate a time-integrated version of the transport equation introduced in [115] and applied in different mixed formulations [9, 133, 155]. To develop the time-integrated finite element discretization, we rewrite (1) by integrating in time to obtain

$$\omega C + (1-\omega)\rho_s q(C) + \int_0^t u \cdot \boldsymbol{\nabla} C dt' - \boldsymbol{\nabla} \cdot \int_0^t D\boldsymbol{\nabla} C dt' = \int_0^t f dt' + \omega C_0 + (1-\omega) q(C_0). \quad (21)$$

Multiplying (21) by $v \in H^1_{0,\Gamma_{in}}(\Omega)$ and integrating over Ω, we get,

$$\begin{aligned} &(\omega C, v) + ((1-\omega)\rho_s q(C), v) + (\int_0^t u \cdot \boldsymbol{\nabla} C dt', v) - (\boldsymbol{\nabla} \cdot \int_0^t D\boldsymbol{\nabla} C dt', v) \\ &= (\int_0^t f dt', v) + (\omega C_0, v) + ((1-\omega) q(C_0), v). \end{aligned} \quad (22)$$

Then the semi-discrete in-space variational formulation is given by the following: Find $C_h \in X^h$ such that $C_h\big|_{\Gamma_{in}} = g_h$ and

$$\begin{aligned} &(\omega C_h, v_h) + ((1-\omega)\rho_s q(C_h), v_h) + (\int_0^t u \cdot \boldsymbol{\nabla} C_h dt', v_h) - (\boldsymbol{\nabla} \cdot \int_0^t D\boldsymbol{\nabla} C_h dt', v_h) \\ &= (\int_0^t f dt', v_h) + (\omega C_0, v_h) + ((1-\omega) q(C_0), v_h), \quad \forall v_h \in X^h_{0,\Gamma_{in}}(\Omega). \end{aligned} \quad (23)$$

2.4 Time-Dependent Analysis

In this section, before we perform the stability and error analysis for the time-dependent problem, first we construct a continuous extension of the Dirichlet data g inside the domain Ω, $\hat{C}$ to deal with the non-homogeneous boundary condition.

2.4.1 Construction of $\hat{C}$

Denote $\hat{C}$ as the solution of the following elliptic problem with nonhomogeneous mixed boundary conditions:

$$\begin{aligned} -\boldsymbol{\nabla} \cdot (D\boldsymbol{\nabla}\hat{C}) + \hat{C} &= 0, \ x \in \Omega, \\ \hat{C} &= g, \ \text{if } x \in \Gamma_{\text{in}}, \\ (D\boldsymbol{\nabla}\hat{C}) \cdot \overrightarrow{n} &= 0, \ \text{if } x \in \Gamma_{\text{n}} \cup \Gamma_{\text{out}}. \end{aligned} \tag{24}$$

Lemma 8. *For every $f \in L^2(\Omega)$ and every $g \in H^{1/2}(\Gamma_{in})$, there exists a unique solution $\hat{C} \in H^2(\Omega)$ of (24) under the compatibility condition $D\boldsymbol{\nabla} g \cdot \overrightarrow{n} = 0$ if $x \in \Gamma_{in} \cap \Gamma_n$. The energy estimates for $\hat{C}$ and $\boldsymbol{\nabla}\hat{C}$ are as follows,*

$$\|\hat{C}\|^2 \leq 4(K\beta_1)^2 \|g\|^2_{L^2(\Gamma_{in})}, \tag{25}$$

$$\|\boldsymbol{\nabla}\hat{C}\|^2 \leq \frac{2(K\beta_1)^2}{\lambda} \|g\|^2_{L^2(\Gamma_{in})}. \tag{26}$$

Remark 9. *The energy bound given in [66, Theorem 2.3.3.6] is*

$$\|\hat{C}\|_{H^2(\Omega)} \leq K \|g\|_{H^{1/2}(\Gamma_{in})}$$

for all $\hat{C} \in H^2(\Omega)$ and some constant K.

Proof. The existence and uniqueness proof for the more general case can be found in [66, Theorem 2.4.2.7]. For energy bounds, we take the dot product with $\hat{C}$, then apply Green's Theorem to the diffusive term to obtain

$$\begin{aligned} -(\boldsymbol{\nabla} \cdot (D\boldsymbol{\nabla}\hat{C}), \hat{C}) &= -\int_{\Gamma} (D\boldsymbol{\nabla}\hat{C}) \cdot \overrightarrow{n} \hat{C} \ ds + (D\boldsymbol{\nabla}\hat{C}, \boldsymbol{\nabla}\hat{C}) \\ &= -\int_{\Gamma_{\text{in}}} (D\boldsymbol{\nabla}\hat{C}) \cdot \overrightarrow{n} g \ ds + (D\boldsymbol{\nabla}\hat{C}, \boldsymbol{\nabla}\hat{C}) \end{aligned}$$

where we used the boundary condition $(D\boldsymbol{\nabla}\hat{C})\cdot n = 0,\ x \in \Gamma_{\rm n} \cup \Gamma_{\rm out}$ and $\hat{C}(x) = g(x)$, $x \in \Gamma_{\rm in}$. Hence, we get the following variational formulation,

$$\|\hat{C}\|^2 + (D\boldsymbol{\nabla}\hat{C}, \boldsymbol{\nabla}\hat{C}) = \int_{\Gamma_{\rm in}} (D\boldsymbol{\nabla}\hat{C})\cdot\overrightarrow{n}g\ ds.$$

Let λ be the minimum eigenvalue of D.

$$(D\boldsymbol{\nabla}\hat{C}, \boldsymbol{\nabla}\hat{C}) \ = \ (D^{1/2}\boldsymbol{\nabla}\hat{C}, D^{1/2}\boldsymbol{\nabla}\hat{C}) \ = \ \|D^{1/2}\boldsymbol{\nabla}\hat{C}\|^2 \geq \lambda\|\boldsymbol{\nabla}\hat{C}\|^2.$$

Hence, we get,

$$\begin{aligned}\|\hat{C}\|^2 + \lambda\|\boldsymbol{\nabla}\hat{C}\|^2 &\leq \int_{\Gamma_{\rm in}} (D\boldsymbol{\nabla}\hat{C})\cdot\overrightarrow{n}g\ ds,\\ &\leq \|D\boldsymbol{\nabla}\hat{C}\cdot\overrightarrow{n}\|_{L^2(\Gamma_{\rm in})}\|g\|_{L^2(\Gamma_{\rm in})},\\ &\leq \beta_1\|\boldsymbol{\nabla}\hat{C}\cdot\overrightarrow{n}\|_{L^2(\Gamma_{\rm in})}\|g\|_{L^2(\Gamma_{\rm in})}.\end{aligned}$$

By using the trace theorem [25, p. 316], we get

$$\|\hat{C}\|^2 + \lambda\|\boldsymbol{\nabla}\hat{C}\|^2 \leq K\beta_1\|\hat{C}\|_{H^2(\Omega)}\|g\|_{L^2(\Gamma_{\rm in})}. \tag{27}$$

We use the following equivalence of norms [25, p. 271],

$$\|\hat{C}\|_{H^2(\Omega)} \leq K(\|\hat{C}\| + \|\boldsymbol{\nabla}\cdot\Big(D\boldsymbol{\nabla}\hat{C}\Big)\|).$$

By using Young and Cauchy-Schwarz inequalities (27) becomes,

$$\frac{1}{2}\|\hat{C}\|^2 + \lambda\|\boldsymbol{\nabla}\hat{C}\|^2 \leq 2(K\beta_1)^2\|g\|^2_{L^2(\Gamma_{\rm in})}.$$

Hence we get the bounds (25) and (26). □

Lemma 10. *Let the domain Ω be a convex polyhedral. Given $g^h \in X^h_{\Gamma_{in}}$, there exists a $\hat{C}^h \in X^h$ such that $\hat{C}^h|_{\Gamma_{in}} = g^h$ and $\|\hat{C}^h\|_{H^1(\Omega)} \leq K\|g^h\|_{H^{1/2}(\Gamma_{in})}$.*

Proof. When Ω is two-dimensional, we use a similar technique as in [67] to prove it. Under the compatibility condition $D\boldsymbol{\nabla} g^h \cdot \overrightarrow{n} = 0$, when $x \in \Gamma_{\text{in}} \cap \Gamma_{\text{n}}$, let $\hat{C} \in H^1(\Omega)$ be the solution of

$$\begin{aligned} -\boldsymbol{\nabla} \cdot (D\boldsymbol{\nabla}\hat{C}) + \hat{C} &= 0, \ x \in \Omega, \\ \hat{C} &= g^h, \text{ when } x \in \Gamma_{\text{in}}, \\ (D\boldsymbol{\nabla}\hat{C}) \cdot \overrightarrow{n} &= 0, \text{ if } x \in \Gamma_{\text{n}} \cup \Gamma_{\text{out}}. \end{aligned} \tag{28}$$

Since X^h is assumed to be a continuous finite element subspace, we see that g^h is continuous and piecewise smooth along the boundary Γ_{in}, so that $g^h \in H^{1/2+\epsilon}(\Gamma_{\text{in}})$ for $0 < \epsilon \leq \frac{1}{2}$. Thus, by elliptic regularity, we derive that $\hat{C} \in H^{1+\epsilon}(\Omega)$ and $\|\hat{C}\|_{1+\epsilon} \leq K\|g^h\|_{1/2+\epsilon,\Gamma_{\text{in}}}$ for $0 < \epsilon \leq \frac{1}{2}$. Let $\hat{C^h} := \Pi_h \hat{C}$ be the X^h-interpolant of $\hat{C}$ so that $\hat{C^h}|_{\Gamma_{\text{in}}} = g^h$. Then, we have the estimates $\|\hat{C} - \Pi_h\hat{C}\|_1 \leq Kh^\epsilon \|\hat{C}\|_{1+\epsilon}$ which can be proven as in, e.g., [56]. Thus, we get the desired result

$$\begin{aligned} \|\hat{C^h}\|_1 = \|\Pi_h\hat{C}\|_1 &\leq \|\hat{C} - \Pi_h\hat{C}\|_1 + \|\hat{C}\|_1, \\ &\leq K(h^\epsilon\|\hat{C}\|_{1+\varepsilon} + \|\hat{C}\|_1), \\ &\leq K(h^\epsilon\|g^h\|_{1/2+\epsilon,\Gamma_{\text{in}}} + \|g^h\|_{1/2,\Gamma_{\text{in}}}), \\ &\leq K\|g^h\|_{1/2,\Gamma_{\text{in}}}. \end{aligned}$$

where in the last step we used an inverse assumption on $X^h_{\Gamma_{\text{in}}}$: there exists a constant K, independent of h, p^h such that

$$\|p^h\|_{s,\Gamma_{\text{in}}} \leq Kh^{t-s}\|p^h\|_{t,\Gamma_{\text{in}}}, \ \forall p^h \in X^h_{\Gamma_{\text{in}}}, \ 0 \leq t \leq s \leq 1.$$

Since the usual interpolant such as the one used in the two-dimensional case, is not defined in three dimensions for $H^r(\Omega)$-functions, $r \leq \frac{3}{2}$, we use Scott-Zhang interpolant [50] when Ω is three-dimensional. Scott-Zhang interpolant is well-defined for any function in $H^1(\Omega)$ [134]. □

Next, to have full insight into the analysis, we start with the simplest case of constant adsorption. Unlike previous work, in [153] we dropped the assumption "$C(x,t)$ is nondecreasing in time at every x" and considered non-homogeneous boundary condition at inflow boundary.

2.4.2 Constant Isotherm

In this subsection, we state and prove a *priori* stability and a *priori* error estimate for the case of constant adsorption. In this case of adsorption, $q(C) = K$ with $K \geq 0$. Since $q(C)$ is constant, it implies $\frac{\partial q}{\partial t} = 0$ and hence the variational formulation given in (10) simplifies to the following: Find $C \in H^1(\Omega)$ such that $C\Big|_{\Gamma_{\text{in}}} = g$ and :

$$(\omega \frac{\partial C}{\partial t}, v) + (\mathbf{u} \cdot \boldsymbol{\nabla} C, v) + (D\boldsymbol{\nabla} C, \boldsymbol{\nabla} v) = (f, v),\ \forall v \in H^1_{0,\Gamma_{\text{in}}}(\Omega). \tag{29}$$

The semi-discrete in space Finite Element formulation with constant adsorption is as follows: Find $C_h \in X^h$ such that $C_h\Big|_{\Gamma_{\text{in}}} = g_h$ and :

$$(\omega \frac{\partial C_h}{\partial t}, v_h) + (\mathbf{u} \cdot \boldsymbol{\nabla} C_h, v_h) + (D\boldsymbol{\nabla} C_h, \boldsymbol{\nabla} v_h) = (f, v_h),\ \forall v_h \in X^h_{0,\Gamma_{\text{in}}}(\Omega). \tag{30}$$

By using Midpoint time discretization, we get a fully discrete approximation: Given $C_h^n \in X^h$, find $C_h^{n+1} \in X^h$ such that $C_h^{n+1}\Big|_{\Gamma_{\text{in}}} = g_h$ satisfying

$$(\omega \frac{C_h^{n+1} - C_h^n}{\Delta t}, v_h) + (u \cdot \boldsymbol{\nabla} C_h^{n+1/2}, v_h) + (D\boldsymbol{\nabla} C_h^{n+1/2}, \boldsymbol{\nabla} v_h) = (f^{n+1/2}, v_h),\ \forall v_h \in X^h_{0,\Gamma_{\text{in}}}(\Omega). \tag{31}$$

For the analysis, we recall the refactorization of midpoint method [29] for time discretization to get the following full discretization: Given $C_h^n \in X^h$, find $C_h^{n+1} \in X^h$ such that $C_h^{n+1}\Big|_{\Gamma_{\text{in}}} = g_h$ satisfying

Step 1: Backward Euler step at the half-integer time step $t_{n+1/2}$,

$$(\omega \frac{C_h^{n+1/2} - C_h^n}{\Delta t/2}, v_h) + (u \cdot \boldsymbol{\nabla} C_h^{n+1/2}, v_h) + (D\boldsymbol{\nabla} C_h^{n+1/2}, \boldsymbol{\nabla} v_h) = (f^{n+1/2}, v_h),\ \forall v_h \in X^h_{0,\Gamma_{\text{in}}}(\Omega). \tag{32}$$

Step 2: Forward Euler step at t_{n+1},

$$\begin{aligned}&(\omega\frac{C_h^{n+1}-C_h^{n+1/2}}{\Delta t/2},v_h)+(u\cdot\boldsymbol{\nabla}C_h^{n+1/2},v_h)+(D\boldsymbol{\nabla}C_h^{n+1/2},\boldsymbol{\nabla}v_h)\\&=(f^{n+1/2},v_h),\ \forall v_h\in X^h_{0,\Gamma_{\text{in}}}(\Omega).\end{aligned}\tag{33}$$

The next theorem gives a stability bound in the sense that the solution is bounded in space.

Theorem 11. *Assume that (F1)-(F6) are satisfied and the variational formulation with constant adsorption given by* (29) *has a solution* $C\in L^\infty(0,T,L^2(\Omega))\cap L^2(0,T,H^1(\Omega))$ *with* $f\in L^2(0,T;L^2(\Omega))$. *Let* $\hat{C}$ *be the continuous extension of the Dirichlet data* g *inside the domain* Ω *and satisfies (24). The bounds on* $\|\hat{C}\|^2$ *and* $\|\boldsymbol{\nabla}\hat{C}\|^2$ *are given in* (25) *and* (26) *respectively. Then we get the following bound:*

$$\begin{aligned}&\|C(t)\|^2+\frac{\lambda}{\omega}\int_0^t\|\boldsymbol{\nabla}C(r)\|^2\,dr+\frac{2}{\omega}\int_0^t\int_{\Gamma_{out}}((C)^2)(\mathbf{u}\cdot\overrightarrow{n})dsdr\le\frac{4}{\omega}\int_0^t\frac{\|\mathbf{u}\|_\infty^2}{\lambda}\|\hat{C}\|^2\,dr+8\|\hat{C}\|^2\\&+\Big(\frac{\lambda}{\omega}+\frac{4\beta_1^2}{\lambda\omega}\Big)\int_0^t\|\boldsymbol{\nabla}\hat{C}\|^2\,dr-\frac{2}{\omega}\int_0^t\int_{\Gamma_{in}}((g)^2)(\mathbf{u}\cdot\overrightarrow{n})dsdr+3\|C_0\|^2+\frac{8K_{PF}^2}{\lambda\omega}\int_0^t\|f\|^2\,dr.\end{aligned}$$

Proof. Let $\hat{C}\in H^1(\Omega)$ such that $\hat{C}\Big|_{\Gamma_{\text{in}}}=g$. Take $v=C-\hat{C}\in H^1_{0,\Gamma_{\text{in}}}(\Omega)$. Then (29) yields to

$$(\omega\frac{\partial C}{\partial t},C-\hat{C})+(\mathbf{u}\cdot\boldsymbol{\nabla}C,C-\hat{C})+(D\boldsymbol{\nabla}C,\boldsymbol{\nabla}\Big(C-\hat{C}\Big))=(f,C-\hat{C}).$$

Thus, we get,

$$(\omega\frac{\partial C}{\partial t},C)+(\mathbf{u}\cdot\boldsymbol{\nabla}C,C)+(D\boldsymbol{\nabla}C,\boldsymbol{\nabla}C)=(\omega\frac{\partial C}{\partial t},\hat{C})+(\mathbf{u}\cdot\boldsymbol{\nabla}C,\hat{C})+(D\boldsymbol{\nabla}C,\boldsymbol{\nabla}\hat{C})+(f,C-\hat{C}).\tag{34}$$

We rewrite the first term in (34),

$$(\omega\frac{\partial C}{\partial t},C)=\omega(\frac{\partial C}{\partial t},C)=\frac{\omega}{2}\frac{\partial}{\partial t}\|C\|^2.\tag{35}$$

By using the divergence theorem and boundary conditions, we get

$$(\mathbf{u}\cdot\boldsymbol{\nabla}C,C)=\frac{1}{2}\Big(\int_{\Gamma_{\text{in}}}((g)^2)(\mathbf{u}\cdot\overrightarrow{n})ds\Big)+\frac{1}{2}\Big(\int_{\Gamma_{\text{out}}}((C)^2)(\mathbf{u}\cdot\overrightarrow{n})ds\Big).\tag{36}$$

Let λ be the minimum eigenvalue of D. Then we get,

$$(D\boldsymbol{\nabla}C, \boldsymbol{\nabla}C) \;=\; (D^{1/2}\boldsymbol{\nabla}C, D^{1/2}\boldsymbol{\nabla}C) \;=\; \|D^{1/2}\boldsymbol{\nabla}C\|^2 \geq \lambda\|\boldsymbol{\nabla}C\|^2. \tag{37}$$

In the right-hand side terms, we get the following estimates,

$$(\mathbf{u}\cdot\boldsymbol{\nabla}C, \hat{C}) \leq \|\mathbf{u}\cdot\boldsymbol{\nabla}C\|\|\hat{C}\| \leq \frac{\lambda}{4\|\mathbf{u}\|_\infty^2}\|\mathbf{u}\cdot\boldsymbol{\nabla}C\|^2 + \frac{\|\mathbf{u}\|_\infty^2}{\lambda}\|\hat{C}\|^2.$$

Then by using boundedness of $\mathbf{u}$, we get

$$(\mathbf{u}\cdot\boldsymbol{\nabla}C, \hat{C}) \leq \frac{\lambda}{4}\|\boldsymbol{\nabla}C\|^2 + \frac{\|\mathbf{u}\|_\infty^2}{\lambda}\|\hat{C}\|^2. \tag{38}$$

Next,

$$(D\boldsymbol{\nabla}C, \boldsymbol{\nabla}\hat{C}) \;\leq \|D\|_\infty\|\boldsymbol{\nabla}C\|\|\boldsymbol{\nabla}\hat{C}\| \leq \beta_1\|\boldsymbol{\nabla}C\|\|\boldsymbol{\nabla}\hat{C}\| \leq \frac{\lambda}{4}\|\boldsymbol{\nabla}C\|^2 + \frac{\beta_1^2}{\lambda}\|\boldsymbol{\nabla}\hat{C}\|^2. \tag{39}$$

$$(f, C-\hat{C}) \leq \|f\|\|C-\hat{C}\| \leq \frac{2K_{\mathrm{PF}}^2}{\lambda}\|f\|^2 + \frac{\lambda}{4}\|\boldsymbol{\nabla}C\|^2 + \frac{\lambda}{4}\|\boldsymbol{\nabla}\hat{C}\|^2. \tag{40}$$

Next,

$$(\omega\frac{\partial C}{\partial t}, \hat{C}) = \omega\frac{\partial}{\partial t}(C, \hat{C}) - \omega(C, \frac{\partial\hat{C}}{\partial t}) = \omega\frac{\partial}{\partial t}(C, \hat{C}). \tag{41}$$

Combining (35)-(41), we get

$$\begin{aligned}
&\frac{\partial}{\partial t}\Big(\frac{\omega}{2}\|C\|^2\Big) + \frac{\lambda}{4}\|\boldsymbol{\nabla}C\|^2 + \frac{1}{2}\int_{\Gamma_{\mathrm{out}}}((C)^2)(\mathbf{u}\cdot\overrightarrow{n})ds \leq \frac{\|\mathbf{u}\|_\infty^2}{\lambda}\|\hat{C}\|^2 \\
&+ \Big(\frac{\lambda}{4} + \frac{\beta_1^2}{\lambda}\Big)\|\boldsymbol{\nabla}\hat{C}\|^2 - \frac{1}{2}\Big(\int_{\Gamma_{\mathrm{in}}}((g)^2)(\mathbf{u}\cdot\overrightarrow{n})ds\Big) + \frac{2K_{\mathrm{PF}}^2}{\lambda}\|f\|^2 + \omega\frac{\partial}{\partial t}(C, \hat{C}).
\end{aligned}$$

Next, integrating both sides from 0 to t, we obtain

$$\begin{aligned}
&\frac{\omega}{2}\|C(t)\|^2 + \frac{\lambda}{4}\int_0^t \|\boldsymbol{\nabla}C(r)\|^2\, dr + \frac{1}{2}\int_0^t \Big(\int_{\Gamma_{\mathrm{out}}}((C)^2)(\mathbf{u}\cdot\overrightarrow{n})ds\Big)\, dr \\
&\leq \int_0^t \frac{\|\mathbf{u}\|_\infty^2}{\lambda}\|\hat{C}\|^2\, dr + \Big(\frac{\lambda}{4} + \frac{\beta_1^2}{\lambda}\Big)\int_0^t \|\boldsymbol{\nabla}\hat{C}\|^2\, dr + \frac{\omega}{2}\|C(0)\|^2 \\
&- \frac{1}{2}\int_0^t \Big(\int_{\Gamma_{\mathrm{in}}}((g)^2)(\mathbf{u}\cdot\overrightarrow{n})ds\Big)\, dr - \omega(C(0), \hat{C}) + \frac{2K_{\mathrm{PF}}^2}{\lambda}\int_0^t \|f\|^2\, dr + \omega(C(t), \hat{C}).
\end{aligned} \tag{42}$$

Here,

$$\omega(C(t),\hat{C}) \leq \omega\|C(t)\|\|\hat{C}\| \leq \frac{\omega}{4}\|C(t)\|^2 + \omega\|\hat{C}\|^2.$$
$$-\omega(C(0),\hat{C}) \leq \omega|(C(0),\hat{C})| \leq \omega\|C(0)\|\|\hat{C}\| \leq \frac{\omega}{4}\|C(0)\|^2 + \omega\|\hat{C}\|^2$$

Hence (42) becomes

$$\begin{aligned}
&\frac{\omega}{4}\|C(t)\|^2 + \frac{\lambda}{4}\int_0^t \|\boldsymbol{\nabla} C(r)\|^2\, dr + \frac{1}{2}\int_0^t \Big(\int_{\Gamma_{\text{out}}} ((C)^2)(\mathbf{u}\cdot\overrightarrow{n})ds\Big)\, dr \\
&\leq \int_0^t \frac{\|\mathbf{u}\|_\infty^2}{\lambda}\|\hat{C}\|^2\, dr + \Big(\frac{\lambda}{4} + \frac{\beta_1^2}{\lambda}\Big)\int_0^t \|\boldsymbol{\nabla}\hat{C}\|^2\, dr - \frac{1}{2}\int_0^t \Big(\int_{\Gamma_{\text{in}}} ((g)^2)(\mathbf{u}\cdot\overrightarrow{n})ds\Big)\, dr \\
&+ \frac{\omega}{4}\|C(0)\|^2 + \omega\|\hat{C}\|^2 + \frac{2K_{\text{PF}}^2}{\lambda}\int_0^t \|f\|^2\, dr + \frac{\omega}{4}\|C(t)\|^2 + \omega\|\hat{C}\|^2 + \frac{\omega}{2}\|C(0)\|^2.
\end{aligned}$$

Simplifying the above inequality and using $C(0) = C_0$, we get the claimed result. □

Remark 12. *Putting* (35), (36) *and* (41) *into* (34), *we get,*

$$\begin{aligned}
&\frac{\omega}{2}\frac{\partial}{\partial t}\|C\|^2 + \Big(\int_{\Gamma_{out}} (C^2)(\mathbf{u}\cdot\overrightarrow{n})ds\Big) + (D\boldsymbol{\nabla} C, \boldsymbol{\nabla} C) = -\Big(\int_{\Gamma_{in}} (g^2)(\mathbf{u}\cdot\overrightarrow{n})ds\Big) + (f, C-\hat{C}) \\
&\omega\frac{\partial}{\partial t}(C,\hat{C}) + (\mathbf{u}\cdot\boldsymbol{\nabla} C,\hat{C}) + (D\boldsymbol{\nabla} C, \boldsymbol{\nabla}\hat{C}).
\end{aligned} \tag{43}$$

If $f = 0$ *and* $\hat{C} = 0$ *in* (43), *we get the balance of mass as follows*

$$\frac{\omega}{2}\frac{\partial}{\partial t}\|C\|^2 + \Big(\int_{\Gamma_{out}} (C^2)(\mathbf{u}\cdot\overrightarrow{n})ds\Big) + (D\boldsymbol{\nabla} C, \boldsymbol{\nabla} C) = -\Big(\int_{\Gamma_{in}} (g^2)(\mathbf{u}\cdot\overrightarrow{n})ds\Big). \tag{44}$$

Recall that $\mathbf{u}\cdot\overrightarrow{n} > 0$ *on* Γ_{out} *and* $\mathbf{u}\cdot\overrightarrow{n} < 0$ *on* Γ_{in}.

Next theorem gives a *priori* error estimate for the case of constant adsorption and semi-discrete in space where we will use the notation:

$$K^2 = \max\Big\{\Big(2 + \frac{8K_{\text{PF}}^2\|\mathbf{u}\|_\infty^2 + 8\beta_1^2}{\lambda^2}\Big)K_1^2, \frac{8K_{\text{PF}}^2\omega^2}{\lambda^2}K_1^2, \frac{4\omega}{\lambda}\Big\}.$$

Theorem 13. *Assume that (F1)-(F6) are satisfied and the variational formulation with constant adsorption given by* (29) *has an exact solution* $C \in H^1(0,T,H^{k+1}(\Omega))$ *and* C_h *solves the semi-discrete in space Finite Element formulation with constant adsorption given by* (30)*. Then for* $1 \leq r \leq k+1$ *there exists a positive constant* K *independent of* h *such that:*

$$\|C - C_h\|_{L^2(0,T;H^1(\Omega))} \leq K\Big(h^{r-1}\|C\|_{L^2(0,T;H^r(\Omega))} + h^{r-1}\Big\|\frac{\partial C}{\partial t}\Big\|_{L^2(0,T;H^r(\Omega))} + \|(C_h - \hat{C}_h)(0)\|\Big).$$

Proof. The weak formulation of continuous and discrete problems are given by (29) and (30), respectively, where $C\Big|_{\Gamma_{\text{in}}} = g$ and $C_h\Big|_{\Gamma_{\text{in}}} = g_h$ are required.
First we let $v = v_h \in X^h_{0,\Gamma_{\text{in}}} \subset H^1_{0,\Gamma_{\text{in}}}(\Omega)$ in (29) and then subtract (30) from (29) to get

$$(\omega\frac{\partial(C - C_h)}{\partial t}, v_h) + (\mathbf{u}\cdot\boldsymbol{\nabla}(C - C_h), v_h) + (D\boldsymbol{\nabla}(C - C_h), \boldsymbol{\nabla}v_h) = 0, \text{ for all } v_h \in X^h_{0,\Gamma_{\text{in}}}. \quad (45)$$

Then for any $\hat{C}_h \in X^h$ such that $\hat{C}_h\Big|_{\Gamma_{\text{in}}} = g_h$, we have that

$$\begin{aligned}&(\omega\frac{\partial(C_h - \hat{C}_h)}{\partial t}, v_h) + (\mathbf{u}\cdot\boldsymbol{\nabla}\Big(C_h - \hat{C}_h\Big), v_h) + (D\boldsymbol{\nabla}\Big(C_h - \hat{C}_h\Big), \boldsymbol{\nabla}v_h) \quad (46)\\ &= (\omega\frac{\partial(C - \hat{C}_h)}{\partial t}, v_h) + (\mathbf{u}\cdot\boldsymbol{\nabla}\Big(C - \hat{C}_h\Big), v_h) + (D\boldsymbol{\nabla}\Big(C - \hat{C}_h\Big), \boldsymbol{\nabla}v_h),\ \forall v_h \in X^h_{0,\Gamma_{\text{in}}}.\end{aligned}$$

We choose $v_h = C_h - \hat{C}_h \in X^h_{0,\Gamma_{\text{in}}}$. Then, we get

$$\begin{aligned}&(\omega\frac{\partial(C_h - \hat{C}_h)}{\partial t}, C_h - \hat{C}_h) + (\mathbf{u}\cdot\boldsymbol{\nabla}\Big(C_h - \hat{C}_h\Big), C_h - \hat{C}_h) + (D\boldsymbol{\nabla}\Big(C_h - \hat{C}_h\Big), \boldsymbol{\nabla}\Big(C_h - \hat{C}_h\Big)) \quad (47)\\ &= (\omega\frac{\partial(C - \hat{C}_h)}{\partial t}, C_h - \hat{C}_h) + (\mathbf{u}\cdot\boldsymbol{\nabla}\Big(C - \hat{C}_h\Big), C_h - \hat{C}_h) + (D\boldsymbol{\nabla}\Big(C - \hat{C}_h\Big), \boldsymbol{\nabla}\Big(C_h - \hat{C}_h\Big)).\end{aligned}$$

Let $\phi_h = C_h - \hat{C}_h$ and $\eta = C - \hat{C}_h$. Notice that both C_h and $\hat{C}_h$ are equal to g_h on Γ_{in}. Hence $\phi_h\Big|_{\Gamma_{\text{in}}} = 0$. Hence, (47) becomes

$$(\omega\frac{\partial\phi_h}{\partial t}, \phi_h) + (\mathbf{u}\cdot\boldsymbol{\nabla}\phi_h, \phi_h) + (D\boldsymbol{\nabla}\phi_h, \boldsymbol{\nabla}\phi_h) = (\omega\frac{\partial\eta}{\partial t}, \phi_h) + (\mathbf{u}\cdot\boldsymbol{\nabla}\eta, \phi_h) + (D\boldsymbol{\nabla}\eta, \boldsymbol{\nabla}\phi_h). \quad (48)$$

We obtain lower bounds for the terms on the left and upper bounds for the term on the right of (48) by using the assumptions and Young's and Cauchy-Schwarz inequalities. We rewrite the first term in (48),

$$(\omega\frac{\partial\phi_h}{\partial t},\phi_h)=\omega(\frac{\partial\phi_h}{\partial t},\phi_h)=\frac{\omega}{2}\frac{\partial}{\partial t}\|\phi_h\|^2. \tag{49}$$

Next,

$$\begin{aligned}(\mathbf{u}\cdot\boldsymbol{\nabla}\phi_h,\phi_h)&=\frac{1}{2}\Big(\int_\Gamma((\phi_h)^2)(\mathbf{u}\cdot\overrightarrow{n})ds\Big),\\&=\frac{1}{2}\Big(\int_{\Gamma_{\text{in}}}((\phi_h)^2)(\mathbf{u}\cdot\overrightarrow{n})ds+\int_{\Gamma_{\text{out}}}((\phi_h)^2)(\mathbf{u}\cdot\overrightarrow{n})ds+\int_{\Gamma_{\text{n}}}((\phi_h)^2)(\mathbf{u}\cdot\overrightarrow{n})ds\Big).\end{aligned}$$

We know that $\phi_h\Big|_{\Gamma_{\text{in}}}=0$, on $\Gamma_{\text{out}},\ \mathbf{u}\cdot\overrightarrow{n}>0$ and on $\Gamma_{\text{n}},\ \mathbf{u}\cdot\overrightarrow{n}=0$.
Hence, we get,

$$(\mathbf{u}\cdot\boldsymbol{\nabla}\phi_h,\phi_h)=\frac{1}{2}\Big(\int_{\Gamma_{\text{out}}}((\phi_h)^2)(\mathbf{u}\cdot\overrightarrow{n})ds\Big)\geq 0. \tag{50}$$

Following the same steps in Theorem 11, we get the following bounds

$$(D\boldsymbol{\nabla}\phi_h,\boldsymbol{\nabla}\phi_h)\geq\lambda\|\boldsymbol{\nabla}\phi_h\|^2. \tag{51}$$

$$(\mathbf{u}\cdot\boldsymbol{\nabla}\eta,\phi_h)\leq\frac{K_{\text{PF}}^2}{\lambda}\|\mathbf{u}\|_\infty^2\|\eta\|_1^2+\frac{\lambda}{4}\|\boldsymbol{\nabla}\phi_h\|^2. \tag{52}$$

$$(D\boldsymbol{\nabla}\eta,\boldsymbol{\nabla}\phi_h)\ \leq\frac{\beta_1^2}{\lambda}\|\eta\|_1^2+\frac{\lambda}{4}\|\boldsymbol{\nabla}\phi_h\|^2. \tag{53}$$

Next,

$$(\omega\frac{\partial\eta}{\partial t},\phi_h)\leq\omega\Big\|\frac{\partial\eta}{\partial t}\Big\|\|\phi_h\|\leq\frac{K_{\text{PF}}^2\omega^2}{\lambda}\Big\|\frac{\partial\eta}{\partial t}\Big\|^2+\frac{\lambda}{4K_{\text{PF}}^2}\|\phi_h\|^2\leq\frac{K_{\text{PF}}^2\omega^2}{\lambda}\Big\|\frac{\partial\eta}{\partial t}\Big\|^2+\frac{\lambda}{4}\|\boldsymbol{\nabla}\phi_h\|^2. \tag{54}$$

Combining (49)-(54) and integrating from 0 to T, we get

$$\|\phi_h(T)\|^2+\frac{\lambda}{2\omega}\int_0^T\|\boldsymbol{\nabla}\phi_h\|^2\ dt$$

$$\leq \Big(\frac{2K_{\mathrm{PF}}^2\|\mathbf{u}\|_\infty^2+2\beta_1^2}{\omega\lambda}\Big)\int_0^T \|\eta\|_1^2\ dt+\frac{2K_{\mathrm{PF}}^2\omega}{\lambda}\int_0^T\Big\|\frac{\partial\eta}{\partial t}\Big\|^2\ dt+\|\phi_h(0)\|^2. \tag{55}$$

Hence, (55) implies

$$\int_0^T \|\boldsymbol{\nabla}\phi_h\|^2\ dt \leq \Big(\frac{4K_{\mathrm{PF}}^2\|\mathbf{u}\|_\infty^2+4\beta_1^2}{\lambda^2}\Big)\int_0^T \|\eta\|_1^2\ dt+\frac{4K_{\mathrm{PF}}^2\omega^2}{\lambda^2}\int_0^T\Big\|\frac{\partial\eta}{\partial t}\Big\|^2\ dt+\frac{2\omega}{\lambda}\|\phi_h(0)\|^2. \tag{56}$$

By using the Lemma 1, we get

$$\int_0^T \|\phi_h\|_1^2\ dt \leq \Big(\frac{4K_{\mathrm{PF}}^2\|\mathbf{u}\|_\infty^2+4\beta_1^2}{\lambda^2}\Big)\int_0^T \|\eta\|_1^2\ dt+\frac{4K_{\mathrm{PF}}^2\omega^2}{\lambda^2}\int_0^T\Big\|\frac{\partial\eta}{\partial t}\Big\|^2\ dt+\frac{2\omega}{\lambda}\|\phi_h(0)\|^2. \tag{57}$$

Triangle inequality gives

$$\|C-C_h\|_1 \leq \|\eta\|_1+\|\phi_h\|_1.$$

Thus, we get

$$\int_0^T \|C-C_h\|_1^2\ dt \leq 2\int_0^T \|\eta\|_1^2\ dt+2\int_0^T \|\phi_h\|_1^2\ dt. \tag{58}$$

Now using inequality (57) in (58) yields

$$\int_0^T \|C-C_h\|_1^2\ dt \leq \Big(2+\frac{8K_{\mathrm{PF}}^2\|\mathbf{u}\|_\infty^2+8\beta_1^2}{\lambda^2}\Big)\int_0^T \|\eta\|_1^2\ dt+\frac{8K_{\mathrm{PF}}^2\omega^2}{\lambda^2}\int_0^T\Big\|\frac{\partial\eta}{\partial t}\Big\|^2\ dt + \frac{4\omega}{\lambda}\|\phi_h(0)\|^2.$$

Since $\hat{C}_h$ is arbitrary, we have the following inequality

$$\int_0^T \|C-C_h\|_1^2\ dt \leq \Big(2+\frac{8K_{\mathrm{PF}}^2\|\mathbf{u}\|_\infty^2+8\beta_1^2}{\lambda^2}\Big)\int_0^T \inf_{\substack{\hat{C_h}\in X^h\\ \hat{C_h}|_{\Gamma_{\mathrm{in}}}=g_h}} \|C-\hat{C}_h\|_1^2\ dt$$
$$+\frac{8K_{\mathrm{PF}}^2\omega^2}{\lambda^2}\int_0^T \inf_{\substack{\hat{C_h}\in X^h\\ \hat{C_h}|_{\Gamma_{\mathrm{in}}}=g_h}} \Big\|\frac{\partial(C-\hat{C}_h)}{\partial t}\Big\|^2\ dt+\frac{4\omega}{\lambda}\|\phi_h(0)\|^2.$$

Let g_h be the interpolant of g in $X^h_{\Gamma_{\text{in}}}$. Then by using Lemma 4, for $1 \le r \le k+1$ we get,

$$\begin{aligned}\int_0^T \|C - C_h\|_1^2 \, dt &\le \Big(2 + \frac{8K_{\text{PF}}^2\|\mathbf{u}\|_\infty^2 + 8\beta_1^2}{\lambda^2}\Big) K_1^2 h^{2r-2} \int_0^T \|C\|_r^2 \, dt \\ &+ \frac{8K_{\text{PF}}^2\omega^2 K_1^2 h^{2r-2}}{\lambda^2} \int_0^T \Big\|\frac{\partial C}{\partial t}\Big\|_r^2 \, dt + \frac{4\omega}{\lambda}\|\phi_h(0)\|^2.\end{aligned} \tag{59}$$

Let

$$K^2 = \max\Big\{\Big(2 + \frac{8K_{\text{PF}}^2\|\mathbf{u}\|_\infty^2 + 8\beta_1^2}{\lambda^2}\Big) K_1^2, \frac{8K_{\text{PF}}^2\omega^2}{\lambda^2} K_1^2, \frac{4\omega}{\lambda}\Big\}.$$

Thus (59) implies

$$\|C - C_h\|^2_{L^2(0,T;H^1(\Omega))} \le K^2\Big(h^{2r-2}\|C\|^2_{L^2(0,T;H^r(\Omega))} + h^{2r-2}\Big\|\frac{\partial C}{\partial t}\Big\|^2_{L^2(0,T;H^r(\Omega))} + \|\phi_h(0)\|^2\Big).$$

Consequently, we prove the claim. □

Next, we find the energy bound for the discrete version of the adsorption equation (1) for constant isotherm using the midpoint method for the time discretization. At a continuous level, we proved $C > 0$ and bounded by initial and boundary conditions. But at a discrete level, the Maximum Principle is very hard to implement, usually, the timestep has to be $\mathcal{O}(h^2)$ [147].

Theorem 14. *Suppose the assumptions (F1)-F(7) are satisfied so that the fully discrete formulation given by (31) has a smooth solution* $\{C_h^n\}_{n=0}^N \in L^2(0,T;H^1(\Omega))$. *Then for all* $N > 0$,

$$\begin{aligned}&\|C_h^{N+1}\|^2 + \frac{2}{\omega}\Delta t \sum_{n=0}^{N}\Big(\int_{\Gamma_{out}}((C_h^{n+1/2})^2)(\mathbf{u}\cdot\overrightarrow{n})ds\Big) + \frac{\lambda}{\omega}\Delta t\sum_{n=0}^{N}\|\boldsymbol{\nabla} C_h^{n+1/2}\|^2 \\ &\le \frac{4N\Delta t\|\mathbf{u}\|_\infty^2 + 8\lambda\omega}{\omega\lambda}\|\hat{C_h}\|^2 + \frac{2N\Delta t}{\omega}\Big(\int_{\Gamma_{in}}((g_h)^2)(-\mathbf{u}\cdot\overrightarrow{n})ds\Big) + \frac{4N\Delta t\beta_1^2 + N\Delta t\lambda^2}{\omega\lambda}\|\boldsymbol{\nabla}\hat{C_h}\|^2 \\ &+ \frac{8K_{PF}^2}{\omega\lambda}\Delta t\sum_{n=0}^{N}\|f^{n+1/2}\|^2 + 3\|C_h^0\|^2.\end{aligned}$$

Proof. Let $\hat{C}_h \in X^h$ such that $\hat{C}_h\Big|_{\Gamma_{\text{in}}} = g_h$. Take $v_h = C_h^{n+1/2} - \hat{C}_h \in X^h_{0,\Gamma_{\text{in}}}(\Omega)$. Then (32) yields to

$$\begin{aligned}
&(\omega(C_h^{n+1/2} - C_h^n), C_h^{n+1/2}) + \frac{\Delta t}{2}(\mathbf{u}\cdot\boldsymbol{\nabla} C_h^{n+1/2}, C_h^{n+1/2}) + \frac{\Delta t}{2}(D\boldsymbol{\nabla} C_h^{n+1/2}, \boldsymbol{\nabla} C_h^{n+1/2}) \\
=&\frac{\Delta t}{2}(f^{n+1/2}, C_h^{n+1/2} - \hat{C}_h) + (\omega(C_h^{n+1/2} - C_h^n), \hat{C}_h) + \frac{\Delta t}{2}(\mathbf{u}\cdot\boldsymbol{\nabla} C_h^{n+1/2}, \hat{C}_h) \\
&+ \frac{\Delta t}{2}(D\boldsymbol{\nabla} C_h^{n+1/2}, \boldsymbol{\nabla}\hat{C}_h).
\end{aligned}$$

Using polarization identity in the first term, we get,

$$\begin{aligned}
&(\frac{\omega}{2}\|C_h^{n+1/2}\|^2 - \frac{\omega}{2}\|C_h^n\|^2 + \frac{\omega}{2}\|C_h^{n+1/2} - C_h^n\|^2) + \frac{\Delta t}{2}(\mathbf{u}\cdot\boldsymbol{\nabla} C_h^{n+1/2}, C_h^{n+1/2}) \\
&+ \frac{\Delta t}{2}(D\boldsymbol{\nabla} C_h^{n+1/2}, \boldsymbol{\nabla} C_h^{n+1/2}) \\
&= \frac{\Delta t}{2}(f^{n+1/2}, C_h^{n+1/2} - \hat{C}_h) + (\omega(C_h^{n+1/2} - C_h^n), \hat{C}_h) + \frac{\Delta t}{2}(\mathbf{u}\cdot\boldsymbol{\nabla} C_h^{n+1/2}, \hat{C}_h) \\
&+ \frac{\Delta t}{2}(D\boldsymbol{\nabla} C_h^{n+1/2}, \boldsymbol{\nabla}\hat{C}_h).
\end{aligned} \tag{60}$$

Next, (33) yields to

$$\begin{aligned}
&(\omega(C_h^{n+1} - C_h^{n+1/2}), C_h^{n+1/2}) + \frac{\Delta t}{2}(\mathbf{u}\cdot\boldsymbol{\nabla} C_h^{n+1/2}, C_h^{n+1/2}) + \frac{\Delta t}{2}(D\boldsymbol{\nabla} C_h^{n+1/2}, \boldsymbol{\nabla} C_h^{n+1/2}) \\
=&\frac{\Delta t}{2}(f^{n+1/2}, C_h^{n+1/2} - \hat{C}_h) + (\omega(C_h^{n+1} - C_h^{n+1/2}), \hat{C}_h) + \frac{\Delta t}{2}(\mathbf{u}\cdot\boldsymbol{\nabla} C_h^{n+1/2}, \hat{C}_h) \\
&+ \frac{\Delta t}{2}(D\boldsymbol{\nabla} C_h^{n+1/2}, \boldsymbol{\nabla}\hat{C}_h).
\end{aligned}$$

Using polarization identity first term, we get

$$\begin{aligned}
&\frac{\omega}{2}(\|C_h^{n+1}\|^2 - \|C_h^{n+1/2}\|^2 - \|C_h^{n+1} - C_h^{n+1/2}\|^2) + \frac{\Delta t}{2}(\mathbf{u}\cdot\boldsymbol{\nabla} C_h^{n+1/2}, C_h^{n+1/2}) \\
&+ \frac{\Delta t}{2}(D\boldsymbol{\nabla} C_h^{n+1/2}, \boldsymbol{\nabla} C_h^{n+1/2}) \\
&= \frac{\Delta t}{2}(f^{n+1/2}, C_h^{n+1/2} - \hat{C}_h) + (\omega(C_h^{n+1} - C_h^{n+1/2}), \hat{C}_h) + \frac{\Delta t}{2}(\mathbf{u}\cdot\boldsymbol{\nabla} C_h^{n+1/2}, \hat{C}_h) \\
&+ \frac{\Delta t}{2}(D\boldsymbol{\nabla} C_h^{n+1/2}, \boldsymbol{\nabla}\hat{C}_h).
\end{aligned} \tag{61}$$

Adding (60) and (61), we get

$$\begin{aligned}&\frac{\omega}{2}(\|C_h^{n+1}\|^2-\|C_h^n\|^2+\|C_h^{n+1/2}-C_h^n\|^2-\|C_h^{n+1}-C_h^{n+1/2}\|^2)+\Delta t(\mathbf{u}\cdot\boldsymbol{\nabla}C_h^{n+1/2},C_h^{n+1/2})\\&+\Delta t(D\boldsymbol{\nabla}C_h^{n+1/2},\boldsymbol{\nabla}C_h^{n+1/2})=\Delta t(f^{n+1/2},C_h^{n+1/2}-\hat{C}_h)+(\omega(C_h^{n+1}-C_h^n),\hat{C}_h)\\&+\Delta t(\mathbf{u}\cdot\boldsymbol{\nabla}C_h^{n+1/2},\hat{C}_h)+\Delta t(D\boldsymbol{\nabla}C_h^{n+1/2},\boldsymbol{\nabla}\hat{C}_h).\end{aligned}\tag{62}$$

Using (32) and (33), we get,

$$\frac{1}{2}\|C_h^{n+1/2}-C_h^n\|^2-\frac{1}{2}\|C_h^{n+1}-C_h^{n+1/2}\|^2=0.$$

Consequently, we have,

$$\begin{aligned}&\frac{\omega}{2}(\|C_h^{n+1}\|^2-\|C_h^n\|^2)+\Delta t(\mathbf{u}\cdot\boldsymbol{\nabla}C_h^{n+1/2},C_h^{n+1/2})+\Delta t(D\boldsymbol{\nabla}C_h^{n+1/2},\boldsymbol{\nabla}C_h^{n+1/2})\\&=\Delta t(f^{n+1/2},C_h^{n+1/2}-\hat{C}_h)+(\omega(C_h^{n+1}-C_h^n),\hat{C}_h)+\Delta t(\mathbf{u}\cdot\boldsymbol{\nabla}C_h^{n+1/2},\hat{C}_h)\\&+\Delta t(D\boldsymbol{\nabla}C_h^{n+1/2},\boldsymbol{\nabla}\hat{C}_h).\end{aligned}\tag{63}$$

Doing a similar analysis as in the continuous case, we get,

$$(\mathbf{u}\cdot\boldsymbol{\nabla}C_h^{n+1/2},C_h^{n+1/2})=\frac{1}{2}\Big(\int_{\Gamma_{\text{in}}}((g_h)^2)(\mathbf{u}\cdot\overrightarrow{n})ds\Big)+\frac{1}{2}\Big(\int_{\Gamma_{\text{out}}}((C_h^{n+1/2})^2)(\mathbf{u}\cdot\overrightarrow{n})ds\Big).\tag{64}$$

Next,

$$(D\boldsymbol{\nabla}C_h^{n+1/2},\boldsymbol{\nabla}C_h^{n+1/2})\geq\lambda\|\boldsymbol{\nabla}C_h^{n+1/2}\|^2.\tag{65}$$

The bounded term on the right side using similar techniques as in continuous case is shown below:

$$(\mathbf{u}\cdot\boldsymbol{\nabla}C_h^{n+1/2},\hat{C}_h)\leq\frac{\lambda}{4}\|\boldsymbol{\nabla}C_h^{n+1/2}\|^2+\frac{\|\mathbf{u}\|_\infty^2}{\lambda}\|\hat{C}_h\|^2.\tag{66}$$

$$(D\boldsymbol{\nabla}C_h^{n+1/2},\boldsymbol{\nabla}\hat{C}_h)\leq\frac{\lambda}{4}\|\boldsymbol{\nabla}C_h^{n+1/2}\|^2+\frac{\beta_1^2}{\lambda}\|\boldsymbol{\nabla}\hat{C}_h\|^2.\tag{67}$$

$$(f^{n+1/2},C_h^{n+1/2}-\hat{C}_h)\leq\frac{2K_{\text{PF}}^2}{\lambda}\|f^{n+1/2}\|^2+\frac{\lambda}{4}\|\boldsymbol{\nabla}C_h^{n+1/2}\|^2+\frac{\lambda}{4}\|\boldsymbol{\nabla}\hat{C}_h\|^2.\tag{68}$$

Putting (64)-(68) into (63), we get,

$$\begin{aligned}
&\frac{\omega}{2}\|C_h^{n+1}\|^2-\frac{\omega}{2}\|C_h^{n}\|^2+\frac{\Delta t}{2}\Big(\int_{\Gamma_{\text{out}}}((C_h^{n+1/2})^2)(\mathbf{u}\cdot\overrightarrow{n})ds\Big)+\frac{\Delta t\lambda}{4}\|\boldsymbol{\nabla} C_h^{n+1/2}\|^2\\
&\leq\frac{\|\mathbf{u}\|_\infty^2\Delta t}{\lambda}\|\hat{C}_h\|^2-\frac{\Delta t}{2}\Big(\int_{\Gamma_{\text{in}}}((g_h)^2)(\mathbf{u}\cdot\overrightarrow{n})ds\Big)+\frac{\Delta t\beta_1^2}{\lambda}\|\boldsymbol{\nabla}\hat{C}_h\|^2\\
&+\frac{2K_{\text{PF}}^2\Delta t}{\lambda}\|f^{n+1/2}\|^2+\frac{\Delta t\lambda}{4}\|\boldsymbol{\nabla}\hat{C}_h\|^2+(\omega(C_h^{n+1}-C_h^n),\hat{C}_h).
\end{aligned}\tag{69}$$

Next, we sum over $n=0$ to $n=N$ to get

$$\begin{aligned}
&\frac{\omega}{2}\|C_h^{N+1}\|^2-\frac{\omega}{2}\|C_h^{0}\|^2+\frac{\Delta t}{2}\sum_{n=0}^{N}\Big(\int_{\Gamma_{\text{out}}}((C_h^{n+1/2})^2)(\mathbf{u}\cdot\overrightarrow{n})ds\Big)+\frac{\Delta t\lambda}{4}\sum_{n=0}^{N}\|\boldsymbol{\nabla} C_h^{n+1/2}\|^2\\
&\leq\frac{N\|\mathbf{u}\|_\infty^2\Delta t}{\lambda}\|\hat{C}_h\|^2-\frac{N\Delta t}{2}\Big(\int_{\Gamma_{\text{in}}}((g_h)^2)(\mathbf{u}\cdot\overrightarrow{n})ds\Big)+\frac{N\Delta t\beta_1^2}{\lambda}\|\boldsymbol{\nabla}\hat{C}_h\|^2\\
&+\frac{2K_{\text{PF}}^2\Delta t}{\lambda}\sum_{n=0}^{N}\|f^{n+1/2}\|^2+\frac{N\Delta t\lambda}{4}\|\boldsymbol{\nabla}\hat{C}_h\|^2+(\omega(C_h^{N+1}-C_h^0),\hat{C}_h).
\end{aligned}\tag{70}$$

Here,

$$(\omega(C_h^{N+1}-C_h^0),\hat{C}_h)\leq\frac{\omega}{4}\|C_h^{N+1}\|^2+\frac{\omega}{4}\|C_h^0\|^2+2\omega\|\hat{C}_h\|^2.$$

After simplification, we get the desired result. □

Remark 15. *Putting (64) into (63), we get,*

$$\begin{aligned}
&\frac{\omega}{2}\|C_h^{n+1}\|^2-\frac{\omega}{2}\|C_h^{n}\|^2+\frac{\Delta t}{2}\Big(\int_{\Gamma_{out}}((C_h^{n+1/2})^2)(\mathbf{u}\cdot\overrightarrow{n})ds\Big)+\Delta t(D\boldsymbol{\nabla} C_h^{n+1/2},\boldsymbol{\nabla} C_h^{n+1/2})\\
&=-\frac{\Delta t}{2}\Big(\int_{\Gamma_{in}}((g_h)^2)(\mathbf{u}\cdot\overrightarrow{n})ds\Big)+\Delta t(f^{n+1/2},C_h^{n+1/2}-\hat{C}_h)\\
&+(\omega(C_h^{n+1}-C_h^n),\hat{C}_h)+\Delta t(\mathbf{u}\cdot\boldsymbol{\nabla} C_h^{n+1/2},\hat{C}_h)+\Delta t(D\boldsymbol{\nabla} C_h^{n+1/2},\boldsymbol{\nabla}\hat{C}_h).
\end{aligned}\tag{71}$$

If $f=0$ and $\hat{C}_h=0$ in (71), we get the balance of mass as follows

$$\begin{aligned}
&\frac{\omega}{2}(\|C_h^{n+1}\|^2-\|C_h^{n}\|^2)+\frac{\Delta t}{2}\Big(\int_{\Gamma_{out}}((C_h^{n+1/2})^2)(\mathbf{u}\cdot\overrightarrow{n})ds\Big)+\Delta t(D\boldsymbol{\nabla} C_h^{n+1/2},\boldsymbol{\nabla} C_h^{n+1/2})\\
&=\frac{\Delta t}{2}\Big(\int_{\Gamma_{in}}((g_h)^2)(-\mathbf{u}\cdot\overrightarrow{n})ds\Big).
\end{aligned}\tag{72}$$

Recall that $\mathbf{u}\cdot\overrightarrow{n}>0$ on Γ_{out} and $\mathbf{u}\cdot\overrightarrow{n}<0$ on Γ_{in}.

Next theorem gives a *priori* error estimate for the case of constant adsorption in the fully discrete case where we will use the notation

$$K^2 = \max\Big\{\Big(2 + \frac{8K_{\rm PF}^2\|\mathbf{u}\|_\infty^2 + 8\beta_1^2}{\lambda^2}\Big)K_2^2, \frac{8K_{\rm PF}^2\omega^2}{\lambda^2}K_2^2, \frac{8K_1TK_{\rm PF}^2}{\lambda^2}, \frac{2\omega}{\lambda}\Big\}.$$

Theorem 16. *Suppose the assumptions (F1)-F(7) are satisfied so that the fully discrete formulation given by (31) has a smooth solution* $\{C_h^n\}_{n=0}^N \in L^2(0,T;H^1(\Omega))$ *and the variational formulation with constant adsorption given by* (29) *has an exact solution* $C \in H^1(0,T,H^{k+1}(\Omega))$. *Let* $\phi_h^n = \hat{C}_h - C_h^n$. *Then for* $1 \le r \le k+1$ *and* $N > 0$ *there exists a positive constant* K *such that:*

$$\Delta t\sum_{n=0}^{N+1}\|C(t_{n+1/2}) - C_h(t_{n+1/2})\|_1^2 \le K^2\Big(h^{2r-2}\Delta t\sum_{n=0}^{N+1}\|C(t_{n+1/2})\|_r^2 + h^{2r-2}\Big\|\frac{\partial C}{\partial t}\Big\|^2_{L^2(0,T;H^r(\Omega))}$$
$$+ (\Delta t)^4\|C_{ttt}\|^2_{L^\infty(0,T;L^\infty)} + \|\phi_h^0\|^2\Big).$$

Proof. Let the approximate solution at time $t^{n+1/2}$ be $C_h^{n+1/2}$. Then by using the midpoint method, we get, the fully discrete variational formulation as follows:
Given $C_h^n \in X^h$, find $C_h^{n+1} \in X^h$ such that $C_h^{n+1}\Big|_{\Gamma_{\rm in}} = g_h$ and satisfying,

$$(\omega\frac{C_h^{n+1} - C_h^n}{\Delta t}, v_h) + (u\cdot\boldsymbol{\nabla}C_h^{n+1/2}, v_h) + (D\boldsymbol{\nabla}C_h^{n+1/2}, \boldsymbol{\nabla}v_h) = (f^{n+1/2}, v_h),\ \forall v_h \in X^h_{0,\Gamma_{\rm in}}(\Omega). \tag{73}$$

Let C_t represent $\frac{\partial C}{\partial t}$. We write the following variational formulation for the exact solution C.

$$\begin{aligned}&(\omega\frac{C(t_{n+1}) - C(t_n)}{\Delta t}, v) + (\mathbf{u}\cdot\boldsymbol{\nabla}C(t_{n+1/2}), v) + (D\boldsymbol{\nabla}C(t_{n+1/2}), \boldsymbol{\nabla}v)\\ &= (f^{n+1/2}, v) + (r^n, v),\ \forall\ v \in H^1_{0,\Gamma_{\rm in}}(\Omega).\end{aligned} \tag{74}$$

where time discretization error, $r^n = \frac{C(t_{n+1})-C(t_n)}{\Delta t} - \frac{C_t(t_{n+1})+C_t(t_n)}{2}$.
Let $e^n = C(t_n) - C_h^n$ and $v = v_h \in X^h_{0,\Gamma_{\rm in}} \subset H^1_{0,\Gamma_{\rm in}}(\Omega)$ in (74) and then subtract (73) from (74) to get

$$(\omega\frac{e^{n+1} - e^n}{\Delta t}, v_h) + (\mathbf{u}\cdot\boldsymbol{\nabla}e^{n+1/2}, v_h) + (D\boldsymbol{\nabla}e^{n+1/2}, \boldsymbol{\nabla}v_h) = (r^n, v_h),\ \forall\ v_h \in X^h_{0,\Gamma_{\rm in}}(\Omega). \tag{75}$$

Then for any $\hat{C}_h \in X^h$ such that $\hat{C}_h\Big|_{\Gamma_{\text{in}}} = g_h$, we write that $e^n = C(t_n) - C_h^n = C(t_n) - \hat{C}_h + \hat{C}_h - C_h^n$. Let $\phi_h^n = \hat{C}_h - C_h^n$ and $\eta^n = \hat{C}_h - C(t_n)$. Notice that both C_h^n and $\hat{C}_h{}^n$ are equal to g_h on Γ_{in}. Hence $\phi_h^n\Big|_{\Gamma_{\text{in}}} = 0$. We choose $v_h = \phi_h^{n+1/2} \in X^h_{0,\Gamma_{\text{in}}}$. Then (75) becomes

$$
\begin{aligned}
&(\omega\frac{\phi_h^{n+1} - \phi_h^n}{\Delta t}, \phi_h^{n+1/2}) + (\mathbf{u}\cdot\boldsymbol{\nabla}\phi_h^{n+1/2}, \phi_h^{n+1/2}) + (D\boldsymbol{\nabla}\phi_h^{n+1/2}, \boldsymbol{\nabla}\phi_h^{n+1/2}) \\
&= (\omega\frac{\eta^{n+1} - \eta^n}{\Delta t}, \phi_h^{n+1/2}) + (\mathbf{u}\cdot\boldsymbol{\nabla}\eta^{n+1/2}, \phi_h^{n+1/2}) + (D\boldsymbol{\nabla}\eta^{n+1/2}, \boldsymbol{\nabla}\phi_h^{n+1/2}) + (r^n, \phi_h^{n+1/2}).
\end{aligned}
$$

We obtain lower bounds for the terms on the left and upper bounds for the term on the right of (76) by using the assumptions and Young's and Cauchy-Schwarz inequalities. We rewrite the first term in (76),

$$
(\omega\frac{\phi_h^{n+1} - \phi_h^n}{\Delta t}, \phi_h^{n+1/2}) = \frac{\omega}{2\Delta t}(\|\phi_h^{n+1}\|^2 - \|\phi_h^n\|^2). \tag{76}
$$

Following the same steps in Theorem 13, we get the following bounds

$$
(\mathbf{u}\cdot\boldsymbol{\nabla}\phi_h^{n+1/2}, \phi_h^{n+1/2}) \geq 0. \tag{77}
$$

$$
(D\boldsymbol{\nabla}\phi_h^{n+1/2}, \boldsymbol{\nabla}\phi_h^{n+1/2}) \geq \lambda\|\boldsymbol{\nabla}\phi_h^{n+1/2}\|^2. \tag{78}
$$

$$
(\mathbf{u}\cdot\boldsymbol{\nabla}\eta^{n+1/2}, \phi_h^{n+1/2}) \leq \frac{2K_{\text{PF}}^2\|\mathbf{u}\|_\infty^2}{\lambda}\|\eta^{n+1/2}\|_1^2 + \frac{\lambda}{8}\|\boldsymbol{\nabla}\phi_h^{n+1/2}\|^2. \tag{79}
$$

$$
(D\boldsymbol{\nabla}\eta^{n+1/2}, \boldsymbol{\nabla}\phi_h^{n+1/2}) \ \leq \frac{2\beta_1^2}{\lambda}\|\eta^{n+1/2}\|_1^2 + \frac{\lambda}{8}\|\boldsymbol{\nabla}\phi_h^{n+1/2}\|^2. \tag{80}
$$

Next,

$$
\begin{aligned}
(\omega\frac{\eta^{n+1} - \eta^n}{\Delta t}, \phi_h^{n+1/2}) &= \big(\frac{\omega}{\Delta t}\int_{t_n}^{t_{n+1}} \eta_t d\tau, \phi_h^{n+1/2}\big), \\
&\leq \frac{2K_{\text{PF}}^2\omega^2}{\lambda\Delta t^2}\big(\int_{t_n}^{t_{n+1}} \|\eta_t\| d\tau\big)^2 + \frac{\lambda}{8}\|\boldsymbol{\nabla}\phi_h^{n+1/2}\|^2.
\end{aligned}
$$

Hence, after applying Cauchy-Schwarz inequality we get,

$$
(\omega\frac{\eta^{n+1} - \eta^n}{\Delta t}, \phi_h^{n+1/2}) \leq \frac{2K_{\text{PF}}^2\omega^2}{\lambda\Delta t^2}\big(\int_{t_n}^{t_{n+1}} \|\eta_t\|^2 d\tau\big) + \frac{\lambda}{8}\|\boldsymbol{\nabla}\phi_h^{n+1/2}\|^2. \tag{81}
$$

Next,

$$(r^n, \phi_h^{n+1/2}) \leq \frac{\lambda}{8}\|\boldsymbol{\nabla}\phi_h^{n+1/2}\|^2 + \frac{2K_{\mathrm{PF}}^2}{\lambda}\|r^n\|^2. \tag{82}$$

Combining (76)-(82), we get

$$\begin{aligned}&\frac{\omega}{2\Delta t}(\|\phi_h^{n+1}\|^2 - \|\phi_h^n\|^2) + \frac{\lambda}{2}\|\boldsymbol{\nabla}\phi_h^{n+1/2}\|^2 \\ &\leq \frac{2K_{\mathrm{PF}}^2\|\mathbf{u}\|_\infty^2\|\eta^{n+1/2}\|_1^2}{\lambda} + \frac{2\beta_1^2\|\eta^{n+1/2}\|_1^2}{\lambda} + \frac{2K_{\mathrm{PF}}^2\omega^2}{\lambda\Delta t}\Big(\int_{t_n}^{t_{n+1}}\|\eta_t\|^2 d\tau\Big) + \frac{2K_{\mathrm{PF}}^2}{\lambda}\|r^n\|^2.\end{aligned} \tag{83}$$

Multiplying (83) by $\frac{2\Delta t}{\omega}$ and summing over $n = 0$ to $n = N$, we get

$$\begin{aligned}\|\phi_h^{N+1}\|^2 + \frac{\lambda}{\omega}\sum_{n=0}^{N+1}\Delta t\|\boldsymbol{\nabla}\phi_h^{n+1/2}\|^2 \ &\leq \Big(\frac{4K_{\mathrm{PF}}^2\|\mathbf{u}\|_\infty^2 + 4\beta_1^2}{\omega\lambda}\Big)\sum_{n=0}^{N+1}\Delta t\|\eta^{n+1/2}\|_1^2 \\ + \frac{4K_{\mathrm{PF}}^2}{\lambda\omega}\int_0^T\|\eta_t\|^2 dt + \frac{4K_{\mathrm{PF}}^2}{\omega\lambda}\sum_{n=0}^{N+1}\Delta t\|r^n\|^2 + \|\phi_h^0\|^2.&\end{aligned} \tag{84}$$

To bound r^n, we use Taylor expansion about $t^{n+1/2}$. Hence,

$$\begin{aligned}\sum_{n=0}^{N+1}\Delta t\|r^n\|^2 &\leq K_1\sum_{n=0}^{N+1}\Delta t(\Delta t^2\|C_{ttt}\|_{L^\infty}(0,T;L^\infty))^2, \\ &\leq K_1 N\Delta t(\Delta t^2\|C_{ttt}\|_{L^\infty(0,T;L^\infty)})^2, \\ &\leq K_1 T(\Delta t^2\|C_{ttt}\|_{L^\infty(0,T;L^\infty)})^2.\end{aligned}$$

Therefore, (84) implies

$$\begin{aligned}\|\phi_h^{N+1}\|^2 + \frac{\lambda}{\omega}\sum_{n=0}^{N+1}\Delta t\|\boldsymbol{\nabla}\phi_h^{n+1/2}\|^2 &\leq \Big(\frac{4K_{\mathrm{PF}}^2\|\mathbf{u}\|_\infty^2 + 4\beta_1^2}{\omega\lambda}\Big)\sum_{n=0}^{N+1}\Delta t\|\eta^{n+1/2}\|_1^2 \\ + \frac{4K_{\mathrm{PF}}^2\omega}{\lambda}\int_0^T\|\eta_t\|^2 dt + \frac{4K_1TK_{\mathrm{PF}}^2}{\omega\lambda}(\Delta t^2\|C_{ttt}\|_{L^\infty(0,T;L^\infty)})^2 + \|\phi_h^0\|^2.&\end{aligned}$$

Hence, we can write,

$$\begin{aligned}\sum_{n=0}^{N+1}\Delta t\|\boldsymbol{\nabla}\phi_h^{n+1/2}\|^2 &\leq \Big(\frac{4K_{\mathrm{PF}}^2\|\mathbf{u}\|_\infty^2 + 4\beta_1^2}{\lambda^2}\Big)\sum_{n=0}^{N+1}\Delta t\|\eta^{n+1/2}\|^2 \\ + \frac{4K_{\mathrm{PF}}^2\omega^2}{\lambda^2}\int_0^T\|\eta_t\|_1^2 dt + \frac{4K_1TK_{\mathrm{PF}}^2}{\lambda^2}(\Delta t^2\|C_{ttt}\|_{L^\infty(0,T;L^\infty)})^2 + \frac{\omega}{\lambda}\|\phi_h^0\|^2.&\end{aligned}$$

By using the Lemma 1, we get

$$\sum_{n=0}^{N+1}\Delta t\|\phi_h^{n+1/2}\|_1^2 \le \Big(\frac{4K_{\rm PF}^2\|\mathbf{u}\|_\infty^2+4\beta_1^2}{\lambda^2}\Big)\sum_{n=0}^{N+1}\Delta t\|\eta^{n+1/2}\|_1^2$$
$$+\frac{4K_{\rm PF}^2\omega^2}{\lambda^2}\int_0^T\|\eta_t\|^2dt+\frac{4K_1TK_{\rm PF}^2}{\lambda^2}(\Delta t^2\|C_{ttt}\|_{L^\infty(0,T;L^\infty)})^2+\frac{\omega}{\lambda}\|\phi_h^0\|^2.$$

Triangle inequality gives

$$\sum_{n=0}^{N+1}\Delta t\|e^{n+1/2}\|_1^2 \le \sum_{n=0}^{N+1}2\Delta t\big(\|\phi_h^{n+1/2}\|_1^2+\|\eta^{n+1/2}\|_1^2\big).$$

Thus, we get

$$\sum_{n=0}^{N+1}\Delta t\|e^{n+1/2}\|_1^2 \le \Big(2+\frac{8K_{\rm PF}^2\|\mathbf{u}\|_\infty^2+8\beta_1^2}{\lambda^2}\Big)\sum_{n=0}^{N+1}\Delta t\|\eta^{n+1/2}\|_1^2$$
$$+\frac{8K_{\rm PF}^2\omega^2}{\lambda^2}\int_0^T\|\eta_t\|^2dt+\frac{8K_1TK_{\rm PF}^2}{\lambda^2}(\Delta t^2\|C_{ttt}\|_{L^\infty(0,T;L^\infty)})^2+\frac{2\omega}{\lambda}\|\phi_h^0\|^2.$$

Since $\hat{C}_h$ is arbitrary, we have the following inequality

$$\sum_{n=0}^{N+1}\Delta t\|e^{n+1/2}\|_1^2 \le \Big(2+\frac{8K_{\rm PF}^2\|\mathbf{u}\|_\infty^2+8\beta_1^2}{\lambda^2}\Big)\sum_{n=0}^{N+1}\Delta t\inf_{\substack{\hat{C_h}\in X^h\\ \hat{C_h}|_{\Gamma_{\rm in}}=g_h}}\|C^{n+1/2}-\hat{C}_h\|_1^2$$
$$+\frac{8K_{\rm PF}^2\omega^2}{\lambda^2}\int_0^T\inf_{\substack{\hat{C_h}\in X^h\\ \hat{C_h}|_{\Gamma_{\rm in}}=g_h}}\Big\|\frac{\partial(C-\hat{C}_h)}{\partial t}\Big\|^2dt+\frac{8K_1TK_{\rm PF}^2}{\lambda^2}(\Delta t^2\|C_{ttt}\|_{L^\infty(0,T;L^\infty)})^2+\frac{2\omega}{\lambda}\|\phi_h^0\|^2.$$

Let g_h be the interpolant of g in $X^h_{\Gamma_{\rm in}}$. Then by using Lemma 4, for $1\le r\le k+1$ we get,

$$\sum_{n=0}^{N+1}\Delta t\|e^{n+1/2}\|_1^2 \le \Big(2+\frac{8K_{\rm PF}^2\|\mathbf{u}\|_\infty^2+8\beta_1^2}{\lambda^2}\Big)K_2^2h^{2r-2}\sum_{n=0}^{N+1}\Delta t\|C^{n+1/2}\|_r^2$$
$$+\frac{8K_{\rm PF}^2\omega^2}{\lambda^2}K_2^2h^{2r-2}\int_0^T\Big\|\frac{\partial C}{\partial t}\Big\|_r^2dt+\frac{8K_1TK_{\rm PF}^2}{\lambda^2}(\Delta t^2\|C_{ttt}\|_{L^\infty(0,T;L^\infty)})^2+\frac{2\omega}{\lambda}\|\phi_h^0\|^2. \tag{85}$$

Let

$$K^2=\max\Big\{\Big(2+\frac{8K_{\rm PF}^2\|\mathbf{u}\|_\infty^2+8\beta_1^2}{\lambda^2}\Big)K_2^2,\frac{8K_{\rm PF}^2\omega^2}{\lambda^2}K_2^2,\frac{8K_1TK_{\rm PF}^2}{\lambda^2},\frac{2\omega}{\lambda}\Big\}.$$

Thus (85) implies the claim. □

2.4.3 Affine Isotherm

In the case of affine adsorption, $q(C) = K_1 + K_2 C$ with $K_1,\ K_2 \geq 0$. It implies $\frac{\partial q}{\partial t} = K_2 \frac{\partial C}{\partial t}$. Let $\bar{\omega} = (\omega + (1-\omega)\rho_s K_2)$. Hence, the variational formulation given in (10) simplifies to the following: Find $C \in H^1(\Omega)$ such that $C\Big|_{\Gamma_{\text{in}}} = g$ and :

$$(\bar{\omega}\frac{\partial C}{\partial t}, v) + (\mathbf{u}\cdot\boldsymbol{\nabla} C, v) + (D\boldsymbol{\nabla} C, \boldsymbol{\nabla} v) = (f, v),\ \text{for all}\ \ v \in H^1_{0,\Gamma_{\text{in}}}(\Omega). \tag{86}$$

The semi-discrete in space Finite Element formulation with affine adsorption is as follows: Find $C_h \in X^h$ such that $C_h\Big|_{\Gamma_{\text{in}}} = g_h$ and

$$(\bar{\omega}\frac{\partial C_h}{\partial t}, v_h) + (\mathbf{u}\cdot\boldsymbol{\nabla} C_h, v_h) + (D\boldsymbol{\nabla} C_h, \boldsymbol{\nabla} v_h) = (f, v_h),\ \text{for all}\ \ v_h \in X^h_{0,\Gamma_{\text{in}}}(\Omega). \tag{87}$$

For the analysis, we recall the refactorization of midpoint method [29] for time discretization, and we get the following full discretization: Given $C_h^n \in X^h$, find $C_h^{n+1} \in X^h$ such that $C_h^{n+1}\Big|_{\Gamma_{\text{in}}} = g_h$ satisfying
Step 1: Backward Euler step at the half-integer time step $t_{n+1/2}$

$$(\bar{\omega}\frac{C_h^{n+1/2} - C_h^n}{\Delta t/2}, v_h) + (u\cdot\boldsymbol{\nabla} C_h^{n+1/2}, v_h) + (D\boldsymbol{\nabla} C_h^{n+1/2}, \boldsymbol{\nabla} v_h) = (f^{n+1/2}, v_h),\ \forall v_h \in X^h_{0,\Gamma_{\text{in}}}(\Omega). \tag{88}$$

Step 2: Forward Euler step at t_{n+1}

$$(\bar{\omega}\frac{C_h^{n+1} - C_h^{n+1/2}}{\Delta t/2}, v_h) + (u\cdot\boldsymbol{\nabla} C_h^{n+1/2}, v_h) + (D\boldsymbol{\nabla} C_h^{n+1/2}, \boldsymbol{\nabla} v_h) = (f^{n+1/2}, v_h),\ \forall v_h \in X^h_{0,\Gamma_{\text{in}}}(\Omega). \tag{89}$$

Remark 17. *All the theorems proved for the constant adsorption are true for the affine adsorption where ω is replaced by $\bar{\omega}$.*

2.4.4 Nonlinear, Explicit Isotherm

We consider the nonlinear isotherm with an explicit representation, for example, Langmuir's isotherm [20, 138] is as follows:

$$q(C) = \frac{q_{max} K_{eq} C}{1 + K_{eq} C}, \tag{90}$$

where K_{eq} is Langmuir equilibrium constant, q_{max} is the maximum binding capacity of the porous medium. Recall that for the case of nonlinear isotherm with explicit representation,

$$\frac{\partial q}{\partial t} = \frac{\partial q}{\partial C}\frac{\partial C}{\partial t} = q'(C)\frac{\partial C}{\partial t}.$$

We consider the variational formulation given in (10). The semi-discrete in space formulation is given in (12) and the fully discrete formulation is given in the Section 2.3.2. Next, we show the total mass balance for this isotherm. Unlike previous work, in [153] we dropped the assumption "$C(x,t)$ is nondecreasing in time at every x" and considered non-homogeneous boundary conditions at inflow boundary.

Theorem 18. *Assume that (F1)-(F6) are satisfied and the variational formulation given by* (10) *has a solution* $C \in L^\infty(0,T,L^2(\Omega)) \cap L^2(0,T,H^1(\Omega))$ *with* $f \in L^2(0,T;L^2(\Omega))$. *Let* $\hat{C}$ *be the continuous extension of the Dirichlet data* g *inside the domain* Ω *and satisfies (24). The bounds on* $\|\hat{C}\|^2$ *and* $\|\boldsymbol{\nabla}\hat{C}\|^2$ *are given in* (25) *and* (26) *respectively. Let the antiderivative be* $A(C) = \int_0^C sq'(s)ds$. *Then we get the following bound:*

$$\begin{aligned}
&\|C(t)\|^2 + \frac{4}{\omega}\int_\Omega (1-\omega)\rho_s A(C(t))d\Omega + \frac{\lambda}{\omega}\int_0^t \|\boldsymbol{\nabla} C(r)\|^2\, dr + \frac{2}{\omega}\int_0^t \Big(\int_{\Gamma_{out}} ((C)^2)(\mathbf{u}\cdot\overrightarrow{n})ds\Big)\, dr \\
&\leq \frac{4}{\omega}\int_0^t \frac{\|\mathbf{u}\|_\infty^2}{\lambda}\|\hat{C}\|^2\, dr + \Big(\frac{\lambda}{\omega} + \frac{4\beta_1^2}{\lambda\omega}\Big)\int_0^t \|\boldsymbol{\nabla}\hat{C}\|^2\, dr - \frac{2}{\omega}\int_0^t \Big(\int_{\Gamma_{in}} ((g)^2)(\mathbf{u}\cdot\overrightarrow{n})ds\Big)\, dr \\
&+ 3\|C(0)\|^2 + \frac{8K_{PF}^2}{\lambda\omega}\int_0^t \|f\|^2\, dr + \frac{16(\omega^2 + (1-\omega)^2\rho_s^2 K^2)}{\omega^2}\|\hat{C}\|^2 + \frac{4}{\omega}\int_\Omega (1-\omega)\rho_s A(C(0))d\Omega.
\end{aligned}$$

Proof. Let $\hat{C} \in H^1(\Omega)$ such that $\hat{C}\Big|_{\Gamma_{\text{in}}} = g$. Take $v = C - \hat{C} \in H^1_{0,\Gamma_{\text{in}}}(\Omega)$. Then (10) yields to

$$((\omega + (1-\omega)\rho_s q'(C))\frac{\partial C}{\partial t}, C - \hat{C}) + (\mathbf{u}\cdot\boldsymbol{\nabla} C, C - \hat{C}) + (D\boldsymbol{\nabla} C, \boldsymbol{\nabla}\Big(C - \hat{C}\Big)) = (f, C - \hat{C}).$$

Thus, we get,

$$\begin{aligned} &((\omega + (1-\omega)\rho_s q'(C))\frac{\partial C}{\partial t}, C) + (\mathbf{u}\cdot\boldsymbol{\nabla} C, C) + (D\boldsymbol{\nabla} C, \boldsymbol{\nabla} C) \\ &= ((\omega + (1-\omega)\rho_s q'(C))\frac{\partial C}{\partial t}, \hat{C}) + (\mathbf{u}\cdot\boldsymbol{\nabla} C, \hat{C}) + (D\boldsymbol{\nabla} C, \boldsymbol{\nabla}\hat{C}) + (f, C - \hat{C}). \end{aligned} \tag{91}$$

Let the antiderivative be

$$A(C(t)) = \int_0^C a(s)ds = \int_0^C sq'(s)ds.$$

We rewrite the first term in (91),

$$\begin{aligned} &((\omega + (1-\omega)\rho_s q'(C))\frac{\partial C}{\partial t}, C) = \int_\Omega (\omega + (1-\omega)\rho_s q'(C))C\frac{\partial C}{\partial t}d\Omega \\ &= \frac{\partial}{\partial t}\int_\Omega \left(\frac{\omega}{2}|C|^2 + (1-\omega)\rho_s A(C(t))\right)d\Omega. \end{aligned} \tag{92}$$

Next using the same steps in Theorem (11), we get the following bounds:

$$(\mathbf{u}\cdot\boldsymbol{\nabla} C, C) = \frac{1}{2}\Big(\int_{\Gamma_{\text{in}}}((g)^2)(\mathbf{u}\cdot\overrightarrow{n})ds\Big) + \frac{1}{2}\Big(\int_{\Gamma_{\text{out}}}((C)^2)(\mathbf{u}\cdot\overrightarrow{n})ds\Big). \tag{93}$$

$$(D\boldsymbol{\nabla} C, \boldsymbol{\nabla} C) \geq \lambda\|\boldsymbol{\nabla} C\|^2. \tag{94}$$

$$(\mathbf{u}\cdot\boldsymbol{\nabla} C, \hat{C}) \leq \frac{\lambda}{4}\|\boldsymbol{\nabla} C\|^2 + \frac{\|\mathbf{u}\|^2_\infty}{\lambda}\|\hat{C}\|^2. \tag{95}$$

$$(D\boldsymbol{\nabla} C, \boldsymbol{\nabla}\hat{C}) \leq \frac{\lambda}{4}\|\boldsymbol{\nabla} C\|^2 + \frac{\beta_1^2}{\lambda}\|\boldsymbol{\nabla}\hat{C}\|^2. \tag{96}$$

$$(f, C - \hat{C}) \leq \frac{2K^2_{\text{PF}}}{\lambda}\|f\|^2 + \frac{\lambda}{4}\|\boldsymbol{\nabla} C\|^2 + \frac{\lambda}{4}\|\boldsymbol{\nabla}\hat{C}\|^2. \tag{97}$$

Next,

$$((\omega+(1-\omega)\rho_s q'(C))\frac{\partial C}{\partial t},\hat{C})=\omega\frac{\partial}{\partial t}(C,\hat{C})+(1-\omega)\rho_s\frac{\partial}{\partial t}(q(C),\hat{C}). \tag{98}$$

Combining (92)-(98), we get

$$\begin{aligned}
&\frac{\partial}{\partial t}\int_\Omega\Big(\frac{\omega}{2}|C|^2+(1-\omega)\rho_s A(C(t))\Big)d\Omega+\frac{\lambda}{4}\|\boldsymbol{\nabla}C\|^2+\frac{1}{2}\int_{\Gamma_{\text{out}}}((C)^2)(\mathbf{u}\cdot\overrightarrow{n})ds\leq\frac{\|\mathbf{u}\|_\infty^2}{\lambda}\|\hat{C}\|^2\\
&+\Big(\frac{\lambda}{4}+\frac{\beta_1^2}{\lambda}\Big)\|\boldsymbol{\nabla}\hat{C}\|^2-\frac{1}{2}\Big(\int_{\Gamma_{\text{in}}}((g)^2)(\mathbf{u}\cdot\overrightarrow{n})ds\Big)+\frac{2K_{\text{PF}}^2}{\lambda}\|f\|^2+\omega\frac{\partial}{\partial t}(C,\hat{C})\\
&+(1-\omega)\rho_s\frac{\partial}{\partial t}(q(C),\hat{C}).
\end{aligned}$$

Let $C(0)=C_0$ and $A(C_0)=A_0$. Integrating both sides from 0 to t, we obtain

$$\begin{aligned}
&\int_\Omega\Big(\frac{\omega}{2}|C(t)|^2+(1-\omega)\rho_s A(C(t))\Big)d\Omega+\frac{\lambda}{4}\int_0^t\|\boldsymbol{\nabla}C(r)\|^2dr+\frac{1}{2}\int_0^t\Big(\int_{\Gamma_{\text{out}}}((C)^2)(\mathbf{u}\cdot\overrightarrow{n})ds\Big)\,dr\\
&\leq\int_0^t\frac{\|\mathbf{u}\|_\infty^2}{\lambda}\|\hat{C}\|^2dr+\Big(\frac{\lambda}{4}+\frac{\beta_1^2}{\lambda}\Big)\int_0^t\|\boldsymbol{\nabla}\hat{C}\|^2dr-\frac{1}{2}\int_0^t\Big(\int_{\Gamma_{\text{in}}}((g)^2)(\mathbf{u}\cdot\overrightarrow{n})ds\Big)\,dr\\
&+\frac{2K_{\text{PF}}^2}{\lambda}\int_0^t\|f\|^2dr+\omega(C(t)-C_0,\hat{C})+(1-\omega)\rho_s(q(C(t))-q(C_0),\hat{C})\\
&+\int_\Omega\Big(\frac{\omega}{2}|C_0|^2+(1-\omega)\rho_s A_0\Big)d\Omega.
\end{aligned} \tag{99}$$

Next,

$$\begin{aligned}
\omega(C(t),\hat{C})&\leq\omega\|C(t)\|\|\hat{C}\|\leq\frac{\omega}{8}\|C(t)\|^2+2\omega\|\hat{C}\|^2.\\
-\omega(C_0,\hat{C})&\leq\omega|(C_0,\hat{C})|\leq\omega\|C_0\|\|\hat{C}\|\leq\frac{\omega}{8}\|C_0\|^2+2\omega\|\hat{C}\|^2.
\end{aligned}$$

By using Cauchy-Schwarz and Young's inequalities, we get,

$$(1-\omega)\rho_s(q(C(t))-q(C_0),\hat{C})\leq\frac{4(1-\omega)^2\rho_s^2K^2}{\omega}\|\hat{C}\|^2+\frac{\omega}{8}(\|C(t)\|^2+\|C_0\|^2).$$

Hence after simplification, we prove the claim. □

Remark 19. *In the case of Langmuir's isotherm* (90)*,*

$$A(C(t))=\ln(1+C)+\frac{1}{1+C}+\textit{constant}.$$

Remark 20. *Substituting* (92) *and* (93) *into* (91)*, we get,*

$$\begin{aligned}
&\frac{\partial}{\partial t}\int_\Omega \Big(\frac{\omega}{2}\|C\|^2+(1-\omega)\rho_s A(C(t))\Big)d\Omega+\Big(\int_{\Gamma_{out}}(C^2)(\mathbf{u}\cdot\overrightarrow{n})ds\Big)+(D\boldsymbol{\nabla}C,\boldsymbol{\nabla}C)\\
&=-\Big(\int_{\Gamma_{in}}(g^2)(\mathbf{u}\cdot\overrightarrow{n})ds\Big).+(f,C-\hat{C})((\omega+(1-\omega)\rho_s q'(C))\frac{\partial C}{\partial t},\hat{C})++(\mathbf{u}\cdot\boldsymbol{\nabla}C,\hat{C})\\
&+(D\boldsymbol{\nabla}C,\boldsymbol{\nabla}\hat{C})
\end{aligned}\tag{100}$$

If $f=0$ *and* $\hat{C}=0$ *in* (100)*, we get the balance of mass as follows*

$$\begin{aligned}
&\frac{\partial}{\partial t}\int_\Omega \Big(\frac{\omega}{2}\|C\|^2+(1-\omega)\rho_s A(C(t))\Big)d\Omega+\Big(\int_{\Gamma_{out}}(C^2)(\mathbf{u}\cdot\overrightarrow{n})ds\Big)+(D\boldsymbol{\nabla}C,\boldsymbol{\nabla}C)\\
&=-\Big(\int_{\Gamma_{in}}(g^2)(\mathbf{u}\cdot\overrightarrow{n})ds\Big).
\end{aligned}\tag{101}$$

Recall that $\mathbf{u}\cdot\overrightarrow{n}>0$ *on* Γ_{out} *and* $\mathbf{u}\cdot\overrightarrow{n}<0$ *on* Γ_{in}*.*

Next, we do another approach to the stability analysis where we will use the following notation: $Q(\alpha)=\int_0^\alpha q(s)ds$,

$$\begin{aligned}
\mathcal{E}(t)=&\frac{3\omega}{4}\int_0^t\|D^{1/2}\boldsymbol{\nabla}C-\frac{8}{3}D^{-1/2}\hat{C}\mathbf{u}\|^2\,dr+\frac{3\omega}{4}\int_0^t\|D^{1/2}\boldsymbol{\nabla}C-\frac{8\rho_s q(\hat{C})(1-\omega)}{3\omega}D^{-1/2}\mathbf{u}\|^2\,dr\\
&+\frac{3\omega}{4}\int_0^t\|D^{1/2}\boldsymbol{\nabla}C-\frac{8}{3}D^{-1/2}\boldsymbol{\nabla}\hat{C}\|^2\,dr+\frac{3\omega}{4}\int_0^t\|D^{1/2}\boldsymbol{\nabla}C-\frac{8(1-\omega)\rho_s q'(\hat{C})}{3\omega}D^{-1/2}\boldsymbol{\nabla}\hat{C}\|^2\,dr\\
&+\|\omega C(t)+(1-\omega)\rho_s q(C(t))-2(\omega\hat{C}+(1-\omega)\rho_s q(\hat{C}))\|^2,
\end{aligned}$$

and

$$\begin{aligned}
\mathcal{B}(t)=&\frac{3\omega}{4}\int_0^t\|\frac{8}{3}D^{-1/2}\hat{C}\mathbf{u}\|^2\,dr+\frac{3\omega}{4}\int_0^t\|\frac{8\rho_s q(\hat{C})(1-\omega)}{3\omega}D^{-1/2}\mathbf{u}\|^2\,dr+\frac{3\omega}{4}\int_0^t\|\frac{8}{3}D^{-1/2}\boldsymbol{\nabla}\hat{C}\|^2\,dr\\
&+\frac{3\omega}{4}\int_0^t\|\frac{8(1-\omega)\rho_s q'(\hat{C})}{3\omega}D^{-1/2}\boldsymbol{\nabla}\hat{C}\|^2\,dr\\
&+\|\omega C(0)+(1-\omega)\rho_s q(C(0))-2(\omega\hat{C}+(1-\omega)\rho_s q(\hat{C}))\|^2.
\end{aligned}$$

Theorem 21. *Assume that (F1)-(F6) are satisfied. The variational formulation given by (10) has a solution $C \in L^\infty(0,T,L^2(\Omega)) \cap L^2(0,T,H^1(\Omega))$ with $f \in L^2(0,T;L^2(\Omega))$. Let $\hat{C}$ be the continuous extension of the Dirichlet data g inside the domain Ω and solution of (24). We get the following result:*

$$
\begin{aligned}
&\|\omega C(t) + (1-\omega)\rho_s q(C(t))\|^2 + \omega \int_0^t \|D^{1/2}\boldsymbol{\nabla} C(r)\|^2\, dr \\
&+ 4(1-\omega)\rho_s \int_0^t \left(\int_\Omega q'(C(r))(D^{1/2}\boldsymbol{\nabla} C(r))^2\, d\Omega \right) dr + + \mathcal{E}(t) \\
&+ 4(1-\omega)\rho_s \int_0^t \Big(\int_{\Gamma_{out}} Q(C(r))(\mathbf{u}\cdot\overrightarrow{n})ds \Big)\, dr + 2\omega \int_0^t \Big(\int_{\Gamma_{out}} C^2(\mathbf{u}\cdot\overrightarrow{n})ds \Big)\, dr \\
&= \|\omega C_0 + (1-\omega)\rho_s q(C_0)\|^2 + 4\int_0^t (f, \omega C + (1-\omega)\rho_s q(C) - (\omega\hat{C} + (1-\omega)\rho_s q(\hat{C})))\, dr \\
&+ \mathcal{B}(t) - 2\omega \int_0^t \Big(\int_{\Gamma_{in}} g^2(\mathbf{u}\cdot\overrightarrow{n})ds \Big)\, dr - 4(1-\omega)\rho_s \int_0^t \Big(\int_{\Gamma_{in}} Q(g)(\mathbf{u}\cdot\overrightarrow{n})ds \Big)\, dr.
\end{aligned}
$$

Proof. Let $\hat{C} \in H^1(\Omega)$ such that $\hat{C}\Big|_{\Gamma_{\text{in}}} = g$. Take $v = (\omega C + (1-\omega)\rho_s q(C)) - (\omega\hat{C} + (1-\omega)\rho_s q(\hat{C})) \in H^1_{0,\Gamma_{\text{in}}}(\Omega)$. Then (9) yields to

$$
\begin{aligned}
&\left(\frac{\partial}{\partial t}(\omega C + (1-\omega)\rho_s q(C)), \omega C + (1-\omega)\rho_s q(C) - (\omega\hat{C} + (1-\omega)\rho_s q(\hat{C})) \right) \\
&+ \left(\mathbf{u}\cdot\boldsymbol{\nabla} C, \omega C + (1-\omega)\rho_s q(C) - (\omega\hat{C} + (1-\omega)\rho_s q(\hat{C})) \right) \\
&+ \left(D\boldsymbol{\nabla} C, \boldsymbol{\nabla}\Big(\omega C + (1-\omega)\rho_s q(C) - (\omega\hat{C} + (1-\omega)\rho_s q(\hat{C}))\Big) \right) \\
&= (f, \omega C + (1-\omega)\rho_s q(C) - (\omega\hat{C} + (1-\omega)\rho_s q(\hat{C}))).
\end{aligned}
$$

Thus, we get,

$$
\begin{aligned}
&\left(\frac{\partial}{\partial t}(\omega C + (1-\omega)\rho_s q(C)), \omega C + (1-\omega)\rho_s q(C) \right) \\
&+ \big(\mathbf{u}\cdot\boldsymbol{\nabla} C, \omega C + (1-\omega)\rho_s q(C)\big) + \omega(D\boldsymbol{\nabla} C, \boldsymbol{\nabla} C) + (1-\omega)\rho_s(q'(C)D\boldsymbol{\nabla} C, \boldsymbol{\nabla} C) \\
&= (f, \omega C + (1-\omega)\rho_s q(C) - (\omega\hat{C} + (1-\omega)\rho_s q(\hat{C}))) \qquad (102) \\
&+ \left(\frac{\partial}{\partial t}(\omega C + (1-\omega)\rho_s q(C)), (\omega\hat{C} + (1-\omega)\rho_s q(\hat{C})) \right) \\
&+ \big(\mathbf{u}\cdot\boldsymbol{\nabla} C, (\omega\hat{C} + (1-\omega)\rho_s q(\hat{C}))\big) + \omega(D\boldsymbol{\nabla} C, \boldsymbol{\nabla}\hat{C}) + (1-\omega)\rho_s(q'(\hat{C})D\boldsymbol{\nabla} C, \boldsymbol{\nabla}\hat{C}).
\end{aligned}
$$

We rewrite the first term in (102),

$$\left(\frac{\partial}{\partial t}(\omega C+(1-\omega)\rho_s q(C)), \omega C+(1-\omega)\rho_s q(C)\right)=\frac{1}{2}\frac{\partial}{\partial t}\|\omega C+(1-\omega)\rho_s q(C)\|^2. \quad (103)$$

By using the divergence theorem and boundary conditions, we get

$$\begin{aligned}&(\mathbf{u}\cdot\boldsymbol{\nabla}C, \omega C+(1-\omega)\rho_s q(C))\\ &=\frac{\omega}{2}\int_{\Gamma_{\text{in}}} g^2(\mathbf{u}\cdot\overrightarrow{n})ds+\frac{\omega}{2}\int_{\Gamma_{\text{out}}} C^2(\mathbf{u}\cdot\overrightarrow{n})ds+(1-\omega)\rho_s\int_{\Gamma_{\text{in}}} Q(g)(\mathbf{u}\cdot\overrightarrow{n})ds\\ &+(1-\omega)\rho_s\int_{\Gamma_{\text{out}}} Q(C)(\mathbf{u}\cdot\overrightarrow{n})ds.\end{aligned} \quad (104)$$

Next,

$$\begin{aligned}&\omega(D\boldsymbol{\nabla}C,\boldsymbol{\nabla}C)+(1-\omega)\rho_s(q'(C)D\boldsymbol{\nabla}C,\boldsymbol{\nabla}C)\\ &=\omega(D^{1/2}\boldsymbol{\nabla}C, D^{1/2}\boldsymbol{\nabla}C)+(1-\omega)\rho_s(q'(C)D^{1/2}\boldsymbol{\nabla}C, D^{1/2}\boldsymbol{\nabla}C)\\ &=\omega\|D^{1/2}\boldsymbol{\nabla}C\|^2+(1-\omega)\rho_s\int_\Omega q'(C)(D^{1/2}\boldsymbol{\nabla}C)^2\,d\Omega.\end{aligned}$$

Next, in the right-hand side terms, we get the following equalities,

$$\begin{aligned}(\mathbf{u}\cdot\boldsymbol{\nabla}C,\omega\hat{C}) &=(\boldsymbol{\nabla}C\cdot\mathbf{u},\omega\hat{C})\\ &=(\boldsymbol{\nabla}C,\omega\hat{C}\mathbf{u})\\ &=\omega(D^{1/2}\boldsymbol{\nabla}C, D^{-1/2}\hat{C}\mathbf{u})\\ &=\frac{3\omega}{8}(D^{1/2}\boldsymbol{\nabla}C,\frac{8}{3}D^{-1/2}\hat{C}\mathbf{u})\\ &=\frac{3\omega}{16}\|D^{1/2}\boldsymbol{\nabla}C\|^2+\frac{3\omega}{16}\|\frac{8}{3}D^{-1/2}\hat{C}\mathbf{u}\|^2-\frac{3\omega}{16}\|D^{1/2}\boldsymbol{\nabla}C-\frac{8}{3}D^{-1/2}\hat{C}\mathbf{u}\|^2,\end{aligned} \quad (105)$$

and

$$
\begin{aligned}
&(\mathbf{u}\cdot\boldsymbol{\nabla}C,(1-\omega)\rho_s q(\hat{C}))\\
&=(\boldsymbol{\nabla}C\cdot\mathbf{u},(1-\omega)\rho_s q(\hat{C}))\\
&=(\boldsymbol{\nabla}C,(1-\omega)\rho_s q(\hat{C})\mathbf{u})\\
&=\omega(D^{1/2}\boldsymbol{\nabla}C,\frac{\rho_s q(\hat{C})(1-\omega)}{\omega}D^{-1/2}\mathbf{u})\\
&=\frac{3\omega}{8}(D^{1/2}\boldsymbol{\nabla}C,\frac{8\rho_s q(\hat{C})(1-\omega)}{3\omega}D^{-1/2}\mathbf{u})\\
&=\frac{3\omega}{16}\|D^{1/2}\boldsymbol{\nabla}C\|^2+\frac{3\omega}{16}\|\frac{8\rho_s q(\hat{C})(1-\omega)}{3\omega}D^{-1/2}\mathbf{u}\|^2\\
&-\frac{3\omega}{16}\|D^{1/2}\boldsymbol{\nabla}C-\frac{8\rho_s q(\hat{C})(1-\omega)}{3\omega}D^{-1/2}\mathbf{u}\|^2.
\end{aligned}
\tag{106}
$$

Furthermore,

$$
\begin{aligned}
&\omega(D\boldsymbol{\nabla}C,\boldsymbol{\nabla}\hat{C})\\
&=\omega(D^{1/2}\boldsymbol{\nabla}C,D^{-1/2}\boldsymbol{\nabla}\hat{C})\\
&=\frac{3\omega}{8}(D^{1/2}\boldsymbol{\nabla}C,\frac{8}{3}D^{-1/2}\boldsymbol{\nabla}\hat{C})\\
&=\frac{3\omega}{16}\|D^{1/2}\boldsymbol{\nabla}C\|^2+\frac{3\omega}{16}\|\frac{8}{3}D^{-1/2}\boldsymbol{\nabla}\hat{C}\|^2-\frac{3\omega}{16}\|D^{1/2}\boldsymbol{\nabla}C-\frac{8}{3}D^{-1/2}\boldsymbol{\nabla}\hat{C}\|^2,
\end{aligned}
\tag{107}
$$

and

$$
\begin{aligned}
&(D\boldsymbol{\nabla}C,(1-\omega)\rho_s q'(\hat{C})\boldsymbol{\nabla}\hat{C})\\
&=\omega(D^{1/2}\boldsymbol{\nabla}C,\frac{(1-\omega)\rho_s q'(\hat{C})}{\omega}D^{-1/2}\boldsymbol{\nabla}\hat{C})\\
&=\frac{3\omega}{8}(D^{1/2}\boldsymbol{\nabla}C,\frac{8(1-\omega)\rho_s q'(\hat{C})}{3\omega}D^{-1/2}\boldsymbol{\nabla}\hat{C})\\
&=\frac{3\omega}{16}\|D^{1/2}\boldsymbol{\nabla}C\|^2+\frac{3\omega}{16}\|\frac{8(1-\omega)\rho_s q'(\hat{C})}{3\omega}D^{-1/2}\boldsymbol{\nabla}\hat{C}\|^2\\
&-\frac{3\omega}{16}\|D^{1/2}\boldsymbol{\nabla}C-\frac{8(1-\omega)\rho_s q'(\hat{C})}{3\omega}D^{-1/2}\boldsymbol{\nabla}\hat{C}\|^2.
\end{aligned}
\tag{108}
$$

We also have,

$$\begin{aligned}
&\left(\frac{\partial}{\partial t}(\omega C+(1-\omega)\rho_s q(C)), \omega\hat{C}+(1-\omega)\rho_s q(\hat{C})\right)\\
&=\frac{\partial}{\partial t}(\omega C+(1-\omega)\rho_s q(C), \omega\hat{C}+(1-\omega)\rho_s q(\hat{C}))\\
&-(\omega C+(1-\omega)\rho_s q(C), \frac{\partial(\omega\hat{C}+(1-\omega)\rho_s q(\hat{C}))}{\partial t})\\
&=\frac{\partial}{\partial t}(\omega C+(1-\omega)\rho_s q(C), \omega\hat{C}+(1-\omega)\rho_s q(\hat{C})).
\end{aligned} \tag{109}$$

Combining (112)-(118), we get

$$\begin{aligned}
&\frac{1}{2}\frac{\partial}{\partial t}\|\omega C+(1-\omega)\rho_s q(C)\|^2+\frac{\omega}{4}\|D^{1/2}\boldsymbol{\nabla} C\|^2+\frac{\omega}{2}\int_{\Gamma_{\text{out}}} C^2(\mathbf{u}\cdot\overrightarrow{n})ds\\
&+(1-\omega)\rho_s\int_{\Gamma_{\text{out}}} Q(C)(\mathbf{u}\cdot\overrightarrow{n})ds+(1-\omega)\rho_s\int_{\Omega} q'(C)(D^{1/2}\boldsymbol{\nabla} C)^2\ d\Omega\\
&+\frac{3\omega}{16}\|D^{1/2}\boldsymbol{\nabla} C-\frac{8}{3}D^{-1/2}\hat{C}\mathbf{u}\|^2+\frac{3\omega}{16}\|D^{1/2}\boldsymbol{\nabla} C-\frac{8\rho_s q(\hat{C})(1-\omega)}{3\omega}D^{-1/2}\mathbf{u}\|^2\\
&+\frac{3\omega}{16}\|D^{1/2}\boldsymbol{\nabla} C-\frac{8}{3}D^{-1/2}\boldsymbol{\nabla}\hat{C}\|^2\\
&+\frac{3\omega}{16}\|D^{1/2}\boldsymbol{\nabla} C-\frac{8(1-\omega)\rho_s q'(\hat{C})}{3\omega}D^{-1/2}\boldsymbol{\nabla}\hat{C}\|^2\\
&=(f,\omega C+(1-\omega)\rho_s q(C)-(\omega\hat{C}+(1-\omega)\rho_s q(\hat{C})))+\frac{3\omega}{16}\|\frac{8}{3}D^{-1/2}\hat{C}\mathbf{u}\|^2\\
&+\frac{3\omega}{16}\|\frac{8\rho_s q(\hat{C})(1-\omega)}{3\omega}D^{-1/2}\mathbf{u}\|^2+\frac{3\omega}{16}\|\frac{8}{3}D^{-1/2}\boldsymbol{\nabla}\hat{C}\|^2+\frac{3\omega}{16}\|\frac{8(1-\omega)\rho_s q'(\hat{C})}{3\omega}D^{-1/2}\boldsymbol{\nabla}\hat{C}\|^2\\
&-\frac{\omega}{2}\int_{\Gamma_{\text{in}}} g^2(\mathbf{u}\cdot\overrightarrow{n})ds-(1-\omega)\rho_s\int_{\Gamma_{\text{in}}} Q(g)(\mathbf{u}\cdot\overrightarrow{n})ds\\
&+\frac{\partial}{\partial t}(\omega C+(1-\omega)\rho_s q(C), \omega\hat{C}+(1-\omega)\rho_s q(\hat{C})).
\end{aligned}$$

Next, integrating both sides from 0 to t, we obtain

$$
\begin{aligned}
&\frac{1}{2}\|\omega C(t)+(1-\omega)\rho_s q(C(t))\|^2+\frac{\omega}{4}\int_0^t\|\boldsymbol{\nabla} C(r)\|^2\,dr+\frac{\omega}{2}\int_0^t\Big(\int_{\Gamma_{\text{out}}}C^2(\mathbf{u}\cdot\overrightarrow{n})ds\Big)\,dr\\
&+(1-\omega)\rho_s\int_0^t\Big(\int_{\Gamma_{\text{out}}}Q(C(r))(\mathbf{u}\cdot\overrightarrow{n})ds\Big)\,dr\\
&+(1-\omega)\rho_s\int_0^t\left(\int_\Omega q'(C(r))(D^{1/2}\boldsymbol{\nabla} C(r))^2\,d\Omega\right)dr\\
&+\frac{3\omega}{16}\int_0^t\|D^{1/2}\boldsymbol{\nabla} C(r)-\frac{8}{3}D^{-1/2}\hat{C}\mathbf{u}\|^2\,dr+\frac{3\omega}{16}\int_0^t\|D^{1/2}\boldsymbol{\nabla} C(r)-\frac{8\rho_s q(\hat{C})(1-\omega)}{3\omega}D^{-1/2}\mathbf{u}\|^2\,dr\\
&+\frac{3\omega}{16}\int_0^t\|D^{1/2}\boldsymbol{\nabla} C(r)-\frac{8}{3}D^{-1/2}\boldsymbol{\nabla}\hat{C}\|^2\,dr\\
&+\frac{3\omega}{16}\int_0^t\|D^{1/2}\boldsymbol{\nabla} C(r)-\frac{8(1-\omega)\rho_s q'(\hat{C})}{3\omega}D^{-1/2}\boldsymbol{\nabla}\hat{C}\|^2\,dr\\
&=\int_0^t(f,\omega C+(1-\omega)\rho_s q(C)-(\omega\hat{C}+(1-\omega)\rho_s q(\hat{C})))\,dr+\frac{3\omega}{16}\int_0^t\|\frac{8}{3}D^{-1/2}\hat{C}\mathbf{u}\|^2\,dr\\
&+\frac{3\omega}{16}\int_0^t\|\frac{8\rho_s q(\hat{C})(1-\omega)}{3\omega}D^{-1/2}\mathbf{u}\|^2\,dr+\frac{3\omega}{16}\int_0^t\|\frac{8}{3}D^{-1/2}\boldsymbol{\nabla}\hat{C}\|^2\,dr\\
&+\frac{3\omega}{16}\int_0^t\|\frac{8(1-\omega)\rho_s q'(\hat{C})}{3\omega}D^{-1/2}\boldsymbol{\nabla}\hat{C}\|^2\,dr+\frac{1}{2}\|\omega C(0)+(1-\omega)\rho_s q(C(0))\|^2\\
&-\frac{\omega}{2}\int_0^t\Big(\int_{\Gamma_{\text{in}}}g^2(\mathbf{u}\cdot\overrightarrow{n})ds\Big)\,dr-(1-\omega)\rho_s\int_0^t\Big(\int_{\Gamma_{\text{in}}}Q(g)(\mathbf{u}\cdot\overrightarrow{n})ds\Big)\,dr\\
&+(\omega C(t)+(1-\omega)\rho_s q(C(t)),\omega\hat{C}+(1-\omega)\rho_s q(\hat{C}))\\
&-(\omega C(0)+(1-\omega)\rho_s q(C(0)),\omega\hat{C}+(1-\omega)\rho_s q(\hat{C})).
\end{aligned}
\tag{110}
$$

Here,

$$
\begin{aligned}
&(\omega C(t)+(1-\omega)\rho_s q(C(t)),\omega\hat{C}+(1-\omega)\rho_s q(\hat{C}))\\
&=\frac{1}{2}(\omega C(t)+(1-\omega)\rho_s q(C(t)),2(\omega\hat{C}+(1-\omega)\rho_s q(\hat{C})))\\
&=\frac{1}{4}\|(\omega C(t)+(1-\omega)\rho_s q(C(t))\|^2+\frac{1}{4}\|2(\omega\hat{C}+(1-\omega)\rho_s q(\hat{C}))\|^2\\
&-\frac{1}{4}\|\omega C(t)+(1-\omega)\rho_s q(C(t))-2(\omega\hat{C}+(1-\omega)\rho_s q(\hat{C}))\|^2,
\end{aligned}
$$

and

$$
\begin{aligned}
&- (\omega C(0) + (1-\omega)\rho_s q(C(0)), \omega\hat{C} + (1-\omega)\rho_s q(\hat{C})) \\
&= -\frac{1}{2}(\omega C(0) + (1-\omega)\rho_s q(C(0)), 2(\omega\hat{C} + (1-\omega)\rho_s q(\hat{C}))) \\
&= -\frac{1}{4}\|(\omega C(0) + (1-\omega)\rho_s q(C(0))\|^2 - \frac{1}{4}\|2(\omega\hat{C} + (1-\omega)\rho_s q(\hat{C}))\|^2 \\
&+ \frac{1}{4}\|\omega C(0) + (1-\omega)\rho_s q(C(0)) - 2(\omega\hat{C} + (1-\omega)\rho_s q(\hat{C}))\|^2.
\end{aligned}
$$

Hence (119) becomes

$$
\begin{aligned}
&\frac{1}{4}\|\omega C(t) + (1-\omega)\rho_s q(C(t))\|^2 + \frac{\omega}{4}\int_0^t \|\boldsymbol{\nabla} C(r)\|^2 \, dr + \frac{\omega}{2}\int_0^t \Big(\int_{\Gamma_{\text{out}}} C^2(\mathbf{u}\cdot\overrightarrow{n})ds\Big)\, dr + \frac{1}{4}\mathcal{E}(t) \\
&+ (1-\omega)\rho_s \int_0^t \Big(\int_{\Gamma_{\text{out}}} Q(C(r))(\mathbf{u}\cdot\overrightarrow{n})ds\Big)\, dr \\
&+ (1-\omega)\rho_s \int_0^t \left(\int_\Omega q'(C(r))(D^{1/2}\boldsymbol{\nabla} C(r))^2 \, d\Omega\right) dr \\
&= \frac{1}{4}\|\omega C(0) + (1-\omega)\rho_s q(C(0))\|^2 + \int_0^t (f, \omega C + (1-\omega)\rho_s q(C) - (\omega\hat{C} + (1-\omega)\rho_s q(\hat{C})))\, dr \\
&- \frac{\omega}{2}\int_0^t \Big(\int_{\Gamma_{\text{in}}} g^2(\mathbf{u}\cdot\overrightarrow{n})ds\Big)\, dr - (1-\omega)\rho_s \int_0^t \Big(\int_{\Gamma_{\text{in}}} Q(g)(\mathbf{u}\cdot\overrightarrow{n})ds\Big)\, dr + \frac{1}{4}\mathcal{B}(t).
\end{aligned}
$$

Simplifying the above inequality and setting $C(0) = C_0$, we get the claimed result. □

Next, for stability in the case of semi-discrete in space, we will use the following notation: $Q_h(\alpha) = \int_0^\alpha \mathcal{P}(q(s))ds$,

$$
\begin{aligned}
\mathcal{E}_h(t) &= \frac{3\omega}{4}\int_0^t \|D^{1/2}\boldsymbol{\nabla} C_h - \frac{8}{3}D^{-1/2}\hat{C}_h\mathbf{u}\|^2 \, dr \\
&+ \frac{3\omega}{4}\int_0^t \|D^{1/2}\boldsymbol{\nabla} C_h - \frac{8(1-\omega)\rho_s\mathcal{P}^1(q'(\hat{C}_h))}{3\omega}D^{-1/2}\boldsymbol{\nabla}\hat{C}_h\|^2 \, dr \\
&+ \|\omega C_h(t) + (1-\omega)\rho_s\mathcal{P}(q(C_h(t))) - 2(\omega\hat{C}_h + (1-\omega)\rho_s\mathcal{P}(q(\hat{C}_h)))\|^2 \\
&+ \frac{3\omega}{4}\int_0^t \|D^{1/2}\boldsymbol{\nabla} C_h - \frac{8}{3}D^{-1/2}\boldsymbol{\nabla}\hat{C}_h\|^2 \, dr \\
&+ \frac{3\omega}{4}\int_0^t \|D^{1/2}\boldsymbol{\nabla} C_h - \frac{8\rho_s\mathcal{P}(q(\hat{C}_h))(1-\omega)}{3\omega}D^{-1/2}\mathbf{u}\|^2 \, dr.
\end{aligned}
$$

and

$$\begin{aligned}\mathcal{B}_h(t) &= \frac{3\omega}{4}\int_0^t \|\frac{8}{3}D^{-1/2}\hat{C}\mathbf{u}\|^2\ dr + \frac{3\omega}{4}\int_0^t \|\frac{8\rho_s\mathcal{P}(q(\hat{C}_h))(1-\omega)}{3\omega}D^{-1/2}\mathbf{u}\|^2\ dr\\ &+ \frac{3\omega}{4}\int_0^t \|\frac{8(1-\omega)\rho_s\mathcal{P}^1(q'(\hat{C}))}{3\omega}D^{-1/2}\boldsymbol{\nabla}\hat{C}_h\|^2\ dr + \frac{3\omega}{4}\int_0^t \|\frac{8}{3}D^{-1/2}\boldsymbol{\nabla}\hat{C}_h\|^2\ dr\\ &+ \|\omega C(0) + (1-\omega)\rho_s\mathcal{P}(q(C(0))) - 2(\omega\hat{C}_h + (1-\omega)\rho_s\mathcal{P}(q(\hat{C}_h)))\|^2.\end{aligned}$$

Theorem 22. *Assume that (F1)-(F6) are satisfied. The variational formulation given by (10) has a solution $C \in L^\infty(0,T,L^2(\Omega)) \cap L^2(0,T,H^1(\Omega))$ with $f \in L^2(0,T;L^2(\Omega))$. Let $\hat{C}$ be the continuous extension of the Dirichlet data g inside the domain Ω and solution of (24). We assume $Q(\alpha) = \int_0^\alpha \mathcal{P}(q(s))ds \geq 0$ and $\mathcal{P}^1(q'(C_h)) \geq 0$. We get the following result:*

$$\begin{aligned}&\|\omega C_h(t) + (1-\omega)\rho_s\mathcal{P}(q(C_h(t)))\|^2 + \omega\int_0^t \|D^{1/2}\boldsymbol{\nabla}C_h(r)\|^2\,dr\\ &+ 4(1-\omega)\rho_s\int_0^t\left(\int_\Omega \mathcal{P}^1(q'(C_h(r)))(D^{1/2}\boldsymbol{\nabla}C_h(r))^2\,d\Omega\right)dr\\ &+ 4(1-\omega)\rho_s\int_0^t\Big(\int_{\Gamma_{out}} Q_h(C_h(r))(\mathbf{u}\cdot\overrightarrow{n})ds\Big)\,dr + 2\omega\int_0^t\Big(\int_{\Gamma_{out}} C_h^2(\mathbf{u}\cdot\overrightarrow{n})ds\Big)\,dr + \mathcal{E}_h(t)\\ &= \|\omega C_h(0) + (1-\omega)\rho_s\mathcal{P}(q(C_h(0)))\|^2 + \mathcal{B}_h(t)\\ &+ 4\int_0^t (f, \omega C_h + (1-\omega)\rho_s\mathcal{P}(q(C_h)) - (\omega\hat{C}_h + (1-\omega)\rho_s\mathcal{P}(q(\hat{C}_h))))\,dr\\ &- 2\omega\int_0^t\Big(\int_{\Gamma_{in}} g_h^2(\mathbf{u}\cdot\overrightarrow{n})ds\Big)\,dr - 4(1-\omega)\rho_s\int_0^t\Big(\int_{\Gamma_{in}} Q_h(g_h)(\mathbf{u}\cdot\overrightarrow{n})ds\Big)\,dr.\end{aligned}$$

Proof. Let $\hat{C}_h \in X^h(\Omega)$ such that $\hat{C}_h\Big|_{\Gamma_{\text{in}}} = g_h$. Let $\mathcal{P}$ and $\mathcal{P}^1$ be the orthogonal projections with respect to the L^2 inner product and H^1 inner product, respectively. Take $v_h = (\omega C_h + (1-\omega)\rho_s\mathcal{P}(q(C_h))) - (\omega\hat{C}_h + (1-\omega)\rho_s\mathcal{P}(q(\hat{C}_h))) \in X^h_{0,\Gamma_{\text{in}}}(\Omega)$. Then (11) yields to

$$\begin{aligned}&\left(\frac{\partial}{\partial t}(\omega C_h + (1-\omega)\rho_s q(C_h)), (\omega C_h + (1-\omega)\rho_s\mathcal{P}(q(C_h))) - (\omega\hat{C}_h + (1-\omega)\rho_s\mathcal{P}(q(\hat{C}_h)))\right)\\ &+ \left(\mathbf{u}\cdot\boldsymbol{\nabla}C_h, (\omega C_h + (1-\omega)\rho_s\mathcal{P}(q(C_h))) - (\omega\hat{C}_h + (1-\omega)\rho_s\mathcal{P}(q(\hat{C}_h)))\right)\\ &+ \left(D\boldsymbol{\nabla}C_h, \boldsymbol{\nabla}\Big((\omega C_h + (1-\omega)\rho_s\mathcal{P}(q(C_h))) - (\omega\hat{C}_h + (1-\omega)\rho_s\mathcal{P}(q(\hat{C}_h)))\Big)\right)\end{aligned}$$

$$= (f, (\omega C_h + (1-\omega)\rho_s \mathcal{P}(q(C_h))) - (\omega \hat{C}_h + (1-\omega)\rho_s \mathcal{P}(q(\hat{C}_h)))).$$

Thus, we get,

$$\begin{aligned}
&\left(\frac{\partial}{\partial t}(\omega C_h + (1-\omega)\rho_s q(C_h)), \omega C_h + (1-\omega)\rho_s \mathcal{P}(q(C_h))\right) \\
&+ \left(\mathbf{u}\cdot\boldsymbol{\nabla} C_h, \omega C_h + (1-\omega)\rho_s \mathcal{P}(q(C_h))\right) + \omega(D\boldsymbol{\nabla} C_h, \boldsymbol{\nabla} C_h) \\
&+ (1-\omega)\rho_s (D\boldsymbol{\nabla} C_h, \mathcal{P}^1(q'(C_h)\boldsymbol{\nabla} C_h)) \\
&= (f, \omega C_h + (1-\omega)\rho_s \mathcal{P}(q(C_h)) - (\omega \hat{C}_h + (1-\omega)\rho_s \mathcal{P}(q(\hat{C}_h)))) \\
&+ \left(\frac{\partial}{\partial t}(\omega C_h + (1-\omega)\rho_s q(C_h)), (\omega \hat{C}_h + (1-\omega)\rho_s \mathcal{P}(q(\hat{C}_h)))\right) \\
&+ \left(\mathbf{u}\cdot\boldsymbol{\nabla} C, (\omega \hat{C}_h + (1-\omega)\rho_s \mathcal{P}(q(\hat{C}_h)))\right) + \omega(D\boldsymbol{\nabla} C_h, \boldsymbol{\nabla} \hat{C}_h) \\
&+ (1-\omega)\rho_s (D\boldsymbol{\nabla} C_h, \mathcal{P}^1(q'(\hat{C}_h)\boldsymbol{\nabla} \hat{C}_h)).
\end{aligned} \tag{111}$$

We rewrite the first term in (102),

$$\left(\frac{\partial}{\partial t}(\omega C_h + (1-\omega)\rho_s q(C_h)), \omega C_h + (1-\omega)\rho_s \mathcal{P}(q(C_h))\right) = \frac{1}{2}\frac{\partial}{\partial t}\|\omega C_h + (1-\omega)\rho_s \mathcal{P}(q(C_h))\|^2. \tag{112}$$

By using the divergence theorem and boundary conditions, we get

$$\begin{aligned}
&(\mathbf{u}\cdot\boldsymbol{\nabla} C_h, \omega C_h + (1-\omega)\rho_s \mathcal{P}(q(C_h))) \\
&= \frac{\omega}{2}\int_{\Gamma_{\text{in}}} g_h^2 (\mathbf{u}\cdot\overrightarrow{n}) ds + \frac{\omega}{2}\int_{\Gamma_{\text{out}}} C_h^2 (\mathbf{u}\cdot\overrightarrow{n}) ds \\
&+ (1-\omega)\rho_s \int_{\Gamma_{\text{in}}} Q_h(g_h)(\mathbf{u}\cdot\overrightarrow{n}) ds + (1-\omega)\rho_s \int_{\Gamma_{\text{out}}} Q_h(C_h)(\mathbf{u}\cdot\overrightarrow{n}) ds.
\end{aligned} \tag{113}$$

Next,

$$\begin{aligned}
&\omega(D\boldsymbol{\nabla} C_h, \boldsymbol{\nabla} C_h) + (1-\omega)\rho_s \mathcal{P}^1(q'(C_h) D\boldsymbol{\nabla} C_h, \boldsymbol{\nabla} C_h) \\
&= \omega(D^{1/2}\boldsymbol{\nabla} C_h, D^{1/2}\boldsymbol{\nabla} C_h) + (1-\omega)\rho_s (\mathcal{P}^1(q'(C_h)) D^{1/2}\boldsymbol{\nabla} C_h, D^{1/2}\boldsymbol{\nabla} C_h) \\
&= \omega\|D^{1/2}\boldsymbol{\nabla} C_h\|^2 + (1-\omega)\rho_s \int_\Omega \mathcal{P}^1(q'(C_h))(D^{1/2}\boldsymbol{\nabla} C_h)^2 \, d\Omega.
\end{aligned}$$

Next, in the right-hand side terms, we get the following equalities,

$$
\begin{aligned}
&(\mathbf{u}\cdot\boldsymbol{\nabla}C_h,\omega\hat{C}_h)\\
&=(\boldsymbol{\nabla}C_h\cdot\mathbf{u},\omega\hat{C}_h)\\
&=(\boldsymbol{\nabla}C_h,\omega\hat{C}_h\mathbf{u})\\
&=\omega(D^{1/2}\boldsymbol{\nabla}C_h,D^{-1/2}\hat{C}_h\mathbf{u})\\
&=\frac{3\omega}{8}(D^{1/2}\boldsymbol{\nabla}C_h,\frac{8}{3}D^{-1/2}\hat{C}_h\mathbf{u})\\
&=\frac{3\omega}{16}\|D^{1/2}\boldsymbol{\nabla}C_h\|^2+\frac{3\omega}{16}\|\frac{8}{3}D^{-1/2}\hat{C}_h\mathbf{u}\|^2-\frac{3\omega}{16}\|D^{1/2}\boldsymbol{\nabla}C_h-\frac{8}{3}D^{-1/2}\hat{C}_h\mathbf{u}\|^2,
\end{aligned}
\tag{114}
$$

and

$$
\begin{aligned}
&(\mathbf{u}\cdot\boldsymbol{\nabla}C_h,(1-\omega)\rho_s\mathcal{P}(q(\hat{C}_h)))\\
&=(\boldsymbol{\nabla}C_h\cdot\mathbf{u},(1-\omega)\rho_s\mathcal{P}(q(\hat{C}_h)))\\
&=(\boldsymbol{\nabla}C_h,(1-\omega)\rho_s\mathcal{P}(q(\hat{C}_h))\mathbf{u})\\
&=\omega(D^{1/2}\boldsymbol{\nabla}C_h,\frac{\rho_s\mathcal{P}(q(\hat{C}_h))(1-\omega)}{\omega}D^{-1/2}\mathbf{u})\\
&=\frac{3\omega}{8}(D^{1/2}\boldsymbol{\nabla}C_h,\frac{8\rho_s\mathcal{P}(q(\hat{C}_h))(1-\omega)}{3\omega}D^{-1/2}\mathbf{u})\\
&=\frac{3\omega}{16}\|D^{1/2}\boldsymbol{\nabla}C_h\|^2+\frac{3\omega}{16}\|\frac{8\rho_s\mathcal{P}(q(\hat{C}_h))(1-\omega)}{3\omega}D^{-1/2}\mathbf{u}\|^2\\
&-\frac{3\omega}{16}\|D^{1/2}\boldsymbol{\nabla}C_h-\frac{8\rho_s\mathcal{P}(q(\hat{C}_h))(1-\omega)}{3\omega}D^{-1/2}\mathbf{u}\|^2.
\end{aligned}
\tag{115}
$$

Next,

$$
\begin{aligned}
&\omega(D\boldsymbol{\nabla}C_h,\boldsymbol{\nabla}\hat{C}_h)\\
&=\omega(D^{1/2}\boldsymbol{\nabla}C_h,D^{-1/2}\boldsymbol{\nabla}\hat{C}_h)\\
&=\frac{3\omega}{8}(D^{1/2}\boldsymbol{\nabla}C_h,\frac{8}{3}D^{-1/2}\boldsymbol{\nabla}\hat{C}_h)\\
&=\frac{3\omega}{16}\|D^{1/2}\boldsymbol{\nabla}C_h\|^2+\frac{3\omega}{16}\|\frac{8}{3}D^{-1/2}\boldsymbol{\nabla}\hat{C}_h\|^2-\frac{3\omega}{16}\|D^{1/2}\boldsymbol{\nabla}C_h-\frac{8}{3}D^{-1/2}\boldsymbol{\nabla}\hat{C}_h\|^2,
\end{aligned}
\tag{116}
$$

and

$$
\begin{aligned}
&(D\boldsymbol{\nabla} C_h, (1-\omega)\rho_s \mathcal{P}^1(q'(\hat{C}_h))\boldsymbol{\nabla}\hat{C}_h) \\
&= \omega(D^{1/2}\boldsymbol{\nabla} C_h, \frac{(1-\omega)\rho_s \mathcal{P}^1(q'(\hat{C}_h))}{\omega} D^{-1/2}\boldsymbol{\nabla}\hat{C}_h) \\
&= \frac{3\omega}{8}(D^{1/2}\boldsymbol{\nabla} C_h, \frac{8(1-\omega)\rho_s \mathcal{P}^1(q'(\hat{C}_h))}{3\omega} D^{-1/2}\boldsymbol{\nabla}\hat{C}_h) \\
&= \frac{3\omega}{16}\|D^{1/2}\boldsymbol{\nabla} C_h\|^2 + \frac{3\omega}{16}\|\frac{8(1-\omega)\rho_s \mathcal{P}^1(q'(\hat{C}_h))}{3\omega} D^{-1/2}\boldsymbol{\nabla}\hat{C}_h\|^2 \\
&- \frac{3\omega}{16}\|D^{1/2}\boldsymbol{\nabla} C_h - \frac{8(1-\omega)\rho_s \mathcal{P}^1(q'(\hat{C}_h))}{3\omega} D^{-1/2}\boldsymbol{\nabla}\hat{C}_h\|^2.
\end{aligned} \tag{117}
$$

Next,

$$
\begin{aligned}
&\left(\frac{\partial}{\partial t}(\omega C_h + (1-\omega)\rho_s q(C_h)), \omega\hat{C}_h + (1-\omega)\rho_s \mathcal{P}(q(\hat{C}_h))\right) \\
&= \frac{\partial}{\partial t}(\omega C_h + (1-\omega)\rho_s q(C_h), \omega\hat{C}_h + (1-\omega)\rho_s \mathcal{P}(q(\hat{C}_h))) \\
&- (\omega C_h + (1-\omega)\rho_s q(C_h), \frac{\partial(\omega\hat{C}_h + (1-\omega)\rho_s \mathcal{P}(q(\hat{C}_h)))}{\partial t}) \\
&= \frac{\partial}{\partial t}(\omega C_h + (1-\omega)\rho_s q(C_h), \omega\hat{C}_h + (1-\omega)\rho_s \mathcal{P}(q(\hat{C}_h))).
\end{aligned} \tag{118}
$$

Combining (112)-(118), we get

$$
\begin{aligned}
&\frac{1}{2}\frac{\partial}{\partial t}\|\omega C_h + (1-\omega)\rho_s \mathcal{P}(q(C_h))\|^2 + \frac{\omega}{4}\|D^{1/2}\boldsymbol{\nabla} C_h\|^2 + \frac{\omega}{2}\int_{\Gamma_{\text{out}}} C_h^2(\mathbf{u}\cdot\overrightarrow{n})ds \\
&+ (1-\omega)\rho_s \int_{\Gamma_{\text{out}}} Q_h(C_h)(\mathbf{u}\cdot\overrightarrow{n})ds + (1-\omega)\rho_s \int_\Omega \mathcal{P}^1(q'(C_h))(D^{1/2}\boldsymbol{\nabla} C_h)^2 \, d\Omega \\
&+ \frac{3\omega}{16}\|D^{1/2}\boldsymbol{\nabla} C_h - \frac{8}{3}D^{-1/2}\hat{C}_h\mathbf{u}\|^2 \\
&+ \frac{3\omega}{16}\|D^{1/2}\boldsymbol{\nabla} C_h - \frac{8\rho_s \mathcal{P}(q(\hat{C}))(1-\omega)}{3\omega} D^{-1/2}\mathbf{u}\|^2 + \frac{3\omega}{16}\|D^{1/2}\boldsymbol{\nabla} C_h - \frac{8}{3}D^{-1/2}\boldsymbol{\nabla}\hat{C}_h\|^2 \\
&+ \frac{3\omega}{16}\|D^{1/2}\boldsymbol{\nabla} C_h - \frac{8(1-\omega)\rho_s \mathcal{P}^1(q'(\hat{C}_h))}{3\omega} D^{-1/2}\boldsymbol{\nabla}\hat{C}_h\|^2 \\
&= (f, \omega C_h + (1-\omega)\rho_s \mathcal{P}(q(C_h)) - (\omega\hat{C}_h + (1-\omega)\rho_s \mathcal{P}(q(\hat{C}_h)))) + \frac{3\omega}{16}\|\frac{8}{3}D^{-1/2}\hat{C}_h\mathbf{u}\|^2 \\
&+ \frac{3\omega}{16}\|\frac{8\rho_s \mathcal{P}(q(\hat{C}))(1-\omega)}{3\omega} D^{-1/2}\mathbf{u}\|^2 + \frac{3\omega}{16}\|\frac{8}{3}D^{-1/2}\boldsymbol{\nabla}\hat{C}_h\|^2 \\
&+ \frac{3\omega}{16}\|\frac{8(1-\omega)\rho_s \mathcal{P}^1(q'(\hat{C}_h))}{3\omega} D^{-1/2}\boldsymbol{\nabla}\hat{C}_h\|^2 \\
&- \frac{\omega}{2}\int_{\Gamma_{\text{in}}} g_h^2(\mathbf{u}\cdot\overrightarrow{n})ds - (1-\omega)\rho_s \int_{\Gamma_{\text{in}}} Q_h(g_h)(\mathbf{u}\cdot\overrightarrow{n})ds
\end{aligned}
$$

$$+\frac{\partial}{\partial t}(\omega C_h+(1-\omega)\rho_s q(C_h),\omega\hat{C}_h+(1-\omega)\rho_s\mathcal{P}(q(\hat{C}_h))).$$

Next, integrating both sides from 0 to t, we obtain

$$\begin{aligned}
&\frac{1}{2}\|\omega C_h(t)+(1-\omega)\rho_s\mathcal{P}(q(C(t)))\|^2+\frac{\omega}{4}\int_0^t\|\boldsymbol{\nabla}C_h(r)\|^2\,dr+\frac{\omega}{2}\int_0^t\Big(\int_{\Gamma_{\text{out}}}C_h^2(\mathbf{u}\cdot\overrightarrow{n})ds\Big)\,dr\\
&+(1-\omega)\rho_s\int_0^t\Big(\int_{\Gamma_{\text{out}}}Q_h(C_h(r))(\mathbf{u}\cdot\overrightarrow{n})ds\Big)\,dr\\
&+(1-\omega)\rho_s\int_0^t\left(\int_\Omega\mathcal{P}^1(q'(C_h(r)))(D^{1/2}\boldsymbol{\nabla}C_h(r))^2\,d\Omega\right)dr\\
&+\frac{3\omega}{16}\int_0^t\|D^{1/2}\boldsymbol{\nabla}C_h(r)-\frac{8}{3}D^{-1/2}\hat{C}_h\mathbf{u}\|^2\,dr\\
&+\frac{3\omega}{16}\int_0^t\|D^{1/2}\boldsymbol{\nabla}C_h(r)-\frac{8\rho_s\mathcal{P}(q(\hat{C}_h))(1-\omega)}{3\omega}D^{-1/2}\mathbf{u}\|^2\,dr\\
&+\frac{3\omega}{16}\int_0^t\|D^{1/2}\boldsymbol{\nabla}C_h(r)-\frac{8}{3}D^{-1/2}\boldsymbol{\nabla}\hat{C}_h\|^2\,dr\\
&+\frac{3\omega}{16}\int_0^t\|D^{1/2}\boldsymbol{\nabla}C_h(r)-\frac{8(1-\omega)\rho_s\mathcal{P}^1(q'(\hat{C}_h))}{3\omega}D^{-1/2}\boldsymbol{\nabla}\hat{C}_h\|^2\,dr\\
&=\int_0^t(f,\omega C_h+(1-\omega)\rho_s\mathcal{P}(q(C_h))-(\omega\hat{C}_h+(1-\omega)\rho_s\mathcal{P}(q(\hat{C}_h))))\,dr\\
&+\frac{3\omega}{16}\int_0^t\|\frac{8\rho_s\mathcal{P}(q(\hat{C}_h))(1-\omega)}{3\omega}D^{-1/2}\mathbf{u}\|^2\,dr+\frac{3\omega}{16}\int_0^t\|\frac{8}{3}D^{-1/2}\boldsymbol{\nabla}\hat{C}_h\|^2\,dr\\
&+\frac{3\omega}{16}\int_0^t\|\frac{8(1-\omega)\rho_s\mathcal{P}^1(q'(\hat{C}_h))}{3\omega}D^{-1/2}\boldsymbol{\nabla}\hat{C}_h\|^2\,dr+\frac{1}{2}\|\omega C_h(0)+(1-\omega)\rho_s\mathcal{P}(q(C_h(0)))\|^2\\
&-\frac{\omega}{2}\int_0^t\Big(\int_{\Gamma_{\text{in}}}g_h^2(\mathbf{u}\cdot\overrightarrow{n})ds\Big)\,dr-(1-\omega)\rho_s\int_0^t\Big(\int_{\Gamma_{\text{in}}}Q_h(g_h)(\mathbf{u}\cdot\overrightarrow{n})ds\Big)\,dr\\
&+(\omega C_h(t)+(1-\omega)\rho_s q(C_h(t)),\omega\hat{C}_h+(1-\omega)\rho_s\mathcal{P}(q(\hat{C}_h)))\\
&-(\omega C_h(0)+(1-\omega)\rho_s q(C_h(0)),\omega\hat{C}_h+(1-\omega)\rho_s\mathcal{P}(q(\hat{C}_h)))+\frac{3\omega}{16}\int_0^t\|\frac{8}{3}D^{-1/2}\hat{C}_h\mathbf{u}\|^2\,dr.
\end{aligned}\tag{119}$$

Here,

$$\begin{aligned}
&(\omega C_h(t)+(1-\omega)\rho_s q(C_h(t)),\omega\hat{C}_h+(1-\omega)\rho_s\mathcal{P}(q(\hat{C}_h)))\\
&=\frac{1}{2}(\omega C_h(t)+(1-\omega)\rho_s q(C_h(t)),2(\omega\hat{C}_h+(1-\omega)\rho_s\mathcal{P}(q(\hat{C}_h))))
\end{aligned}$$

$$= \frac{1}{4}\|(\omega C_h(t) + (1-\omega)\rho_s q(C_h(t))\|^2 + \frac{1}{4}\|2(\omega\hat{C_h} + (1-\omega)\rho_s\mathcal{P}(q(\hat{C_h})))\|^2$$
$$- \frac{1}{4}\|\omega C_h(t) + (1-\omega)\rho_s q(C_h(t)) - 2(\omega\hat{C_h} + (1-\omega)\rho_s\mathcal{P}(q(\hat{C_h})))\|^2,$$

and

$$- (\omega C_h(0) + (1-\omega)\rho_s q(C_h 0)), \omega\hat{C_h} + (1-\omega)\rho_s\mathcal{P}(q(\hat{C_h})))$$
$$= -\frac{1}{2}(\omega C_h(0) + (1-\omega)\rho_s q(C_h(0)), 2(\omega\hat{C_h} + (1-\omega)\rho_s\mathcal{P}(q(\hat{C_h}))))$$
$$= -\frac{1}{4}\|(\omega C_h(0) + (1-\omega)\rho_s q(C_h(0))\|^2 - \frac{1}{4}\|2(\omega\hat{C_h} + (1-\omega)\rho_s\mathcal{P}(q(\hat{C_h})))\|^2$$
$$+ \frac{1}{4}\|\omega C_h(0) + (1-\omega)\rho_s q(C_h(0)) - 2(\omega\hat{C_h} + (1-\omega)\rho_s\mathcal{P}(q(\hat{C_h})))\|^2.$$

Hence (119) becomes

$$\frac{1}{4}\|\omega C_h(t) + (1-\omega)\rho_s\mathcal{P}(q(C_h(t)))\|^2 + \frac{\omega}{4}\int_0^t \|\boldsymbol{\nabla} C_h(r)\|^2\, dr + \frac{\omega}{2}\int_0^t \Big(\int_{\Gamma_{\text{out}}} C_h^2(\mathbf{u}\cdot\overrightarrow{n})ds\Big)\, dr$$
$$+ (1-\omega)\rho_s\int_0^t \Big(\int_{\Gamma_{\text{out}}} Q_h(C_h(r))(\mathbf{u}\cdot\overrightarrow{n})ds\Big)\, dr$$
$$+ (1-\omega)\rho_s\int_0^t \left(\int_\Omega \mathcal{P}^1(q'(C_h(r)))(D^{1/2}\boldsymbol{\nabla} C_h(r))^2\, d\Omega\right) dr + \frac{1}{4}\mathcal{E}_h(t)$$
$$= \frac{1}{4}\|\omega C_h(0) + (1-\omega)\rho_s\mathcal{P}(q(C_h(0)))\|^2 + \frac{1}{4}\mathcal{B}_h(t)$$
$$+ \int_0^t (f, \omega C_h + (1-\omega)\rho_s\mathcal{P}(q(C_h)) - (\omega\hat{C_h} + (1-\omega)\rho_s\mathcal{P}(q(\hat{C_h})))\, dr$$
$$- \frac{\omega}{2}\int_0^t \Big(\int_{\Gamma_{\text{in}}} g_h^2(\mathbf{u}\cdot\overrightarrow{n})ds\Big)\, dr - (1-\omega)\rho_s\int_0^t \Big(\int_{\Gamma_{\text{in}}} Q(g_h)(\mathbf{u}\cdot\overrightarrow{n})ds\Big)\, dr$$

Simplifying the above inequality, we get the claimed result. □

2.4.5 Semi-discrete in space error Estimate

Next theorem gives a *priori* error estimate for the case of nonlinear adsorption and semi-discrete in space where we will use the notation:

$$K_2 := \exp\left(T+\frac{3T\|u\|_\infty^2\|D^{-1/2}\|_\infty^2}{\omega}\right)\left(4\|D^{1/2}\|_\infty^2+3\omega+4\|u\|_\infty^2\|D^{-1/2}\|_\infty^2+\frac{3(1-\omega)^2\rho_s^2K^2}{\omega}\right)K_1^2.$$

Theorem 23. *Assume that (F1)-(F7) are satisfied and the time-integrated method variational formulation with nonlinear adsorption given by* (22) *has an exact solution* $C \in H^1(0,T,H^{k+1}(\Omega))$ *and* C_h *solves the semi-discrete in space method Finite Element formulation with nonlinear adsorption given by* (23). *Then for* $1 \le r \le k+1$ *and for each* $T>0$, *there exists a constant* $K_2>0$ *independent of* h *such that*

$$\omega\int_0^T \|C-C_h\|^2dt + \|\int_0^T D^{1/2}\boldsymbol{\nabla}(C-C_h)dt'\|^2 \le K_2h^{2r-2}\int_0^T\|C\|_r^2dt. \tag{120}$$

Proof. The weak formulation of continuous and semidiscrete problems are given by (22) and (23), respectively, where $C\Big|_{\Gamma_{\text{in}}} = g$ and $C_h\Big|_{\Gamma_{\text{in}}} = g_h$ are required.
First we let $v = v_h \in X^h_{0,\Gamma_{\text{in}}} \subset H^1_{0,\Gamma_{\text{in}}}(\Omega)$ in (22) and then subtract (23) from (22) to get

$$\begin{aligned}&(\omega(C-C_h),v_h)+((1-\omega)\rho_s(q(C)-q(C_h)),v_h)+(\int_0^t u\cdot\boldsymbol{\nabla}(C-C_h)dt',v_h)\\&-(\boldsymbol{\nabla}\cdot\int_0^t D\boldsymbol{\nabla}(C-C_h)dt',v_h)=0,\quad \forall v_h\in X^h_{0,\Gamma_{in}}(\Omega).\end{aligned} \tag{121}$$

We choose $v_h = C_h - \hat{C}_h = C_h - C + C - \hat{C}_h \in X^h_{0,\Gamma_{\text{in}}}$. Then, we get

$$\begin{aligned}&(\omega(C-C_h),C-C_h)+((1-\omega)\rho_s(q(C)-q(C_h)),C-C_h)\\&+(\int_0^t u\cdot\boldsymbol{\nabla}(C-C_h)dt',C-C_h)+(\int_0^t D\boldsymbol{\nabla}(C-C_h)dt',\boldsymbol{\nabla}(C-C_h))\\&=(\omega(C-C_h),C-\hat{C}_h)+((1-\omega)\rho_s(q(C)-q(C_h)),C-\hat{C}_h)\\&+(\int_0^t u\cdot\boldsymbol{\nabla}(C-C_h)dt',C-\hat{C}_h)+(\int_0^t D\boldsymbol{\nabla}(C-C_h)dt',\boldsymbol{\nabla}\Big(C-\hat{C}_h\Big)).\end{aligned} \tag{122}$$

Here,

$$(\omega(C-C_h),C-C_h)=\omega\|C-C_h\|^2,$$

$$
\begin{aligned}
((1-\omega)\rho_s(q(C)-q(C_h)),C-C_h) &= (1-\omega)\rho_s\int_\Omega(\int_0^1(q'(\theta C+(1-\theta)C_h))d\theta)(C-C_h)^2d\Omega,\\
(\int_0^t D\boldsymbol{\nabla}(C-C_h)dt',\boldsymbol{\nabla}(C-C_h)) &= (\int_0^t D^{1/2}\boldsymbol{\nabla}(C-C_h)dt',\frac{d}{dt}\int_0^t D^{1/2}\boldsymbol{\nabla}(C-C_h)dt')\\
&= \frac{1}{2}\frac{d}{dt}\|\int_0^t D^{1/2}\boldsymbol{\nabla}(C-C_h)dt'\|^2.
\end{aligned}
$$

Next, we get the following bounds for the right-hand side terms,

$$
\begin{aligned}
(\omega(C-C_h),C-\hat{C}_h) &\le \frac{\varepsilon_1}{2}\omega\|C-C_h\|^2+\frac{\omega}{2\varepsilon_1}\|C-\hat{C}_h\|^2,\\
(\int_0^t D\boldsymbol{\nabla}(C-C_h)dt',\boldsymbol{\nabla}\Big(C-\hat{C}_h\Big)) &= (\int_0^t D^{1/2}\boldsymbol{\nabla}(C-C_h)dt',D^{1/2}\boldsymbol{\nabla}\Big(C-\hat{C}_h\Big))\\
&\le \|\int_0^t D^{1/2}\boldsymbol{\nabla}(C-C_h)dt'\|\|D^{1/2}\|_\infty\|\boldsymbol{\nabla}\Big(C-\hat{C}_h\Big)\|\\
&\le \frac{\varepsilon_2}{2}\|\int_0^t D^{1/2}\boldsymbol{\nabla}(C-C_h)dt'\|^2+\frac{\|D^{1/2}\|_\infty^2}{2\varepsilon_2}\|\boldsymbol{\nabla}\Big(C-\hat{C}_h\Big)\|^2,\\
(\int_0^t u\cdot\boldsymbol{\nabla}(C-C_h)dt',C-\hat{C}_h) &= (\int_0^t D^{1/2}\boldsymbol{\nabla}(C-C_h)dt',D^{-1/2}u(C-\hat{C}_h))\\
&\le \frac{\varepsilon_3}{2}\|\int_0^t D^{1/2}\boldsymbol{\nabla}(C-C_h)dt'\|^2+\frac{\|u\|_\infty^2\|D^{-1/2}\|_\infty^2}{2\varepsilon_3}\|C-\hat{C}_h\|^2,\\
\Big|(\int_0^t u\cdot\boldsymbol{\nabla}(C-C_h)dt',C-C_h)\Big| &= \Big|(\int_0^t D^{1/2}\boldsymbol{\nabla}(C-C_h)dt',D^{-1/2}u(C-C_h))\Big|\\
&\le \frac{\varepsilon_4}{2}\|\int_0^t D^{1/2}\boldsymbol{\nabla}(C-C_h)dt'\|^2+\frac{\|u\|_\infty^2\|D^{-1/2}\|_\infty^2}{2\varepsilon_4}\|C-C_h\|^2,\\
((1-\omega)\rho_s(q(C)-q(C_h)),C-\hat{C}_h) &\le (1-\omega)\rho_s\|q(C)-q(C_h)\|\|C-\hat{C}_h\|\\
&\le (1-\omega)\rho_sK\|C-C_h\|\|C-\hat{C}_h\|\\
&\le \frac{\varepsilon_5}{2}\|C-C_h\|^2+\frac{(1-\omega)^2\rho_s^2K^2}{2\varepsilon_5}\|C-\hat{C}_h\|^2.
\end{aligned}
$$

Let $\varepsilon_1=\frac{1}{3}$, $\varepsilon_2=\varepsilon_3=\frac{1}{4}$, $\varepsilon_4=\frac{3\|u\|_\infty^2\|D^{-1/2}\|_\infty^2}{\omega}$, $\varepsilon_5=\frac{\omega}{3}$. Combining all terms, (122) yields

$$
\begin{aligned}
&\frac{\omega}{2}\|C-C_h\|^2+(1-\omega)\rho_s\int_\Omega(\int_0^1(q'(\theta C+(1-\theta)C_h))d\theta)(C-C_h)^2d\Omega\\
&+\frac{1}{2}\frac{d}{dt}\|\int_0^t D^{1/2}\boldsymbol{\nabla}(C-C_h)dt'\|^2\\
&\le (\frac{1}{2}+\frac{3\|u\|_\infty^2\|D^{-1/2}\|_\infty^2}{2\omega})\|\int_0^t D^{1/2}\boldsymbol{\nabla}(C-C_h)dt'\|^2+2\|D^{1/2}\|_\infty^2\|\boldsymbol{\nabla}\Big(C-\hat{C}_h\Big)\|^2\\
&+(\frac{3\omega}{2}+2\|u\|_\infty^2\|D^{-1/2}\|_\infty^2+\frac{3(1-\omega)^2\rho_s^2K^2}{2\omega})\|C-\hat{C}_h\|^2.
\end{aligned}
\tag{123}
$$

After integrating (123) in time from $t = 0$ to $t = T$, we obtain,

$$\begin{aligned}
&\omega \int_0^T \|C - C_h\|^2 dt + 2(1-\omega)\rho_s \int_0^T \int_\Omega (\int_0^1 (q'(\theta C + (1-\theta)C_h))d\theta)(C - C_h)^2 d\Omega dt \\
&+ \| \int_0^T D^{1/2} \boldsymbol{\nabla}(C - C_h) dt' \|^2 \\
&\leq \big(1 + \frac{3\|u\|_\infty^2 \|D^{-1/2}\|_\infty^2}{\omega}\big) \int_0^T \| \int_0^t D^{1/2} \boldsymbol{\nabla}(C - C_h) dt' \|^2 dt \\
&+ 4\|D^{1/2}\|_\infty^2 \int_0^T \|\boldsymbol{\nabla}\Big(C - \hat{C}_h\Big)\|^2 dt \\
&+ \big(3\omega + 4\|u\|_\infty^2 \|D^{-1/2}\|_\infty^2 + \frac{3(1-\omega)^2 \rho_s^2 K^2}{\omega}\big) \int_0^T \|C - \hat{C}_h\|^2 dt.
\end{aligned} \tag{124}$$

Then continuous Gronwall's inequality applied to (124) gives us

$$\begin{aligned}
&\omega \int_0^T \|C - C_h\|^2 dt + 2(1-\omega)\rho_s \int_0^T \int_\Omega (\int_0^1 (q'(\theta C + (1-\theta)C_h))d\theta)(C - C_h)^2 d\Omega dt \\
&+ \| \int_0^T D^{1/2} \boldsymbol{\nabla}(C - C_h) dt' \|^2 \\
&\leq \exp\Big(T + \frac{3T\|u\|_\infty^2 \|D^{-1/2}\|_\infty^2}{\omega}\Big) \\
&\times \Big(4\|D^{1/2}\|_\infty^2 + +3\omega + 4\|u\|_\infty^2 \|D^{-1/2}\|_\infty^2 + \frac{3(1-\omega)^2 \rho_s^2 K^2}{\omega}\Big) \int_0^T \|C - \hat{C}_h\|_1^2 dt\Big).
\end{aligned} \tag{125}$$

Here $2(1-\omega)\rho_s \int_0^T \int_\Omega (\int_0^1 (q'(\theta C + (1-\theta)C_h))d\theta)(C - C_h)^2 d\Omega dt$ is a positive term. Hence we can rewrite (125),

$$\begin{aligned}
&\omega \int_0^T \|C - C_h\|^2 dt + \| \int_0^T D^{1/2} \boldsymbol{\nabla}(C - C_h) dt' \|^2 \\
&\leq \exp\Big(T + \frac{3T\|u\|_\infty^2 \|D^{-1/2}\|_\infty^2}{\omega}\Big) \\
&\times \Big(4\|D^{1/2}\|_\infty^2 + +3\omega + 4\|u\|_\infty^2 \|D^{-1/2}\|_\infty^2 + \frac{3(1-\omega)^2 \rho_s^2 K^2}{\omega}\Big) \int_0^T \|C - \hat{C}_h\|_1^2 dt\Big).
\end{aligned} \tag{126}$$

Since $\hat{C}_h$ is arbitrary, we have the following inequality,

$$\begin{aligned}
&\omega \int_0^T \|C - C_h\|^2 dt + \| \int_0^T D^{1/2} \boldsymbol{\nabla} (C - C_h) dt' \|^2 \\
&\leq \exp\left(T + \frac{3T\|u\|_\infty^2 \|D^{-1/2}\|_\infty^2}{\omega} \right) \\
&\times \left(4\|D^{1/2}\|_\infty^2 + +3\omega + 4\|u\|_\infty^2 \|D^{-1/2}\|_\infty^2 + \frac{3(1-\omega)^2 \rho_s^2 K^2}{\omega} \right) \int_0^T \inf_{\substack{\hat{C_h} \in X^h \\ \hat{C_h}|_{\Gamma_{\text{in}}} = g_h}} \|C - \hat{C}_h\|_1^2 dt \Big).
\end{aligned} \tag{127}$$

Let g_h be the interpolant of g in $X^h_{\Gamma_{\text{in}}}$. Then by using Lemma 4, for $1 \leq r \leq k+1$ we get,

$$\begin{aligned}
&\omega \int_0^T \|C - C_h\|^2 dt + \| \int_0^T D^{1/2} \boldsymbol{\nabla} (C - C_h) dt' \|^2 \\
&\leq \exp\left(T + \frac{3T\|u\|_\infty^2 \|D^{-1/2}\|_\infty^2}{\omega} \right) \\
&\times \left(4\|D^{1/2}\|_\infty^2 + +3\omega + 4\|u\|_\infty^2 \|D^{-1/2}\|_\infty^2 + \frac{3(1-\omega)^2 \rho_s^2 K^2}{\omega} \right) K_1^2 h^{2r-2} \int_0^T \|C\|_r^2 dt \Big).
\end{aligned} \tag{128}$$

Let

$$K_2 = \exp\left(T + \frac{3T\|u\|_\infty^2 \|D^{-1/2}\|_\infty^2}{\omega} \right) \left(4\|D^{1/2}\|_\infty^2 + 3\omega + 4\|u\|_\infty^2 \|D^{-1/2}\|_\infty^2 + \frac{3(1-\omega)^2 \rho_s^2 K^2}{\omega} \right) K_1^2.$$

Thus (128) implies

$$\omega \int_0^T \|C - C_h\|^2 dt + \| \int_0^T D^{1/2} \boldsymbol{\nabla} (C - C_h) dt' \|^2 \leq K_2 h^{2r-2} \int_0^T \|C\|_r^2 dt.$$

Consequently, we prove the claim (120). □

2.4.5.1 Existence of solution of approximate system

In this subsection, we prove the solvability of the approximating system (15) for the nonlinear, explicit isotherm (90). We first define all necessary operators and prove associated lemmas to do that. Then, we use the Leray-Schauder fixed-point Thoerem [100, Theorem 16] to prove the existence of the solution of the approximate system. By adding and subtracting $\hat{C}_h$, we can rewrite the fully discretized form Equation (15) as follows:
Given $C_h^n - \hat{C}_h \in X_{0,\Gamma_{\text{in}}}^h$, find $C_h^{n+1} - \hat{C}_h \in X_{0,\Gamma_{\text{in}}}^h$ such that

$$\begin{aligned}
&(D\boldsymbol{\nabla}\Big(C_h^{n+1} - \hat{C}_h\Big), \boldsymbol{\nabla} v_h) \\
&= -2\Bigg(\Big(\omega + (1-\omega)\rho_s q'(\frac{C_h^{n+1} - \hat{C}_h + C_h^n + \hat{C}_h}{2})\Big)\frac{(C_h^{n+1} - \hat{C}_h) - (C_h^n - \hat{C}_h)}{\Delta t}, v_h\Bigg) \\
&+ 2(f^{n+1/2}, v_h) - (\mathbf{u}\cdot\boldsymbol{\nabla}\Big(C_h^{n+1} - \hat{C}_h + C_h^n + \hat{C}_h\Big), v_h) \\
&+ (\boldsymbol{\nabla}\cdot(D\boldsymbol{\nabla}\Big(C_h^n + \hat{C}_h\Big)), v_h),\ \forall v \in X_{0,\Gamma_{\text{in}}}^h.
\end{aligned} \tag{129}$$

For simplicity, we drop h throughout this section. By the Lax-Milgram Theorem [25, corollary 5.8],

$$\forall\ l \in X^*,\ \text{there exists an unique solution } \Psi \in X_{0,\Gamma_{\text{in}}} \text{ of } (D\boldsymbol{\nabla}\Psi, \boldsymbol{\nabla} v) = (l, v),\ \forall v \in X_{0,\Gamma_{\text{in}}}.$$

Then, the operator $T : X^* \to X_{0,\Gamma_{\text{in}}}$ defined by $T(l) = \Psi$ is a well-defined linear and continuous operator. Indeed, T is a bounded operator:

$$\|T\| = \sup_{l\in X^*}\frac{\|T(l)\|_{X_{0,\Gamma_{\text{in}}}}}{\|l\|_*} = \sup_{l\in X^*}\frac{\|\boldsymbol{\nabla}\Psi\|}{\|l\|_*} \le \frac{1}{\lambda},\ \text{since } \|\boldsymbol{\nabla}\Psi\| \le \frac{1}{\lambda}\|l\|_*.$$

Next, we define the nonlinear operator $N : X_{0,\Gamma_{\text{in}}} \to X^*$ by

$$\begin{aligned}
&N(\psi) \\
&= 2f^{n+\frac{1}{2}} - 2\big(\omega + (1-\omega)\rho_s q'(\frac{\psi + C^n + \hat{C}}{2})\big)\frac{\psi - (C^n - \hat{C})}{\Delta t} - \mathbf{u}\cdot\boldsymbol{\nabla}\Big(\psi + C^n + \hat{C}\Big) \\
&+ \boldsymbol{\nabla}\cdot(D\boldsymbol{\nabla}\Big(C^n + \hat{C}\Big))
\end{aligned}$$

and the operator $\mathcal{F} : X_{0,\Gamma_{\text{in}}} \to X_{0,\Gamma_{\text{in}}}$ by $\mathcal{F} = T(N(\psi))$.

Lemma 24. *$N : X_{0,\Gamma_{in}} \to X^*$ is a bounded operator, i.e.,*

$$\|N(\psi)\|_* \leq \|\mathbf{u}\|_\infty \|\boldsymbol{\nabla}\psi\| + \frac{2\omega + 2(1-\omega)\kappa_2}{\Delta t}\|\psi\| + \frac{2\omega + 2(1-\omega)\kappa_2}{\Delta t}\|C^n - \hat{C}\| + \|2f^{n+\frac{1}{2}}\|_*$$
$$+ \|\boldsymbol{\nabla}\cdot(D\boldsymbol{\nabla}\Big(C^n + \hat{C}\Big))\|_* + \|\mathbf{u}\|_\infty \|\boldsymbol{\nabla}\Big(C^n + \hat{C}\Big)\|.$$

Proof. Using the definition, triangle inequality, and Cauchy-Schwarz inequality, we get,

$$\begin{aligned}
&\|N(\psi)\|_* \\
&= \|2f^{n+\frac{1}{2}} - 2\big(\omega + (1-\omega)\rho_s q'(\frac{\psi + C^n + \hat{C}}{2})\big)\frac{\psi - (C^n - \hat{C})}{\Delta t} - \mathbf{u}\cdot\boldsymbol{\nabla}\Big(\psi + C^n + \hat{C}\Big) \\
&+ \boldsymbol{\nabla}\cdot(D\boldsymbol{\nabla}\Big(C^n + \hat{C}\Big))\|_*, \\
&\leq \|2f^{n+\frac{1}{2}}\|_* + \|\boldsymbol{\nabla}\cdot(D\boldsymbol{\nabla}\Big(C^n + \hat{C}\Big))\|_* + \|2\omega\frac{\psi - (C^n - \hat{C})}{\Delta t}\|_* \\
&+ \|2\big((1-\omega)\rho_s q'(\frac{\psi + C^n + \hat{C}}{2})\big)\frac{\psi - (C^n - \hat{C})}{\Delta t}\|_* + \|\mathbf{u}\cdot\boldsymbol{\nabla}\Big(\psi + C^n + \hat{C}\Big)\|_*.
\end{aligned}$$

Notice,

$$\|\mathbf{u}\cdot\boldsymbol{\nabla}\Big(\psi + C^n + \hat{C}\Big)\|_* \leq \|\mathbf{u}\|_\infty\|\boldsymbol{\nabla}\psi\| + \|\mathbf{u}\|_\infty\|\boldsymbol{\nabla}\Big(C^n + \hat{C}\Big)\|.$$

$$\|2\omega\frac{\psi - (C^n - \hat{C})}{\Delta t}\|_* \leq \frac{2\omega}{\Delta t}\|\psi\| + \frac{2\omega}{\Delta t}\|C^n - \hat{C}\|.$$

Next,

$$\|2(1-\omega)\rho_s q'(\frac{\psi + C^n + \hat{C}}{2})\frac{\psi - (C^n - \hat{C})}{\Delta t}\|_* \leq \frac{2(1-\omega)\kappa_2}{\Delta t}\|\psi\| + \frac{2(1-\omega)\kappa_2}{\Delta t}\|C^n - \hat{C}\|.$$

Combining all concludes the argument. □

Lemma 25. *$N : X_{0,\Gamma_{in}} \to X^*$ is a continuous operator.*

Proof. It suffices to show that $\|N(\psi_1) - N(\psi_2)\|_* \to 0$ if $\|\boldsymbol{\nabla}(\psi_1 - \psi_2)\|_* \to 0$. Here,

$$\begin{aligned}
&\|N(\psi_1) - N(\psi_2)\|_* \\
&\leq \frac{2\omega}{\Delta t}\|\psi_2 - \psi_1\|_* + \|\mathbf{u}\cdot\boldsymbol{\nabla}(\psi_2 - \psi_1)\|_* \\
&+ \frac{2(1-\omega)\rho_s}{\Delta t}\|q'(\frac{\psi_2 + C^n + \hat{C}}{2})(\psi_2 - (C^n - \hat{C})) - q'(\frac{\psi_1 + C^n + \hat{C}}{2})(\psi_1 - (C^n - \hat{C}))\|_*.
\end{aligned}$$

Notice, $\frac{2\omega}{\Delta t}\|\psi_2 - \psi_1\|_* \leq \frac{2\omega K_{\mathrm{PF}}}{\Delta t}\|\boldsymbol{\nabla}(\psi_2 - \psi_1)\|$ and $\|\mathbf{u}\cdot\boldsymbol{\nabla}(\psi_2 - \psi_1)\|_* \leq \|\mathbf{u}\|_\infty\|\boldsymbol{\nabla}(\psi_2 - \psi_1)\|$. Next,

$$\|q'(\frac{\psi_2 + C^n + \hat{C}}{2})(\psi_2 - \psi_1)\|_* \leq \kappa_2 K_{\mathrm{PF}}\|\boldsymbol{\nabla}(\psi_2 - \psi_1)\|.$$

Using Lipschitz continuity of q' we get,

$$\begin{aligned}
&\|\left(q'(\frac{\psi_2 + C^n + \hat{C}}{2}) - q'(\frac{\psi_1 + C^n + \hat{C}}{2})\right)(\psi_1 - (C^n - \hat{C}))\|_* \\
&\leq KK_{\mathrm{PF}}\|\boldsymbol{\nabla}(\psi_2 - \psi_1)\|\|\psi_1 - (C^n - \hat{C})\|.
\end{aligned}$$

Hence, using Cauchy-Schwarz, Poincaré-Friedrichs inequalities and Lipschitz continuity of q' we get,

$$\begin{aligned}
&\|N(\psi_1) - N(\psi_2)\|_* \\
&\leq \left(\frac{2\omega K_{\mathrm{PF}}}{\Delta t} + \|\mathbf{u}\|_\infty + \frac{2(1-\omega)\rho_s\kappa_2 K_{\mathrm{PF}}}{\Delta t} + \frac{2(1-\omega)\rho_s K K_{\mathrm{PF}}}{\Delta t}\|\psi_1 - (C^n - \hat{C})\|\right) \\
&\times \|\boldsymbol{\nabla}(\psi_2 - \psi_1)\|
\end{aligned}$$

which concludes the argument. □

Lemma 26. *If $N : X_{0,\Gamma_{in}} \to X^*$ is a compact operator and $T : X^* \to X_{0,\Gamma_{in}}$ is a bounded linear operator, $T \circ N$ is compact .*

Proof. Let $x_n \in X_{0,\Gamma_{\mathrm{in}}}$ be a sequence such that $\|x_n\| \leq 1$. Then, since N is compact Nx_n has convergent subsequence , say, $Nx_{n_k} \to y$. Since T is a bounded linear operator, we get $TNx_{n_k} \to Ty$ which shows that $T \circ N$ has a convergent subsequence proving $T \circ N$ is compact. □

Lemma 27. *$\mathcal{F} : X_{0,\Gamma_{in}} \to X_{0,\Gamma_{in}}$ is a compact map.*

Proof. Since $T : X^* \to X_{0,\Gamma_{\text{in}}}$ is a bounded linear operator, all we need to show that $N : X_{0,\Gamma_{\text{in}}} \to X^*$ is a compact map. In Lemma 24 and Lemma 25, we proved that $N : X_{0,\Gamma_{\text{in}}} \to X^*$ is a bounded and continuous operator respectively. The Rellich-Kondrachov Compactness Theorem [59, page 272] ensures the embedding $X_{0,\Gamma_{\text{in}}} \hookrightarrow L^2(\Omega)$ is compact. Hence, $N : X_{0,\Gamma_{\text{in}}} \hookrightarrow L^2 \to X^*$ is compact. The following diagram gives a better explanation.

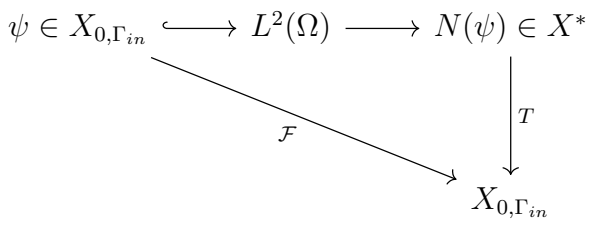

□

To prove the solvability of the problem Equation (129), it suffices to show that $\mathcal{F}$ has a fixed point, i.e., a fixed point ψ of $\psi = \mathcal{F}(\psi)$ in $X_{0,\Gamma_{\text{in}}}$ exists.

Theorem 28. *For any $v \in X_{0,\Gamma_{in}}$ and $f \in X^*$, a solution $\psi = C^{n+1} - \hat{C} \in X_{0,\Gamma_{in}}$ exists to the problem Equation* (129).

Proof. Consider $\psi_\alpha = \alpha\mathcal{F}(\psi_\alpha)$ in $X_{0,\Gamma_{\text{in}}}$, $0 \le \alpha \le 1$. Hence, we write,

$$\begin{aligned}\psi_\alpha = T\bigg(&2\alpha f^{n+\frac{1}{2}} - 2\alpha\big(\omega + (1-\omega)\rho_s q'(\frac{\psi + C^n + \hat{C}}{2})\big)\frac{\psi - (C^n - \hat{C})}{\Delta t}\\ &- \alpha\mathbf{u}\cdot\boldsymbol{\nabla}\Big(\psi + C^n + \hat{C}\Big) + \alpha\boldsymbol{\nabla}\cdot(D\boldsymbol{\nabla}\Big(C^n + \hat{C}\Big))\bigg),\end{aligned}$$

which holds if and only if $\psi_\alpha \in X_{0,\Gamma_{\text{in}}}$ satisfies

$$\begin{aligned}(D\boldsymbol{\nabla}\psi_\alpha, \boldsymbol{\nabla}v) = -2\alpha\bigg(&\big(\omega + (1-\omega)\rho_s q'(\frac{\psi_\alpha + C^n + \hat{C}}{2})\big)\frac{\psi_\alpha - (C^n - \hat{C})}{\Delta t}, v\bigg)\\ &+ 2(\alpha f^{n+1/2}, v) - (\alpha\mathbf{u}\cdot\boldsymbol{\nabla}\Big(\psi_\alpha + C^n + \hat{C}\Big), v) - (\alpha D\boldsymbol{\nabla}\Big(C^n + \hat{C}\Big), \boldsymbol{\nabla}v),\ \forall v \in X_{0,\Gamma_{\text{in}}}.\end{aligned} \tag{130}$$

By the Leray-Schauder fixed-point Thoerem [100, Theorem 16], we only need to prove a priori bound on $\|\boldsymbol{\nabla}\psi_\alpha\|$, independent of α. Setting $v = \psi_\alpha$ in Equation (130) and using Cauchy-Schwarz, Poincaré-Friedrichs inequalities, we get,

$$\begin{aligned}\lambda\|\boldsymbol{\nabla}\psi_\alpha\| \leq 2\alpha K_{\mathrm{PF}}\|f^{n+1/2}\| + \alpha K_{\mathrm{PF}}\|\mathbf{u}\cdot\boldsymbol{\nabla}\Big(C^n + \hat{C}\Big)\| + \alpha\beta_1\|\boldsymbol{\nabla}\Big(C^n + \hat{C}\Big)\| \\ + \frac{2\alpha K_{\mathrm{PF}}(\omega + \alpha(1-\omega)\rho_s\kappa_2)}{\Delta t}\|C^n - \hat{C}\|.\end{aligned}$$

Thus, for $0 \leq \alpha \leq 1$,

$$\begin{aligned}\|\boldsymbol{\nabla}\psi_\alpha\| \leq \frac{2K_{\mathrm{PF}}}{\lambda}\|f^{n+1/2}\| + \frac{K_{\mathrm{PF}}}{\lambda}\|\mathbf{u}\cdot\boldsymbol{\nabla}\Big(C^n + \hat{C}\Big)\| + \frac{\beta_1}{\lambda}\|\boldsymbol{\nabla}\Big(C^n + \hat{C}\Big)\| \\ + \frac{2K_{\mathrm{PF}}(\omega + (1-\omega)\rho_s\kappa_2)}{\lambda\Delta t}\|C^n - \hat{C}\| := K,\end{aligned}$$

and a solution exists. □

Next, we find the energy bound for the fully discrete version of the adsorption equation (1) for nonlinear, explicit isotherm using the midpoint method for the time discretization. At a continuous level, we proved $C > 0$ and bounded by initial and boundary conditions. But at a discrete level, the Maximum Principle is very hard to implement, usually, the timestep has to be $\mathcal{O}(h^2)$ [147]. We will use the following notation: $Q_h(\alpha) = \int_0^\alpha \mathcal{P}(q(s))ds$,

$$\begin{aligned}\mathcal{E}_h^n = \frac{3\Delta t\omega}{4}\sum_{n=0}^{N}\|D^{1/2}\boldsymbol{\nabla}C_h^{n+1/2} - \frac{8}{3}D^{-1/2}\hat{C}_h\mathbf{u}\|^2 \\ + \frac{3\Delta t\omega}{4}\sum_{n=0}^{N}\|D^{1/2}\boldsymbol{\nabla}C_h^{n+1/2} - \frac{8\rho_s\mathcal{P}(q(\hat{C}_h))(1-\omega)}{3\omega}D^{-1/2}\mathbf{u}\|^2 \\ + \frac{3\Delta t\omega}{4}\sum_{n=0}^{N}\|D^{1/2}\boldsymbol{\nabla}C_h^{n+1/2} - \frac{8}{3}D^{-1/2}\boldsymbol{\nabla}\hat{C}_h\|^2 \\ + \frac{3\Delta t\omega}{4}\sum_{n=0}^{N}\|D^{1/2}\boldsymbol{\nabla}C_h^{n+1/2} - \frac{8(1-\omega)\rho_s\mathcal{P}^1(q'(\hat{C}_h))}{3\omega}D^{-1/2}\boldsymbol{\nabla}\hat{C}_h\|^2 \\ + \|\omega C_h^{N+1} + (1-\omega)\rho_s q(C_h^{N+1}) - 2(\omega\hat{C}_h + (1-\omega)\rho_s\mathcal{P}(q(\hat{C}_h)))\|^2,\end{aligned}$$

and

$$\begin{aligned}\mathcal{B}_h^n &= \frac{3N\Delta t\omega}{4}\|\frac{8}{3}D^{-1/2}\hat{C}_h\mathbf{u}\|^2 + \frac{3N\Delta t\omega}{4}\|\frac{8\rho_s\mathcal{P}(q(\hat{C}_h))(1-\omega)}{3\omega}D^{-1/2}\mathbf{u}\|^2 \\ &+ \frac{3N\Delta t\omega}{4}\|\frac{8}{3}D^{-1/2}\boldsymbol{\nabla}\hat{C}_h\|^2 + \frac{3N\Delta t\omega}{4}\|\frac{8(1-\omega)\rho_s\mathcal{P}^1(q'(\hat{C}_h))}{3\omega}D^{-1/2}\boldsymbol{\nabla}\hat{C}_h\|^2 \\ &+ \|\omega C_h^0 + (1-\omega)\rho_s q(C_h^0) - 2(\omega\hat{C}_h + (1-\omega)\rho_s\mathcal{P}(q(\hat{C}_h)))\|^2.\end{aligned}$$

Theorem 29. *Suppose the assumptions (F1)-F(7) are satisfied so that the fully discrete formulation given by (15) has a smooth solution* $\{C_h^n\}_{n=0}^N \in L^2(0,T;H^1(\Omega))$. *Then for all* $N > 0$,

$$\begin{aligned}&\|\omega C_h^{N+1} + (1-\omega)\rho_s\mathcal{P}(q(C_h^{N+1})\|^2 + \Delta t\omega\sum_{n=0}^{N}\|\boldsymbol{\nabla}C_h^{n+1/2}\|^2 + 2\Delta t\omega\sum_{n=0}^{N}\int_{\Gamma_{out}}(C_h^{n+1/2})^2(\mathbf{u}\cdot\overrightarrow{n})ds \\ &+ 4(1-\omega)\Delta t\rho_s\sum_{n=0}^{N}\int_{\Gamma_{out}}Q_h(C_h^{n+1/2})(\mathbf{u}\cdot\overrightarrow{n})ds \\ &+ 4(1-\omega)\Delta t\rho_s\sum_{n=0}^{N}\int_{\Omega}\mathcal{P}^1(q'(C_h^{n+1/2}))(D^{1/2}\boldsymbol{\nabla}C_h^{n+1/2})^2\ d\Omega + \frac{1}{4}\mathcal{E}_h^n \\ &= \|\omega C_h^0 + (1-\omega)\rho_s\mathcal{P}(q(C_h^0)\|^2 + \mathcal{B}_h^n \\ &+ 4\Delta t\sum_{n=0}^{N}(f,\omega C_h^{n+1/2} + (1-\omega)\rho_s\mathcal{P}(q(C_h^{n+1/2})) - (\omega\hat{C}_h + (1-\omega)\rho_s\mathcal{P}(q(\hat{C}_h)))) \\ &- 2N\Delta t\omega\int_{\Gamma_{in}}g_h^2(\mathbf{u}\cdot\overrightarrow{n})ds - 4(1-\omega)N\Delta t\rho_s\int_{\Gamma_{in}}Q_h(g_h)(\mathbf{u}\cdot\overrightarrow{n})ds.\end{aligned}$$

Proof. Let $\hat{C}_h \in X^h$ such that $\hat{C}_h\Big|_{\Gamma_{\text{in}}} = g_h$. Take

$$v_h = \omega C_h^{n+1/2} + (1-\omega)\mathcal{P}(q(C_h^{n+1/2})) - (\omega\hat{C}_h + (1-\omega)\rho_s\mathcal{P}(q(\hat{C}_h))) \in X^h_{0,\Gamma_{\text{in}}}(\Omega).$$

Then (17) yields to

$$\begin{aligned}&(\omega C_h^{n+1/2} + (1-\omega)\rho_s q(C_h^{n+1/2}) - \omega C_h^n - (1-\omega)\rho_s q(C_h^n), \omega C_h^{n+1/2} + (1-\omega)\mathcal{P}(q(C_h^{n+1/2}))) \\ &+ \frac{\Delta t}{2}(\mathbf{u}\cdot\boldsymbol{\nabla}C_h^{n+1/2}, \omega C_h^{n+1/2} + (1-\omega)\mathcal{P}(q(C_h^{n+1/2}))) \\ &+ \frac{\Delta t}{2}(D\boldsymbol{\nabla}C_h^{n+1/2}, \boldsymbol{\nabla}\Big(\omega C_h^{n+1/2} + (1-\omega)\mathcal{P}(q(C_h^{n+1/2}))\Big))\end{aligned}$$

$$
\begin{aligned}
&= \frac{\Delta t}{2}(f^{n+1/2}, \omega C_h^{n+1/2} + (1-\omega)\mathcal{P}(q(C_h^{n+1/2})) - (\omega \hat{C}_h + (1-\omega)\rho_s \mathcal{P}(q(\hat{C}_h))))\\
&+ (\omega C_h^{n+1/2} + (1-\omega)\rho_s q(C_h^{n+1/2}) - \omega C_h^n - (1-\omega)\rho_s q(C_h^n), (\omega \hat{C}_h + (1-\omega)\rho_s \mathcal{P}(q(\hat{C}_h)))\\
&+ \frac{\Delta t}{2}(\mathbf{u}\cdot\boldsymbol{\nabla} C_h^{n+1/2}, (\omega \hat{C}_h + (1-\omega)\rho_s \mathcal{P}(q(\hat{C}_h)))\\
&+ \frac{\Delta t}{2}(D\boldsymbol{\nabla} C_h^{n+1/2}, \boldsymbol{\nabla}\Big((\omega \hat{C}_h + (1-\omega)\rho_s \mathcal{P}(q(\hat{C}_h)\Big)))
\end{aligned}
$$

Using polarization identity in the first term, we get,

$$
\begin{aligned}
&\frac{1}{2}(\|\omega C_h^{n+1/2} + (1-\omega)\rho_s \mathcal{P}(q(C_h^{n+1/2}))\|^2 + \|\omega C_h^n + (1-\omega)\rho_s \mathcal{P}(q(C_h^n))\|^2\\
&- \|\omega C_h^{n+1/2} + (1-\omega)\rho_s \mathcal{P}((C_h^{n+1/2})) - (\omega C_h^n + (1-\omega)\rho_s \mathcal{P}(q(C_h^n)))\|^2)\\
&+ \frac{\Delta t}{2}(\mathbf{u}\cdot\boldsymbol{\nabla} C_h^{n+1/2}, \omega C_h^{n+1/2} + (1-\omega)\mathcal{P}(q(C_h^{n+1/2})))\\
&+ \frac{\Delta t}{2}(D\boldsymbol{\nabla} C_h^{n+1/2}, \boldsymbol{\nabla}\Big(\omega C_h^{n+1/2} + (1-\omega)\mathcal{P}(q(C_h^{n+1/2}))\Big))\\
&= \frac{\Delta t}{2}(f^{n+1/2}, \omega C_h^{n+1/2} + (1-\omega)\mathcal{P}(q(C_h^{n+1/2})) - (\omega \hat{C}_h + (1-\omega)\rho_s \mathcal{P}(q(\hat{C}_h))))\\
&+ (\omega C_h^{n+1/2} + (1-\omega)\rho_s q(C_h^{n+1/2}) - \omega C_h^n - (1-\omega)\rho_s q(C_h^n), (\omega \hat{C}_h + (1-\omega)\rho_s \mathcal{P}(q(\hat{C}_h)))\\
&+ \frac{\Delta t}{2}(\mathbf{u}\cdot\boldsymbol{\nabla} C_h^{n+1/2}, (\omega \hat{C}_h + (1-\omega)\rho_s \mathcal{P}(q(\hat{C}_h)))\\
&+ \frac{\Delta t}{2}(D\boldsymbol{\nabla} C_h^{n+1/2}, \boldsymbol{\nabla}\Big((\omega \hat{C}_h + (1-\omega)\rho_s \mathcal{P}(q(\hat{C}_h)\Big))).
\end{aligned}
\tag{131}
$$

Next, (19) yields to

$$
\begin{aligned}
&(\omega C_h^{n+1} + (1-\omega)\rho_s q(C_h^{n+1}) - \omega C_h^{n+1/2} - (1-\omega)\rho_s q(C_h^{n+1/2})\\
&, \omega C_h^{n+1/2} + (1-\omega)\mathcal{P}(q(C_h^{n+1/2})))\\
&+ \frac{\Delta t}{2}(\mathbf{u}\cdot\boldsymbol{\nabla} C_h^{n+1/2}, \omega C_h^{n+1/2} + (1-\omega)\mathcal{P}(q(C_h^{n+1/2})))\\
&+ \frac{\Delta t}{2}(D\boldsymbol{\nabla} C_h^{n+1/2}, \boldsymbol{\nabla}\Big(\omega C_h^{n+1/2} + (1-\omega)\mathcal{P}(q(C_h^{n+1/2}))\Big))\\
&= \frac{\Delta t}{2}(f^{n+1/2}, \omega C_h^{n+1/2} + (1-\omega)\mathcal{P}(q(C_h^{n+1/2})) - (\omega \hat{C}_h + (1-\omega)\rho_s \mathcal{P}(q(\hat{C}_h))))\\
&+ (\omega C_h^{n+1} + (1-\omega)\rho_s q(C_h^{n+1}) - \omega C_h^{n+1/2} - (1-\omega)\rho_s q(C_h^{n+1/2}), (\omega \hat{C}_h + (1-\omega)\rho_s \mathcal{P}(q(\hat{C}_h)))\\
&+ \frac{\Delta t}{2}(\mathbf{u}\cdot\boldsymbol{\nabla} C_h^{n+1/2}, \omega \hat{C}_h + (1-\omega)\rho_s \mathcal{P}(q(\hat{C}_h)))
\end{aligned}
$$

$$+\frac{\Delta t}{2}(D\boldsymbol{\nabla}C_h^{n+1/2},\boldsymbol{\nabla}\Big((\omega\hat{C}_h+(1-\omega)\rho_s\mathcal{P}(q(\hat{C}_h)\Big)))$$

Using polarization identity first term, we get

$$\begin{aligned}
&\frac{1}{2}(\|\omega C_h^{n+1}+(1-\omega)\rho_s\mathcal{P}(q(C_h^{n+1}))\|^2-\|\omega C_h^{n+1/2}+(1-\omega)\rho_s\mathcal{P}(q(C_h^{n+1/2}))\|^2\\
&-\|\omega C_h^{n+1/2}+(1-\omega)\rho_s\mathcal{P}((C_h^{n+1/2}))-(\omega C_h^{n+1}+(1-\omega)\rho_s\mathcal{P}(q(C_h^{n+1})))\|^2)\\
&+\frac{\Delta t}{2}(\mathbf{u}\cdot\boldsymbol{\nabla}C_h^{n+1/2},\omega C_h^{n+1/2}+(1-\omega)\mathcal{P}(q(C_h^{n+1/2})))\\
&+\frac{\Delta t}{2}(D\boldsymbol{\nabla}C_h^{n+1/2},\boldsymbol{\nabla}\Big(\omega C_h^{n+1/2}+(1-\omega)\mathcal{P}(q(C_h^{n+1/2}))\Big))\\
&=\frac{\Delta t}{2}(f^{n+1/2},\omega C_h^{n+1/2}+(1-\omega)\mathcal{P}(q(C_h^{n+1/2}))-(\omega\hat{C}_h+(1-\omega)\rho_s\mathcal{P}(q(\hat{C}_h))))\\
&+(\omega C_h^{n+1}+(1-\omega)\rho_s q(C_h^{n+1})-\omega C_h^{n+1/2}-(1-\omega)\rho_s q(C_h^{n+1/2}),\omega\hat{C}_h+(1-\omega)\rho_s\mathcal{P}(q(\hat{C}_h)))\\
&+\frac{\Delta t}{2}(\mathbf{u}\cdot\boldsymbol{\nabla}C_h^{n+1/2},\omega\hat{C}_h+(1-\omega)\rho_s\mathcal{P}(q(\hat{C}_h)))\\
&+\frac{\Delta t}{2}(D\boldsymbol{\nabla}C_h^{n+1/2},\boldsymbol{\nabla}\Big((\omega\hat{C}_h+(1-\omega)\rho_s\mathcal{P}(q(\hat{C}_h)\Big)))
\end{aligned}\tag{132}$$

Adding (131) and (132), we get

$$\begin{aligned}
&\frac{1}{2}(\|\omega C_h^{n+1}+(1-\omega)\rho_s\mathcal{P}(q(C_h^{n+1}))\|^2-\|\omega C_h^{n}+(1-\omega)\rho_s\mathcal{P}(q(C_h^{n}))\|^2\\
&-\|\omega C_h^{n+1/2}+(1-\omega)\rho_s\mathcal{P}((C_h^{n+1/2}))-(\omega C_h^{n+1}+(1-\omega)\rho_s\mathcal{P}(q(C_h^{n+1})))\|^2\\
&+\|\omega C_h^{n+1/2}+(1-\omega)\rho_s\mathcal{P}((C_h^{n+1/2}))-(\omega C_h^{n}+(1-\omega)\rho_s\mathcal{P}(q(C_h^{n})))\|^2)\\
&+\Delta t(\mathbf{u}\cdot\boldsymbol{\nabla}C_h^{n+1/2},\omega C_h^{n+1/2}+(1-\omega)\mathcal{P}(q(C_h^{n+1/2})))\\
&+\Delta t(D\boldsymbol{\nabla}C_h^{n+1/2},\boldsymbol{\nabla}\Big(\omega C_h^{n+1/2}+(1-\omega)\mathcal{P}(q(C_h^{n+1/2}))\Big))\\
&=\Delta t(f^{n+1/2},\omega C_h^{n+1/2}+(1-\omega)\mathcal{P}(q(C_h^{n+1/2}))-(\omega\hat{C}_h+(1-\omega)\rho_s\mathcal{P}(q(\hat{C}_h))))\\
&+(\omega C_h^{n+1}+(1-\omega)\rho_s q(C_h^{n+1})-\omega C_h^{n}-(1-\omega)\rho_s q(C_h^{n}),(\omega\hat{C}_h+(1-\omega)\rho_s\mathcal{P}(q(\hat{C}_h)))\\
&+\Delta t(\mathbf{u}\cdot\boldsymbol{\nabla}C_h^{n+1/2},\omega\hat{C}_h+(1-\omega)\rho_s\mathcal{P}(q(\hat{C}_h)))\\
&+\Delta t(D\boldsymbol{\nabla}C_h^{n+1/2},\boldsymbol{\nabla}\Big((\omega\hat{C}_h+(1-\omega)\rho_s\mathcal{P}(q(\hat{C}_h)\Big))).
\end{aligned}\tag{133}$$

Using (17) and (19), we get,

$$-\|\omega C_h^{n+1/2}+(1-\omega)\rho_s\mathcal{P}((C_h^{n+1/2}))-(\omega C_h^{n+1}+(1-\omega)\rho_s\mathcal{P}(q(C_h^{n+1})))\|^2$$

$$+ \|\omega C_h^{n+1/2} + (1-\omega)\rho_s \mathcal{P}((C_h^{n+1/2})) - (\omega C_h^n + (1-\omega)\rho_s \mathcal{P}(q(C_h^n)))\|^2 = 0$$

Consequently, we have,

$$\begin{aligned}
&\frac{1}{2}(\|\omega C_h^{n+1} + (1-\omega)\rho_s \mathcal{P}(q(C_h^{n+1}))\|^2 - \|\omega C_h^n + (1-\omega)\rho_s \mathcal{P}(q(C_h^n))\|^2) \\
&+ \Delta t(\mathbf{u}\cdot\boldsymbol{\nabla} C_h^{n+1/2}, \omega C_h^{n+1/2} + (1-\omega)\mathcal{P}(q(C_h^{n+1/2}))) \\
&+ \Delta t(D\boldsymbol{\nabla} C_h^{n+1/2}, \boldsymbol{\nabla}\Big(\omega C_h^{n+1/2} + (1-\omega)\mathcal{P}(q(C_h^{n+1/2}))\Big)) \\
&= \Delta t(f^{n+1/2}, \omega C_h^{n+1/2} + (1-\omega)\mathcal{P}(q(C_h^{n+1/2})) - (\omega \hat{C}_h + (1-\omega)\rho_s \mathcal{P}(q(\hat{C}_h)))) \\
&+ (\omega C_h^{n+1} + (1-\omega)\rho_s q(C_h^{n+1}) - \omega C_h^n - (1-\omega)\rho_s q(C_h^n), (\omega \hat{C}_h + (1-\omega)\rho_s \mathcal{P}(q(\hat{C}_h))) \\
&+ \Delta t(\mathbf{u}\cdot\boldsymbol{\nabla} C_h^{n+1/2}, (\omega \hat{C}_h + (1-\omega)\rho_s \mathcal{P}(q(\hat{C}_h))) \\
&+ \Delta t(D\boldsymbol{\nabla} C_h^{n+1/2}, \boldsymbol{\nabla}\Big((\omega \hat{C}_h + (1-\omega)\rho_s \mathcal{P}(q(\hat{C}_h)\Big))).
\end{aligned} \tag{134}$$

Doing a similar analysis as in the semidiscrete case, we get,

$$\begin{aligned}
&\Delta t(\mathbf{u}\cdot\boldsymbol{\nabla} C_h^{n+1/2}, \omega C_h^{n+1/2} + (1-\omega)\rho_s \mathcal{P}(q(C_h^{n+1/2}))) \\
&= \frac{\Delta t\omega}{2}\int_{\Gamma_{\text{in}}} g_h^2(\mathbf{u}\cdot\overrightarrow{n})ds + \frac{\Delta t\omega}{2}\int_{\Gamma_{\text{out}}} (C_h^{n+1/2})^2(\mathbf{u}\cdot\overrightarrow{n})ds \\
&+ \Delta t(1-\omega)\rho_s \int_{\Gamma_{\text{in}}} Q_h(g_h)(\mathbf{u}\cdot\overrightarrow{n})ds + \Delta t(1-\omega)\rho_s \int_{\Gamma_{\text{out}}} Q_h(C_h^{n+1/2})(\mathbf{u}\cdot\overrightarrow{n})ds.
\end{aligned} \tag{135}$$

Next,

$$\begin{aligned}
&\Delta t\omega(D\boldsymbol{\nabla} C_h^{n+1/2}, \boldsymbol{\nabla} C_h^{n+1/2}) + \Delta t(1-\omega)\rho_s \mathcal{P}^1(q'(C_h^{n+1/2}))D\boldsymbol{\nabla} C_h^{n+1/2}, \boldsymbol{\nabla} C_h^{n+1/2}) \\
&= \Delta t\omega(D^{1/2}\boldsymbol{\nabla} C_h^{n+1/2}, D^{1/2}\boldsymbol{\nabla} C_h^{n+1/2}) \\
&+ \Delta t(1-\omega)\rho_s(\mathcal{P}^1(q'(C_h^{n+1/2}))D^{1/2}\boldsymbol{\nabla} C_h^{n+1/2}, D^{1/2}\boldsymbol{\nabla} C_h^{n+1/2}) \\
&= \Delta t\omega\|D^{1/2}\boldsymbol{\nabla} C_h^{n+1/2}\|^2 + \Delta t(1-\omega)\rho_s \int_\Omega \mathcal{P}^1(q'(C_h^{n+1/2}))(D^{1/2}\boldsymbol{\nabla} C_h^{n+1/2})^2 \, d\Omega.
\end{aligned}$$

Next, in the right-hand side terms, we get the following equalities,

$$\begin{aligned}
&\Delta t(\mathbf{u}\cdot\boldsymbol{\nabla}C_h^{n+1/2},\omega\hat{C}_h)\\
&=\Delta t(\boldsymbol{\nabla}C_h^{n+1/2}\cdot\mathbf{u},\omega\hat{C}_h)\\
&=\Delta t(\boldsymbol{\nabla}C_h^{n+1/2},\omega\hat{C}_h\mathbf{u})\\
&=\Delta t\omega(D^{1/2}\boldsymbol{\nabla}C_h^{n+1/2},D^{-1/2}\hat{C}_h\mathbf{u})\\
&=\frac{3\Delta t\omega}{8}(D^{1/2}\boldsymbol{\nabla}C_h^{n+1/2},\frac{8}{3}D^{-1/2}\hat{C}_h\mathbf{u})\\
&=\frac{3\Delta t\omega}{16}\|D^{1/2}\boldsymbol{\nabla}C_h^{n+1/2}\|^2+\frac{3\Delta t\omega}{16}\|\frac{8}{3}D^{-1/2}\hat{C}_h\mathbf{u}\|^2-\frac{3\Delta t\omega}{16}\|D^{1/2}\boldsymbol{\nabla}C_h^{n+1/2}-\frac{8}{3}D^{-1/2}\hat{C}_h\mathbf{u}\|^2,
\end{aligned}\tag{136}$$

and

$$\begin{aligned}
&\Delta t(\mathbf{u}\cdot\boldsymbol{\nabla}C_h^{n+1/2},(1-\omega)\rho_s\mathcal{P}(q(\hat{C}_h)))\\
&=(\boldsymbol{\nabla}C_h^{n+1/2}\cdot\mathbf{u},(1-\omega)\rho_s\mathcal{P}(q(\hat{C}_h)))\\
&=\Delta t(\boldsymbol{\nabla}C_h^{n+1/2},(1-\omega)\rho_s\mathcal{P}(q(\hat{C}_h))\mathbf{u})\\
&=\Delta t\omega(D^{1/2}\boldsymbol{\nabla}C_h^{n+1/2},\frac{\rho_s\mathcal{P}(q(\hat{C}_h))(1-\omega)}{\omega}D^{-1/2}\mathbf{u})\\
&=\frac{3\Delta t\omega}{8}(D^{1/2}\boldsymbol{\nabla}C_h^{n+1/2},\frac{8\rho_s\mathcal{P}(q(\hat{C}_h))(1-\omega)}{3\omega}D^{-1/2}\mathbf{u})\\
&=\frac{3\Delta t\omega}{16}\|D^{1/2}\boldsymbol{\nabla}C_h^{n+1/2}\|^2+\frac{3\Delta t\omega}{16}\|\frac{8\rho_s\mathcal{P}(q(\hat{C}_h))(1-\omega)}{3\omega}D^{-1/2}\mathbf{u}\|^2\\
&-\frac{3\Delta t\omega}{16}\|D^{1/2}\boldsymbol{\nabla}C_h^{n+1/2}-\frac{8\rho_s\mathcal{P}(q(\hat{C}_h))(1-\omega)}{3\omega}D^{-1/2}\mathbf{u}\|^2.
\end{aligned}\tag{137}$$

Next,

$$\begin{aligned}
&\Delta t\omega(D\boldsymbol{\nabla}C_h^{n+1/2},\boldsymbol{\nabla}\hat{C}_h)\\
&=\Delta t\omega(D^{1/2}\boldsymbol{\nabla}C_h^{n+1/2},D^{-1/2}\boldsymbol{\nabla}\hat{C}_h)\\
&=\frac{3\Delta t\omega}{8}(D^{1/2}\boldsymbol{\nabla}C_h^{n+1/2},\frac{8}{3}D^{-1/2}\boldsymbol{\nabla}\hat{C}_h)\\
&=\frac{3\Delta t\omega}{16}\|D^{1/2}\boldsymbol{\nabla}C_h^{n+1/2}\|^2+\frac{3\Delta t\omega}{16}\|\frac{8}{3}D^{-1/2}\boldsymbol{\nabla}\hat{C}_h\|^2-\frac{3\Delta t\omega}{16}\|D^{1/2}\boldsymbol{\nabla}C_h^{n+1/2}-\frac{8}{3}D^{-1/2}\boldsymbol{\nabla}\hat{C}_h\|^2,
\end{aligned}\tag{138}$$

and

$$
\begin{aligned}
&\Delta t(D\boldsymbol{\nabla} C_h^{n+1/2}, (1-\omega)\rho_s \mathcal{P}^1(q'(\hat{C}_h))\boldsymbol{\nabla}\hat{C}_h) \\
&= \Delta t\omega(D^{1/2}\boldsymbol{\nabla} C_h^{n+1/2}, \frac{(1-\omega)\rho_s \mathcal{P}^1(q'(\hat{C}_h))}{\omega} D^{-1/2}\boldsymbol{\nabla}\hat{C}_h) \\
&= \frac{3\Delta t\omega}{8}(D^{1/2}\boldsymbol{\nabla} C_h^{n+1/2}, \frac{8(1-\omega)\rho_s \mathcal{P}^1(q'(\hat{C}_h))}{3\omega} D^{-1/2}\boldsymbol{\nabla}\hat{C}_h) \qquad (139) \\
&= \frac{3\Delta t\omega}{16}\|D^{1/2}\boldsymbol{\nabla} C_h^{n+1/2}\|^2 + \frac{3\Delta t\omega}{16}\|\frac{8(1-\omega)\rho_s \mathcal{P}^1(q'(\hat{C}_h))}{3\omega} D^{-1/2}\boldsymbol{\nabla}\hat{C}_h\|^2 \\
&- \frac{3\Delta t\omega}{16}\|D^{1/2}\boldsymbol{\nabla} C_h^{n+1/2} - \frac{8(1-\omega)\rho_s \mathcal{P}^1(q'(\hat{C}_h))}{3\omega} D^{-1/2}\boldsymbol{\nabla}\hat{C}_h\|^2.
\end{aligned}
$$

Combining (135)-(138), we get

$$
\begin{aligned}
&\frac{1}{2}(\|\omega C_h^{n+1} + (1-\omega)\rho_s \mathcal{P}(q(C_h^{n+1}))\|^2 - \|\omega C_h^n + (1-\omega)\rho_s \mathcal{P}(q(C_h^n))\|^2) + \frac{\omega\Delta t}{4}\|D^{1/2}\boldsymbol{\nabla} C_h^{n+1/2}\|^2 \\
&+ (1-\omega)\Delta t\rho_s \int_{\Gamma_{\text{out}}} Q_h(C_h^{n+1/2})(\mathbf{u}\cdot\overrightarrow{n})ds + \Delta t(1-\omega)\rho_s \int_\Omega \mathcal{P}^1(q'(C_h^{n+1/2}))(D^{1/2}\boldsymbol{\nabla} C_h^{n+1/2})^2\, d\Omega \\
&+ \frac{\Delta t\omega}{2}\int_{\Gamma_{\text{out}}} (C_h^{n+1/2})^2(\mathbf{u}\cdot\overrightarrow{n})ds + \frac{3\Delta t\omega}{16}\|D^{1/2}\boldsymbol{\nabla} C_h^{n+1/2} - \frac{8}{3}D^{-1/2}\hat{C}_h\mathbf{u}\|^2 \\
&+ \frac{3\Delta t\omega}{16}\|D^{1/2}\boldsymbol{\nabla} C_h^{n+1/2} - \frac{8\rho_s \mathcal{P}(q(\hat{C}_h))(1-\omega)}{3\omega} D^{-1/2}\mathbf{u}\|^2 \\
&+ \frac{3\Delta t\omega}{16}\|D^{1/2}\boldsymbol{\nabla} C_h^{n+1/2} - \frac{8}{3}D^{-1/2}\boldsymbol{\nabla}\hat{C}_h\|^2 \\
&+ \frac{3\Delta t\omega}{16}\|D^{1/2}\boldsymbol{\nabla} C_h^{n+1/2} - \frac{8(1-\omega)\rho_s \mathcal{P}^1(q'(\hat{C}_h))}{3\omega} D^{-1/2}\boldsymbol{\nabla}\hat{C}_h\|^2 \\
&= \Delta t(f^{n+1/2}, \omega C_h^{n+1/2} + (1-\omega)\rho_s \mathcal{P}(q(C_h^{n+1/2})) - (\omega\hat{C}_h + (1-\omega)\rho_s \mathcal{P}(q(\hat{C}_h)))) \\
&- \frac{\Delta t\omega}{2}\int_{\Gamma_{\text{in}}} g_h^2(\mathbf{u}\cdot\overrightarrow{n})ds + \frac{3\Delta t\omega}{16}\|\frac{8}{3}D^{-1/2}\hat{C}_h\mathbf{u}\|^2 \\
&+ \frac{3\Delta t\omega}{16}\|\frac{8\rho_s \mathcal{P}(q(\hat{C}_h))(1-\omega)}{3\omega} D^{-1/2}\mathbf{u}\|^2 + \frac{3\Delta t\omega}{16}\|\frac{8}{3}D^{-1/2}\boldsymbol{\nabla}\hat{C}_h\|^2 \\
&+ \frac{3\Delta t\omega}{16}\|\frac{8(1-\omega)\rho_s \mathcal{P}^1(q'(\hat{C}_h))}{3\omega} D^{-1/2}\boldsymbol{\nabla}\hat{C}_h\|^2 - (1-\omega)\rho_s\Delta t\int_{\Gamma_{\text{in}}} Q_h(g_h)(\mathbf{u}\cdot\overrightarrow{n})ds \\
&+ (\omega C_h^{n+1} + (1-\omega)\rho_s q(C_h^{n+1}) - \omega C_h^n - (1-\omega)\rho_s q(C_h^n), (\omega\hat{C}_h + (1-\omega)\rho_s \mathcal{P}(q(\hat{C}_h)))).
\end{aligned}
$$

Next, we sum over $n = 0$ to $n = N$ to obtain

$$
\begin{aligned}
&\frac{1}{2}\|\omega C_h^{N+1} + (1-\omega)\rho_s \mathcal{P}(q(C_h^{N+1}))\|^2 + \frac{\omega \Delta t}{4}\sum_{n=0}^{N}\|D^{1/2}\boldsymbol{\nabla} C_h^{n+1/2}\|^2 \\
&+ \frac{\Delta t \omega}{2}\sum_{n=0}^{N}\Big(\int_{\Gamma_{\text{out}}}(C_h^{n+1/2})^2(\mathbf{u}\cdot\overrightarrow{n})ds\Big) + \Delta t(1-\omega)\rho_s\sum_{n=0}^{N}\Big(\int_{\Gamma_{\text{out}}} Q_h(C_h^{n+1/2}(\mathbf{u}\cdot\overrightarrow{n})ds\Big) \\
&+ \Delta t(1-\omega)\rho_s\sum_{n=0}^{N}\left(\int_{\Omega}\mathcal{P}^1(q'(C_h^{n+1/2})(D^{1/2}\boldsymbol{\nabla} C_h^{n+1/2})^2\ d\Omega\right) \\
&+ \frac{3\Delta t\omega}{16}\sum_{n=0}^{N}\|D^{1/2}\boldsymbol{\nabla} C_h^{n+1/2} - \frac{8}{3}D^{-1/2}\hat{C}_h\mathbf{u}\|^2 \\
&+ \frac{3\Delta t\omega}{16}\sum_{n=0}^{N}\|D^{1/2}\boldsymbol{\nabla} C_h^{n+1/2} - \frac{8\rho_s\mathcal{P}(q(\hat{C}_h))(1-\omega)}{3\omega}D^{-1/2}\mathbf{u}\|^2 \\
&+ \frac{3\Delta t\omega}{16}\sum_{n=0}^{N}\|D^{1/2}\boldsymbol{\nabla} C_h^{n+1/2} - \frac{8}{3}D^{-1/2}\boldsymbol{\nabla}\hat{C}_h\|^2 \\
&+ \frac{3\Delta t\omega}{16}\sum_{n=0}^{N}\|D^{1/2}\boldsymbol{\nabla} C_h^{n+1/2} - \frac{8(1-\omega)\rho_s\mathcal{P}^1(q'(\hat{C}_h))}{3\omega}D^{-1/2}\boldsymbol{\nabla}\hat{C}_h\|^2 \\
&= \Delta t\sum_{n=0}^{N}(f^{n+1/2}, \omega C_h^{n+1/2} + (1-\omega)\rho_s\mathcal{P}(q(C_h^{n+1/2})) - (\omega\hat{C}_h + (1-\omega)\rho_s\mathcal{P}(q(\hat{C}_h)))) \\
&+ \frac{3N\Delta t\omega}{16}\|\frac{8}{3}D^{-1/2}\hat{C}_h\mathbf{u}\|^2 + \frac{3N\Delta t\omega}{16}\|\frac{8\rho_s\mathcal{P}(q(\hat{C}_h))(1-\omega)}{3\omega}D^{-1/2}\mathbf{u}\|^2 \\
&+ \frac{3N\Delta t\omega}{16}\|\frac{8(1-\omega)\rho_s\mathcal{P}^1(q'(\hat{C}_h))}{3\omega}D^{-1/2}\boldsymbol{\nabla}\hat{C}_h\|^2 + \frac{1}{2}\|\omega C_h^0 + (1-\omega)\rho_s\mathcal{P}(q(C_h^0)\|^2 \\
&- \frac{N\Delta t\omega}{2}\int_{\Gamma_{\text{in}}} g_h^2(\mathbf{u}\cdot\overrightarrow{n})ds - (1-\omega)N\Delta t\rho_s\int_{\Gamma_{\text{in}}} Q(g_h)(\mathbf{u}\cdot\overrightarrow{n})ds \\
&+ (\omega C_h^{N+1} + (1-\omega)\rho_s q(C_h^{N+1}, \omega\hat{C}_h + (1-\omega)\rho_s\mathcal{P}(q(\hat{C}_h))) \\
&- (\omega C_h^0 + (1-\omega)\rho_s q(C_h^0, \omega\hat{C}_h + (1-\omega)\rho_s\mathcal{P}(q(\hat{C}_h))) + \frac{3N\Delta t\omega}{16}\|\frac{8}{3}D^{-1/2}\boldsymbol{\nabla}\hat{C}_h\|^2.
\end{aligned}
\tag{140}
$$

Here,

$$
\begin{aligned}
&(\omega C_h^{N+1} + (1-\omega)\rho_s q(C_h^{N+1}), \omega\hat{C}_h + (1-\omega)\rho_s\mathcal{P}(q(\hat{C}_h))) \\
&= \frac{1}{2}(\omega C_h^{N+1} + (1-\omega)\rho_s q(C_h^{N+1}), 2(\omega\hat{C}_h + (1-\omega)\rho_s\mathcal{P}(q(\hat{C}_h))))
\end{aligned}
$$

$$= \frac{1}{4}\|(\omega C_h^{N+1} + (1-\omega)\rho_s q(C_h^{N+1})\|^2 + \frac{1}{4}\|2(\omega\hat{C}_h + (1-\omega)\rho_s\mathcal{P}(q(\hat{C}_h)))\|^2$$
$$- \frac{1}{4}\|\omega C_h^{N+1} + (1-\omega)\rho_s q(C_h^{N+1}) - 2(\omega\hat{C}_h + (1-\omega)\rho_s\mathcal{P}(q(\hat{C}_h)))\|^2,$$

and

$$- (\omega C_h^0 + (1-\omega)\rho_s q(C_h^0)), \omega\hat{C}_h + (1-\omega)\rho_s\mathcal{P}(q(\hat{C}_h)))$$
$$= -\frac{1}{2}(\omega C_h^0 + (1-\omega)\rho_s q(C_h^0, 2(\omega\hat{C}_h + (1-\omega)\rho_s\mathcal{P}(q(\hat{C}_h))))$$
$$= -\frac{1}{4}\|(\omega C_h^0 + (1-\omega)\rho_s q(C_h^0)\|^2 - \frac{1}{4}\|2(\omega\hat{C}_h + (1-\omega)\rho_s\mathcal{P}(q(\hat{C}_h)))\|^2$$
$$+ \frac{1}{4}\|\omega C_h^0 + (1-\omega)\rho_s q(C_h^0) - 2(\omega\hat{C}_h + (1-\omega)\rho_s\mathcal{P}(q(\hat{C}_h)))\|^2.$$

Hence (140) becomes

$$\frac{1}{4}\|\omega C_h^{N+1} + (1-\omega)\rho_s\mathcal{P}(q(C_h^{N+1})\|^2 + \frac{\Delta t\omega}{4}\sum_{n=0}^{N}\|\boldsymbol{\nabla} C_h^{n+1/2}\|^2$$
$$+ \frac{\Delta t\omega}{2}\sum_{n=0}^{N}\int_{\Gamma_{\text{out}}}(C_h^{n+1/2})^2(\mathbf{u}\cdot\overrightarrow{n})ds + \frac{1}{4}\mathcal{E}_h^n + (1-\omega)\Delta t\rho_s\sum_{n=0}^{N}\int_{\Gamma_{\text{out}}}Q(C_h^{n+1/2})(\mathbf{u}\cdot\overrightarrow{n})ds$$
$$+ (1-\omega)\Delta t\rho_s\sum_{n=0}^{N}\int_{\Omega}\mathcal{P}^1(q'(C_h^{n+1/2}))(D^{1/2}\boldsymbol{\nabla} C_h^{n+1/2})^2\ d\Omega$$
$$= \frac{1}{4}\|\omega C_h^0 + (1-\omega)\rho_s\mathcal{P}(q(C_h^0)\|^2 + \frac{1}{4}\mathcal{B}_h^n$$
$$+ \Delta t\sum_{n=0}^{N}(f, \omega C_h^{n+1/2} + (1-\omega)\rho_s\mathcal{P}(q(C_h^{n+1/2})) - (\omega\hat{C}_h + (1-\omega)\rho_s\mathcal{P}(q(\hat{C}_h))))$$
$$- \frac{N\Delta t\omega}{2}\int_{\Gamma_{\text{in}}}g_h^2(\mathbf{u}\cdot\overrightarrow{n})ds - (1-\omega)N\Delta t\rho_s\int_{\Gamma_{\text{in}}}Q(g_h)(\mathbf{u}\cdot\overrightarrow{n})ds$$

Simplifying the above inequality, we get the claimed result. □

2.5 Numerical Test

In this section, we perform numerical tests to show that the midpoint method described in Section 2.3.2 gives a second-order convergence rate for the considered PDE model for the constant, affine, and nonlinear, explicit adsorptions. For checking the order of convergence, we assume the following: $\mathbf{u} = (1, 1)$, $D = I$, $\Omega = [0, 1] \times [0, 1]$, $\omega = 0.5$, $X^h =$ the space of continuous piecewise affine functions, the exact solution is $C(x, y, t) = t^2(x^3 - \frac{3}{2}x^2 + 1)\cos(\frac{\pi}{4}y)$. The true solution determines the body force f, initial condition C_0, and boundary conditions. The norms used in the table are defined as follows,

$$\|C\|_{\infty,0} := \operatorname{ess\,sup}_{0<t<T} \|C(\cdot, t)\|_{L^2(\Omega)} \text{ and } \|C\|_{0,0} := \left(\int_0^T \|C(\cdot, t)\|^2_{L^2(\Omega)} \, dt \right)^{1/2}.$$

Next, for the plot of the concentration profile in each case, we consider the following: $f = 0$, $g = 1$, $T = 3.0$, $h = 1/128$, $dt = 1/128$, $\mathbf{u} = (0, 2x(x - 2))$, $D = I$, $\Omega = [0, 2] \times [0, 10]$, $\omega = 0.5$, $X^h =$ the space of continuous piecewise affine functions.

2.5.1 Tests for the case of constant isotherm

In this subsection, we first check the convergence rate for the case of constant isotherm in the first test, and in the second test, we plot the concentration profile. We also show the comparison of evolution of total mass

$$(\int_\Omega (\omega C + (1 - \omega)\rho_s q(C)) d\Omega)$$

after each test.

$(h, \Delta t) \ \rightarrow$	$(\frac{1}{128}, \frac{1}{2})$	$(\frac{1}{128}, \frac{1}{4})$	$(\frac{1}{128}, \frac{1}{8})$	$(\frac{1}{128}, \frac{1}{16})$	$(\frac{1}{128}, \frac{1}{32})$
$\|C - C_h\|_{\infty,0}$	0.0871011	0.0462486	0.0238288	0.0120901	0.00608901
Rate	-	0.91328	0.9567	0.97888	0.98955
$\|C - C_h\|_{0,0}$	0.0622419	0.0340122	0.0179402	0.00923882	0.00469204
Rate	-	0.87183	0.92286	0.95742	0.97749
$\|\boldsymbol{\nabla} C - \boldsymbol{\nabla} C_h\|_{0,0}$	0.100308	0.0548173	0.0289367	0.0149649	0.00773043
Rate	-	0.87173	0.92173	0.95132	0.95296
$\|C - C_h\|_{0,1}$	0.11805	0.0645117	0.0340468	0.017587	0.00904294
Rate	-	0.87177	0.92204	0.95301	0.95965

Table 1: Temporal convergence rates for the BE approximation with a constant adsorption model to the non-steady-state problem.

$(h, \Delta t) \ \rightarrow$	$(\frac{1}{128}, \frac{1}{2})$	$(\frac{1}{128}, \frac{1}{4})$	$(\frac{1}{128}, \frac{1}{8})$	$(\frac{1}{128}, \frac{1}{16})$	$(\frac{1}{128}, \frac{1}{32})$
$\|C - C_h\|_{\infty,0}$	0.0465279	0.011173	0.00269747	0.000664032	0.000164628
Rate	-	2.0581	2.0503	2.0223	2.012
$\|C - C_h\|_{0,0}$	0.0385999	0.00906892	0.00219412	0.000539591	0.000133763
Rate	-	2.0896	2.0473	2.0237	2.0122
$\|\boldsymbol{\nabla} C - \boldsymbol{\nabla} C_h\|_{0,0}$	0.714751	0.178008	0.0442268	0.0110284	0.00312606
Rate	-	2.0055	2.0089	2.0037	1.8188
$\|C - C_h\|_{0,1}$	0.715792	0.178239	0.0442812	0.0110416	0.00312892
Rate	-	2.0057	2.009	2.0037	1.8192

Table 2: Temporal convergence rates for the midpoint approximation with a constant adsorption model to the non-steady-state problem.

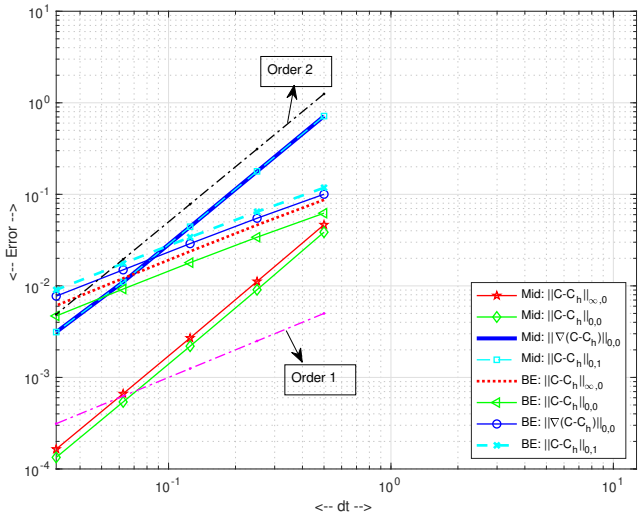

Figure 2: Constant Isotherm: Temporal rate of convergence of BE and Midpoint, $T = 1.0, h = 1/128$. Notice that Midpoint is giving order 2 whereas BE is giving order 1.

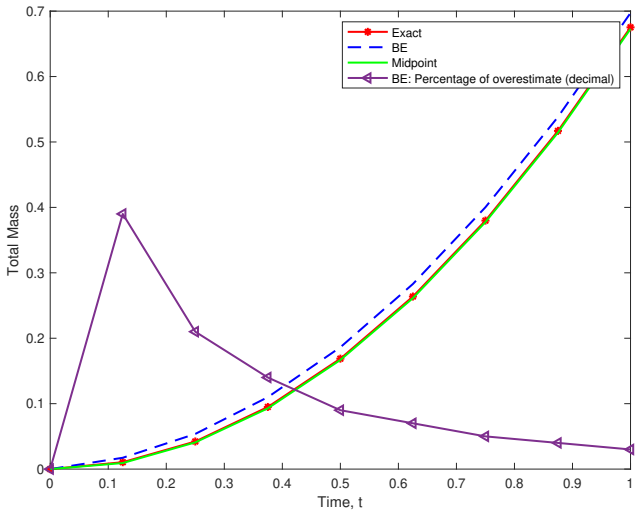

Figure 3: Constant Isotherm: Comparison of total mass for exact solution, BE, Midpoint, $T = 1.0$, $h = 1/128$, $dt = 1/8$. Notice that BE overestimates total mass rather than underestimates.

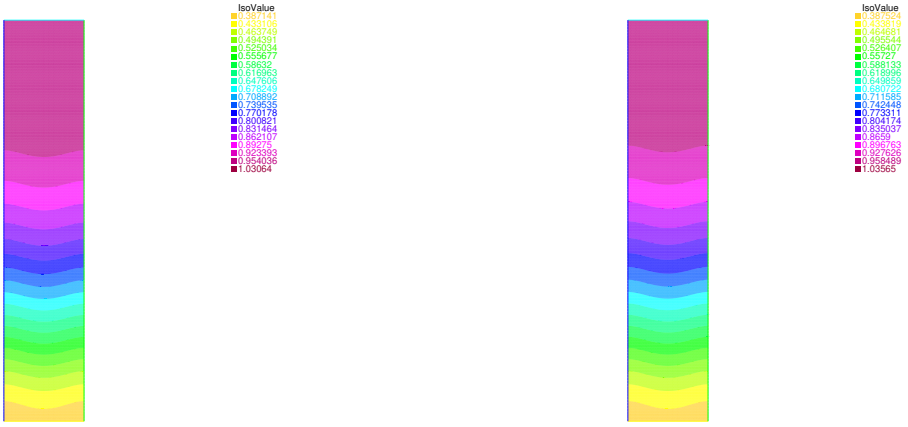

Figure 4: Constant isotherm: Plot of concentration while using BE (Left) & Midpoint (Right), $f = 0$, $g = 1$, $T = 3.0$, $h = 1/128$, $dt = 1/128$, $\mathbf{u} = (0, 2x(x-2))$, $D = I$.

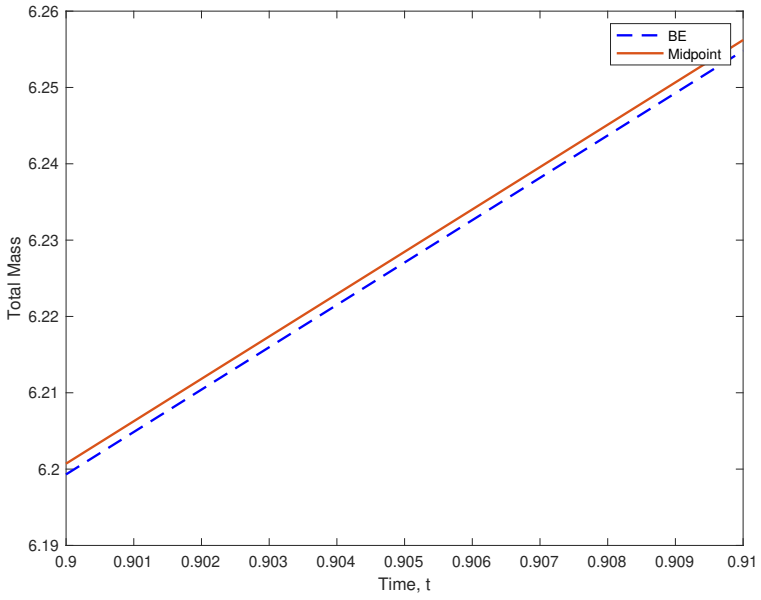

Figure 5: Constant isotherm: Comparison of total mass, $f = 0$, $g = 1$, $T = 3.0$, $h = 1/128$, $dt = 1/128$, $\mathbf{u} = (0, 2x(x-2))$, $D = I$.

2.5.2 Tests for the case of affine isotherm

In this subsection, we first check the convergence rate for the case of affine isotherm in the first test, and in the second test, we plot the concentration profile. We also show the comparison of total mass

$$(\int_{\Omega} (\omega C + (1-\omega)\rho_s q(C)) d\Omega)$$

after each test.

$(h, \Delta t) \ \rightarrow$	$(\frac{1}{128}, \frac{1}{2})$	$(\frac{1}{128}, \frac{1}{4})$	$(\frac{1}{128}, \frac{1}{8})$	$(\frac{1}{128}, \frac{1}{16})$	$(\frac{1}{128}, \frac{1}{32})$
$\|C - C_h\|_{\infty,0}$	0.141342	0.075632	0.039242	0.0200057	0.0101035
Rate	-	0.90212	0.9466	0.97199	0.98556
$\|C - C_h\|_{0,0}$	0.0954833	0.0510779	0.0266862	0.0136784	0.00693
Rate	-	0.90255	0.93661	0.96419	0.98097
$\|\boldsymbol{\nabla} C - \boldsymbol{\nabla} C_h\|_{0,0}$	0.154705	0.0827994	0.0432733	0.0222213	0.0113464
Rate	-	0.90183	0.93614	0.96153	0.96971
$\|C - C_h\|_{0,1}$	0.181798	0.0972866	0.0508403	0.0260938	0.0132953
Rate	-	0.90202	0.93627	0.96227	0.97279

Table 3: Temporal convergence rates for the BE approximation with an affine adsorption model to the non-steady-state problem.

$(h, \Delta t) \ \rightarrow$	$(\frac{1}{128}, \frac{1}{2})$	$(\frac{1}{128}, \frac{1}{4})$	$(\frac{1}{128}, \frac{1}{8})$	$(\frac{1}{128}, \frac{1}{16})$	$(\frac{1}{128}, \frac{1}{32})$
$\|C - C_h\|_{\infty,0}$	0.0362764	0.00901857	0.00224664	0.000561211	0.000140536
Rate	-	2.0081	2.0051	2.0012	1.9976
$\|C - C_h\|_{0,0}$	0.0306995	0.00722705	0.00174822	0.000429612	0.000106604
Rate	-	2.0867	2.0475	2.0248	2.0108
$\|\boldsymbol{\nabla} C - \boldsymbol{\nabla} C_h\|_{0,0}$	0.712515	0.177229	0.0439172	0.0108973	0.00307773
Rate	-	2.0073	2.0128	2.0108	1.824
$\|C - C_h\|_{0,1}$	0.713176	0.177376	0.043952	0.0109057	0.00307958
Rate	-	2.0074	2.0128	2.0108	1.8243

Table 4: Temporal convergence rates for the midpoint approximation with an affine adsorption model to the non-steady-state problem.

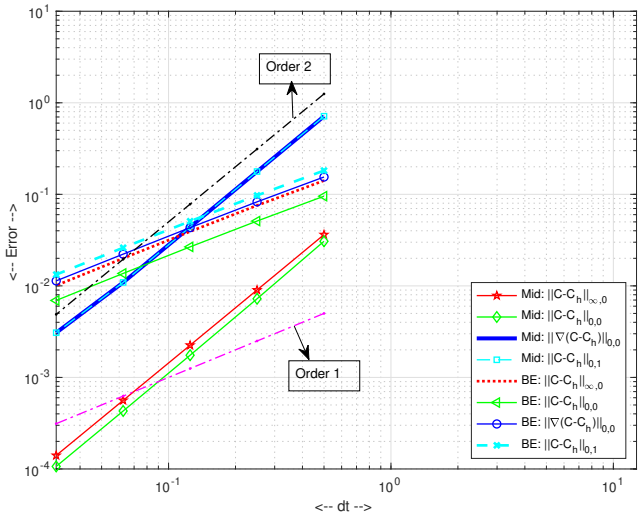

Figure 6: Affine Isotherm: Temporal rate of convergence of BE and Midpoint, $T = 1.0$, $h = 1/128$. Notice that Midpoint is giving order 2 whereas BE is giving order 1.

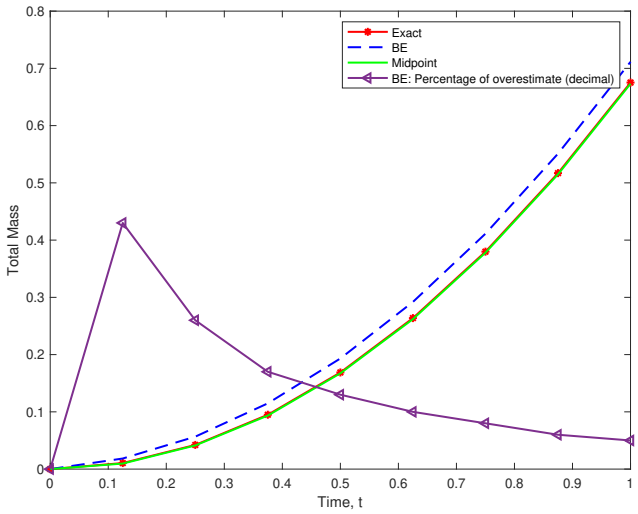

Figure 7: Affine Isotherm: Comparison of total mass for exact solution, BE, Midpoint, $T = 1.0$, $h = 1/128$, $dt = 1/8$. Notice that BE overestimates total mass rather than underestimates.

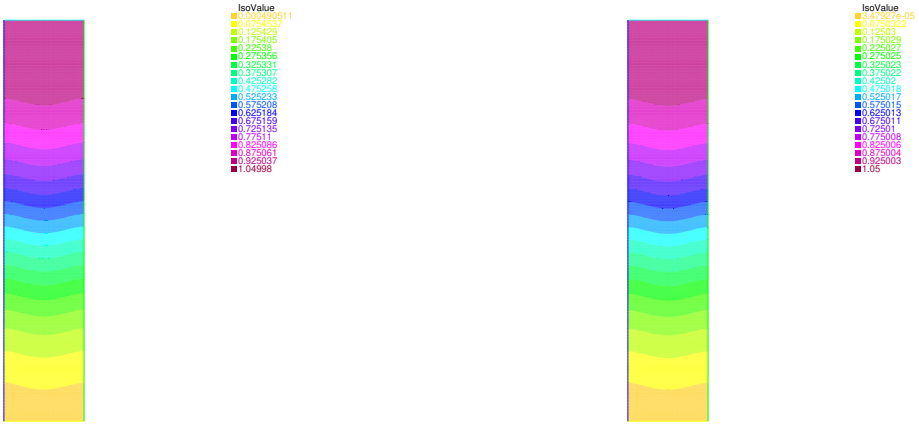

Figure 8: Affine isotherm: Plot of concentration while using BE (Left) & Midpoint (Right), $f = 0$, $g = 1$, $T = 3.0$, $h = 1/128$, $dt = 1/128$, $\mathbf{u} = (0, 2x(x-2))$, $D = I$.

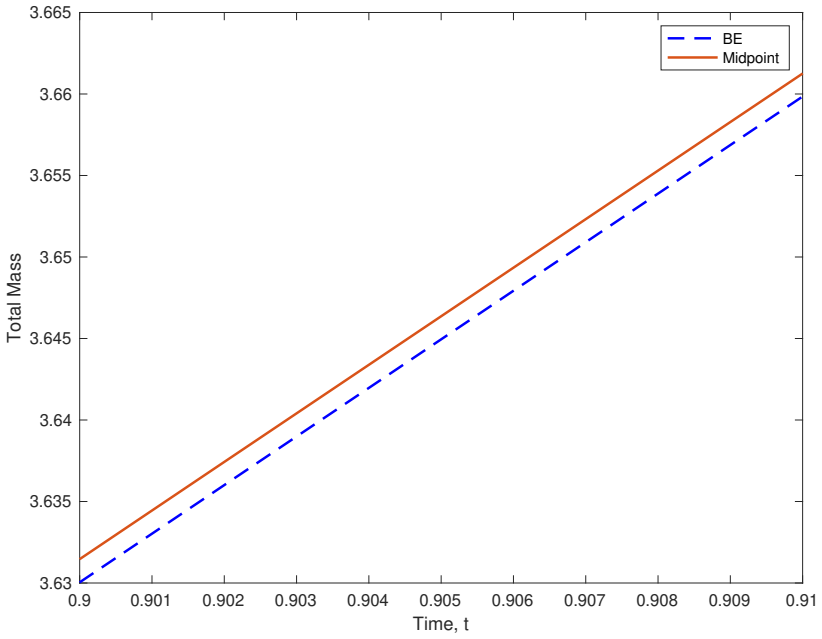

Figure 9: Affine isotherm: Comparison of total mass, $f = 0$, $g = 1$, $T = 3.0$, $h = 1/128$, $dt = 1/128$, $\mathbf{u} = (0, 2x(x-2))$, $D = I$.

2.5.3 Tests for the case of nonlinear, explicit isotherm

In this subsection, we first check the convergence rate for the case of nonlinear, explicit isotherm in the first test, and in the second test, we plot the concentration profile. We also show the comparison of total mass ($\int_\Omega(\omega C + (1-\omega)\rho_s q(C))d\Omega$) after each test. In these test problems, we use Langmuir's isotherm with $q_{max} = K_{eq} = 1$ where $q(C) = \frac{q_{max}K_{eq}C}{1+K_{eq}C} = \frac{C}{1+C}$. We simplify the problem formulation to a single (nonlinear) transport equation in one unknown C using

$$\frac{\partial q}{\partial t} = \frac{\partial q}{\partial C}\frac{\partial C}{\partial t} = \frac{1}{(1+C)^2}\frac{\partial C}{\partial t}.$$

While using Backward Euler discretization, we compute solutions by lagging the nonlinearity $q'(C_h^{n+1})$ as [49]

$$q'(C_h^{n+1})\frac{C_h^{n+1} - C_h^n}{\Delta t} \approx q'(C_h^n)\frac{C_h^{n+1} - C_h^n}{\Delta t}.$$

For the midpoint method, we use the standard (second order) linear extrapolation [95] of $C_h^{n+1/2}$ while computing $q'(C_h^{n+1/2})$ as

$$q'(C_h^{n+1/2})\frac{C_h^{n+1}-C_h^n}{\Delta t} \approx q'(\frac{3C_h^n - C_h^{n-1}}{2})\frac{C_h^{n+1}-C_h^n}{\Delta t}.$$

$(h, \Delta t) \ \rightarrow$	$(\frac{1}{128}, \frac{1}{2})$	$(\frac{1}{128}, \frac{1}{4})$	$(\frac{1}{128}, \frac{1}{8})$	$(\frac{1}{128}, \frac{1}{16})$	$(\frac{1}{128}, \frac{1}{32})$
$\|C - C_h\|_{\infty,0}$	0.0636074	0.0374917	0.0206665	0.0108985	0.00558454
Rate	-	0.76262	0.85928	0.92316	0.96462
$\|C - C_h\|_{0,0}$	0.0522838	0.0310798	0.0169125	0.00883222	0.00451535
Rate	-	0.75039	0.87789	0.93724	0.96794
$\|\boldsymbol{\nabla} C - \boldsymbol{\nabla} C_h\|_{0,0}$	0.0847469	0.0502647	0.0273473	0.0143409	0.00746467
Rate	-	0.75362	0.87815	0.93126	0.94199
$\|C - C_h\|_{0,1}$	0.0995773	0.0590973	0.0321544	0.0168424	0.00872408
Rate	-	0.75272	0.87808	0.93292	0.94902

Table 5: Temporal convergence rates for the BE approximation with a Langmuir adsorption model to the non-steady-state problem.

$(h, \Delta t) \ \rightarrow$	$(\frac{1}{128}, \frac{1}{2})$	$(\frac{1}{128}, \frac{1}{4})$	$(\frac{1}{128}, \frac{1}{8})$	$(\frac{1}{128}, \frac{1}{16})$	$(\frac{1}{128}, \frac{1}{32})$
$\|C - C_h\|_{\infty,0}$	0.0357416	0.00951864	0.00242801	0.000611192	0.000153313
Rate	-	1.9088	1.971	1.9901	1.9951
$\|C - C_h\|_{0,0}$	0.0307399	0.00741601	0.00181065	0.00044712	0.000111214
Rate	-	2.0514	2.0341	2.0178	2.0073
$\|\boldsymbol{\nabla} C - \boldsymbol{\nabla} C_h\|_{0,0}$	0.744766	0.191186	0.0475431	0.0117471	0.00323681
Rate	-	1.9618	2.0077	2.0169	1.8597
$\|C - C_h\|_{0,1}$	0.7454	0.19133	0.0475776	0.0117556	0.00323872
Rate	-	1.962	2.0077	2.0169	1.8599

Table 6: Temporal convergence rates for the midpoint approximation with a Langmuir adsorption model to the non-steady-state problem.

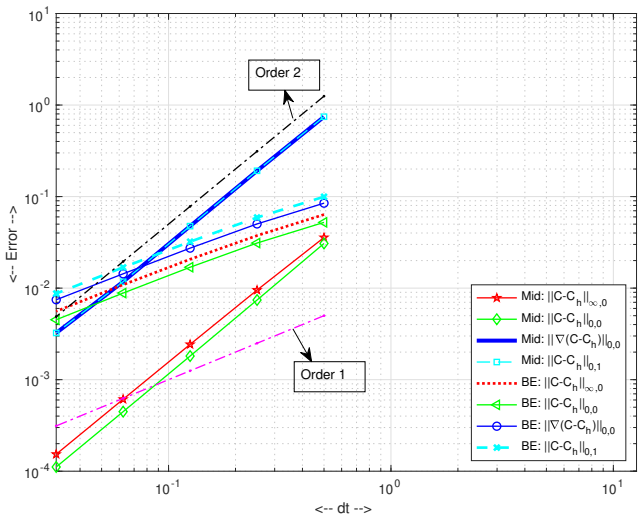

Figure 10: Langmuir Isotherm: Temporal rate of convergence of BE and Midpoint, $T = 1.0$, $h = 1/128$. Notice that Midpoint is giving order 2 whereas BE is giving order 1.

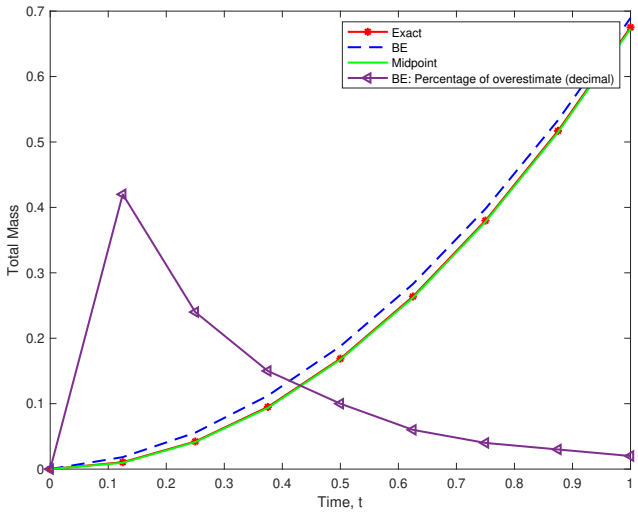

Figure 11: Langmuir Isotherm: Comparison of total mass for exact solution, BE, Midpoint, $T = 1.0$, $h = 1/128$, $dt = 1/8$. Notice that BE overestimates total mass rather than underestimates.

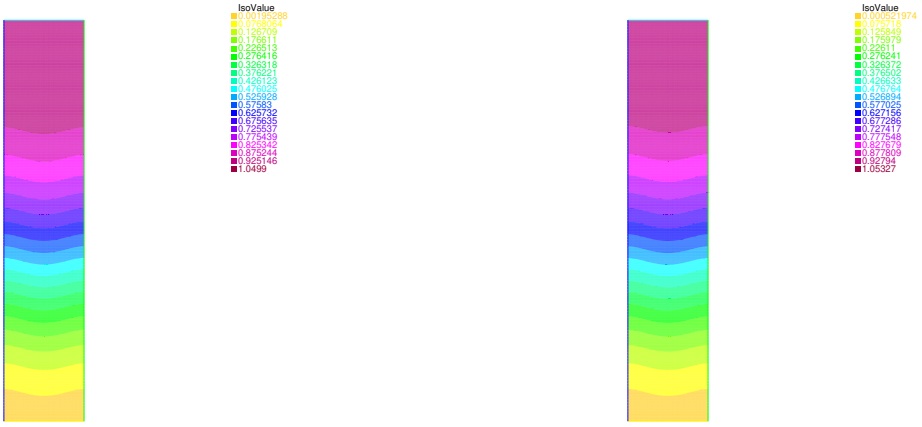

Figure 12: Langmuir isotherm: Plot of concentration while using BE (Left) & Midpoint (Right), $f = 0$, $g = 1$, $T = 3.0$, $h = 1/128$, $dt = 1/128$, $\mathbf{u} = (0, 2x(x-2))$, $D = I$.

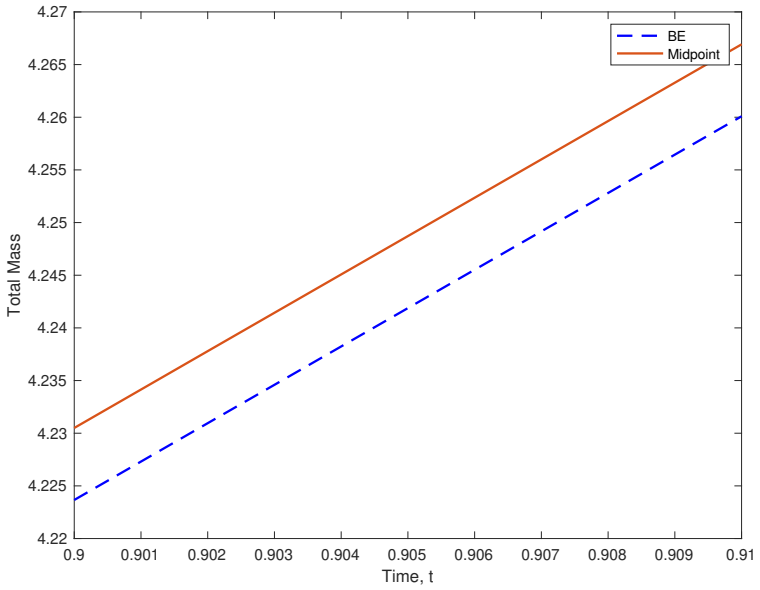

Figure 13: Langmuir isotherm: Comparison of total mass, $f = 0$, $g = 1$, $T = 3.0$, $h = 1/128$, $dt = 1/128$, $\mathbf{u} = (0, 2x(x-2))$, $D = I$.

In Figure 3, Figure 7, and Figure 11, it is observed that the midpoint method gives exact total mass evolution and BE has an error in total mass evolution. In the Figure 4, Figure 8 and Figure 12, the concentration front gradually advances through the height of the membrane over time as it evolves following the contour of the velocity profile. Though we can't visibly see the difference among two plots for BE and midpoint in Figure 4, Figure 8 and Figure 12, we can see the significant difference in total mass evolution in Figure 5, Figure 9, and Figure 13.

3.0 Numerical Analysis of a Corrected Smagorinsky Model

The classical Smagorinsky model's solution is an approximation to a (resolved) mean velocity. Since it is an eddy viscosity model, it cannot represent a flow of energy from unresolved fluctuations to the (resolved) mean velocity. This model has recently been corrected to incorporate this flow and still be well-posed. Herein we first develop some basic properties of the corrected model. Next, we perform a complete numerical analysis of two algorithms for its approximation. They are tested and proven to be effective.

3.1 Introduction

Consider the Smagorinksy model [139][1], with prescribed body force f, kinematic viscosity ν in the regular and bounded flow domain $\Omega \subset \mathbb{R}^d$ $(d = 2,\ 3)$, which was later advanced independently by Ladyzhenskaya [90, 91]: $\boldsymbol{\nabla} \cdot w = 0$ and

$$w_t + w \cdot \boldsymbol{\nabla} w - \nu \Delta w + \boldsymbol{\nabla} q - \boldsymbol{\nabla} \cdot \left((C_s \delta)^2 |\boldsymbol{\nabla} w| \boldsymbol{\nabla} w \right) = f(x). \tag{141}$$

Here (w, q) approximate an ensemble average of Navier-Stokes solutions, $(\overline{u}, \overline{p})$. This is an eddy viscosity model with turbulent viscosity, $\nu_T = (C_s \delta)^2 |\boldsymbol{\nabla} w|$, where $C_s \approx 0.1$, Lilly [107], δ is a length scale (or grid-scale). Like all eddy viscosity models, the Smagorinsky model represents a flow of energy from means to unresolved fluctuations ($u' = u - \overline{u}$, for a precise formula, see Definition 40) and has errors by not representing any intermittent energy flow from fluctuations back to means. Corrections have recently been made representing this flow in Jiang and Layton [78] and Rong, Layton, and Zhao [131]. Following their ideas, we

[1] The mechanically correct formulation is with the $\boldsymbol{\nabla}^s w$ instead of $\boldsymbol{\nabla} w$ in the term $-\boldsymbol{\nabla} \cdot \left((C_s \delta)^2 |\boldsymbol{\nabla} w| \boldsymbol{\nabla} w \right)$ where $\boldsymbol{\nabla}^s$ is the symmetric part of the gradient tensor. But since the estimates are the same and analyses are simpler with $\boldsymbol{\nabla} w$ due to Korn's inequality $\|v\|^2_{H^1(\Omega)} \leq C[\|v\|^2_{L^2(\Omega)} + \|\boldsymbol{\nabla}^s v\|^2_{L^2(\Omega)}]$, we use $\boldsymbol{\nabla} w$ throughout the chapter.

develop a corrected model in Section 3.3. We also analyze and test numerical algorithms for effective approximation of the resulting corrected model: $\boldsymbol{\nabla} \cdot w = 0$ and

$$w_t - C_s^4 \delta^2 \mu^{-2} \Delta w_t + w \cdot \boldsymbol{\nabla} w - \nu \Delta w + \boldsymbol{\nabla} q - \boldsymbol{\nabla} \cdot \Big((C_s \delta)^2 |\boldsymbol{\nabla} w| \boldsymbol{\nabla} w \Big) = f(x). \tag{142}$$

Here μ is a constant from Kolmogorov-Prandtl relation [85, 119].

The main result of this chapter is the complete numerical analysis and computational testing of effective algorithms for this model. This chapter gives detailed numerical analyses in Section 3.4 and Section 3.5. This model can capture the phenomenon of transferring energy from fluctuation to means, which is tested numerically in Section 3.6.2. There were few attempts made to extend the model that represents flow from statistical equilibrium to non-equilibrium. For instance, in a previous work by Jiang and Layton [78], there was an extra fitting parameter β in the second term of (142) which is needlessly complicated. In this work, a different idea results in a simpler model with no new fitting parameters other than from the Smagorinsky model (141).

3.1.1 Related Work

For simulating turbulent flow, there are different approaches, see [57, 63, 109, 116, 128, 146, 152]. A summary of some recent work in eddy viscosity models of turbulence is presented in [79]. One of the recent approaches is by adding a term of Kelvin-Voigt form to the equations for the mean-field [7]. Smagorinsky model is a classical model. Its positive and negative features are well understood. There has been a lot of work correcting negative features, for example, Tommy K. Kim [84] did a different modification than ours which corrects near-wall behavior. The new term in our model has a similarity to the Voigt term used in Voigt/Kelvin-Voigt/Kelvin Model [141] for viscoelastic fluids. There have been lot of recent works on the Voigt Model, see for example [13, 86, 92, 93]. Recently, Rong, Layton and Zhao [131] and Berselli, Lewandowski and Nguyen [17] all studied the extension of the Baldwin & Lomax model [11] to non-equilibrium ($\frac{d}{dt}\overline{\|u'\|^2} \neq 0$, for a precise definition see Remark 43) problems. A variant of the Smagorinsky model and detailed analysis is presented

in chapter [36]. Jiang and Layton [78] derived a corrected eddy viscosity model for flow not at a statistical equilibrium state.

3.2 Notation and Preliminaries

In this section, we introduce some of the notations and results used in this chapter. We denote by $\|\cdot\|$ and $(\cdot,\cdot)$ the $L^2(\Omega)$ norm and inner product, respectively. We denote the $L^p(\Omega)$ norm by $\|\cdot\|_{L^p}$. The solution spaces X for the velocity and Q for the pressure are defined as:

$$X := \{v \in L^3(\Omega) : \boldsymbol{\nabla} v \in L^3(\Omega) \text{ and } v = 0 \text{ on } \partial\Omega\},$$
$$Q := L_0^2(\Omega) = \{q \in L^2(\Omega) : \int_\Omega q \; dx = 0\},$$
$$\text{and} \quad V := \{v \in X : (q, \boldsymbol{\nabla} \cdot v) = 0, \; \forall q \in Q\}.$$

The space $H^{-1}(\Omega)$ denotes the dual space of bounded linear functionals defined on $H_0^1(\Omega) = \{v \in H^1(\Omega) : v = 0 \text{ on } \partial\Omega\}$ and this space is equipped with the norm:

$$\|f\|_{-1} = \sup_{0 \neq v \in X} \frac{(f, v)}{\|\boldsymbol{\nabla} v\|}.$$

The finite element method for this problem involves picking finite element spaces [100] $X^h \subset X$ and $Q^h \subset Q$. We assume that (X^h, Q^h) satisfies the discrete inf-sup condition:

$$\inf_{\lambda^h \in Q^h} \sup_{v^h \in X^h} \frac{(\lambda^h, \boldsymbol{\nabla} \cdot v^h)}{\|\lambda^h\| \|\boldsymbol{\nabla} v^h\|} \geq \beta^h > 0,$$

where β^h is bounded away from zero uniformly in h.

Definition 30. *(Trilinear Form) Define the skew symmetrized trilinear form* $b^* : X \times X \times X \to \mathbb{R}$ *as follows*

$$b^*(u, v, w) := \frac{1}{2}(u \cdot \boldsymbol{\nabla} v, w) - \frac{1}{2}(u \cdot \boldsymbol{\nabla} w, v).$$

Lemma 31. *(p.114, Girault and Raviart [65]) For any $u \in V$ and $v, w \in X$,*

$$b^*(u, v, w) = (u \cdot \boldsymbol{\nabla} v, w), \text{ and } b^*(u, v, v) = 0, \quad \forall\ u,\ v \in X.$$

Lemma 32. *For any $u,\ v,\ w \in X$,*

$$\left| \int_\Omega u \cdot \boldsymbol{\nabla} v \cdot w \ dx \right| \leq C \|\boldsymbol{\nabla} u\| \|\boldsymbol{\nabla} v\| \|\boldsymbol{\nabla} w\|,$$
$$\left| \int_\Omega u \cdot \boldsymbol{\nabla} v \cdot w \ dx \right| \leq C \|u\|^{1/2} \|\boldsymbol{\nabla} u\|^{1/2} \|\boldsymbol{\nabla} v\| \|\boldsymbol{\nabla} w\|.$$

Lemma 33. *(Polarization identity)*

$$(u, v) = \frac{1}{2}\|u\|^2 + \frac{1}{2}\|v\|^2 - \frac{1}{2}\|u - v\|^2. \tag{143}$$

Lemma 34. *(The Poincaré-Friedrichs' inequality) There is a positive constant $C_{PF} = C_{PF}(\Omega)$ such that*

$$\|u\| \leq C_{PF} \|\boldsymbol{\nabla} u\|, \ \ \forall u \in X. \tag{144}$$

Next is a Discrete Gronwall lemma see Lemma 5.1 p.369 [71].

Lemma 35. *Let $\Delta t,\ B,\ a_n,\ b_n, c_n,\ d_n$ for integers $n \geq 0$ be nonnegative numbers such that for $l \geq 1$, if*

$$a_l + \Delta t \sum_{n=0}^{l} b_n \leq \Delta t \sum_{n=0}^{l-1} d_n a_n + \Delta t \sum_{n=0}^{l} c_n + B, \ \text{for } l \geq 0,$$

then for all $\Delta t > 0$,

$$a_l + \Delta t \sum_{n=0}^{l} b_n \leq \exp\left(\Delta t \sum_{n=0}^{l-1} d_n \right) \Big(\Delta t \sum_{n=0}^{l} c_n + B \Big), \ \text{for } l \geq 0.$$

In this chapter, we will need the following well-known lemma, see, e.g., [55, 81, 99]

Lemma 36. *(***Strong Monotonicity (SM) and Local Lipschitz Continuity (LLC)***)*
There exists $C_1,\ C_2 > 0$ such that for all $u,\ v,\ w \in L^3(\Omega),\ \boldsymbol{\nabla} u,\ \boldsymbol{\nabla} v,\ \boldsymbol{\nabla} w \in L^3(\Omega)$

$$\textbf{\textit{(SM)}} \quad (|\boldsymbol{\nabla} u| \boldsymbol{\nabla} u - |\boldsymbol{\nabla} w| \boldsymbol{\nabla} w, \boldsymbol{\nabla}(u - w)) \geq C_1 \|\boldsymbol{\nabla}(u - w)\|^3_{L^3(\Omega)}, \tag{145}$$

$$\textbf{\textit{(LLC)}} \quad (|\boldsymbol{\nabla} u| \boldsymbol{\nabla} u - |\boldsymbol{\nabla} w| \boldsymbol{\nabla} w, \boldsymbol{\nabla} v) \leq C_2 r \|\boldsymbol{\nabla}(u - w)\|_{L^3(\Omega)} \|\boldsymbol{\nabla} v\|_{L^3(\Omega)}, \tag{146}$$

where $r = \max\{\|\boldsymbol{\nabla} u\|_{L^3(\Omega)},\ \|\boldsymbol{\nabla} w\|_{L^3(\Omega)}\}$.

Proposition 37. *(see p.173 [23]) Let $W^{m,p}(\Omega)$ denote the Sobolev space, let $p \in [1, +\infty]$ and $q \in [p, p^*]$, where $\frac{1}{p^\star} = \frac{1}{p} - \frac{1}{d}$ if $p < dim(\Omega) = d$. There is a $C > 0$ such that*

$$\|u\|_{L^q(\Omega)} \leq C\|u\|_{L^p(\Omega)}^{1+d/q-d/p}\|u\|_{W^{1,p}(\Omega)}^{d/p-d/q}, \quad \forall u \in W^{1,p}(\Omega) \tag{147}$$

The weak formulation of (142) is: Find $(w, p) \in (X, Q)$ such that

$$\begin{aligned} (w_t, v) + \frac{C_s^4}{\mu^2}\delta^2(\boldsymbol{\nabla} w_t, \boldsymbol{\nabla} v) + (w \cdot \boldsymbol{\nabla} w, v) + \nu(\boldsymbol{\nabla} w, \boldsymbol{\nabla} v) \\ -(p, \boldsymbol{\nabla} \cdot v) + \Big((C_s\delta)^2|\boldsymbol{\nabla} w|\boldsymbol{\nabla} w, \boldsymbol{\nabla} v\Big) = (f, v) \text{ for all } v \in X, \\ (q, \boldsymbol{\nabla} \cdot w) = 0 \text{ for all } q \in Q. \end{aligned} \tag{148}$$

For the stationary Smagorinsky model, Du and Gunzburger [54, 55] proved that the discrete solution converges to the continuous problem under minimal regularity assumptions. The existence and uniqueness of the strong solution of the Smagorinsky model (141) on a periodic domain have been discussed [101, 103, 108]. Recently, the error estimates for Smagorinsky model have also been studied in [30] and it showed that both the accuracy and the stability are enhanced for flows with high Reynolds numbers. The existence and uniqueness of strong solutions of the incompressible Navier-Stokes-Voigt model is studied in [13].

Here we omit the proof for the existence of a strong solution for the new CSM Model. We assume the model has a solution in the following sense.

Definition 38. *A solution w of the Corrected Smagorinsky Model* (142) *is a strong solution if w satisfies the following*

1. $w \in L^\infty(0, T; H^1(\Omega)) \cap L^2(0, T; W^{1,3}(\Omega)) \cap L^2(0, T; L^6(\Omega))$,
2. $w(x, t) \to w_0(x)$ *in* $L^2(\Omega)$ *as* $t \to 0$,
3. w *satisfies the model's weak form* (148) *for all* $v \in L^\infty(0, T; H^1(\Omega)) \cap L^2(0, T; W^{1,3}(\Omega)) \cap L^2(0, T; L^6(\Omega))$.

Remark 39. *Though the existence of strong solutions is not yet proven for the new model, we believe it is reasonable to assume existence because it is known for the Smagorinsky Model and the extra Voigt term is linear and regularizing.*

Definition 40. *(Mean, Fluctuation and Variance) The ensembles* $u(x,t;\omega_j)$, $j=1,\dots,J$ *where* ω *is a a random variable, mean* $\overline{u}$ *and fluctuation* u' *are defined as follows:*

$$\overline{u}(x,t)=\frac{1}{J}\sum_{j=1}^{J}u(x,t;\omega_j),\quad u'(x,t,\omega_j)=u(x,t;\omega_j)-\overline{u}(x,t).$$

The variance of u *and* $\boldsymbol{\nabla} u$ *are, respectively,*

$$V(u):=\int_\Omega \overline{|u|^2}-|\overline{u}|^2\,dx,\quad V(\boldsymbol{\nabla}u):=\int_\Omega \overline{|\boldsymbol{\nabla}u|^2}-|\boldsymbol{\nabla}\overline{u}|^2\,dx.$$

Definition 41. *(Reynolds Stresses) The Reynolds stresses are*

$$R(u,u):=\overline{u}\otimes\overline{u}-\overline{u\otimes u}=-\overline{u'\otimes u'}.$$

Ensemble averaging satisfies the following properties, e.g., [110, 113, 117]

$$\overline{\overline{u}}=\overline{u},\qquad \overline{u'}=0,\quad \overline{\overline{w}\cdot v}=\overline{w}\cdot\overline{v},\qquad \overline{\overline{w}\cdot v'}=\overline{w}\cdot\overline{v'}=0,$$

$$\overline{\overline{w}\otimes v}=\overline{w}\otimes\overline{v},\qquad \overline{\overline{w}\otimes v'}=\overline{w}\otimes\overline{v'}=0,\quad \frac{\partial}{\partial t}\overline{u}=\overline{\frac{\partial}{\partial t}u},\qquad \frac{\partial}{\partial x}\overline{u}=\overline{\frac{\partial}{\partial x}u}.$$

Theorem 42. *Suppose that each realization is a strong solution of the NSE. The ensemble is generated by different initial data and* $u(x,0;\omega_j)\in L^2(\Omega)$, $f(x,t)\in L^\infty(0,\infty;L^2(\Omega))$. *Then the following two properties are satisfied.*

Property 1 : *(Time averaged dissipativity)*

$$\lim_{T\to\infty}\frac{1}{T}\int_0^T\int_\Omega R(u,u):\boldsymbol{\nabla}\bar{u}\;dxdt=\lim_{T\to\infty}\frac{1}{T}\int_\Omega \nu\overline{|\boldsymbol{\nabla}u'|^2}\;dxdt\geq 0.$$

Property 2 : *(Equation for the evolution of variance of fluctuations)*

$$\int_\Omega R(u,u):\boldsymbol{\nabla}\bar{u}\;dx=\frac{1}{2}\frac{d}{dt}\int_\Omega\overline{|u'|^2}\;dx+\int_\Omega\nu\overline{|\boldsymbol{\nabla}u'|^2}\;dx. \tag{149}$$

Proof. Proof of this theorem can be found in Section 2 of [78]. □

Remark 43. *(Statistical steady state and statistical equilibrium, see [78]) The statistical steady state is* $\mathcal{P}/\epsilon=1$ *where*

$$\epsilon=\textit{dissipation of turbulent kinetic energy (TKE)}=\nu\overline{\|\boldsymbol{\nabla}u'\|^2},$$

$$\mathcal{P}=\textit{production of TKE}=\int_\Omega R(u,u):\boldsymbol{\nabla}\overline{u}dx.$$

Hence, $\frac{\mathcal{P}}{\epsilon}=1$ *implies* $\int_\Omega R(u,u):\boldsymbol{\nabla}\overline{u}\;dx=\int_\Omega\nu\overline{|\boldsymbol{\nabla}u'|^2}\;dx$.

3.3 Model derivation

In this section, we develop a model for turbulence not at statistical equilibrium unlike the Smagorinsky model (141).

Consider the Navier-Stokes Equations (NSE) which govern the flow of an incompressible fluid with velocity $u(x,t)$, pressure $p(x,t)$, prescribed body force f and kinematic viscosity ν in the regular and bounded flow domain $\Omega \subset \mathbb{R}^d (d = 2,\ 3)$:

$$u_t + u \cdot \boldsymbol{\nabla} u - \nu \Delta u + \boldsymbol{\nabla} p = f(x) \text{ in } \Omega, \text{ and } \boldsymbol{\nabla} \cdot u = 0 \text{ in } \Omega. \tag{150}$$

To derive the Corrected Smagorinsky model, following the work in [78], we begin with an ensemble of NSE solution $u(x,t;w_j)$ with perturbed initial data $u(x,0;\omega_j) = u_0(x;\omega_j),\ j = 1,\ 2, \ldots,\ J,\ x \in \Omega$.

The goal of a turbulent model solution of (141) and (142) is to approximate $\overline{u}(x,t)$. By ensemble averaging the NSE gives a system that is not closed since $\overline{uu} \neq \bar{u}\bar{u}$. Hence the Reynolds stress tensor, $R(u,u) = \bar{u}\bar{u} - \overline{uu}$ which is accountable for all effects of the fluctuations on the mean flow must be modeled [131]. We rewrite $\overline{uu}$ as $\overline{uu} = \bar{u}\bar{u} - R(u,u)$. Note that by using properties in (41), we get $R = -\overline{u'u'}$. Hence we get,

$$\overline{u_t} + \bar{u} \cdot \boldsymbol{\nabla} \bar{u} - \nu \Delta \bar{u} + \boldsymbol{\nabla} \bar{p} - \boldsymbol{\nabla} \cdot R = f(x) \text{ in } \Omega, \text{ and } \boldsymbol{\nabla} \cdot \bar{u} = 0 \text{ in } \Omega. \tag{151}$$

Take the dot product of the first and second equation in ((151)) with mean flow $\bar{u}$ and $\bar{p}$ respectively and doing integration by parts, we get the energy estimate as follows [78, 131]

$$\underbrace{\frac{1}{2}\frac{d}{dt}\|\bar{u}\|^2}_{\text{rate of change of kinetic energy}} + \underbrace{\nu\|\boldsymbol{\nabla}\bar{u}\|^2}_{\text{energy dissipation due to viscous forces}} + \underbrace{\int_\Omega R(u,u) : \boldsymbol{\nabla}\bar{u}\ dx}_{\text{effect of fluctuation}} = \underbrace{(f,\bar{u}).}_{\text{energy input through body force-flow interaction}} \tag{152}$$

In ((152)), if the term $\int_\Omega R(u,u) : \boldsymbol{\nabla}\bar{u}\ dx > 0$, the effect of $R(u,u)$ is dissipative while if $\int_\Omega R(u,u) : \boldsymbol{\nabla}\bar{u}\ dx < 0$, fluctuations u' transfers energy back to mean $\bar{u}$ which causes increased energy in mean flow.

Property 1 in Theorem 42 is consistent with the assumption of Boussinesq [22] that turbulent fluctuations are dissipative on the mean in the time-averaged case. In property 2 of Theorem 42, the term $\int_\Omega \nu\overline{|\boldsymbol{\nabla} u'|^2}\, dx$ is clearly dissipative while $\frac{d}{dt}\int_\Omega \overline{|u'|^2}\, dx = 0$ for flows at statistical equilibrium. The idea of any EV model is based on three assumptions [78]. Firstly, the statistical equilibrium assumption that dissipativity holds at each instant time

$$\int_\Omega R(u,u) : \boldsymbol{\nabla}\bar{u}\, dx \simeq \int_\Omega \nu\overline{|\boldsymbol{\nabla} u'|^2}\, dx. \tag{153}$$

The second assumption is that $\boldsymbol{\nabla} u'$ aligns with $\boldsymbol{\nabla}\bar{u}$. Third, calibration [78] provides that the action of fluctuating velocities can be represented in terms of mean flow

$$action(\boldsymbol{\nabla} u') \simeq a(\bar{u})\boldsymbol{\nabla}\bar{u}.$$

Combining all these three assumptions results in the eddy viscosity closure,

$$-\boldsymbol{\nabla}\cdot R(u,u) \Leftarrow -\boldsymbol{\nabla}\cdot(\nu_T(\bar{u})\boldsymbol{\nabla}\bar{u}) + \text{terms incorporated in } \boldsymbol{\nabla}\bar{p}.$$

Here ν_T denotes the turbulent viscosity. Thus we have the eddy viscosity (EV) model: $\boldsymbol{\nabla}\cdot w = 0$ and

$$w_t + w\cdot\boldsymbol{\nabla} w - \nu\Delta w + \boldsymbol{\nabla} q - \boldsymbol{\nabla}\cdot(\nu_T(w)\boldsymbol{\nabla} w) = f(x). \tag{154}$$

The solution (w,q) of ((154)) is an approximation of the ensemble average $(\bar{u},\bar{p})$. In 1963, Smagorinsky [139] model ν_T by

$$\nu_T = (C_s\delta)^2|\boldsymbol{\nabla} w|, \tag{155}$$

where $C_s \approx 0.1$, Lilly [107]. Let Δx to be the mesh size and $\delta = \Delta x << 1$ is the model length scale [140]. Thus we get the classic Smagorinsky model (141).

By taking the dot product with w, here we have the energy equality for Smagorinsky model:

$$\frac{1}{2}\frac{d}{dt}\|w\|^2 + \nu\|\boldsymbol{\nabla} w\|^2 + (C_s\delta)^2\|\boldsymbol{\nabla} w\|^3_{L^3} = (f,w).$$

$(C_s\delta)^2\|\boldsymbol{\nabla} w\|^3 \geq 0$ approximates the average energy dissipated by fluctuation. Since it is positive, it prevents the energy from returning to the mean flow. We aim to remove this flaw

in the corrected model. Notice that in (153), the term $\frac{d}{dt}\int_\Omega \overline{|u'|^2}\,dx$ is omitted for flows at statistical equilibrium. This term is accountable for backscatter and other non-equilibrium effects. To model this term, we must express u' in terms of $\bar{u}$. One idea in [78] is that since the Smagorinsky model is dimensionally consistent, it must conform to the Kolmogorov-Prandtl relation [85, 119]

$$\nu_T = \mu l\sqrt{k'}, \tag{156}$$

where $\mu \approx 0.3$ to 0.55, l = turbulent length scale and k' is the turbulent kinetic energy: $k'(x,t) = \frac{1}{2}\overline{|u'(x,t)|^2}$. Thus, the Smagorinsky model contains an implicit model of l and k'. Equating (155) with (156) gives

$$\mu l\sqrt{k'} = \nu_T = (C_s\delta)^2|\boldsymbol{\nabla} w| = \mu\delta\Big(\frac{C_s^2\delta}{\mu}|\boldsymbol{\nabla} w|\Big).$$

Here δ is the obvious choice for l. With $\delta = l$, the Smagorinsky Model yields the model $k' = C_s^4\delta^2\mu^{-2}|\boldsymbol{\nabla} w|^2$. Hence, the omitted term responsible for non-equilibrium effects is modeled as

$$\frac{d}{dt}\int_\Omega k'\,dx = \frac{d}{dt}C_s^4\delta^2\mu^{-2}(\boldsymbol{\nabla} w, \boldsymbol{\nabla} w) = C_s^4\delta^2\mu^{-2}(-\Delta w_t, w).$$

By including $C_s^4\delta^2\mu^{-2}\Delta w_t$ in the model, its energy balance has a consistent representation of the term $\frac{1}{2}\frac{d}{dt}\overline{\|u'\|^2}$. As a result, the Corrected Smagorinsky Model (CSM) is: $\boldsymbol{\nabla}\cdot w = 0$ and

$$w_t - C_s^4\delta^2\mu^{-2}\Delta w_t + w\cdot\boldsymbol{\nabla} w - \nu\Delta w + \boldsymbol{\nabla} q - \boldsymbol{\nabla}\cdot\Big((C_s\delta)^2|\boldsymbol{\nabla} w|\boldsymbol{\nabla} w\Big) = f(x). \tag{157}$$

Here we impose the no-slip boundary condition, $w = 0$ on $\partial\Omega$.

3.4 Basic Properties of the Model

In this section, we develop some basic properties of the model which are useful in numerical analysis. In particular, we derive the basic energy estimate, we prove a stability bound and the uniqueness of the solution. We also analyze the modeling error and numerical error of the model.

3.4.1 Energy Estimate for the CSM

We will identify the model's kinetic energy and energy dissipation in Theorem 44.

Theorem 44. *Let w be a strong solution of the Corrected Smagorinsky Model* (157)*, then the following energy estimate holds*

$$\begin{aligned} &\frac{1}{2}\frac{1}{|\Omega|}\frac{d}{dt}\Big(\|w\|^2+\frac{C_s^4\delta^2}{\mu^2}\|\boldsymbol{\nabla} w\|^2\Big)\\ &+\frac{1}{|\Omega|}\nu\|\boldsymbol{\nabla} w\|^2+\frac{1}{|\Omega|}(C_s\delta)^2\|\boldsymbol{\nabla} w\|_{L^3}^3=\frac{1}{|\Omega|}\langle f,w\rangle. \end{aligned} \tag{158}$$

Proof. First, we take dot product in ((157)) with w and do integration by parts which is shown below,

$$\begin{aligned} &\int_\Omega\Big(w_t-C_s^4\delta^2\mu^{-2}\Delta w_t+w\cdot\boldsymbol{\nabla} w-\nu\Delta w+\boldsymbol{\nabla} q-\boldsymbol{\nabla}\cdot\Big((C_s\delta)^2|\boldsymbol{\nabla} w|\boldsymbol{\nabla} w\Big)\Big)\cdot w dx\\ &=\int_\Omega f\cdot w\ dx. \end{aligned}$$

Here, $\int_\Omega w_t\cdot w\ dx=\frac{d}{dt}\Big(\frac{1}{2}\int_\Omega|w|^2\ dx\Big)$. By Lemma (31), $\int_\Omega w\cdot\boldsymbol{\nabla} w\cdot w\ dx=0$. Next, $-\nu\int_\Omega\Delta w\cdot w\ dx=\int_\Omega\nu|\boldsymbol{\nabla} w|^2\ dx$. The next term, $\int_\Omega\boldsymbol{\nabla} q\cdot w\ dx=\int_{\partial\Omega}pw\cdot\hat{n}\ \ ds-\int_\Omega p\boldsymbol{\nabla}\cdot w\ dx=0$. The final term,

$$\int_\Omega-\boldsymbol{\nabla}\cdot\big((C_s\delta)^2|\boldsymbol{\nabla} w|\boldsymbol{\nabla} w\big)\,w\ dx=\int_\Omega(C_s\delta)^2|\boldsymbol{\nabla} w|\boldsymbol{\nabla} w\cdot\boldsymbol{\nabla} w\ dx=\int_\Omega(C_s\delta)^2|\boldsymbol{\nabla} w|^3\ dx.$$

Hence combining all these terms we get the following energy estimate per unit volume,

$$\frac{1}{2}\frac{1}{|\Omega|}\frac{d}{dt}\Big(\|w\|^2+\frac{C_s^4\delta^2}{\mu^2}\|\boldsymbol{\nabla} w\|^2\Big)$$
$$+\frac{1}{|\Omega|}\nu\|\boldsymbol{\nabla} w\|^2+\frac{1}{|\Omega|}(C_s\delta)^2\|\boldsymbol{\nabla} w\|_{L^3}^3=\frac{1}{|\Omega|}\langle f,w\rangle.$$

□

Remark 45. *In* (158)*, we can identify the following quantities:*

1. *Model kinetic energy of mean flow per unit volume*

$$MKE:=\frac{1}{2}\frac{1}{|\Omega|}\Big(\|w\|^2+\frac{C_s^4}{\mu^2}\delta^2\|\boldsymbol{\nabla} w\|^2\Big).$$

   The second term in MKE coming from the Corrected Smagorinsky Model is the turbulent kinetic energy per unit volume.

2. *Rate of energy dissipation of mean flow per unit volume*

$$\varepsilon_{CSM}(t):=\frac{1}{|\Omega|}\Big(\nu\|\boldsymbol{\nabla} w\|^2+(C_s\delta)^2\|\boldsymbol{\nabla} w\|_{L^3}^3\Big).$$

   This controls the time rate of change of kinetic energy. It's always positive and it reduces the accumulation of kinetic energy.

3. *Rate of energy input to mean flow per unit volume is* $\frac{1}{|\Omega|}\langle f,w\rangle$.

3.4.2 Stability

Next, we give the stability bound of the Corrected Smagorinsky Model (157) in Theorem 46. We prove the model kinetic energy is bounded uniformly in time and the time-averaged model energy dissipation rate is bounded as well in the same Theorem.

Theorem 46. *(Stability of w)* (157) *is unconditionally stable. The solution w of* (157) *satisfies the following inequality*

$$\|w(T)\|^2 + \frac{C_s^4}{\mu^2}\delta^2\|\boldsymbol{\nabla} w(T)\|^2 \leq e^{-\alpha T}\Big\{\|w(0)\|^2 + \frac{C_s^4}{\mu^2}\delta^2\|\boldsymbol{\nabla} w(0)\|^2 + \frac{C}{\alpha}(e^{\alpha T}-1)\Big\},$$

where $\alpha = \min\{\frac{\nu}{2C_{PF}^2},\ \frac{\mu^2\nu}{C_s^4\delta^2}\}$, *and if* $f \in L^2(\Omega)$, *we get*

$$\max_{0\leq t<\infty}\Big(\|w\|^2 + \frac{C_s^4\delta^2}{\mu^2}\|\boldsymbol{\nabla} w\|^2\Big) \leq C' < \infty.$$

and

$$\mathcal{O}(\frac{1}{T}) + \frac{1}{|\Omega|}\frac{1}{T}\int_0^T \Big(\frac{\nu}{2}\|\boldsymbol{\nabla} w\|^2 + (C_s\delta)^2\|\boldsymbol{\nabla} w\|_{L^3}^3\Big)\ dt \leq \frac{1}{|\Omega|}\frac{1}{T}\int_0^T \frac{C_{PF}^2}{2\nu}\|f\|^2\ dt.$$

Proof. Take L^2 inner product of (157) with w, we get the following energy equality,

$$\frac{1}{2}\frac{d}{dt}\Big(\|w\|^2 + \frac{c_s^4}{\mu^2}\delta^2\|\boldsymbol{\nabla} w\|^2\Big) + \nu\|\boldsymbol{\nabla} w\|^2 + (C_s\delta)^2\|\boldsymbol{\nabla} w\|_{L^3}^3 = (f, w). \tag{159}$$

Consider the RHS of (159), $(f,w) \leq \frac{\epsilon}{2}\|w\|^2 + \frac{1}{2\epsilon}\|f\|^2$. Thus (159) implies

$$\frac{d}{dt}\Big(\|w\|^2 + \frac{C_s^4}{\mu^2}\delta^2\|\boldsymbol{\nabla} w\|^2\Big) + \nu\|\boldsymbol{\nabla} w\|^2 + \nu\|\boldsymbol{\nabla} w\|^2 + 2(C_s\delta)^2\|\boldsymbol{\nabla} w\|_{L^3}^3 \leq \epsilon\|w\|^2 + \frac{1}{\epsilon}\|f\|^2.$$

Using the inequality $\|w\| \leq C_{PF}\|\boldsymbol{\nabla} w\|$, we have

$$\frac{d}{dt}\Big(\|w\|^2 + \frac{C_s^4}{\mu^2}\delta^2\|\boldsymbol{\nabla} w\|^2\Big) + \frac{\nu}{C_{PF}^2}\|w\|^2 + \nu\|\boldsymbol{\nabla} w\|^2 + 2(C_s\delta)^2\|\boldsymbol{\nabla} w\|_{L^3}^3 \leq \epsilon\|w\|^2 + \frac{1}{\epsilon}\|f\|^2.$$

Pick $\epsilon = \frac{\nu}{2C_{PF}^2}$ and drop the term $2(C_s\delta)^2\|\boldsymbol{\nabla} w\|_{L^3}^3$. We obtain

$$\frac{d}{dt}\Big(\|w\|^2 + \frac{C_s^4}{\mu^2}\delta^2\|\boldsymbol{\nabla} w\|^2\Big) + \frac{\nu}{2C_{PF}^2}\|w\|^2 + \frac{\mu^2}{C_s^4\delta^2}\nu\Big(\frac{C_s^4}{\mu^2}\delta^2\|\boldsymbol{\nabla} w\|^2\Big) \leq \frac{2}{\nu}C_{PF}^2\|f\|^2.$$

Let $\alpha = \min\{\frac{\nu}{2C_{PF}^2},\ \frac{\mu^2}{C_s^4\delta^2}\nu\}$, resulting in

$$\frac{d}{dt}\Big(\|w\|^2 + \frac{C_s^4}{\mu^2}\delta^2\|\boldsymbol{\nabla} w\|^2\Big) + \alpha\Big(\|w\|^2 + \frac{C_s^4}{\mu^2}\delta^2\|\boldsymbol{\nabla} w\|^2\Big) \leq \frac{2}{\nu}C_{PF}^2\|f\|^2.$$

Multiply by the integrating factor $e^{\alpha t}$ and integrate from $t = 0$ to $t = T$, leading to

$$\|w(T)\|^2 + \frac{C_s^4}{\mu^2}\delta^2\|\boldsymbol{\nabla} w(T)\|^2 \leq e^{-\alpha T}\Big\{\|w(0)\|^2 + \frac{C_s^4}{\mu^2}\delta^2\|\boldsymbol{\nabla} w(0)\|^2 + \frac{C}{\alpha}(e^{\alpha T} - 1)\Big\},$$

where $C = \frac{2}{\nu}C_{PF}^2\|f\|^2$.

This implies that kinetic energy is uniformly bounded, i.e. if $f \in L^2(\Omega)$, we get

$$\max_{0\leq t<\infty}\Big(\|w\|^2 + \frac{C_s^4\delta^2}{\mu^2}\|\boldsymbol{\nabla} w\|^2\Big) \leq C' < \infty.$$

Integrate (159) from $t = 0$ to $t = T$ and divide by $|\Omega|$ and T, we have

$$\begin{aligned}\frac{1}{|\Omega|}\frac{1}{2T}\Big\{\Big(\|w(T)\|^2 + \frac{C_s^4}{\mu^2}\delta^2\|\boldsymbol{\nabla} w(T)\|^2\Big) - \Big(\|w(0)\|^2 + \frac{C_s^4}{\mu^2}\delta^2\|\boldsymbol{\nabla} w(0)\|^2\Big)\Big\} \\ + \frac{1}{|\Omega|}\frac{1}{T}\int_0^T \Big(\nu\|\boldsymbol{\nabla} w\|^2 + (C_s\delta)^2\|\boldsymbol{\nabla} w\|_{L^3}^3\Big)\ dt = \frac{1}{|\Omega|}\frac{1}{T}\int_0^T (f, w)\ dt.\end{aligned} \tag{160}$$

Consider the term on the right. Using the Poincaré-Friedrichs' inequality (144), Cauchy Schwarz and Young's inequality gives

$$\begin{aligned}\frac{1}{|\Omega|}\frac{1}{T}\int_0^T (f, w)\ dt &\leq \frac{1}{|\Omega|}\frac{1}{T}\int_0^T \frac{1}{\sqrt{\nu}}\|f\|C_{PF}\sqrt{\nu}\|\boldsymbol{\nabla} w\|\ dt, \\ &\leq \frac{1}{|\Omega|}\frac{1}{T}\int_0^T \frac{\nu}{2}\|\boldsymbol{\nabla} w\|^2\ dt + \frac{1}{|\Omega|}\frac{1}{T}\int_0^T \frac{C_{PF}^2}{2\nu}\|f\|^2\ dt.\end{aligned}$$

The first term in (160) is bounded by the previous result. Thus,

$$\mathcal{O}(\frac{1}{T}) + \frac{1}{|\Omega|}\frac{1}{T}\int_0^T \Big(\frac{\nu}{2}\|\boldsymbol{\nabla} w\|^2 + (C_s\delta)^2\|\boldsymbol{\nabla} w\|_{L^3}^3\Big)\ dt \leq \frac{1}{|\Omega|}\frac{1}{T}\int_0^T \frac{C_{PF}^2}{2\nu}\|f\|^2\ dt.$$

The time-averaged dissipation is bounded. □

3.4.3 Uniqueness

In this subsection, we prove the uniqueness of the strong solution to (157) in Theorem 47.

Theorem 47. *The solution w of* (157) *is unique.*

Proof. Suppose (w_1, q_1) and (w_2, q_2) are two different solution of (157) and let $\phi,\ q$ denote the difference between two solutions: $\phi = w_1 - w_2$, $q = q_1 - q_2$, ϕ satisfies $\boldsymbol{\nabla} \cdot \phi = 0$ and

$$\frac{\partial}{\partial t}\left(\phi - \frac{C_s^4}{\mu^2}\delta^2\Delta\phi\right) + w_1 \cdot \boldsymbol{\nabla} w_1 - w_2 \cdot \boldsymbol{\nabla} w_2 - \nu\Delta\phi + \boldsymbol{\nabla} q$$
$$-(C_s\delta)^2\boldsymbol{\nabla} \cdot (|\boldsymbol{\nabla} w_1|\boldsymbol{\nabla} w_1 - |\boldsymbol{\nabla} w_2|\boldsymbol{\nabla} w_2) = 0.$$

Take the L^2 inner product with ϕ and let $\tilde{w}$ represent either w_1 or w_2, we obtain

$$\frac{1}{2}\frac{d}{dt}\left(\|\phi\|^2 + \frac{C_s^4}{\mu^2}\delta^2\|\boldsymbol{\nabla}\phi\|^2\right) + \nu\|\boldsymbol{\nabla}\phi\|^2$$
$$+(C_s\delta)^2\int_\Omega [|\boldsymbol{\nabla} w_1|\boldsymbol{\nabla} w_1 - |\boldsymbol{\nabla} w_2|\boldsymbol{\nabla} w_2] \cdot \boldsymbol{\nabla}(w_1 - w_2)\ dx = -\int_\Omega \phi \cdot \boldsymbol{\nabla}\tilde{w} \cdot \phi\ dx.$$

Using the Strong Monotonicity (145), we get

$$\frac{1}{2}\frac{d}{dt}\left(\|\phi\|^2 + \frac{C_s^4}{\mu^2}\delta^2\|\boldsymbol{\nabla}\phi\|^2\right) + \nu\|\boldsymbol{\nabla}\phi\|^2 + C_1(C_s\delta)^2\|\boldsymbol{\nabla}\phi\|_{L_3}^3 \le -\int_\Omega \phi \cdot \boldsymbol{\nabla} w \cdot \phi\ dx.$$

Consider the RHS, using (147) in 3D space,

$$\left|-\int_\Omega \phi \cdot \boldsymbol{\nabla} w \cdot \phi\ dx\right| \le \|\boldsymbol{\nabla} w\|_{L^3}\|\phi\|_{L^3}^2,$$
$$\le C\|\boldsymbol{\nabla} w\|_{L^3}(\|\phi\|^{1/2}\|\boldsymbol{\nabla}\phi\|^{1/2})^2,$$
$$\le \frac{\epsilon}{2}\|\boldsymbol{\nabla}\phi\|^2 + C(\epsilon)\|\boldsymbol{\nabla} w\|_{L^3}^2\|\phi\|^2.$$

Pick $\epsilon = 2\frac{C_s^4}{\mu^2}\delta^2$, leading to

$$\frac{1}{2}\frac{d}{dt}(\|\boldsymbol{\phi}\|^2 + \frac{C_s^4}{\mu^2}\delta^2\|\boldsymbol{\nabla}\phi\|^2) + \nu\|\boldsymbol{\nabla}\phi\|^2 + C_1(C_s\delta)^2\|\boldsymbol{\nabla}\phi\|_{L^3}^3$$
$$\le \frac{C_s^4}{\mu^2}\delta^2\|\boldsymbol{\nabla}\phi\|^2 + C(\epsilon)\|\boldsymbol{\nabla} w\|_{L^3}^2\|\phi\|^2,$$
$$\le \max\{1, C(\epsilon)\|\boldsymbol{\nabla} w\|_{L^3}^2\}(\frac{C_s^4}{\mu^2}\delta^2\|\boldsymbol{\nabla}\phi\|^2 + \|\phi\|^2).$$

Here $a(t) := \max\{1,\ C(\epsilon)\|\boldsymbol{\nabla} w_1\|_{L^3}^2\} \in L^1(0,T)$, because

$$\begin{aligned}\int_0^T 1 \cdot \|\boldsymbol{\nabla} w_1\|_{L^3}^2\ dt &\leq \left(\int_0^T 1^3\ dt\right)^{1/3} \cdot \left(\int_0^T \|\boldsymbol{\nabla} w_1\|_{L^3}^{2\times\frac{3}{2}}\ dt\right)^{2/3} \\ &= \left(\int_0^T 1^3\ dt\right)^{1/3} \cdot \left(\int_0^T \|\boldsymbol{\nabla} w_1\|_{L^3}^3\ dt\right)^{2/3} < \infty.\end{aligned}$$

Then we can form its antiderivative

$$A(T) := \int_0^T a(t)\ dt < \infty,\ \text{for } \boldsymbol{\nabla} w \in L^3(0,T;L^3(\Omega)).$$

Multiplying through by the integrating factor $e^{-A(t)}$ gives

$$\frac{d}{dt}\left[\frac{1}{2}e^{-A(t)}\left(\|\phi\|^2 + \frac{C_s^4\delta^2}{\mu^2}\|\boldsymbol{\nabla}\phi\|^2\right)\right] + e^{-A(t)}[\nu\|\boldsymbol{\nabla}\phi\|^2 + C_1(C_s\delta)^2\|\boldsymbol{\nabla}\phi\|_{L^3}^3] \leq 0.$$

Then, integrating over $[0,T]$ and multiplying through by $e^{A(t)}$ gives

$$\begin{aligned}\frac{1}{2}\Big(\|\phi(T)\|^2 + \frac{C_s^4}{\mu^2}\delta^2\|\boldsymbol{\nabla}\phi(T)\|^2\Big) + \int_0^T \Big(\nu\|\boldsymbol{\nabla}\phi\|^2 + C_1(C_s\delta)^2\|\boldsymbol{\nabla}\phi\|_{L^3}^3\Big)\ dt \\ \leq e^{A(t)}\frac{1}{2}\Big(\|\phi(0)\|^2 + \frac{C_s^4}{\mu^2}\delta^2\|\boldsymbol{\nabla}\phi(0)\|^2\Big).\end{aligned}$$

□

3.4.4 Modelling error

In this subsection, we analyze the error between the solution to the NSE (150) and the Corrected Smagorinksy Model (157) in Theorem 48.

Theorem 48. *Assume $\boldsymbol{\nabla} u_t \in L^2(\Omega)$ and $\boldsymbol{\nabla} w \in L^2(0,T;L^3)$, let $\phi = u_{NSE} - w_{Smag}$ be the modelling error of the Corrected Smagorinsky, then ϕ satisfies the following:*

$$\begin{aligned}
&\frac{1}{2}\Big(\|\phi(T)\|^2 + \frac{C_s^4}{\mu^2}\delta^2\|\boldsymbol{\nabla}\phi(T)\|^2\Big) + \int_0^T \frac{\nu}{2}\|\boldsymbol{\nabla}\phi\|^2 + \frac{C_1}{2}(C_s\delta)^2\|\boldsymbol{\nabla}\phi\|_{L^3}^3\ dt \\
&\leq C^*\left\{\frac{1}{2}\Big(\|\phi(0)\|^2 + \frac{C_s^4}{\mu^2}\delta^2\|\boldsymbol{\nabla}\phi(0)\|^2\Big) + \int_0^T (C_s\delta)^2\|\boldsymbol{\nabla} u\|_{L^3}^3 + \frac{C_s^4}{\mu^2}\delta^2\|\boldsymbol{\nabla} u_t\|^2\ dt\right\}.
\end{aligned}$$

Here C^* depends on ν, T, $\int_0^T \|\boldsymbol{\nabla} w\|_{L^3}^2\ dt$.

Proof. u_{NSE} satisfies $\boldsymbol{\nabla}\cdot u = 0$ and the following equation

$$\begin{aligned}
u_t + u\cdot\boldsymbol{\nabla} u - \nu\Delta u + \boldsymbol{\nabla} p - (C_s\delta)^2\boldsymbol{\nabla}\cdot(|\boldsymbol{\nabla} u|\boldsymbol{\nabla} u) - \frac{C_s^4}{\mu^2}\delta^2\Delta u_t \\
= f - (C_s\delta)^2\boldsymbol{\nabla}\cdot(|\boldsymbol{\nabla} u|\boldsymbol{\nabla} u) - \frac{C_s^4}{\mu^2}\delta^2\Delta u_t.
\end{aligned} \tag{161}$$

Subtract (157) from (161). We obtain, $\boldsymbol{\nabla}\cdot\phi = 0$ and

$$\begin{aligned}
&\phi_t - \frac{C_s^4}{\mu^2}\delta^2\Delta\phi_t + u\cdot\boldsymbol{\nabla} u - w\cdot\boldsymbol{\nabla} w - \nu\Delta\phi + \boldsymbol{\nabla}(p-q) \\
&-(C_s\delta)^2\boldsymbol{\nabla}\cdot(|\boldsymbol{\nabla} u|\boldsymbol{\nabla} u - |\boldsymbol{\nabla} w|\boldsymbol{\nabla} w) = -(C_s\delta)^2\boldsymbol{\nabla}\cdot(|\boldsymbol{\nabla} u|\boldsymbol{\nabla} u) - \frac{C_s^4}{\mu^2}\delta^2\Delta u_t.
\end{aligned}$$

Here, $u\cdot\boldsymbol{\nabla} u - w\cdot\boldsymbol{\nabla} w = u\cdot\boldsymbol{\nabla} u - u\cdot\boldsymbol{\nabla} w + u\cdot\boldsymbol{\nabla} w - w\cdot\boldsymbol{\nabla} w = u\cdot\boldsymbol{\nabla}\phi + \phi\cdot\boldsymbol{\nabla} w$.
Take L^2 inner product with ϕ gives

$$\begin{aligned}
&\frac{1}{2}\frac{d}{dt}\Big(\|\phi\|^2 + \frac{C_s^4}{\mu^2}\delta^2\|\boldsymbol{\nabla}\phi\|^2\Big) + \int_\Omega \phi\cdot\boldsymbol{\nabla} w\cdot\phi\ dx + \nu\|\boldsymbol{\nabla}\phi\|^2\ dx \\
&\qquad +(C_s\delta)^2\int_\Omega (|\boldsymbol{\nabla} u|\boldsymbol{\nabla} u - |\boldsymbol{\nabla} w|\boldsymbol{\nabla} w)\cdot\boldsymbol{\nabla}(u-w)\ dx \\
&= (C_s\delta)^2\int_\Omega |\boldsymbol{\nabla} u|\boldsymbol{\nabla} u : \boldsymbol{\nabla}\phi\ dx + \frac{C_s^4}{\mu^2}\delta^2\int_\Omega \boldsymbol{\nabla} u_t : \boldsymbol{\nabla}\phi\ dx.
\end{aligned}$$

Using Strong Monotonicity (36), we have

$$\begin{aligned}&\frac{1}{2}\frac{d}{dt}\Big(\|\phi\|^2+\frac{C_s^4}{\mu^2}\delta^2\|\boldsymbol{\nabla}\phi\|^2\Big)+\nu\|\boldsymbol{\nabla}\phi\|^2+C_1(C_s\delta)^2\|\boldsymbol{\nabla}\phi\|_{L^3}^3\\ \leq&-\int_\Omega\phi\cdot\boldsymbol{\nabla}w\cdot\phi\;dx+(C_s\delta)^2\int_\Omega|\boldsymbol{\nabla}u|\boldsymbol{\nabla}u:\boldsymbol{\nabla}\phi\;dx+\frac{C_s^4}{\mu^2}\delta^2\int_\Omega\boldsymbol{\nabla}u_t:\boldsymbol{\nabla}\phi\;dx.\end{aligned}\tag{162}$$

Consider the first term in the RHS, similar to the previous steps

$$\Big|-\int_\Omega\phi\cdot\boldsymbol{\nabla}w\cdot\phi\;dx\Big|\leq\frac{\epsilon_1}{2}\|\boldsymbol{\nabla}\phi\|^2+C(\epsilon_1)\|\boldsymbol{\nabla}w\|_{L^3}^2\|\phi\|^2.$$

The second term in the RHS is

$$\begin{aligned}\Big|(C_s\delta)^2\int_\Omega|\boldsymbol{\nabla}u|\boldsymbol{\nabla}u:\boldsymbol{\nabla}\phi\;dx\Big|&\leq(C_s\delta)^2\|\boldsymbol{\nabla}\phi\|_{L^3}\|\boldsymbol{\nabla}u\|_{L^3}^2,\\ &\leq\frac{\epsilon_2}{3}(C_s\delta)^2\|\boldsymbol{\nabla}\phi\|_{L^3}^3+C(\epsilon_2)(C_s\delta)^2(\|\boldsymbol{\nabla}u\|_{L^3}^2)^{3/2},\\ &=\frac{\epsilon_2}{3}(C_s\delta)^2\|\boldsymbol{\nabla}\phi\|_{L^3}^3+C(\epsilon_2)(C_s\delta)^2\|\boldsymbol{\nabla}u\|_{L^3}^3.\end{aligned}$$

The third term in the RHS satisfies

$$\begin{aligned}\Big|\frac{C_s^4}{\mu^2}\delta^2\int_\Omega\boldsymbol{\nabla}u_t:\boldsymbol{\nabla}\phi\;dx\Big|&\leq\frac{C_s^4}{\mu^2}\delta^2\|\boldsymbol{\nabla}u_t\|\|\boldsymbol{\nabla}\phi\|,\\ &\leq\frac{\epsilon_3}{2}\frac{C_s^4}{\mu^2}\delta^2\|\boldsymbol{\nabla}\phi\|^2+C(\epsilon_3)\frac{C_s^4}{\mu^2}\delta^2\|\boldsymbol{\nabla}u_t\|^2.\end{aligned}$$

Pick $\epsilon_1=\nu,\epsilon_2=\frac{3C_1}{2}$, collect all terms, (162) becomes

$$\begin{aligned}&\frac{1}{2}\frac{d}{dt}\Big(\|\phi\|^2+\frac{C_s^4}{\mu^2}\delta^2\|\boldsymbol{\nabla}\phi\|^2\Big)+\frac{\nu}{2}\|\boldsymbol{\nabla}\phi\|^2+\frac{C_1}{2}(C_s\delta)^2\|\boldsymbol{\nabla}\phi\|_{L^3}^3\\ &\quad\leq\max\Big\{C(\epsilon_1)\|\boldsymbol{\nabla}w\|_{L^3}^2,\frac{\epsilon_3}{2}\Big\}(\|\phi\|^2+\frac{C_s^4}{\mu^2}\delta^2\|\boldsymbol{\nabla}\phi\|^2)\\ &\qquad+C(\epsilon_2)(C_s\delta)^2\|\boldsymbol{\nabla}u\|_{L^3}^3+C(\epsilon_3)\frac{C_s^4}{\mu^2}\delta^2\|\boldsymbol{\nabla}u_t\|^2.\end{aligned}$$

Denote $a(t):=\max\big\{C(\epsilon_1)\|\boldsymbol{\nabla}w\|_{L^3}^2,\ \frac{\epsilon_3}{2}\big\}$ and its antiderivative is given by

$$A(T):=\int_0^T a(t)\;dt<\infty\text{ for }\boldsymbol{\nabla}w\in L^2(0,T;L^3).$$

Multiplying through by the integrating factor $e^{-A(t)}$ gives

$$\frac{d}{dt}\left[\frac{1}{2}e^{-A(t)}\left(\|\phi\|^2+\frac{C_s^4\delta^2}{\mu^2}\|\boldsymbol{\nabla}\phi\|^2\right)\right]+e^{-A(t)}\left[\frac{\nu}{2}\|\boldsymbol{\nabla}\phi\|^2+\frac{C_1}{2}(C_s\delta)^2\|\boldsymbol{\nabla}\phi\|_{L^3}^3\right]$$
$$\leq e^{-A(t)}\left\{C(\epsilon_2)(C_s\delta)^2\|\boldsymbol{\nabla}u\|_{L^3}^3+C(\epsilon_3)\frac{C_s^4\delta^2}{\mu^2}\|\boldsymbol{\nabla}u_t\|^2\right\}.$$

Then, integrating over $[0,T]$ and multiplying through by $e^{A(t)}$ gives

$$\frac{1}{2}\Big(\|\phi(T)\|^2+\frac{C_s^4}{\mu^2}\delta^2\|\boldsymbol{\nabla}\phi\|^2\Big)+\int_0^T\frac{\nu}{2}\|\boldsymbol{\nabla}\phi\|^2+\frac{C_1}{2}(C_s\delta)^2\|\boldsymbol{\nabla}\phi\|_{L^3}^3\,dt$$
$$\leq C(\nu,T,\|\boldsymbol{\nabla}w\|_{L^3})\Big\{\frac{1}{2}\Big(\|\phi(0)\|^2+\frac{C_s^4}{\mu^2}\delta^2\|\boldsymbol{\nabla}\phi(0)\|^2\Big)$$
$$+\int_0^T(C_s\delta)^2\|\boldsymbol{\nabla}u\|_{L^3}^3+\frac{C_s^4}{\mu^2}\delta^2\|\boldsymbol{\nabla}u_t\|^2\,dt\Big\},$$

and $C(\nu,T)$ depends on $\nu,\ T,\ \int_0^T\|\boldsymbol{\nabla}w\|_{L^3}^2\,dt$. □

3.5 Numerical error

Consider the semi-discrete approximation of the CSM (157) with grad-div stabilization. Suppose $w^h(x,0)$ is approximation of $w(x,0)$. The approximate velocity and pressure are maps

$$w^h:[0,T]\to X^h\quad,p^h:(0,T]\to Q^h$$

satisfying

$$(w_t^h,v^h)+\frac{C_s^4}{\mu^2}\delta^2(\boldsymbol{\nabla}w_t^h,\boldsymbol{\nabla}v^h)+b^*(w^h,w^h,v^h)+\nu(\boldsymbol{\nabla}w^h,\boldsymbol{\nabla}v^h)+\gamma(\boldsymbol{\nabla}\cdot w^h,\boldsymbol{\nabla}\cdot v^h)$$
$$-(p^h,\boldsymbol{\nabla}\cdot v^h)+\Big((C_s\delta)^2|\boldsymbol{\nabla}w^h|\boldsymbol{\nabla}w^h,\boldsymbol{\nabla}v^h\Big)=(f,v^h)\text{ for all }v^h\in X^h,\quad(163)$$
$$(q^h,\boldsymbol{\nabla}\cdot w^h)=0\text{ for all }q^h\in Q^h.$$

In this section, we analyze the error between the strong solution to the CSM (157) and the semi-discrete solution to (163) in Theorem 49.

Theorem 49. *(Numerical error of semi-discrete case) Let w be the strong solution of the CSM (157) (in particular $\|w\| \in L^\infty(0,T)$, $\|\boldsymbol{\nabla} w\|_{L^2} \in L^2(0,T)$, $w \in L^2(0,T;W^{1,3}(\Omega)) \cap L^2(0,T;L^6(\Omega))$) and w^h be a solution to the semi-discrete problem (163). Let*

$$a(t) := C(\nu)\|\boldsymbol{\nabla} w\|_{L^3}^2 + \frac{1}{4}\|w\|_{L^6}^2.$$

Then, for $T > 0$ the error $w - w^h$ satisfies

$$\begin{aligned}
&\|(w-w^h)(T)\|^2 + \frac{C_s^4\delta^2}{\mu^2}\|\boldsymbol{\nabla}\big(w-w^h\big)(T)\|^2 \\
&+\int_0^T \Big\{\frac{\nu}{4}\|\boldsymbol{\nabla}\big(w-w^h\big)\|^2 + \gamma\|\boldsymbol{\nabla}\cdot(w-w^h)\|^2 + \frac{2}{3}C_1(C_s\delta)^2\|\boldsymbol{\nabla}\big(w-w^h\big)\|_{L^3}^3\Big\}\,dt \\
&\le \exp\Big(\int_0^T a(t)dt\Big)\Big\{\|(w-w^h)(0)\|^2 \\
&+\frac{C_s^4\delta^2}{\mu^2}\|\boldsymbol{\nabla}\big(w-w^h\big)(0)\|^2 + \inf_{v^h\in V^h}\|(w-v^h)(T)\|^2 \\
&+\int_0^T \Big[C(\nu)\inf_{v^h\in V^h}\Big(\|w_t - v_t^h\|_{-1}^2 + (\frac{C_s^4\delta^2}{\mu^2})^2\|\boldsymbol{\nabla}\big(w_t - v_t^h\big)\|^2 + \|\boldsymbol{\nabla}\big(w-v^h\big)\|^2\Big) \\
&+C\inf_{v^h\in V^h}\Big((C_s\delta)^2\|\boldsymbol{\nabla}\big(w-v^h\big)\|_{L^3}^{3/2} + \delta^{-1}\|w-v^h\|_{L^6}^{3/2} + \gamma\|\boldsymbol{\nabla}\cdot(w-v^h)\|^2\Big) \\
&+C(\gamma^{-1})\inf_{q^h\in Q^h}\|p-q^h\|^2\Big]dt\Big\}.
\end{aligned}$$

Proof. Consider the variational problem of the CSM (157): Find $w : [0,T] \to X = L^\infty(0,T;L^2(\Omega)) \cap L^3(0,T;W^{1,3}(\Omega))$ satisfying (148). Let $v^h \in V^h = \{v^h \in X^h : (\boldsymbol{\nabla}\cdot v^h, q^h) = 0 \ \forall\ q^h \in Q^h\}$. Since $v \in X$ & $v^h \in V^h \subset X^h \subset X$, we restrict $v = v^h$ in continuous variational problem. Then subtract semi-discrete problem (163) from continuous problem (148). Let $\boldsymbol{e} = error = w - w^h$. This gives,

$$\begin{aligned}
&(\boldsymbol{e}_t, v^h) + (C_s^4\delta^2\mu^{-2}\boldsymbol{\nabla}\boldsymbol{e}_t, \boldsymbol{\nabla}v^h) + b^*(w,w,v^h) - b^*(w^h,w^h,v^h) \\
&+\nu(\boldsymbol{\nabla}\boldsymbol{e},\boldsymbol{\nabla}v^h) + \gamma(\boldsymbol{\nabla}\cdot e, \boldsymbol{\nabla}\cdot v^h) + (C_s\delta)^2\int_\Omega(|\boldsymbol{\nabla}w|\boldsymbol{\nabla}w - |\boldsymbol{\nabla}w^h|\boldsymbol{\nabla}w^h) : \boldsymbol{\nabla}v^h\,dx \qquad (164)\\
&-(p-p^h, \boldsymbol{\nabla}\cdot v^h) = 0.
\end{aligned}$$

We can write,

$$\begin{aligned}
&b^*(w,w,v^h) - b^*(w^h,w^h,v^h)\\
=&b^*(w,w,v^h) - b^*(w^h,w,v^h) + b^*(w^h,w,v^h) - b^*(w^h,w^h,v^h),\\
=&b^*(\boldsymbol{e},w,v^h) + b^*(w^h,\boldsymbol{e},v^h).
\end{aligned}$$

Also,

$$\begin{aligned}
&\int_\Omega (|\boldsymbol{\nabla} w|\boldsymbol{\nabla} w - |\boldsymbol{\nabla} w^h|\boldsymbol{\nabla} w^h)\cdot\boldsymbol{\nabla} v^h\ dx\\
=&\int_\Omega (|\boldsymbol{\nabla} w|\boldsymbol{\nabla} w - |\boldsymbol{\nabla}\widetilde{w}|\boldsymbol{\nabla}\widetilde{w} + |\boldsymbol{\nabla}\widetilde{w}|\boldsymbol{\nabla}\widetilde{w} - |\boldsymbol{\nabla} w^h|\boldsymbol{\nabla} w^h)\cdot\boldsymbol{\nabla} v^h\ dx.
\end{aligned}$$

Pick $\widetilde{w}\in V^h$. Let $\boldsymbol{\eta} = w-\widetilde{w},\ \phi^h = w^h-\widetilde{w},\ \phi^h\in V^h$. This implies $\boldsymbol{e} = (w-\widetilde{w})-(w^h-\widetilde{w}) = \boldsymbol{\eta}-\phi^h$. Then (164) becomes

$$\begin{aligned}
&(\phi_t^h, v^h) + (C_s^4\delta^2\mu^{-2}\boldsymbol{\nabla}\phi_t^h, \boldsymbol{\nabla} v^h) + b^*(\boldsymbol{e},w,v^h) + b^*(w^h,\boldsymbol{e},v^h)\\
&\qquad +\nu(\boldsymbol{\nabla}\phi^h,\boldsymbol{\nabla} v^h) + \gamma(\boldsymbol{\nabla}\cdot\phi^h,\boldsymbol{\nabla}\cdot v^h)\\
&+(C_s\delta)^2\int_\Omega (|\boldsymbol{\nabla} w^h|\boldsymbol{\nabla} w^h - |\boldsymbol{\nabla}\widetilde{w}|\boldsymbol{\nabla}\widetilde{w}) : (\boldsymbol{\nabla} v^h)\ dx - (p-p^h, \boldsymbol{\nabla}\cdot v^h)\\
&= (\boldsymbol{\eta}_t, v^h) + (C_s^4\delta^2\mu^{-2}\boldsymbol{\nabla}\boldsymbol{\eta}_t, \boldsymbol{\nabla} v^h) + \nu(\boldsymbol{\nabla}\boldsymbol{\eta},\boldsymbol{\nabla} v^h) + \gamma(\boldsymbol{\nabla}\cdot\eta,\boldsymbol{\nabla}\cdot v^h)\\
&\qquad +(C_s\delta)^2\int_\Omega (|\boldsymbol{\nabla} w|\boldsymbol{\nabla} w - |\boldsymbol{\nabla}\widetilde{w}|\boldsymbol{\nabla}\widetilde{w}) : (\boldsymbol{\nabla} v^h)\ dx.
\end{aligned}$$

Take $v^h = \phi^h$ and $\lambda^h\in Q^h$. Here $b^*(w^h,\boldsymbol{e},\phi^h) = b^*(w^h,\boldsymbol{\eta}-\phi^h,\phi^h) = b^*(w^h,\boldsymbol{\eta},\phi^h)$ since $b^*(w^h,\phi^h,\phi^h) = 0$. Using strong monotonocity (36), we get

$$(C_s\delta)^2\int_\Omega (|\boldsymbol{\nabla} w^h|\boldsymbol{\nabla} w^h - |\boldsymbol{\nabla}\widetilde{w}|\boldsymbol{\nabla}\widetilde{w}) : (\boldsymbol{\nabla}\phi^h)\ dx \geq C_1(C_s\delta)^2\|\boldsymbol{\nabla}\phi^h\|_{L^3}^3.$$

Using local Lipschitz continuity (36), we get

$$\begin{aligned}
&(C_s\delta)^2\int_\Omega (|\boldsymbol{\nabla} w|\boldsymbol{\nabla} w - |\boldsymbol{\nabla}\widetilde{w}|\boldsymbol{\nabla}\widetilde{w}) : (\boldsymbol{\nabla}\phi^h)\ dx \leq (C_s\delta)^2 C_2 r\|\boldsymbol{\nabla}\boldsymbol{\eta}\|_{L^3}\|\boldsymbol{\nabla}\phi^h\|_{L^3},\\
&where\ \ r = \max\{\|\boldsymbol{\nabla} w\|_{L^3},\ \|\boldsymbol{\nabla}\widetilde{w}\|_{L^3}\}.
\end{aligned}$$

Hence,

$$\frac{1}{2}\frac{d}{dt}\left\{\|\phi^h\|^2+\frac{C_s^4\delta^2}{\mu^2}\|\boldsymbol{\nabla}\phi^h\|^2\right\}+\nu\|\boldsymbol{\nabla}\phi^h\|^2+\gamma\|\boldsymbol{\nabla}\cdot\phi^h\|^2$$
$$+b^*(\boldsymbol{\eta}-\phi^h,w,\phi^h)+b^*(w^h,\boldsymbol{\eta},\phi^h)+C_1(C_s\delta)^2\|\boldsymbol{\nabla}\phi^h\|_{L^3}^3$$
$$\leq(\boldsymbol{\eta}_t,\phi^h)+(C_s^4\delta^2\mu^{-2}\boldsymbol{\nabla}\boldsymbol{\eta}_t,\boldsymbol{\nabla}\phi^h)+\nu(\boldsymbol{\nabla}\boldsymbol{\eta},\boldsymbol{\nabla}\phi^h)+\gamma(\boldsymbol{\nabla}\cdot\eta,\boldsymbol{\nabla}\cdot\phi^h)$$
$$+(C_s\delta)^2C_2r\|\boldsymbol{\nabla}\boldsymbol{\eta}\|_{L^3}\|\boldsymbol{\nabla}\phi^h\|_{L^3}+(p-\lambda^h,\boldsymbol{\nabla}\cdot\phi^h).$$

We can rewrite it as

$$\frac{1}{2}\frac{d}{dt}\left\{\|\phi^h\|^2+\frac{C_s^4}{\mu^2}\delta^2\|\boldsymbol{\nabla}\phi^h\|^2\right\}+\nu\|\boldsymbol{\nabla}\phi^h\|^2+\gamma\|\boldsymbol{\nabla}\cdot\phi^h\|^2+C_1(C_s\delta)^2\|\boldsymbol{\nabla}\phi^h\|_{L^3}^3$$
$$\leq(\boldsymbol{\eta}_t,\phi^h)+\frac{C_s^4}{\mu^2}\delta^2(\boldsymbol{\nabla}\boldsymbol{\eta}_t,\boldsymbol{\nabla}\phi^h)+\nu(\boldsymbol{\nabla}\boldsymbol{\eta},\boldsymbol{\nabla}\phi^h)+(p-\lambda^h,\boldsymbol{\nabla}\cdot\phi^h)+\gamma(\boldsymbol{\nabla}\cdot\eta,\boldsymbol{\nabla}\cdot\phi^h)$$
$$+(C_s\delta)^2C_2r\|\boldsymbol{\nabla}\boldsymbol{\eta}\|_{L^3}\|\boldsymbol{\nabla}\phi^h\|_{L^3}-b^*(\boldsymbol{\eta},w,\phi^h)+b^*(\phi^h,w,\phi^h)-b^*(w^h,\boldsymbol{\eta},\phi^h).$$

Next, we find the bounds for the terms in the RHS. For the first five terms on the right, use the Cauchy Schwarz and Young's inequality,

$$|(\boldsymbol{\eta}_t,\phi^h)|\leq\|\boldsymbol{\eta}_t\|_{-1}\|\boldsymbol{\nabla}\phi^h\|\leq\frac{\nu}{2}\|\boldsymbol{\nabla}\phi^h\|^2+C(\nu)\|\boldsymbol{\eta}_t\|_{-1}^2.$$

$$\frac{C_s^4}{\mu^2}\delta^2|(\boldsymbol{\nabla}\boldsymbol{\eta}_t,\boldsymbol{\nabla}\phi^h)|\leq\|\boldsymbol{\nabla}\phi^h\|\frac{C_s^4\delta^2}{\mu^2}\|\boldsymbol{\nabla}\boldsymbol{\eta}_t\|,$$
$$\leq\frac{\nu}{4}\|\boldsymbol{\nabla}\phi^h\|^2+C(\nu)\left(\frac{C_s^4\delta^2}{\mu^2}\right)^2\|\boldsymbol{\nabla}\boldsymbol{\eta}_t\|^2.$$

$$\nu|(\boldsymbol{\nabla}\boldsymbol{\eta},\boldsymbol{\nabla}\phi^h)|\leq\nu\|\boldsymbol{\nabla}\boldsymbol{\eta}\|\|\boldsymbol{\nabla}\phi^h\|\leq\frac{\nu}{16}\|\boldsymbol{\nabla}\phi^h\|^2+C(\nu)\|\boldsymbol{\nabla}\boldsymbol{\eta}\|^2.$$
$$|(p-\lambda^h,\boldsymbol{\nabla}\cdot\phi^h)|\leq\|p-\lambda^h\|\|\boldsymbol{\nabla}\cdot\phi^h\|\leq\frac{\gamma}{4}\|\boldsymbol{\nabla}\cdot\phi^h\|^2+C(\gamma^{-1})\|p-\lambda^h\|^2.$$
$$|\gamma(\boldsymbol{\nabla}\cdot\eta,\boldsymbol{\nabla}\cdot\phi^h)|\leq\gamma\|\boldsymbol{\nabla}\cdot\eta\|\|\boldsymbol{\nabla}\cdot\phi^h\|\leq\frac{\gamma}{4}\|\boldsymbol{\nabla}\cdot\phi^h\|^2+C(\gamma)\|\boldsymbol{\nabla}\cdot\eta\|^2.$$

For the fifth term on the right, use the Hölder's inequality,

$$(C_s\delta)^2C_2r\|\boldsymbol{\nabla}\boldsymbol{\eta}\|_{L^3}\|\boldsymbol{\nabla}\phi^h\|_{L^3}\leq(C_s\delta)^2\left\{\frac{C_1}{3}\|\boldsymbol{\nabla}\phi^h\|_{L^3}^3+\frac{2}{3}C_1^{-1/2}r^{3/2}\|\boldsymbol{\nabla}\boldsymbol{\eta}\|_{L^3}^{3/2}\right\}.$$

Next, for the first and the third nonlinear terms, here we follow the estimates in [81, p.1007-1008, equations (4.5) and (4.6)] and we omit the details.

$$|b^*(\boldsymbol{\eta}, w, \phi^h)| \leq \frac{1}{4}\|\boldsymbol{\nabla} w\|_{L^3}^2\|\phi^h\|^2 + \frac{1}{4}\|\boldsymbol{\eta}\|_{L^6}^2 + \epsilon_1\|\boldsymbol{\nabla}\phi^h\|_{L^3}^3 + C\epsilon_1^{-1/2}\|w\|^{3/2}\|\boldsymbol{\eta}\|_{L^6}^{3/2}. \tag{165}$$

$$\begin{aligned}
|b^*(\phi^h, w, \phi^h)| &\leq \|\boldsymbol{\nabla} w\|_{L^3}\|\boldsymbol{\nabla}\phi^h\|_{L^3}^2, \\
&\leq \|\boldsymbol{\nabla} w\|_{L^3}(\|\phi^h\|^{1/2}\|\boldsymbol{\nabla}\phi^h\|^{1/2})^2, \\
&\leq \frac{\nu}{16}\|\boldsymbol{\nabla}\phi^h\|^2 + C(\nu)\|\boldsymbol{\nabla} w\|_{L^3}^2\|\phi^h\|^2.
\end{aligned}$$

$$|b^*(w^h, \boldsymbol{\eta}, \phi^h)| \leq \frac{1}{4}\|w\|_{L^6}^2\|\phi^h\|^2 + \frac{1}{4}\|\boldsymbol{\nabla}\boldsymbol{\eta}\|_{L^3}^2 + \epsilon_2\|\boldsymbol{\nabla}\phi^h\|_{L^3}^3 + C\epsilon_2^{-1/2}\|w^h\|^{3/2}\|\boldsymbol{\eta}\|_{L^6}^{3/2}. \tag{166}$$

Setting $\epsilon_1 = \epsilon_2 = \frac{1}{6}C_1(C_s\delta)^2$ and collecting all the terms gives

$$\begin{aligned}
\frac{1}{2}\frac{d}{dt}\Big\{\|\phi^h\|^2 + \frac{C_s^4}{\mu^2}\delta^2\|\boldsymbol{\nabla}\phi^h\|^2\Big\} + \frac{\nu}{8}\|\boldsymbol{\nabla}\phi^h\|^2 + \frac{\gamma}{2}\|\boldsymbol{\nabla}\cdot\phi^h\|^2 + \frac{1}{3}C_1(C_s\delta)^2\|\boldsymbol{\nabla}\phi^h\|_{L^3}^3 \\
\leq \Big[C(\nu)\|\boldsymbol{\nabla} w\|_{L^3}^2 + \frac{1}{4}\|\boldsymbol{\nabla} w\|_{L^3}^2 + \frac{1}{4}\|w\|_{L^6}^2\Big]\|\phi^h\|^2 \\
+\Big\{C(\nu)\Big[\|\boldsymbol{\eta}_t\|_{-1}^2 + (\frac{C_s^4\delta^2}{\mu^2})^2\|\boldsymbol{\nabla}\boldsymbol{\eta}_t\|^2 + \|\boldsymbol{\nabla}\boldsymbol{\eta}\|^2\Big] \\
+C(\gamma^{-1})\|p - \lambda^h\|^2 + C(\gamma)\|\boldsymbol{\nabla}\cdot\gamma\|^2 + (C_s\delta)^2 r^{3/2}\|\boldsymbol{\nabla}\boldsymbol{\eta}\|_{L^3}^{3/2} \\
+\frac{1}{4}\|\boldsymbol{\eta}\|_{L^6}^2 + \delta^{-1}\|w\|^{3/2}\|\boldsymbol{\eta}\|_{L^6}^{3/2} + \frac{1}{4}\|\boldsymbol{\nabla}\boldsymbol{\eta}\|_{L^3}^2 + \delta^{-1}\|w^h\|^{3/2}\|\boldsymbol{\eta}\|_{L^6}^{3/2}\Big\}.
\end{aligned}$$

Denote $a(t) := C(\nu)\|\boldsymbol{\nabla} w\|_{L^3}^2 + \frac{1}{4}\|\boldsymbol{\nabla} w\|_{L^3}^2 + \frac{1}{4}\|w\|_{L^6}^2$ and its antiderivative is

$$A(t) := \int_0^T a(t)\ dt < \infty \text{ for } w \in L^2(0,T;W^{1,3}(\Omega)) \cap L^2(0,T;L^6(\Omega)).$$

Multiplying through by the integrating factor $e^{-A(t)}$ gives

$$\begin{aligned}
\frac{d}{dt}\left[\frac{1}{2}e^{-A(t)}\left(\|\phi^h\|^2 + \frac{C_s^4\delta^2}{\mu^2}\|\boldsymbol{\nabla}\phi^h\|^2\right)\right] \\
+e^{-A(t)}\left[\frac{\nu}{8}\|\boldsymbol{\nabla}\phi^h\|^2 + \frac{\gamma}{2}\|\boldsymbol{\nabla}\cdot\phi^h\|^2 + \frac{1}{3}C_1(C_s\delta)^2\|\boldsymbol{\nabla}\phi^h\|_{L^3}^3\right] \\
\leq e^{-A(t)}\Big\{C(\nu)\Big[\|\boldsymbol{\eta}_t\|_{-1}^2 + (\frac{C_s^4\delta^2}{\mu^2})^2\|\boldsymbol{\nabla}\boldsymbol{\eta}_t\|^2 + \|\boldsymbol{\nabla}\boldsymbol{\eta}\|^2\Big]
\end{aligned}$$

$$+C(\gamma^{-1})\|p-\lambda^h\|^2+C(\gamma)\|\boldsymbol{\nabla}\cdot\eta\|^2+(C_s\delta)^2r^{3/2}\|\boldsymbol{\nabla}\boldsymbol{\eta}\|_{L^3}^{3/2}+\frac{1}{4}\|\boldsymbol{\eta}\|_{L^6}^2$$
$$+\delta^{-1}\|w\|^{3/2}\|\boldsymbol{\eta}\|_{L^6}^{3/2}+\frac{1}{4}\|\boldsymbol{\nabla}\boldsymbol{\eta}\|_{L^3}^2+\delta^{-1}\|w^h\|^{3/2}\|\boldsymbol{\eta}\|_{L^6}^{3/2}\Big\}.$$

Integrating over $[0,T]$ and multiplying through by $e^{A(t)}$ gives

$$\frac{1}{2}\left\{\|\phi^h(T)\|^2+\frac{C_s^4\delta^2}{\mu^2}\|\boldsymbol{\nabla}\phi^h(T)\|^2\right\}$$
$$+\int_0^T\Big(\frac{\nu}{8}\|\boldsymbol{\nabla}\phi^h\|^2+\frac{\gamma}{2}\|\boldsymbol{\nabla}\cdot\phi^h\|^2+\frac{1}{3}C_1(C_s\delta)^2\|\boldsymbol{\nabla}\phi^h\|_{L^3}^3\Big)dt$$
$$\leq\exp\Big(\int_0^T a(t)dt\Big)\Big\{\frac{1}{2}\Big(\|\phi^h(0)\|^2+\frac{C_s^4\delta^2}{\mu^2}\|\boldsymbol{\nabla}\phi^h(0)\|^2\Big)$$
$$+\int_0^T\Big[C(\nu)\Big(\|\boldsymbol{\eta}_t\|_{-1}^2+(\frac{C_s^4\delta^2}{\mu^2})^2\|\boldsymbol{\nabla}\boldsymbol{\eta}_t\|^2+\|\boldsymbol{\nabla}\boldsymbol{\eta}\|^2\Big)$$
$$+C(\gamma^{-1})\|p-\lambda^h\|^2+C(\gamma)\|\boldsymbol{\nabla}\cdot\eta\|^2+(C_s\delta)^2r^{3/2}\|\boldsymbol{\nabla}\boldsymbol{\eta}\|_{L^3}^{3/2}+\frac{1}{4}\|\boldsymbol{\eta}\|_{L^6}^2$$
$$+\delta^{-1}\|w\|^{3/2}\|\boldsymbol{\eta}\|_{L^6}^{3/2}+\frac{1}{4}\|\boldsymbol{\nabla}\boldsymbol{\eta}\|_{L^3}^2+\delta^{-1}\|w^h\|^{3/2}\|\boldsymbol{\eta}\|_{L^6}^{3/2}\Big]dt\Big\}.$$

Apply the Hölder's inequality gives

$$\int_0^T r^{3/2}\|\boldsymbol{\nabla}\boldsymbol{\eta}\|_{L^3}^{3/2}\,dt\leq\left(\int_0^T r^3\,dt\right)^{1/2}\|\boldsymbol{\nabla}\boldsymbol{\eta}\|_{L^3(0,T;L^3)}^{3/2},$$
$$\int_0^T\|w\|^{3/2}\|\boldsymbol{\eta}\|_{L^6}^{3/2}\,dt\leq\|w\|_{L^2(0,T;L^2)}^{3/2}\|\boldsymbol{\eta}\|_{L^6(0,T;L^6)}^{3/2},$$
$$\int_0^T\|w^h\|^{3/2}\|\boldsymbol{\eta}\|_{L^6}^{3/2}\,dt\leq\|w^h\|_{L^2(0,T;L^2)}^{3/2}\|\boldsymbol{\eta}\|_{L^6(0,T;L^6)}^{3/2}.$$

$\|w\|_{L^2(0,T;L^2)}$ and $\|w^h\|_{L^2(0,T;L^2)}$ are bounded by problem data by stability bound. Here $r=\max\{\|\boldsymbol{\nabla}w\|_{L^3},\|\boldsymbol{\nabla}\widetilde{w}\|_{L^3}\}$ and $\left(\int_0^T r^3\,dt\right)^{1/2}=\|\boldsymbol{\nabla}w\|_{L^3(0,T;L^3)}^{3/2}$ or $\|\boldsymbol{\nabla}\widetilde{w}\|_{L^3(0,T;L^3)}^{3/2}$ also bounded. Using triangle inequality: $\|\boldsymbol{e}\|\leq\|\phi^h\|+\|\boldsymbol{\eta}\|$, we obtain the desired result. □

Remark 50. *If $\tilde{w}$ is taken to be the Stokes projection, then $\|\boldsymbol{\nabla}\boldsymbol{\eta}\|^2$ does not occur at the RHS.*

Remark 51. *Considering the nonlinear terms* (165) *and* (166)*, alternatively we have*

$$
\begin{aligned}
|b^*(\eta, w, \phi^h)| &\le M\|\boldsymbol{\nabla}\eta\|\|\boldsymbol{\nabla} w\|\|\boldsymbol{\nabla}\phi^h\| \le \epsilon\|\boldsymbol{\nabla}\phi^h\|^2 + \frac{1}{4\epsilon}M^2\|\boldsymbol{\nabla} w\|^2\|\boldsymbol{\nabla}\eta\|^2.\\
|b^*(w^h, \eta, \phi^h)| &\le C\|w^h\|^{1/2}\|\boldsymbol{\nabla} w^h\|^{1/2}\|\boldsymbol{\nabla}\eta\|\|\boldsymbol{\nabla}\phi^h\|,\\
&\le \epsilon\|\boldsymbol{\nabla}\phi^h\|^2 + C(\epsilon^{-1})\|w^h\|\|\boldsymbol{\nabla} w^h\|\|\boldsymbol{\nabla}\eta\|^2.
\end{aligned}
$$

By taking $\epsilon = \nu/32$*, we can avoid the term* $\delta^{-1}\|\eta\|_{L^6}^{3/2}$ *at the RHS but instead we have* $\nu^{-1}\|\boldsymbol{\nabla}\eta\|^2$*.*

3.5.1 Time discretization of the Corrected Smagorinsky model

This subsection presents the unconditionally stable, linearly implicit, full discretization of (157). Let the time step and other quantities be denoted by

$$
\begin{aligned}
\text{time-step} = k,\ t_n = nk,\ f_n(x) &= f(x, t_n),\\
w_n^h(x) &= \text{approximation to } w(x, t_n),\\
p_n^h(x) &= \text{approximation to } p(x, t_n).
\end{aligned}
$$

We perform the finite element spatial discretization and the first-order Backward Euler scheme for time discretization to get the following full discretization: Given $(w_n^h, p_n^h) \in (X^h, Q^h)$, find $(w_{n+1}^h, p_{n+1}^h) \in (X^h, Q^h)$ satisfying

$$
\begin{aligned}
&\Big(\frac{w_{n+1}^h - w_n^h}{k}, v^h\Big) + \frac{C_s^4\delta^2}{\mu^2}\Big(\frac{\boldsymbol{\nabla} w_{n+1}^h - \boldsymbol{\nabla} w_n^h}{k}, \boldsymbol{\nabla} v^h\Big) + b^*(w_n^h, w_{n+1}^h, v^h)\\
&\qquad +\nu(\boldsymbol{\nabla} w_{n+1}^h, \boldsymbol{\nabla} v^h) + (C_s\delta)^2(|\boldsymbol{\nabla} w_n^h|\boldsymbol{\nabla} w_{n+1}^h, \boldsymbol{\nabla} v^h)\\
&+\gamma(\boldsymbol{\nabla}\cdot w_{n+1}^h, \boldsymbol{\nabla}\cdot v^h) - (p_{n+1}^h, \boldsymbol{\nabla}\cdot v^h) = (f_{n+1}(x), v^h)\ \forall\ v^h \in X^h,\\
&\qquad (\boldsymbol{\nabla}\cdot w_{n+1}^h, q^h) = 0\ \forall\ q^h \in Q^h.
\end{aligned}
\tag{167}
$$

This method is semi-implicit. We shall prove it is unconditionally stable in Theorem 52.

Theorem 52. (167) *is unconditionally energy stable. For any* $N \geq 1$,

$$\Big(\frac{1}{2}\|w_N^h\|^2 + \frac{1}{2}\frac{C_s^4\delta^2}{\mu^2}\|\boldsymbol{\nabla} w_N^h\|^2\Big) + \sum_{n=0}^{N-1}\frac{1}{2}\Big(\|w_{n+1}^h - w_n^h\|^2$$
$$+\frac{C_s^4\delta^2}{\mu^2}\|\boldsymbol{\nabla} w_{n+1}^h - \boldsymbol{\nabla} w_n^h\|^2\Big) + k\sum_{n=0}^{N-1}\int_\Omega [\nu + (C_s\delta)^2|\boldsymbol{\nabla} w_n^h]|\boldsymbol{\nabla} w_{n+1}^h|^2\ dx + \tag{168}$$
$$+\gamma\|\boldsymbol{\nabla}\cdot w_{n+1}^h\|^2 = \Big(\frac{1}{2}\|w_0^h\|^2 + \frac{1}{2}\frac{C_s^4\delta^2}{\mu^2}\|\boldsymbol{\nabla} w_0^h\|^2\Big) + k\sum_{n=0}^{N-1}(f_{n+1}, w_{n+1}^h).$$

Proof. Multiply (167) by k and take $v^h = w_{n+1}^h$. Use Lemma (31) to get $b^*(w_n^h, w_{n+1}^h, w_{n+1}^h) = 0$. Hence,

$$\|w_{n+1}^h\|^2 - (w_{n+1}^h, w_n^h) + \frac{C_s^4\delta^2}{\mu^2}\|\boldsymbol{\nabla} w_{n+1}^h\|^2 - \frac{C_s^4\delta^2}{\mu^2}(\boldsymbol{\nabla} w_{n+1}^h, \boldsymbol{\nabla} w_n^h)$$
$$+\gamma\|\boldsymbol{\nabla}\cdot w_{n+1}^h\|^2 + k\int_\Omega [\nu + (C_s\delta)^2|\boldsymbol{\nabla} w_n^h]|\boldsymbol{\nabla} w_{n+1}^h|^2\ dx = k(f_{n+1}, w_{n+1}^h).$$

For the second and fourth terms, apply the polarization identity (143),

$$(w_{n+1}^h, w_n^h) = \frac{1}{2}\|w_{n+1}^h\|^2 + \frac{1}{2}\|w_n^h\|^2 - \frac{1}{2}\|w_{n+1}^h - w_n^h\|^2,$$
$$(\boldsymbol{\nabla} w_{n+1}^h, \boldsymbol{\nabla} w_n^h) = \frac{1}{2}\|\boldsymbol{\nabla} w_{n+1}^h\|^2 + \frac{1}{2}\|\boldsymbol{\nabla} w_n^h\|^2 - \frac{1}{2}\|\boldsymbol{\nabla} w_{n+1}^h - \boldsymbol{\nabla} w_n^h\|^2.$$

Collecting terms and summing from $n = 0$ to $N-1$, we get the result. □

Remark 53. (168) *is an energy equality, we can identify the following quantities:*

1. *Model kinetic energy* $= \frac{1}{2}\|w_N^h\|^2 + \frac{1}{2}\frac{C_s^4\delta^2}{\mu^2}\|\boldsymbol{\nabla} w_N^h\|^2$.
2. *Eddy viscosity dissipation* $= \int_\Omega (C_s\delta)^2|\boldsymbol{\nabla} w_n^h||\boldsymbol{\nabla} w_{n+1}^h|^2\ dx$.
3. *Numerical diffusion* $= \frac{1}{2}(\|w_{n+1}^h - w_n^h\|^2 + \frac{C_s^4\delta^2}{\mu^2}\|\boldsymbol{\nabla} w_{n+1}^h - \boldsymbol{\nabla} w_n^h\|^2)$. *This numerical diffusion arises due to the Backward Euler scheme.*

Remark 54. *The energy equality* (168) *can be also written as*

$$\frac{1}{2k}(\|w_{n+1}^h\|^2 - \|w_n^h\|^2) + \frac{1}{2k}\|w_{n+1}^h - w_n^h\|^2 + \nu\|\boldsymbol{\nabla} w_{n+1}^h\|^2 + \gamma\|\boldsymbol{\nabla}\cdot w_{n+1}^h\|^2$$
$$+\left\{\frac{C_s^4\delta^2}{2k\mu^2}(\|\boldsymbol{\nabla} w_{n+1}^h\|^2 - \|\boldsymbol{\nabla} w_n^h\|^2) + \frac{C_s^4\delta^2}{2k\mu^2}\|\boldsymbol{\nabla} w_{n+1}^h - \boldsymbol{\nabla} w_n^h\|^2\right.$$
$$\left. + \int_\Omega (C_s\delta)^2|\boldsymbol{\nabla} w_n^h||\boldsymbol{\nabla} w_{n+1}^h|^2\ dx\right\} = (f_{n+1}, w_{n+1}^h).$$

Line one and the RHS are from the backward Euler discretization of the usual NSE. The bracketed term is a discretized form of model dissipation at $t = t_{n+1}$. Here the term model dissipation in the chapter can be positive or negative. When it is positive, it aggregates energy from mean to fluctuations. When it is negative, energy is transferred from fluctuations back to the mean.

Remark 55. *For* (167)*, the model dissipation is*

$$MD^{n+1} = \frac{C_s^4\delta^2}{2k\mu^2}(\|\boldsymbol{\nabla} w_{n+1}^h\|^2 - \|\boldsymbol{\nabla} w_n^h\|^2) + \frac{C_s^4\delta^2}{2k\mu^2}\|\boldsymbol{\nabla} w_{n+1}^h - \boldsymbol{\nabla} w_n^h\|^2$$
$$+ \int_\Omega (C_s\delta)^2|\boldsymbol{\nabla} w_n^h||\boldsymbol{\nabla} w_{n+1}^h|^2\ dx.$$

In this Test 8.2, we use both Backward Euler and Crank-Nicolson to see the difference. We perform the finite element spatial discretization and the linearly implicit Crank-Nicolson (also called CNLE-CN with Linear Extrapolation) scheme for time discretization to get the following full discretization: for function w, we denote

$$w_{n+\frac{1}{2}}^h = \frac{w_n^h + w_{n+1}^h}{2}, \quad \tilde{w}_{n+\frac{1}{2}}^h = \frac{3w_n^h - w_{n-1}^h}{2}.$$

Given $(w_n^h, p_n^h) \in (X^h, Q^h)$, find $(w_{n+1}^h, p_{n+1}^h) \in (X^h, Q^h)$ satisfying

$$\begin{aligned}
&\Big(\frac{w_{n+1}^h - w_n^h}{k}, v^h\Big) + \frac{C_s^4\delta^2}{\mu^2}\Big(\frac{\boldsymbol{\nabla} w_{n+1}^h - \boldsymbol{\nabla} w_n^h}{k}, \boldsymbol{\nabla} v^h\Big) + b^*(\tilde{w}_{n+\frac{1}{2}}^h, w_{n+\frac{1}{2}}^h, v^h)\\
&+\nu(\boldsymbol{\nabla} w_{n+\frac{1}{2}}^h, \boldsymbol{\nabla} v^h) + (C_s\delta)^2(|\boldsymbol{\nabla}\tilde{w}_{n+\frac{1}{2}}^h|\boldsymbol{\nabla} w_{n+\frac{1}{2}}^h, \boldsymbol{\nabla} v^h)\\
+\gamma(\boldsymbol{\nabla}\cdot w_{n+\frac{1}{2}}^h, \boldsymbol{\nabla}\cdot v^h) - (p_{n+\frac{1}{2}}^h, \boldsymbol{\nabla}\cdot v^h) &= (f_{n+\frac{1}{2}}(x), v^h)\ \forall\ v^h \in X^h,\\
(\boldsymbol{\nabla}\cdot w_{n+\frac{1}{2}}^h, q^h) &= 0\ \forall\ q^h \in Q^h.
\end{aligned} \tag{169}$$

We will prove it is unconditionally stable in Theorem 56.

Theorem 56. (169) *is unconditionally energy stable. For any* $N \geq 1$,

$$\begin{aligned}&\left(\frac{1}{2}\|w_N^h\|^2+\frac{1}{2}\frac{C_s^4\delta^2}{\mu^2}\|\boldsymbol{\nabla} w_N^h\|^2\right)+k\sum_{n=0}^{N-1}\int_\Omega[\nu+(C_s\delta)^2|\boldsymbol{\nabla}\tilde{w}^h_{n+\frac{1}{2}}|]|\boldsymbol{\nabla} w^h_{n+\frac{1}{2}}|^2\ dx\\&+\gamma\|\boldsymbol{\nabla}\cdot w^h_{n+\frac{1}{2}}\|^2=\left(\frac{1}{2}\|w_0^h\|^2+\frac{1}{2}\frac{C_s^4\delta^2}{\mu^2}\|\boldsymbol{\nabla} w_0^h\|^2\right)+k\sum_{n=0}^{N-1}\left(f_{n+\frac{1}{2}},w^h_{n+\frac{1}{2}}\right).\end{aligned}\tag{170}$$

Proof. Multiply (169) by k and take $v^h = w^h_{n+\frac{1}{2}}$. Use Lemma (31) to get $b^*(\tilde{w}^h_{n+\frac{1}{2}}, w^h_{n+\frac{1}{2}}, w^h_{n+\frac{1}{2}}) = 0$. Hence,

$$\begin{aligned}&\frac{1}{2}\|w^h_{n+1}\|^2-\frac{1}{2}\|w^h_n\|^2+\frac{1}{2}\frac{C_s^4\delta^2}{\mu^2}\|\boldsymbol{\nabla} w^h_{n+1}\|^2-\frac{1}{2}\frac{C_s^4\delta^2}{\mu^2}\|\boldsymbol{\nabla} w^h_n\|^2\\&+\gamma\|\boldsymbol{\nabla}\cdot w^h_{n+\frac{1}{2}}\|^2+k\int_\Omega[\nu+(C_s\delta)^2|\boldsymbol{\nabla}\tilde{w}^h_{n+\frac{1}{2}}|]|\boldsymbol{\nabla} w^h_{n+\frac{1}{2}}|^2\ dx=k(f_{n+\frac{1}{2}},w^h_{n+\frac{1}{2}}).\end{aligned}$$

Collecting terms and summing from $n = 0$ to $N - 1$, we get the result. □

Remark 57. (170) *is an energy equality, we can identify the following quantities:*

1. *Model kinetic energy* $= \frac{1}{2}\|w^h_N\|^2 + \frac{1}{2}\frac{C_s^4\delta^2}{\mu^2}\|\boldsymbol{\nabla} w^h_N\|^2$.
2. *Eddy viscosity dissipation* $= \int_\Omega (C_s\delta)^2|\boldsymbol{\nabla}\tilde{w}^h_{n+\frac{1}{2}}||\boldsymbol{\nabla} w^h_{n+\frac{1}{2}}|^2\ dx$.
3. *No Numerical diffusion.*

Remark 58. *The energy equality can be also written as*

$$\begin{aligned}&\frac{1}{2k}(\|w^h_{n+1}\|^2-\|w^h_n\|^2)+\nu\|\boldsymbol{\nabla} w^h_{n+\frac{1}{2}}\|^2+\gamma\|\boldsymbol{\nabla}\cdot w^h_{n+\frac{1}{2}}\|^2\\&+\left\{\frac{C_s^4\delta^2}{2k\mu^2}(\|\boldsymbol{\nabla} w^h_{n+1}\|^2-\|\boldsymbol{\nabla} w^h_n\|^2)+\int_\Omega(C_s\delta)^2|\boldsymbol{\nabla}\tilde{w}^h_{n+\frac{1}{2}}||\boldsymbol{\nabla} w^h_{n+\frac{1}{2}}|^2\ dx\right\}\\&=(f_{n+\frac{1}{2}},w^h_{n+\frac{1}{2}}).\end{aligned}$$

Line one and line three are from the CNLE discretization of the usual NSE. The bracketed term in the second line is a discretized form of model dissipation at $t = t_{n+1}$.

Remark 59. *For* (169)*, the model dissipation is*

$$MD^{n+1}=\frac{C_s^4\delta^2}{2k\mu^2}(\|\boldsymbol{\nabla} w^h_{n+1}\|^2-\|\boldsymbol{\nabla} w^h_n\|^2)+\int_\Omega(C_s\delta)^2|\boldsymbol{\nabla}\tilde{w}^h_{n+\frac{1}{2}}||\boldsymbol{\nabla} w^h_{n+\frac{1}{2}}|^2\ dx.$$

3.6 Numerical Tests

In this section, we perform two numerical tests. In the first test, we show the numerical error and the rate of convergence of the Backward Euler scheme. In the second test, we show among Backward Euler (BE) and Crank-Nicolson with Linear Extrapolation (CNLE), CNLE exhibits intermittent backscatter.

3.6.1 A test with exact solution

(Taken from V. DeCaria, W. J. Layton and M. McLaughlin [52]) The first experiment tests the accuracy of the Corrected Smagorinsky Model (157) and the convergence rate of (167). The following test has an exact solution for the 2D Navier Stokes problem.
Let the domain $\Omega = (-1,1) \times (-1,1)$. The exact solution is as follows:

$$u(x,y,t) = \pi \sin t(\sin 2\pi y \sin^2 \pi x, -\sin 2\pi x \sin^2 \pi y).$$
$$p(x,y,t) = \sin t \cos \pi x \sin \pi y.$$

This is inserted into the CSM and the body force $f(x,t)$ is calculated.
Uniform meshes were used with 270 nodes per side on the boundary and the degrees of freedom for the velocity space is 292681 and for the pressure space is 73441. The mesh is fine enough compared to the time step so that the main error from the time steps is only considered here. Taylor-Hood elements (P2-P1) were used in this test. We ran the test up to $T = 10$. We take $C_s = 0.1,\ \mu = 0.4,\ \delta$ is taken to be the shortest edge of all triangles. The norms used in the table heading are defined as follows,

$$\|w\|_{\infty,0} := \operatorname{ess\,sup}_{0<t<T} \|w\|_{L^2(\Omega)} \text{ and } \|w\|_{0,0} := \left(\int_0^T \|w(\cdot,t)\|^2_{L^2(\Omega)}\, dt \right)^{1/2}.$$

Δt	$\|w-w^h\|_{\infty,0}$	rate	$\|\boldsymbol{\nabla}(w-w^h)\|_{0,0}$	rate	$\|p-p^h\|_{0,0}$	rate
0.05	3.27068	-	5.25129	-	0.640537	-
0.02	0.823036	1.506	1.59313	1.302	0.235862	1.091
0.01	0.348629	1.239	0.739145	1.108	0.108216	1.124
0.005	0.169429	1.041	0.39714	0.89621	0.0470406	1.202

Table 7: Numerical error and temporal convergence rate, $Re = 5,000,\ T_{final} = 10,\ C_s = 0.1,\ \mu = 0.4,\ \delta = 0.0104757$.

$h = \delta$	$\|w-w^h\|_{\infty,0}$	rate	$\|\boldsymbol{\nabla}(w-w^h)\|_{0,0}$	rate	$\|p-p^h\|_{0,0}$	rate
0.08571	57.9769	-	88.1677	-	14.5602	-
0.04221	1.41386	5.244	3.30974	4.635	0.313994	5.418
0.02095	0.407421	1.776	0.95483	1.774	0.0562327	2.455
0.01048	0.169429	1.266	0.39714	1.266	0.0470406	0.258

Table 8: Numerical error and spatial convergence rate, $Re = 5,000,\ T_{final} = 10,\ C_s = 0.1,\ \mu = 0.4,\ \Delta t = 0.005$.

From the Table 7, we see the temporal convergence rate is 1 which is expected from Backward Euler (167) discretization. Using Taylor-Hood elements, Theorem 49 predicts a convergence rate in space of $O(h^{1.75})$, with a moderate constant, for $\|w-w^h\|_{\infty,0}$ and $\|\boldsymbol{\nabla}(w-w^h)\|_{0,0}$. But with the estimates in Remark 51, the order of convergence is $O(h^2)$, with a large constant $\frac{1}{\nu}$. In Table 8, the third and fifth columns show rates $O(h^{1.78})$ until the error plateaus (last line) at the error in the time discretization (last line in Table 7). There is still some gap between the theoretical convergence rate and the actual convergence rate we get in Table 8. The behavior of the pressure error for this test problem is unclear as well in Table 8.

3.6.2 Test2. Flow between offset cylinder

(Taken from N. Jiang and W. J. Layton [78]). This flow problem is tested to show the transfer of energy from fluctuations back to means in the turbulent flow using the Corrected Smagorinksy Model (157).

The domain is a disk with a smaller off-center obstacle inside. Let $r_1 = 1, r_2 = 0.1, c = (c_1, c_2) = (1/2, 0)$, then the domain is given by

$$\Omega = \{(x, y) : x^2 + y^2 < r_1^2 \text{ and } (x - c_1)^2 + (y - c_2)^2 > r_2^2\}.$$

The flow is driven by a counterclockwise rotational body force

$$f(x, y, t) = (-4y * (1 - x^2 - y^2), 4x * (1 - x^2 - y^2))^T,$$

with no-slip boundary conditions on both circles. We discretize in space using Taylor-Hood elements. There are 80 mesh points around the outer circle and 60 mesh points around the inner circle. The flow is driven by a counterclockwise force (f=0 on the outer circle). Thus, the flow rotates about the origin and interacts with the immersed circle.

We start the initial condition by solving the Stokes problem. We compute up to final time $T_{final} = 3$. Take $C_s = 0.1, \mu = 0.3, \delta$ is taken to be the shortest edge of all triangles ≈ 0.0112927, Re=10,000. For Backward Euler (167), we compute the following quantities:

$$\begin{aligned}
\text{Model dissipation } MD &= \int_\Omega \Big(\frac{C_s^4 \delta^2}{\mu^2} \frac{\boldsymbol{\nabla} w_{n+1}^h - \boldsymbol{\nabla} w_n^h}{k} \cdot \boldsymbol{\nabla} w_{n+1}^h \\
&\quad + (C_s \delta)^2 |\boldsymbol{\nabla} w_n^h| |\boldsymbol{\nabla} w_{n+1}^h|^2 \Big)\, dx. \\
\text{Effect of new term from CSM, } CSMD &= \int_\Omega \frac{C_s^4 \delta^2}{\mu^2} \frac{\boldsymbol{\nabla} w_{n+1}^h - \boldsymbol{\nabla} w_n^h}{k} \cdot \boldsymbol{\nabla} w_{n+1}^h \, dx. \\
\text{Eddy viscosity dissipation } EVD &= \int_\Omega (C_s \delta)^2 |\boldsymbol{\nabla} w_n^h| |\boldsymbol{\nabla} w_{n+1}^h|^2 \, dx. \\
\text{Viscous dissipation } VD &= \nu \|\boldsymbol{\nabla} w_{n+1}^h\|^2.
\end{aligned}$$

For Crank-Nicolson CNLE (169), we compute the following quantities:

$$\text{Model dissipation } MD = \int_\Omega \Big(\frac{C_s^4 \delta^2}{\mu^2} \frac{\boldsymbol{\nabla} w_{n+1}^h - \boldsymbol{\nabla} w_n^h}{k} \cdot \boldsymbol{\nabla} w_{n+\frac{1}{2}}^h$$

$$+ (C_s\delta)^2|\boldsymbol{\nabla}\tilde{w}^h_{n+\frac{1}{2}}||\boldsymbol{\nabla}w^h_{n+\frac{1}{2}}|^2\Big)\,dx.$$

$$\text{Effect of new term from CSM, } CSMD = \int_\Omega \frac{C_s^4\delta^2}{\mu^2}\frac{\boldsymbol{\nabla}w^h_{n+1} - \boldsymbol{\nabla}w^h_n}{k}\cdot\boldsymbol{\nabla}w^h_{n+\frac{1}{2}}\,dx.$$

$$\text{Eddy viscosity dissipation } EVD = \int_\Omega (C_s\delta)^2|\boldsymbol{\nabla}\tilde{w}^h_{n+\frac{1}{2}}||\boldsymbol{\nabla}w^h_{n+\frac{1}{2}}|^2\,dx.$$

$$\text{Viscous dissipation } VD = \nu\|\boldsymbol{\nabla}w^h_{n+\frac{1}{2}}\|^2.$$

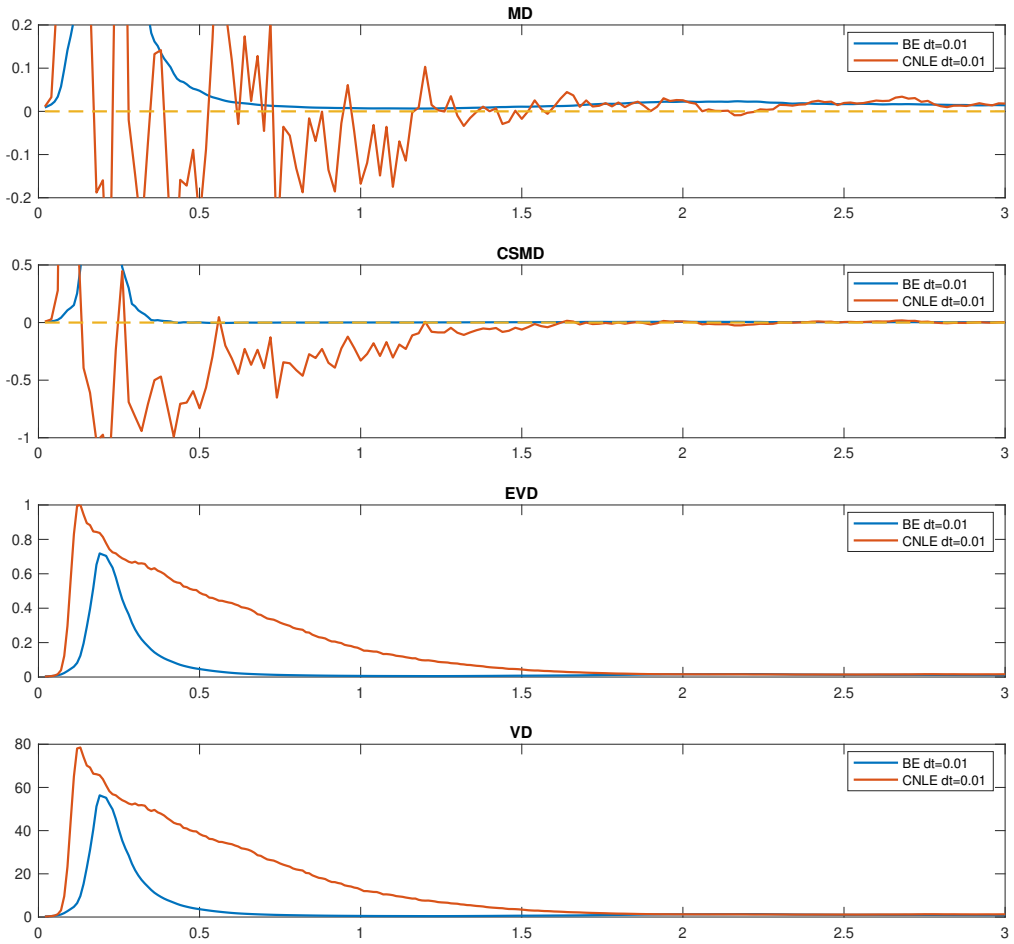

Figure 14: Comparison of Backward Euler (167) and linearized Crank-Nicolson (169) with $\Delta t = 0.01,\ Re = 10,000,\ T_{final} = 3,\ C_s = 0.1,\ \mu = 0.4,\ \delta = 0.0112927.$

It can be seen from the Figure 14, model dissipation MD becomes negative sometimes for linearized Crank-Nicolson (169) and MD are all positive for Backward Euler (167). Only CNLE for the Corrected Smagorinksy has a backscatter, which is consistent with the purpose of this model. Backward Euler has too much numerical diffusion, which makes it harder to see the backscatter from BE.

In the Figure 15, we notice the flow becomes smoother as it approaches statistical equilibrium.

3.6.2.1 Comparison with NSE and standard Smagorinksy

Here we compare the CSM (157) with Navier Stokes (150) and the standard Smagorinsky (141). The Taylor microscale [100] is defined as

$$\lambda_T := \|u\|/\|\nabla u\|$$

, which represents an average length scale for the flow. We use the same setting but with

$$Re = 100,000$$

to compare the Taylor microscale of each model. All numerical tests are calculated using Crank-Nicolson with grad-div stabilization

$$\gamma = 1.$$

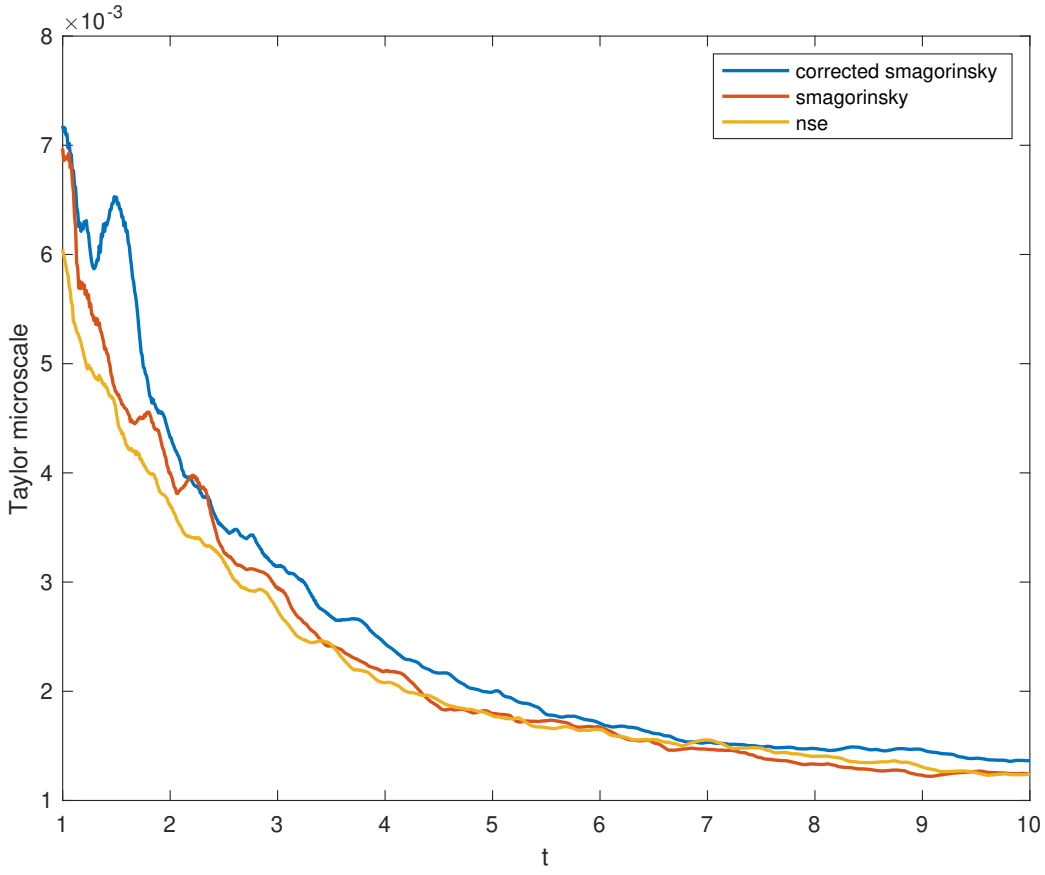

Figure 16: Taylor microscale comparison between CSM, NSE and the standard Smagorinsky with $\Delta t = 0.01,\ Re = 100,000,\ T_{final} = 10,\ C_s = 0.1,\ \mu = 0.4,\ \delta = 0.0112927.$

To further see the difference between these three models, here we focus on time-interval [7,10] and see the relative length-scale

$$\lambda_T/h$$

with h being the mesh size.

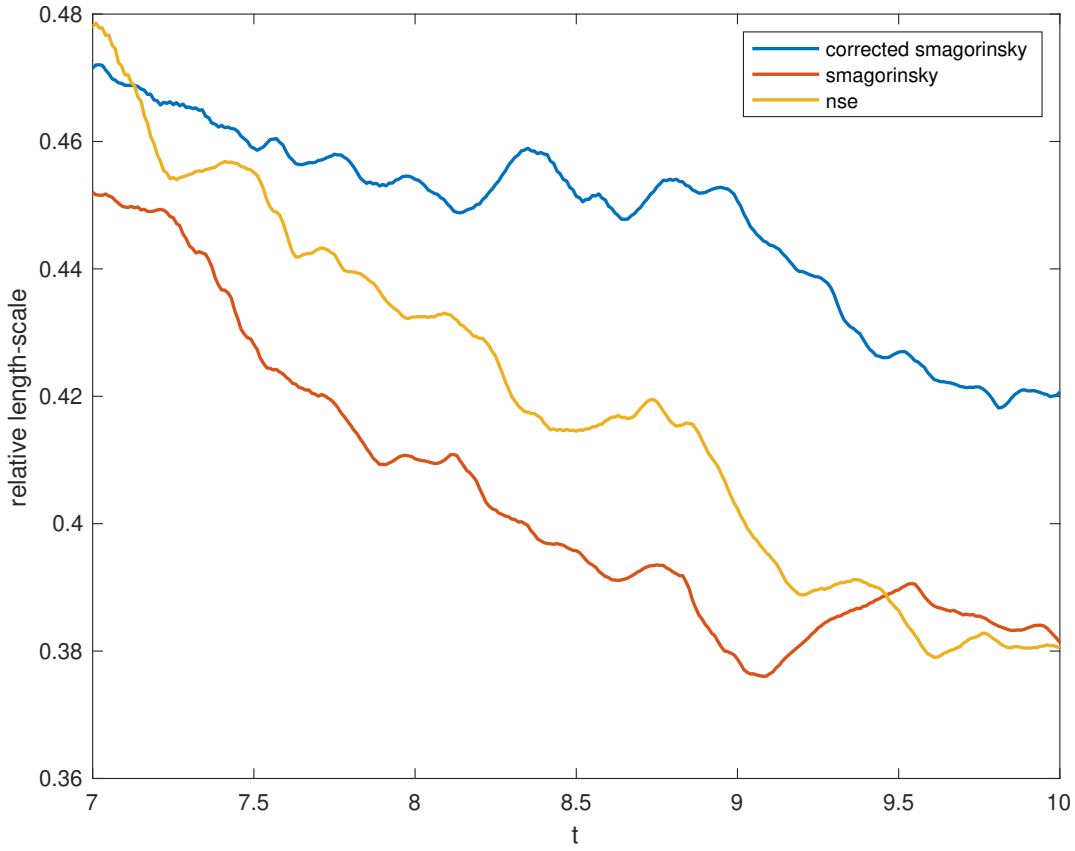

Figure 17: Relative length-scale (λ_T/h) comparison between CSM, NSE and standard Smagorinsky with $\Delta t = 0.01$, $Re = 100,000$, $C_s = 0.1$, $\mu = 0.4$, $\delta = 0.0112927$, time-interval shown as $[7, 10]$.

From Figure 16, notice the CSM has a larger Taylor microscale. Since the CSM models backscatter, more energy is expected in velocity means. Consistent with this, the averaged length scale of CSM is larger than Smagorinsky and NSE. And from Figure 17, the relative length-scale of the CSM at the final time is almost twice as large as the relative length-scale calculated with NSE and standard Smagorinsky.

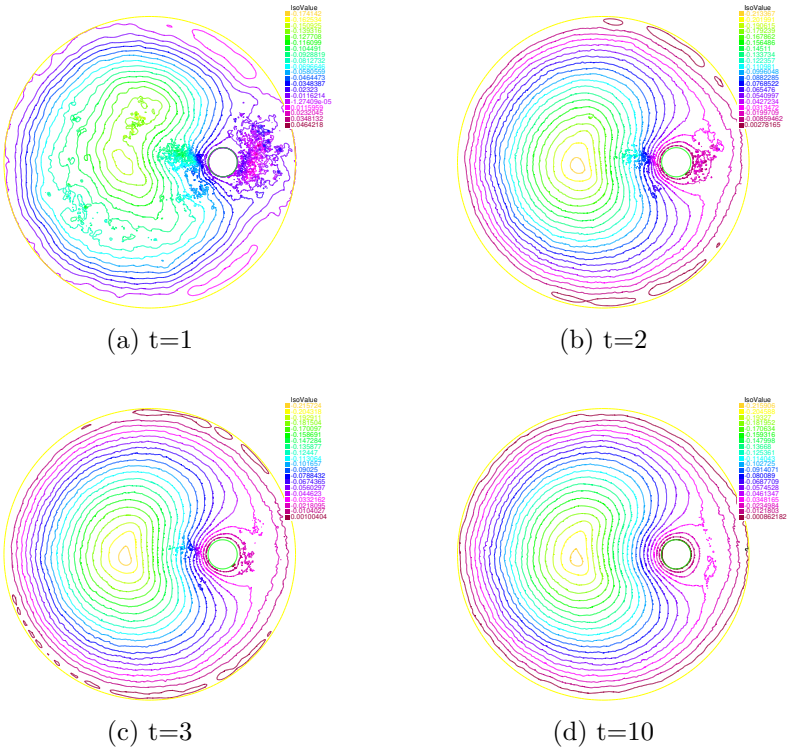

(a) t=1 (b) t=2

(c) t=3 (d) t=10

Figure 15: Streamline plot using CNLE (169). There are 270 mesh points around the outer circle and 180 mesh points around the inner circle.

4.0 Variable Time Step Method of Dahlquist, Liniger and Nevanlinna(DLN) for a Corrected Smagorinsky Model

Turbulent flows strain resources, both memory and CPU speed. The DLN method has greater accuracy and allows larger time steps, requiring less memory and fewer FLOPS. The DLN method can also be implemented adaptively. The classical Smagorinsky model, as an effective way to approximate a (resolved) mean velocity, has recently been corrected to represent a flow of energy from unresolved fluctuations to the (resolved) mean velocity. In this chapter, we apply a family of second-order, G-stable time-stepping methods proposed by Dahlquist, Liniger, and Nevanlinna (the DLN method) to one corrected Smagorinsky model and provide the detailed numerical analysis of the stability and consistency. We prove that the numerical solutions under any arbitrary time step sequences are unconditionally stable in the long term and converge in second order. We also provide error estimates under certain time-step conditions. Numerical tests are given to confirm the rate of convergence and also to show that the adaptive DLN algorithm helps to control numerical dissipation so that backscatter is visible.

4.1 Introduction

Eddy viscosity (EV) models are the most common approaches to depict the average of turbulent flow of Navier-Stokes equations (NSE). Various eddy viscosity models in practical settings are proposed for analytical and numerical study [14, 60, 62, 73, 74]. Unfortunately, most EV models have difficulties in simulating backscatter or complex turbulent flow not at statistical equilibrium due to the neglection of the intermittent energy flow from fluctuations back to means. To overcome this defect, Jiang and Layton [78] calibrated the standard eddy viscosity model by fitting the turbulent viscosity coefficient to flow data. Rong, Layton, and

Zhao [131] extended the usual Baldwin-Lomax model so that the new model can account for statistical backscatter without artificial negative viscosities. Recently, Siddiqua and Xie [137] have corrected the classical Smagorinsky model [139] with no new fitting parameters to reflect a flow of energy from unresolved fluctuations to means in the corrected Smagorinsky model (CSM henceforth). Most recently, Dai, Liu, Liu, Jiang, and Chen [48] proposed a new dynamic Smagorinsky model by an artificial neural network for prediction of outdoor airflow and pollutant dispersion. Herein we give an analysis of the method of Dahlquist, Liniger, and Nevanlinna [47] (the DLN method henceforth) for the CSM [137] with variable time steps. Let $f(x,t)$ be the prescribed body force, ν be the kinematic viscosity in the regular and bounded flow domain $\Omega \subset \mathbb{R}^d$ $(d = 2,\ 3)$. We analyze the variable step, DLN time discretization for the CSM: $\boldsymbol{\nabla} \cdot w = 0$ and

$$w_t - C_s^4 \delta^2 \mu^{-2} \Delta w_t + w \cdot \boldsymbol{\nabla} w - \nu \Delta w + \boldsymbol{\nabla} q - \boldsymbol{\nabla} \cdot \Big((C_s \delta)^2 |\boldsymbol{\nabla} w| \boldsymbol{\nabla} w \Big) = f,\ x \in \Omega,\ 0 \le t \le T. \tag{171}$$

Here μ is a constant from Kolmogorov-Prandtl relation [85, 119] and (w, q) approximate an ensemble average pair of velocity and pressure of Navier-Stokes solutions, $(\overline{u}, \overline{p})$. This is an eddy viscosity model with turbulent viscosity, $\nu_T = (C_s \delta)^2 |\boldsymbol{\nabla} w|$, where $C_s \approx 0.1$, (suggested by Lilly [107]), δ is a length scale (or grid-scale). In [137], the CSM model derivation and some basic properties of the CSM are developed and two algorithms for its numerical simulation are proposed. However, the significant backscatter of model dissipation is not observed in specific examples except for Linearized Crank-Nicolson time discretization. Besides that, constant time discretization in their algorithms (backward Euler and Linearized Crank-Nicolson time-stepping schemes) excludes the use of time adaptivity since the solution pattern (in terms of stability and convergence) under extreme time step ratios is hard to expect. Dahlquist, Liniger, and Nevanlinna designed a one-parameter family of one-leg, second-order methods for evolutionary equations [47]. This time-stepping method (the DLN method) is proved to be G-stable (non-linear stable) under any arbitrary time grids [44–46] and hence the ideal

choice for time discretization of fluid models [1]. Herein we apply the fully-discrete DLN algorithm (finite element space discretization) for the CSM in (171) and present a complete numerical analysis of the algorithm. We prove that the numerical solutions on arbitrary time grids are unconditionally long-term stable, and converge to exact solutions at second order with moderate time step restrictions. Let $\{t_n\}_{n=0}^N$ be the time grids on interval $[0,T]$ and $k_n = t_{n+1} - t_n$ is the local time step. Let w_n^h and q_n^h be the numerical approximations of velocity and pressure at time t_n of the CSM in (171) respectively on certain finite element space with the diameter h, the fully discrete DLN algorithm (with parameter $\theta \in [0,1]$) for the CSM in (171) is written as follows: $\nabla \cdot w_{n+1}^h = 0$ and

$$\begin{aligned}
&\frac{\alpha_2 w_{n+1}^h + \alpha_1 w_n^h + \alpha_0 w_{n-1}^h}{\alpha_2 k_n - \alpha_0 k_{n-1}} - \frac{C_s^4 \delta^2}{\mu^2} \Delta\Big(\frac{\alpha_2 w_{n+1}^h + \alpha_1 w_n^h + \alpha_0 w_{n-1}^h}{\alpha_2 k_n - \alpha_0 k_{n-1}}\Big) \\
&+ \Big(\sum_{\ell=0}^{2} \beta_\ell^{(n)} w_{n-\ell}^h\Big) \cdot \nabla\Big(\sum_{\ell=0}^{2} \beta_\ell^{(n)} w_{n-\ell}^h\Big) - \nu\Delta\Big(\sum_{\ell=0}^{2} \beta_\ell^{(n)} w_{n-\ell}^h\Big) + \nabla\Big(\sum_{\ell=0}^{2} \beta_\ell^{(n)} q_{n-\ell}^h\Big) \\
&+ \nabla \cdot \Big((C_s\delta)^2 \Big|\nabla\Big(\sum_{\ell=0}^{2} \beta_\ell^{(n)} w_{n-\ell}^h\Big)\Big| \nabla\Big(\sum_{\ell=0}^{2} \beta_\ell^{(n)} w_{n-\ell}^h\Big)\Big) = f\Big(\sum_{\ell=0}^{2} \beta_\ell^{(n)} t_{n-\ell}^h\Big), \quad \text{for } 1 \le n \le N-1,
\end{aligned} \tag{172}$$

where $|\cdot|$ is the Euclidian norm on $\mathbb{R}^d$ and the coefficients in (172) are

$$\begin{bmatrix} \alpha_2 \\ \alpha_1 \\ \alpha_0 \end{bmatrix} = \begin{bmatrix} \frac{1}{2}(\theta+1) \\ -\theta \\ \frac{1}{2}(\theta-1) \end{bmatrix}, \quad \begin{bmatrix} \beta_2^{(n)} \\ \beta_1^{(n)} \\ \beta_0^{(n)} \end{bmatrix} = \begin{bmatrix} \frac{1}{4}\Big(1 + \frac{1-\theta^2}{(1+\varepsilon_n\theta)^2} + \varepsilon_n^2 \frac{\theta(1-\theta^2)}{(1+\varepsilon_n\theta)^2} + \theta\Big) \\ \frac{1}{2}\Big(1 - \frac{1-\theta^2}{(1+\varepsilon_n\theta)^2}\Big) \\ \frac{1}{4}\Big(1 + \frac{1-\theta^2}{(1+\varepsilon_n\theta)^2} - \varepsilon_n^2 \frac{\theta(1-\theta^2)}{(1+\varepsilon_n\theta)^2} - \theta\Big) \end{bmatrix}.$$

The step variability $\varepsilon_n = (k_n - k_{n-1})/(k_n + k_{n-1})$ is the function of two step sizes and $\varepsilon_n \in (-1,1)$.

The main result of this chapter is the complete numerical analysis of the DLN method and computational tests showing backscatter phenomena for the CSM model (171). The chapter is organized as follows. We provide some necessary notations and preliminaries for numerical analysis in Section 4.2. We present the fully discrete variational formulation in Section 4.3.

[1] To our knowledge, the DLN method is the **only** variable step method which is both non-linear stable and second-order accurate.

We show that the DLN solutions are long-term, unconditional stable in Theorem 70 of Section 4.4.1 and perform the variable step error analysis with the moderate time step restriction in Theorem 73 of Section 4.4.2. Furthermore, in Section 4.5.1, we present the test problem with exact solutions [52] to confirm the fully discrete DLN algorithm is second-order in time, and in Section 4.5.2, we present the test problem about flow between offset cylinders [77] to check the unconditional stability and the efficiency of the time adaptivity of the DLN algorithm.

4.1.1 Related Work

Due to the fine properties of stability and consistency, the whole DLN family calls great attention to the simulation of evolutionary equations and fluid models. The DLN method with $\theta = \frac{2}{3}$ is suggested in [47] to relieve the conflict between error and stability. Kulikov and Shindin find that the DLN method with $\theta = \frac{2}{\sqrt{5}}$ has the best stability at infinity [87]. The midpoint rule (the DLN method with $\theta = 1$), conserving all quadratic Hamiltonians, has been thoroughly studied and widely used in computational fluid dynamics [10, 26–29, 68, 89]. Recently, the whole DLN family is applied to some time-dependent fluid model and shows its outstanding performance in some specific examples [96, 121, 122]. In addition, the DLN implementation has been simplified by the re-factorization process (adding time filters on backward Euler method) for wide application [97]. Time adaptivity of the DLN method (by the local truncation error criterion) is proposed to solve stiff differential systems for both efficiency and accuracy [98].

4.2 Notations and preliminary results

In this section, we introduce some of the notations and results used in this chapter. Recall that $\Omega \subset \mathbb{R}^d$ $(d = 2,\ 3)$ is the bounded domain of the CSM in Equation (171). Banach space $L^p(\Omega)$ $(p \geq 1)$ contains all Lebesgue measurable function f such that $|f|^p$ is

integrable. For $r \in \{0\} \cup \mathbb{N}$, Sobolev space $W^{m,p}(\Omega)$ with norm $\|.\|_{m,p}$ contains all functions whose weak derivatives up to m-th belong to $L^p(\Omega)$. Thus $W^{m,p}(\Omega)$ is exactly L^p when $m = 0$. We use H^m with norm $\|\cdot\|_m$ and semi-norm $|\cdot|_m$ to denote the inner product space $W^{m,2}(\Omega)$. $\|\cdot\|$ and $(\cdot,\cdot)$ denote the $L^2(\Omega)$ norm and inner product, respectively. The solution spaces X for the velocity and Q for the pressure are defined as:

$$X = \Big\{ v \in \big(L^3(\Omega)\big)^d : \nabla v \in \big(L^3(\Omega)\big)^{d\times d},\ v\big|_{\partial\Omega} = 0 \Big\}, \quad Q = \Big\{ q \in L^2(\Omega) : \int_\Omega q\ dx = 0 \Big\},$$

and the divergence-free velocity space is

$$V = \big\{ v \in X : (q, \nabla \cdot v) = 0,\ \forall q \in Q \big\}.$$

X' is the dual norm of X with the dual norm

$$\|f\|_{-1} = \sup_{0\neq v\in X} \frac{(f,v)}{\|\nabla v\|}, \qquad \forall f \in X'.$$

Definition 60. *(Trilinear Form) Define the trilinear form $b^* : X \times X \times X \to \mathbb{R}$ as follows*

$$b^*(u,v,w) := \frac{1}{2}(u\cdot\boldsymbol{\nabla} v, w) - \frac{1}{2}(u\cdot\boldsymbol{\nabla} w, v), \qquad \forall u,v,w \in X.$$

Lemma 61. *The nonlinear term $b^*(\cdot,\cdot,\cdot)$ is continuous on $X\times X\times X$ (and thus on $V\times V\times V$) which has the following skew-symmetry property,*

$$b^*(u,v,w) = -b^*(u,w,v), \qquad b^*(u,v,v) = 0. \tag{173}$$

As a consequence, we get

$$b^*(u,v,w) = (u\cdot\boldsymbol{\nabla} v, w), \quad \forall\ u \in V \text{and } v,\ w \in X,$$
$$b^*(u,v,v) = 0, \quad \forall\ u,\ v \in X.$$

Proof. Proof of this lemma is standard, see $p.114$ of Girault and Raviart [65]. □

Lemma 62. *For any* $u,\ v,\ w \in X$

$$b^*(u,v,w) \le C(\Omega)\|\nabla u\|\|\nabla v\|\|\nabla w\|,$$
$$b^*(u,v,w) \le C(\Omega)\|u\|^{1/2}\|\nabla u\|^{1/2}\|\nabla v\|\|\nabla w\|. \tag{174}$$

Proof. By Hölder's inequality, Poincaré-Friedrichs's inequality and Ladyzhenskaya's inequality. □

Next is a Discrete Grönwall Lemma, see [71, Lemma 5.1, p.369].

Lemma 63. *Let* $\Delta t,\ B$ *be non-negative real numbers and* $\{a_n\}_{n=0}^{\infty}$, $\{b_n\}_{n=0}^{\infty}$, $\{c_n\}_{n=0}^{\infty}$, $\{d_n\}_{n=0}^{\infty}$ *be non-negative sequences of real numbers such that*

$$a_\ell + \Delta t\sum_{n=0}^{\ell} b_n \le \Delta t\sum_{n=0}^{\ell} d_n a_n + \Delta t\sum_{n=0}^{\ell} c_n + B, \qquad \forall \ell \in \mathbb{N},$$

and $\Delta t d_n < 1$ *for all* n*, then*

$$a_\ell + \Delta t\sum_{n=0}^{\ell} b_n \le \exp\Big(\Delta t\sum_{n=0}^{\ell}\frac{d_n}{1-\Delta t d_n}\Big)\Big(\Delta t\sum_{n=0}^{\ell} c_n + B\Big), \qquad \forall \ell \in \mathbb{N}.$$

Proof. See [71, p.369]. □

Lemma 64. *(***Strong Monotonicity (SM) and Local Lipschitz Continuity (LLC)***)* *There exists* $C_1,\ C_2 > 0$ *such that for all* $u,\ v,\ w \in W^{1,3}(\Omega)$,

$$\textbf{\textit{(SM)}} \quad (|\nabla u|\nabla u - |\nabla w|\nabla w, \nabla(u-w)) \ge C_1\|\nabla(u-w)\|_{0,3}^3, \tag{175}$$

$$\textbf{\textit{(LLC)}} \quad (|\nabla u|\nabla u - |\nabla w|\nabla w, \nabla v) \le C_2\big(\max\{\|\nabla u\|_{0,3}, \|\nabla w\|_{0,3}\}\big)\|\nabla(u-w)\|_{0,3}\|\nabla v\|_{0,3}. \tag{176}$$

Proof. We refer [55, 81, 99] for proof. □

Let $\mathcal{T}_h$ be the edge-to-edge triangulation of the domain Ω with diameter $h > 0$. $X^h \subset X$ and $Q^h \subset Q$ are certain finite element spaces of velocity and pressure respectively. The divergence-free subspace of X^h is

$$V^h := \Big\{ v^h \in X^h : (p^h, \nabla \cdot v^h) = 0, \quad \forall p^h \in Q^h \Big\}.$$

Given $(w, q) \in X \times Q$, the finite element pair (X^h, Q^h) satisfies the approximation theorem (See [24, 38]): for any $r, s \in \{0\} \cup \mathbb{N}$ and $\ell \in \{0, 1\}$,

$$\begin{aligned} \inf_{v^h \in X^h} \|w - v^h\|_\ell &\le C h^{r+\ell-1} \|w\|_{r+1}, \qquad \text{for } \ u \in (H^{r+1})^d \cap X, \\ \inf_{p^h \in Q^h} \|q - p^h\| &\le C h^{s+1} \|q\|_{s+1}, \qquad \text{for } \ q \in H^{s+1} \cap Q, \end{aligned} \tag{177}$$

where r and s are highest degree of polynomials for X^h and Q^h respectively. We need the $L^p - L^2$-type inverse inequality [99].

Theorem 65. *Let Θ be the minimum angle in the triangulation of domain $\Omega \subset \mathbb{R}^d$ $(d = 2, 3)$ and X^h be the finite element space with highest polynomial degree r. For any $v^h \in X^h$ and $2 \le p < \infty$, there is a constant $C = C(\Theta, p, r) > 0$ such that*

$$\|\nabla^h v^h\|_{0,p} \le C h^{\frac{d}{2}(\frac{2-p}{p})} \|\nabla^h v^h\|, \tag{178}$$

where ∇^h is the element-wise defined gradient operator.

Proof. See [99, p.349-350] for proof. □

We assume that (X^h, Q^h) satisfies the discrete inf-sup condition:

$$\inf_{p^h \in Q^h} \sup_{v^h \in X^h} \frac{(p^h, \nabla \cdot v^h)}{\|p^h\| \|\nabla v^h\|} \ge C > 0,$$

where $C > 0$ is some constant independent of h. We define the Stokes projection $\Pi : V \times Q \to V^h \times Q^h$ as follows: given the pair $(w, q) \in V \times Q$, the Stokes projection $\Pi(w, q) = \big(\mathcal{W}, \mathcal{Q}\big)$ satisfies

$$\begin{aligned} &\nu(\nabla w, \nabla v^h) - (q, \nabla \cdot v^h) = \nu(\nabla \mathcal{W}, \nabla v^h) - (\mathcal{Q}, \nabla \cdot v^h), \\ &(p^h, \nabla \cdot \mathcal{W}) = 0, \qquad \forall (v^h, p^h) \in X^h \times Q^h. \end{aligned} \tag{179}$$

The above Stokes projection on $V^h \times Q^h$ is well defined since $X \subset (H_0^1(\Omega))^d$ if the domain Ω is bounded. We need the following approximation of Stokes projection (see [64, 80] for proof)

$$\begin{aligned} \|w - \mathcal{W}\| &\le Ch\big(\nu^{-1} \inf_{q^h \in Q^h} \|q - p^h\| + \inf_{v^h \in X^h} |w - v^h|_1\big), \\ \|w - \mathcal{W}\|_1 &\le C\big(\nu^{-1} \inf_{q^h \in Q^h} \|q - p^h\| + \inf_{v^h \in X^h} |w - v^h|_1\big). \end{aligned} \tag{180}$$

4.3 The variable step DLN method for CSM

We denote $w(t_n)$ by w_n and $q(t_n)$ by q_n in the CSM in (171). $w_n^h \in X^h$ and $q_n^h \in Q^h$ represent the DLN solutions of w_n and q_n respectively. For convenience, we denote

$$\begin{aligned} t_{n,\beta} &= \sum_{\ell=0}^{2} \beta_\ell^{(n)} t_{n-1+\ell}, \qquad w_{n,\beta} = \sum_{\ell=0}^{2} \beta_\ell^{(n)} w(t_{n-1+\ell}), \qquad w_{n,\beta}^h = \sum_{\ell=0}^{2} \beta_\ell^{(n)} w_{n-1+\ell}^h, \\ q_{n,\beta} &= \sum_{\ell=0}^{2} \beta_\ell^{(n)} q(t_{n-1+\ell}), \qquad q_{n,\beta}^h = \sum_{\ell=0}^{2} \beta_\ell^{(n)} q_{n-1+\ell}^h, \qquad f_{n,\beta} = \sum_{\ell=0}^{2} \beta_\ell^{(n)} f(t_{n-1+\ell}), \end{aligned}$$

and represent the average time step $\alpha_2 k_n - \alpha_0 k_{n-1}$ by $\widehat{k}_n$. The variational formulation of the variable time-stepping DLN scheme (with grad-div stabilizer [33]) in (172) is: given $w_n^h,\ w_{n-1}^h \in X^h$ and $q_n^h,\ q_{n-1}^h \in Q^h$, find w_{n+1}^h and q_{n+1}^h satisfying

$$\begin{aligned} &\Big(\frac{\alpha_2 w_{n+1}^h + \alpha_1 w_n^h + \alpha_0 w_{n-1}^h}{\widehat{k}_n}, v^h\Big) + \frac{C_s^4 \delta^2}{\mu^2}\Big(\frac{\alpha_2 \nabla w_{n+1}^h + \alpha_1 \nabla w_n^h + \alpha_0 \nabla w_{n-1}^h}{\widehat{k}_n}, \nabla v^h\Big) \\ &+ \nu(\nabla w_{n,\beta}^h, \nabla v^h) + b^*(w_{n,\beta}^h, w_{n,\beta}^h, v^h) + \gamma(\nabla \cdot w_{n,\beta}^h, \nabla \cdot v^h) - (q_{n,\beta}^h, \nabla \cdot v^h) \\ &+ \Big((C_s\delta)^2 |\nabla w_{n,\beta}^h| \nabla w_{n,\beta}^h, \nabla v^h\Big) = (f_{n,\beta}, v^h), \qquad \forall v^h \in X^h, \\ &(\nabla \cdot w_{n,\beta}^h, p^h) = 0, \qquad \forall p^h \in Q^h, \end{aligned} \tag{181}$$

where constant $\gamma > 0$ needs to be decided by specific problems. Let $\widetilde{w_n^h}$ denote the standard (second order) linear extrapolation [95] of w_n^h

$$\widetilde{w_n^h} = \beta_2^{(n)} \left\{ \left(1 + \frac{k_n}{k_{n-1}}\right) w_n^h - \left(\frac{k_n}{k_{n-1}}\right) w_{n-1}^h \right\} + \beta_1^{(n)} w_n^h + \beta_0^{(n)} w_{n-1}^h.$$

After applying the linearly implicit DLN scheme for time discretization, we get the following discretization:

$$\begin{aligned}
&\left(\frac{\alpha_2 w^h_{n+1}+\alpha_1 w^h_n+\alpha_0 w^h_{n-1}}{\widehat{k_n}}, v^h\right)+\nu(\boldsymbol{\nabla} w^h_{n,\beta},\boldsymbol{\nabla} v^h)\\
&+\frac{C_s^4\delta^2}{\mu^2}\left(\frac{\alpha_2\boldsymbol{\nabla} w^h_{n+1}+\alpha_1\boldsymbol{\nabla} w^h_n+\alpha_0\boldsymbol{\nabla} w^h_{n-1}}{\widehat{k_n}},\boldsymbol{\nabla} v^h\right)+b^*(\widetilde{w^h_n}, w^h_{n,\beta}, v^h)+\gamma(\nabla\cdot w^h_{n,\beta},\nabla\cdot v^h)\\
&-(q^h_{n,\beta},\boldsymbol{\nabla}\cdot v^h)+\left((C_s\delta)^2|\boldsymbol{\nabla}\widetilde{w^h_n}|\boldsymbol{\nabla} w^h_{n,\beta},\boldsymbol{\nabla} v^h\right)=(f(t_{n,\beta}),v^h),\ \forall v^h\in X^h,\\
&(\boldsymbol{\nabla}\cdot w^h_{n,\beta},p^h)=0,\ \forall p^h\in Q^h.
\end{aligned}\tag{182}$$

4.4 Numerical Analysis

We define the discrete Bochner space with time grids $\{t_n\}_{n=0}^N$ on time interval $[0,T]$,

$$\begin{aligned}
\ell^\infty\big(0,N;(W^{m,p})^d\big):=&\big\{f(\cdot,t)\in(W^{m,p})^d:|||f|||_{\infty,m,p}<\infty\big\},\\
\ell^{p_1,\beta}\big(0,N;(W^{m,p_2})^d\big):=&\big\{f(\cdot,t)\in(W^{m,p_2})^d:|||f|||_{p_1,m,p_2,\beta}<\infty\big\},
\end{aligned}$$

where the corresponding discrete norms are

$$|||f|||_{\infty,m,p}:=\max_{0\le n\le N}\|f(\cdot,t_n)\|_{m,p},\quad |||f|||_{p_1,m,p_2,\beta}:=\Big(\sum_{n=1}^N(k_n+k_{n-1})\|f(\cdot,t_{n,\beta})\|^{p_1}_{m,p_2}\Big)^{1/p_1}.$$

Definition 66. *For $0\le\theta\le 1$, define the semi-positive symmetric definite matrix $G(\theta)$ by*

$$G(\theta)=\begin{bmatrix}\frac{1}{4}(1+\theta)\mathbb{I}_d & 0\\ 0 & \frac{1}{4}(1-\theta)\mathbb{I}_d\end{bmatrix}.$$

We present two Lemmas about stability and consistency of the DLN method.

Lemma 67. *Let $\{y_n\}_{n=0}^N$ be any sequence in $L^2(\Omega)$. For any $\theta \in [0,1]$ and $n \in \{1,2,\cdots,N-1\}$, we have*

$$\Big(\sum_{\ell=0}^{2}\alpha_\ell y_{n-1+\ell}, \sum_{\ell=0}^{2}\beta_\ell^{(n)} y_{n-1+\ell}\Big) = \left\|\begin{matrix} y_{n+1} \\ y_n \end{matrix}\right\|_{G(\theta)} - \left\|\begin{matrix} y_n \\ y_{n-1} \end{matrix}\right\|_{G(\theta)} + \Big\|\sum_{\ell=0}^{2}\lambda_\ell^{(n)} y_{n-1+\ell}\Big\|^2, \tag{183}$$

where the $\|\cdot\|_{G(\theta)}$-norm is

$$\left\|\begin{matrix} u \\ v \end{matrix}\right\|_{G(\theta)} = \frac{1}{4}(1+\theta)\|u\|^2 + \frac{1}{4}(1-\theta)\|v\|^2, \qquad \forall u, v \in L^2(\Omega), \tag{184}$$

and the coefficients $\{\lambda_\ell^{(n)}\}_{\ell=0}^2$ are

$$\lambda_1^{(n)} = -\frac{\theta(1-\theta^2)}{\sqrt{2}(1+\varepsilon_n\theta)}, \qquad \lambda_2^{(n)} = -\frac{1-\varepsilon_n}{2}\lambda_1^{(n)}, \qquad \lambda_0^{(n)} = -\frac{1+\varepsilon_n}{2}\lambda_1^{(n)}. \tag{185}$$

Proof. The proof of identity in (183) is just algebraic calculation. □

Remark 68. *If we replace $L^2(\Omega)$ by Euclidian space $\mathbb{R}^d$, the identity in* (183) *still holds and implies G-stability of the DLN method. (See [44, p.2] for the definition of G-stability.)*

Lemma 69. *Let Y be any Banach space over $\mathbb{R}$ with norm $\|\cdot\|_Y$, $\{t_n\}_{n=0}^N$ be time grids on time interval $[0,T]$ and u be the mapping from $[0,T]$ to Y. We set*

$$k_{\max} = \max_{0\le n\le N-1}\{k_n\},$$

and assume that the mapping $u(t)$ is smooth enough about the variable t, then for any $\theta \in [0,1]$,

$$\begin{aligned} \Big\|\sum_{\ell=0}^{2}\beta_\ell^{(n)} u(t_{n-1+\ell}) - u(t_{n,\beta})\Big\|_Y^2 \le & C(\theta)k_{\max}^3 \int_{t_{n-1}}^{t_{n+1}} \|u_{tt}\|_Y^2 dt, \\ \Big\|\frac{1}{\widehat{k}_n}\sum_{\ell=0}^{2}\alpha_\ell u(t_{n-1+\ell}) - u_t(t_{n,\beta})\Big\|_Y^2 \le & C(\theta)k_{\max}^3 \int_{t_{n-1}}^{t_{n+1}} \|u_{ttt}\|_Y^2 dt. \end{aligned} \tag{186}$$

Proof. We use Taylor's Theorem and expand $u(t_{n+1})$, $u(t_n)$, $u(t_{n-1})$ at $t_{n,\beta}$. By Hölder's inequality, we obtain (186). □

4.4.1 Stability of the DLN scheme for the CSM

The DLN method is a one parameter family of A-stable, 2 step, G-stable methods ($0 \leq \theta \leq 1$). It reduces to a one-step midpoint scheme if $\theta = 1$. The important property of it is G-stability matrix does not depend on the time step ratio but on θ in Lemma 67. In this section, we prove the unconditional, long-time, variable time step energy-stability of (181) by using the G-stability property (Lemma 67) of the method.

Theorem 70. *The one-leg variable time step DLN scheme by* (181) *is unconditionally, long-time stable, i.e. for any integer $N > 1$,*

$$\begin{aligned}
&\tfrac{1+\theta}{4}\big(\|w_N^h\|^2+\tfrac{C_s^4\delta^2}{\mu^2}\|\nabla w_N^h\|^2\big) + \tfrac{1-\theta}{4}\big(\|w_{N-1}^h\|^2+\tfrac{C_s^4\delta^2}{\mu^2}\|\nabla w_{N-1}^h\|^2\big)\\
&+\sum_{n=1}^{N-1}\Big(\Big\|\sum_{\ell=0}^{2}\lambda_\ell^{(n)}w_{n-1+\ell}^h\Big\|^2+\tfrac{C_s^4\delta^2}{\mu^2}\Big\|\sum_{\ell=0}^{2}\lambda_\ell^{(n)}\nabla w_{n-1+\ell}^h\Big\|^2\Big)+\sum_{n=1}^{N-1}\widehat{k}_n\big(\tfrac{\nu}{2}\|\nabla w_{n,\beta}^h\|^2+\gamma\|\nabla\cdot w_{n,\beta}^h\|^2\big)\\
&+\sum_{n=1}^{N-1}\widehat{k}_n\int_\Omega\big[(C_s\delta)^2|\nabla w_{n,\beta}^h|\big]|\nabla w_{n,\beta}^h|^2dx\leq\frac{C(\theta)k_{\max}^4}{\nu}\|f_{tt}\|^2_{L^2(0,T;X')}+\frac{1}{\nu}\|\|f\|\|^2_{2,-1,2,\beta}\\
&+\tfrac{1+\theta}{4}\big(\|w_1^h\|^2+\tfrac{C_s^4\delta^2}{\mu^2}\|\nabla w_1^h\|^2\big) + \tfrac{1-\theta}{4}\big(\|w_0^h\|^2+\tfrac{C_s^4\delta^2}{\mu^2}\|\nabla w_0^h\|^2\big).
\end{aligned}\tag{187}$$

Proof. We set $v^h = w_{n,\beta}^h,\ p^h = q_{n,\beta}^h$ in (181). By Lemma 31 and identity (183) in Lemma 67, we obtain

$$\begin{aligned}
&\Big(\sum_{\ell=0}^{2}\alpha_\ell w_{n-1+\ell}^h, w_{n,\beta}^h\Big)+\frac{C_s^4\delta^2}{\mu^2}\Big(\sum_{\ell=0}^{2}\alpha_\ell\nabla w_{n-1+\ell}^h,\nabla w_{n,\beta}^h\Big)+\gamma\widehat{k}_n\|\nabla\cdot w_{n,\beta}^h\|^2\\
&+\widehat{k}_n\int_\Omega\big(\nu+(C_s\delta)^2|\nabla w_{n,\beta}^h|\big)|\nabla w_{n,\beta}^h|^2\,dx=\widehat{k}_n(f_{n,\beta},w_{n,\beta}^h)\leq\widehat{k}_n\|f_{n,\beta}\|_{-1}\|\nabla w_{n,\beta}^h\|.
\end{aligned}$$

The G-stability relation (67) implies

$$\begin{aligned}
&\left\|\begin{matrix}w_{n+1}^h\\ w_n^h\end{matrix}\right\|^2_{G(\theta)}-\left\|\begin{matrix}w_n^h\\ w_{n-1}^h\end{matrix}\right\|^2_{G(\theta)}+\Big\|\sum_{\ell=0}^{2}\lambda_\ell^{(n)}w_{n-1+\ell}^h\Big\|^2+\widehat{k}_n\int_\Omega\big(\tfrac{\nu}{2}+(C_s\delta)^2|\nabla w_{n,\beta}^h|\big)|\nabla w_{n,\beta}^h|^2dx\\
&+\gamma\widehat{k}_n\|\nabla\cdot w_{n,\beta}^h\|^2+\frac{C_s^4\delta^2}{\mu^2}\Big(\left\|\begin{matrix}\nabla w_{n+1}^h\\ \nabla w_n^h\end{matrix}\right\|^2_{G(\theta)}-\left\|\begin{matrix}\nabla w_n^h\\ \nabla w_{n-1}^h\end{matrix}\right\|^2_{G(\theta)}+\Big\|\sum_{\ell=0}^{2}\lambda_\ell^{(n)}\nabla w_{n-1+\ell}^h\Big\|^2\Big)\\
&\leq\frac{\widehat{k}_n}{2\nu}\|f_{n,\beta}\|^2_{-1}.
\end{aligned}\tag{188}$$

By triangle inequality and (186) in Lemma 69, we get,

$$\begin{aligned}\frac{\widehat{k_n}}{2\nu}\|f_{n,\beta}\|_{-1}^2 \leq & \frac{\widehat{k_n}}{\nu}\|f_{n,\beta}-f(t_{n,\beta})\|_{-1}^2+\frac{\widehat{k_n}}{\nu}\|f(t_{n,\beta})\|_{-1}^2 \\ \leq & \frac{C(\theta)k_{\max}^4}{\nu}\int_{t_{n-1}}^{t_{n+1}}\|f_{tt}\|_{-1}^2dt+\frac{(k_n+k_{n-1})}{\nu}\|f(t_{n,\beta})\|_{-1}^2.\end{aligned}$$

Summing (188) over n from 1 to $N-1$, we have desired result (187). □

Remark 71. *We identify the following quantities from the energy equality in* (187)*:*

1. *Model kinetic energy,*

$$\mathcal{E}_N^{\texttt{EN}}=\frac{1+\theta}{4}\big(\|w_N^h\|^2+\frac{C_s^4\delta^2}{\mu^2}\|\nabla w_N^h\|^2\big)+\frac{1-\theta}{4}\big(\|w_{N-1}^h\|^2+\frac{C_s^4\delta^2}{\mu^2}\|\nabla w_{N-1}^h\|^2\big).$$

2. *Energy dissipation due to viscous force,*

$$\mathcal{E}_N^{\texttt{VD}}=\nu\|\nabla w_{N-1,\beta}^h\|^2.$$

3. *Eddy viscosity dissipation,*

$$\mathcal{E}_N^{\texttt{EVD}}=\int_\Omega\big[(C_s\delta)^2|\nabla w_{N-1,\beta}^h|\big]|\nabla w_{N-1,\beta}^h|^2\,dx.$$

4. *Numerical dissipation,*

$$\mathcal{E}_N^{\texttt{ND}}=\left\|\frac{\sum_{l=0}^2\lambda_l^{N-1}w_{N-2+l}^h}{\sqrt{\widehat{k_{N-1}}}}\right\|^2+\frac{C_s^4\delta^2}{\mu^2}\left\|\frac{\sum_{l=0}^2\lambda_l^{N-1}\boldsymbol{\nabla} w_{N-2+l}^h}{\sqrt{\widehat{k_{N-1}}}}\right\|^2.$$

   $\mathcal{E}_N^{\texttt{ND}}$ *vanishes if and only if* $\theta\in\{0,1\}$.

5. *The model dissipation originating from the CSM in* (171)*,*

$$\begin{aligned}\mathcal{E}_N^{\texttt{MD}}=&\frac{C_s^4\delta^2}{\widehat{k_{N-1}}\mu^2}\Big(\left\|\begin{matrix}\nabla w_N^h\\ \nabla w_N^h\end{matrix}\right\|_{G(\theta)}^2-\left\|\begin{matrix}\nabla w_{N-1}\\ \nabla w_{N-1}\end{matrix}\right\|_{G(\theta)}^2+\Big\|\sum_{\ell=0}^2\lambda_\ell^{(N-1)}\nabla w_{N-2+\ell}^h\Big\|^2\Big)\\ &+\int_\Omega\big[(C_s\delta)^2|\nabla w_{N-1,\beta}^h|\big]|\nabla w_{N-1,\beta}^h|^2dx.\end{aligned}$$

   Model dissipation in this chapter can be positive or negative. When it is positive, it aggregates energy from mean to fluctuations. And when it is negative, energy is being transferred from fluctuations back to mean.

Remark 72. *The one-leg linearly implicit DLN method by (182) is unconditionally long-time stable, i.e. for any integer $N > 1$,*

$$\begin{aligned}
&\frac{1+\theta}{4}\big(\|w_N^h\|^2+\frac{C_s^4\delta^2}{\mu^2}\|\nabla w_N^h\|^2\big)+\frac{1-\theta}{4}\big(\|w_{N-1}^h\|^2+\frac{C_s^4\delta^2}{\mu^2}\|\nabla w_{N-1}^h\|^2\big)\\
&+\sum_{n=1}^{N-1}\Big(\Big\|\sum_{\ell=0}^{2}\lambda_\ell^{(n)}w_{n-1+\ell}^h\Big\|^2+\frac{C_s^4\delta^2}{\mu^2}\Big\|\sum_{\ell=0}^{2}\lambda_\ell^{(n)}\nabla w_{n-1+\ell}^h\Big\|^2\Big)+\sum_{n=1}^{N-1}\widehat{k}_n\big(\frac{\nu}{2}\|\nabla w_{n,\beta}^h\|^2+\gamma\|\nabla\cdot w_{n,\beta}^h\|^2\big)\\
&+\sum_{n=1}^{N-1}\widehat{k}_n\int_\Omega\big[(C_s\delta)^2|\widetilde{w_{n,\beta}^h}|\big]|\nabla w_{n,\beta}^h|^2dx\le\frac{C(\theta)k_{\max}^4}{\nu}\|f_{tt}\|_{L^2(0,T;X')}^2+\frac{1}{\nu}|||f|||_{2,-1,\beta}^2\\
&+\frac{1+\theta}{4}\big(\|w_1^h\|^2+\frac{C_s^4\delta^2}{\mu^2}\|\nabla w_1^h\|^2\big)+\frac{1-\theta}{4}\big(\|w_0^h\|^2+\frac{C_s^4\delta^2}{\mu^2}\|\nabla w_0^h\|^2\big).
\end{aligned}\tag{189}$$

4.4.2 Error Analysis of the DLN Scheme for the CSM

In this section, we analyze the error between the semi-discrete solution and the fully discrete solution to (171) in Theorem 73 under the following time step condition [1]:

$$\frac{C(\theta)}{\nu^3}\big(\widehat{k}_{n+1}\|\nabla w_{n+1,\beta}\|^4+\widehat{k}_n\|\nabla w_{n,\beta}\|^4+\widehat{k}_{n-1}\|\nabla w_{n-1,\beta}\|^4\big)<1,\qquad\forall n.\tag{190}$$

Theorem 73. *Let $(w(t),q(t))$ be sufficiently smooth, strong solution of the CSM. We assume that the velocity $w\in X$, pressure $q\in Q$, body force f of the CSM in (171) satisfy*

$$\begin{gathered}
w\in\ell^{2,\beta}(0,N;(H^{r+1})^d)\cap\ell^{4,\beta}(0,N;(H^{r+1})^d)\cap\ell^{3,\beta}(0,N;(H^{r+1})^d)\cap\ell^{3,\beta}(0,N;(W^{1,3})^d),\\
w_t\in L^2\big(0,T;(H^{r+1})^d\big),\qquad w_{ttt}\in L^2\big(0,T;(H^1)^d\big),\\
w_{tt}\in L^2\big(0,T;(H^{r+1})^d\big)\cap L^3\big(0,T;(W^{1,3})^d\big)\cap L^3\big(0,T;(H^{r+1})^d\big)\cap L^4\big(0,T;(H^{r+1})^d\big),\\
q\in\ell^{2,\beta}(0,N;H^{s+1}),\qquad f_{tt}\in L^2(0,T;X')
\end{gathered}$$

Under the time step condition in (190), the variable time-stepping DLN scheme (with $\theta\in[0,1]$) for the CSM in (181) satisfies: for $r,\ s,\in\{0\}\cup\mathbb{N}$ and any integer $N\ge 2$

$$\begin{aligned}
&\max_{0\le n\le N}\|w_n^h-w_n\|+C(\theta)\sqrt{\nu}\Big(\sum_{n=1}^{N-1}\widehat{k}_n\|\nabla(w_{n,\beta}^h-w_{n,\beta})\|^2\Big)^{1/2}\\
&\le\mathcal{O}\big(k_{\max}^2,h^r,h^{s+1},\delta h^{\frac{3r}{4}-\frac{d}{8}},\delta k_{\max}^{3/2}\big).
\end{aligned}\tag{191}$$

[1] To our best knowledge, time step condition like $\Delta t<\mathcal{O}(\nu^{-3})$ cannot be avoided for fully-implicit schemes in error analysis.

Remark 74. *Since δ has the same dimension as h, the spatial convergence rate in* (191) *is* $\min\{r, s+1\}$ *as long as the highest polynomial degree for velocity* $r \in \{1, 2\}$*. Thus the DLN algorithm in* (172) *is second-order accurate in both time and space if we choose Taylor-Hood* $\mathbb{P}2 - \mathbb{P}1$ *finite element space and set the time step* $\Delta t \approx h$*.*

Proof. We start with the CSM at time $t_{n,\beta}$ $(1 \le n \le N-1)$. For any $v^h \in V^h$, the variational formulation becomes

$$
\begin{aligned}
&(w_t(t_{n,\beta}), v^h) + \frac{C_s^4\delta^2}{\mu^2}(\nabla w_t(t_{n,\beta}), \nabla v^h) + b^*\big(w(t_{n,\beta}), w(t_{n,\beta}), v^h\big) - (q(t_{n,\beta}), \nabla\cdot v^h)\\
&+\nu(\nabla w(t_{n,\beta}), \nabla v^h) + \Big((C_s\delta)^2|\nabla w(t_{n,\beta})|\nabla w(t_{n,\beta}), \nabla v^h\Big) = \big(f(t_{n,\beta}), v^h\big), \quad \forall v^h \in V^h.
\end{aligned}
$$

Equivalently,

$$
\begin{aligned}
&\Big(\frac{\alpha_2 w_{n+1} + \alpha_1 w_n + \alpha_0 w_{n-1}}{\widehat{k}_n}, v^h\Big) + \frac{C_s^4\delta^2}{\mu^2}\Big(\frac{\alpha_2\nabla w_{n+1} + \alpha_1\nabla w_n + \alpha_0\nabla w_{n-1}}{\widehat{k}_n}, \nabla v^h\Big)\\
&+ b^*(w_{n,\beta}, w_{n,\beta}, v^h) - \big(q(t_{n,\beta}), \nabla\cdot v^h\big) + \nu(\nabla w_{n,\beta}, \nabla v^h) + \gamma(\nabla\cdot w_{n,\beta}, \nabla\cdot v^h)\\
&+ \Big((C_s\delta)^2|\nabla w_{n,\beta}|\nabla w_{n,\beta}, \nabla v^h\Big) = (f_{n,\beta}, v^h) + \tau_n(v^h),
\end{aligned}
\tag{192}
$$

where the truncation error is

$$
\begin{aligned}
\tau_n(v^h) = &\Big(\frac{\alpha_2 w_{n+1} + \alpha_1 w_n + \alpha_0 w_{n-1}}{\widehat{k}_n} - w_t(t_{n,\beta}), v^h\Big) + \nu\big(\nabla\big(w_{n,\beta} - w(t_{n,\beta})\big), \nabla v^h\big)\\
&+ \frac{C_s^4\delta^2}{\mu^2}\Big(\frac{\alpha_2\nabla w_{n+1} + \alpha_1\nabla w_n + \alpha_0\nabla w_{n-1}}{\widehat{k}_n} - \nabla w_t(t_{n,\beta}), \nabla v^h\Big)\\
&+ b^*(w_{n,\beta}, w_{n,\beta}, v^h) - b^*(w(t_{n,\beta}), w(t_{n,\beta}), v^h) + \big(f(t_{n,\beta}) - f_{n,\beta}, v^h\big)\\
&+ \Big((C_s\delta)^2\big(|\nabla w_{n,\beta}|\nabla w_{n,\beta} - |\nabla w(t_{n,\beta})|\nabla w(t_{n,\beta})\big), \nabla v^h\Big).
\end{aligned}
$$

Let W_n be velocity component of Stokes projection of $(w_n, 0)$ onto $V^h \times Q^h$. We set

$$
\begin{aligned}
&e_n = w_n - w_n^h, \qquad \eta_n = w_n - W_n, \qquad \phi_n^h = w_n^h - W_n,\\
&e_{n,\beta} = \sum_{\ell=0}^{2}\beta_\ell^{(n)} e_{n-1+\ell}, \qquad \eta_{n,\beta} = \sum_{\ell=0}^{2}\beta_\ell^{(n)}\eta_{n-1+\ell}, \qquad \phi_{n,\beta}^h = \sum_{\ell=0}^{2}\beta_\ell^{(n)}\phi_{n-1+\ell}^h.
\end{aligned}
\tag{193}
$$

Then the velocity error e_n can be decomposed as $e_n = \eta_n - \phi_n^h$. We subtract the DLN scheme in (181) from (192) to get the following,

$$\begin{aligned}
&\Big(\frac{\alpha_2 e_{n+1} + \alpha_1 e_n + \alpha_0 e_{n-1}}{\widehat{k}_n}, v^h\Big) + \frac{C_s^4\delta^2}{\mu^2}\Big(\frac{\alpha_2\nabla e_{n+1} + \alpha_1\nabla e_n + \alpha_0\nabla e_{n-1}}{\widehat{k}_n}, \nabla v^h\Big)\\
&+b^*(w_{n,\beta}, w_{n,\beta}, v^h) - b^*(w_{n,\beta}^h, w_{n,\beta}^h, v^h) + \nu(\nabla e_{n,\beta}, \nabla v^h) + \gamma(\nabla\cdot e_{n,\beta}, \nabla\cdot v^h)\\
&+\Big((C_s\delta)^2(|\nabla w_{n,\beta}|\nabla w_{n,\beta} - |\nabla w_{n,\beta}^h|\nabla w_{n,\beta}^h), \nabla v^h\Big) = \big(q(t_{n,\beta}), \nabla\cdot v^h\big) + \tau_n(v^h), \quad \forall v^h \in V^h.
\end{aligned}$$

Notice that,

$$\begin{aligned}
&b^*(w_{n,\beta}, w_{n,\beta}, v^h) - b^*(w_{n,\beta}^h, w_{n,\beta}^h, v^h)\\
=&b^*(w_{n,\beta}, w_{n,\beta}, v^h) - b^*(w_{n,\beta}^h, w_{n,\beta}, v^h) + b^*(w_{n,\beta}^h, w_{n,\beta}, v^h) - b^*(w_{n,\beta}^h, w_{n,\beta}^h, v^h),\\
=&b^*(e_{n,\beta}, w_{n,\beta}, v^h) + b^*(w_{n,\beta}^h, e_{n,\beta}, v^h),
\end{aligned}$$

and

$$\begin{aligned}
&\int_\Omega (|\nabla w_{n,\beta}|\nabla w_{n,\beta} - |\nabla w_{n,\beta}^h|\nabla w_{n,\beta}^h) : \nabla v^h dx\\
=&\int_\Omega (|\nabla w_{n,\beta}|\nabla w_{n,\beta} - |\nabla W_{n,\beta}|\nabla W_{n,\beta} + |\nabla W_{n,\beta}|\nabla W_{n,\beta} - |\nabla w_{n,\beta}^h|\nabla w_{n,\beta}^h) : \nabla v^h dx.
\end{aligned}$$

Hence,

$$\begin{aligned}
&\Big(\frac{\alpha_2\phi_{n+1}^h + \alpha_1\phi_n^h + \alpha_0\phi_{n-1}^h}{\widehat{k}_n}, v^h\Big) + \frac{C_s^4\delta^2}{\mu^2}\Big(\frac{\alpha_2\nabla\phi_{n+1}^h + \alpha_1\nabla\phi_n^h + \alpha_0\nabla\phi_{n-1}^h}{\widehat{k}_n}, \nabla v^h\Big)\\
&- b^*(e_{n,\beta}, w_{n,\beta}, v^h) - b^*(w_{n,\beta}^h, e_{n,\beta}, v^h) + \nu(\nabla\phi_{n,\beta}^h, \nabla v^h) + \gamma(\nabla\cdot\phi_{n,\beta}^h, \nabla\cdot v^h)\\
&+ (C_s\delta)^2\int_\Omega (|\nabla w_{n,\beta}^h|\nabla w_{n,\beta}^h - |\nabla W_{n,\beta}|\nabla W_{n,\beta}) : (\nabla v^h) dx\\
=&\Big(\frac{\alpha_2\eta_{n+1} + \alpha_1\eta_n + \alpha_0\eta_{n-1}}{\widehat{k}_n}, v^h\Big) + \frac{C_s^4\delta^2}{\mu^2}\Big(\frac{\alpha_2\nabla\eta_{n+1} + \alpha_1\nabla\eta_n + \alpha_0\nabla\eta_{n-1}}{\widehat{k}_n}, \nabla v^h\Big)\\
&+ (C_s\delta)^2\int_\Omega (|\nabla w_{n,\beta}|\nabla w_{n,\beta} - |\nabla W_{n,\beta}|\nabla W_{n,\beta}) : \nabla v^h dx\\
&+ \nu(\nabla\eta_{n,\beta}, \nabla v^h) + \gamma(\nabla\cdot\eta_{n,\beta}, \nabla\cdot v^h) - \big(q(t_{n,\beta}), \nabla\cdot v^h\big) - \tau_n(v^h).
\end{aligned} \tag{194}$$

We set $v^h = \phi^h_{n,\beta}$ in (194) and use (183) in Lemma 67,

$$\begin{aligned}
&\left\|\begin{matrix}\phi^h_{n+1}\\ \phi^h_n\end{matrix}\right\|^2_{G(\theta)} - \left\|\begin{matrix}\phi^h_{n}\\ \phi^h_{n-1}\end{matrix}\right\|^2_{G(\theta)} + \Big\|\sum_{\ell=0}^{2}\lambda^{(n)}_\ell \phi^h_{n-1+\ell}\Big\|^2 + \nu\widehat{k}_n\|\nabla\phi^h_{n,\beta}\|^2 + \gamma\widehat{k}_n\|\nabla\cdot\phi^h_{n,\beta}\|^2\\
&+\frac{C_s^4\delta^2}{\mu^2}\Big(\left\|\begin{matrix}\nabla\phi^h_{n+1}\\ \nabla\phi^h_n\end{matrix}\right\|^2_{G(\theta)} - \left\|\begin{matrix}\nabla\phi^h_{n}\\ \nabla\phi^h_{n-1}\end{matrix}\right\|^2_{G(\theta)} + \Big\|\sum_{\ell=0}^{2}\lambda^{(n)}_\ell \nabla\phi^h_{n-1+\ell}\Big\|^2\Big) \qquad (195)\\
&+(C_s\delta)^2\widehat{k}_n\int_\Omega(|\nabla w^h_{n,\beta}|\nabla w^h_{n,\beta} - |\nabla W_{n,\beta}|\nabla W_{n,\beta}) : (\nabla\phi^h_{n,\beta})dx\\
=&\Big(\sum_{\ell=0}^{2}\alpha_\ell\eta_{n-1+\ell},\phi^h_{n,\beta}\Big) + \frac{C_s^4\delta^2}{\mu^2}\Big(\sum_{\ell=0}^{2}\alpha_\ell\nabla\eta_{n-1+\ell},\nabla\phi^h_{n,\beta}\Big) + \nu\widehat{k}_n(\nabla\eta_{n,\beta},\nabla\phi^h_{n,\beta})\\
&+\gamma\widehat{k}_n(\nabla\cdot\eta_{n,\beta},\nabla\cdot\phi^h_{n,\beta}) + \widehat{k}_n b^*(e_{n,\beta},w_{n,\beta},\phi^h_{n,\beta}) + \widehat{k}_n b^*(w^h_{n,\beta},e_{n,\beta},\phi^h_{n,\beta})\\
&+(C_s\delta)^2\widehat{k}_n\int_\Omega(|\nabla w_{n,\beta}|\nabla w_{n,\beta} - |\nabla W_{n,\beta}|\nabla W_{n,\beta}) : \nabla\phi^h_{n,\beta}dx - \widehat{k}_n\big(q(t_{n,\beta}),\nabla\cdot\phi^h_{n,\beta}\big) - \widehat{k}_n\tau_n(\phi^h_{n,\beta}).
\end{aligned}$$

By strong monotonicity property (175) in Lemma 64,

$$(C_s\delta)^2\widehat{k}_n\int_\Omega(|\nabla w^h_{n,\beta}|\nabla w^h_{n,\beta} - |\nabla W_{n,\beta}|\nabla W_{n,\beta}) : (\nabla\phi^h_{n,\beta})dx \geq C_1(C_s\delta)^2\widehat{k}_n\|\nabla\phi^h_{n,\beta}\|^3_{0,3}. \qquad (196)$$

By Cauchy Schwarz inequality, Poincaré inequality and Young's inequality, we obtain

$$\Big(\sum_{\ell=0}^{2}\alpha_\ell\eta_{n-1+\ell},\phi^h_{n,\beta}\Big) \leq \frac{1}{\nu\widehat{k}_n}\Big\|\sum_{\ell=0}^{2}\alpha_\ell\eta_{n-1+\ell}\Big\|^2 + \frac{\nu\widehat{k}_n}{32}\|\nabla\phi^h_{n,\beta}\|^2 \qquad (197)$$

We use the approximation of Stokes projection in (180) and Hölder's inequality

$$\begin{aligned}
\Big\|\sum_{\ell=0}^{2}\alpha_\ell\eta_{n-1+\ell}\Big\|^2 \leq& Ch^{2r+2}\Big\|\sum_{\ell=0}^{2}\alpha_\ell w_{n-1+\ell}\Big\|^2_{r+1} \qquad (198)\\
\leq& C(\theta)h^{2r+2}\big(\|w_{n+1}-w_n\|^2_{r+1} + \|w_{n+1}-w_{n-1}\|^2_{r+1}\big)\\
\leq& C(\theta)h^{2r+2}(k_n+k_{n-1})\int_{t_{n-1}}^{t_{n+1}}\|w_t\|^2_{r+1}dt.
\end{aligned}$$

By (198), (197) becomes

$$\Big(\sum_{\ell=0}^{2}\alpha_\ell\eta_{n-1+\ell},\phi^h_{n,\beta}\Big) \leq C(\theta)h^{2r+2}\int_{t_{n-1}}^{t_{n+1}}\|w_t\|^2_{r+1}dt + \frac{\nu\widehat{k}_n}{32}\|\nabla\phi^h_{n,\beta}\|^2. \qquad (199)$$

Similarly, we have

$$\frac{C_s^4\delta^2}{\mu^2}\Big(\sum_{\ell=0}^{2}\alpha_\ell\nabla\eta_{n-1+\ell},\nabla\phi_{n,\beta}^h\Big)\leq C(\theta)h^{2r}\Big(\frac{C_s^4\delta^2}{\mu^2}\Big)^2\int_{t_{n-1}}^{t_{n+1}}\|w_t\|_{r+1}^2dt+\frac{\nu\widehat{k}_n}{32}\|\nabla\phi_{n,\beta}^h\|^2. \tag{200}$$

By the definition of Stokes projection in (179), $(\nabla\eta_{n,\beta},\nabla\phi_{n,\beta}^h)=0$. By Cauchy Schwarz inequality, Poincaré inequality and Young's inequality,

$$\gamma\widehat{k}_n(\nabla\cdot\eta_{n,\beta},\nabla\cdot\phi_{n,\beta}^h)\leq\gamma d\widehat{k}_n\|\nabla\eta_{n,\beta}\|\|\nabla\phi_{n,\beta}^h\|\leq\frac{C\gamma^2\widehat{k}_n}{\nu}\|\nabla\eta_{n,\beta}\|^2+\frac{\nu\widehat{k}_n}{32}\|\nabla\phi_{n,\beta}^h\|^2. \tag{201}$$

By the approximation of Stokes projection in (180), triangle inequality and (186) in Lemma 69

$$\begin{aligned}\|\nabla\eta_{n,\beta}\|^2\leq&Ch^{2r}\big(\|w_{n,\beta}-w(t_{n,\beta})\|_{r+1}^2+\|w(t_{n,\beta})\|_{r+1}^2\big)\\ \leq&Ch^{2r}\Big(k_{\max}^3\int_{t_{n-1}}^{t_{n+1}}\|w_{tt}\|_{r+1}^2dt+\|w(t_{n,\beta})\|_{r+1}^2\Big).\end{aligned} \tag{202}$$

Hence (201) becomes

$$\begin{aligned}&\gamma\widehat{k}_n(\nabla\cdot\eta_{n,\beta},\nabla\cdot\phi_{n,\beta}^h)\\ \leq&\frac{C\gamma^2h^{2r}}{\nu}\Big(k_{\max}^4\int_{t_{n-1}}^{t_{n+1}}\|w_{tt}\|_{r+1}^2dt+(k_n+k_{n-1})\|w(t_{n,\beta})\|_{r+1}^2\Big)+\frac{\nu\widehat{k}_n}{32}\|\nabla\phi_{n,\beta}^h\|^2.\end{aligned} \tag{203}$$

By (174) in Lemma 62, Young's inequality and approximation of Stokes projection in 177

$$\begin{aligned}&\widehat{k}_nb^*(e_{n,\beta},w_{n,\beta},\phi_{n,\beta}^h)\\ =&\widehat{k}_nb^*(\eta_{n,\beta},w_{n,\beta},\phi_{n,\beta}^h)-\widehat{k}_nb^*(\phi_{n,\beta}^h,w_{n,\beta},\phi_{n,\beta}^h)\\ \leq&C\widehat{k}_n\|\nabla\eta_{n,\beta}\|\|\nabla w_{n,\beta}\|\|\nabla\phi_{n,\beta}^h\|+C\widehat{k}_n\|\phi_{n,\beta}^h\|^{1/2}\|\nabla w_{n,\beta}\|\|\nabla\phi_{n,\beta}^h\|^{3/2}\\ \leq&\frac{C\widehat{k}_n}{\nu}\|\nabla\eta_{n,\beta}\|^2\|\nabla w_{n,\beta}\|^2+\frac{C\widehat{k}_n}{\nu^3}\|\nabla w_{n,\beta}\|^4\|\phi_{n,\beta}^h\|^2+\frac{\nu\widehat{k}_n}{32}\|\nabla\phi_{n,\beta}^h\|^2\\ \leq&\frac{C\widehat{k}_nh^{2r}}{\nu}\big(\|w_{n,\beta}\|_{r+1}^4+\|\nabla w_{n,\beta}\|^4\big)+\frac{C\widehat{k}_n}{\nu^3}\|\nabla w_{n,\beta}\|^4\|\phi_{n,\beta}^h\|^2+\frac{\nu\widehat{k}_n}{32}\|\nabla\phi_{n,\beta}^h\|^2\end{aligned} \tag{204}$$

We use triangle inequality, (186) in Lemma 69 and Hölder's inequality

$$\|w_{n,\beta}\|_{r+1}^4\leq C\big(\|w_{n,\beta}-w(t_{n,\beta})\|_{r+1}^4+\|w(t_{n,\beta})\|_{r+1}^4\big)$$

$$
\begin{aligned}
&\leq C\Big[\big(Ck_{\max}^3\int_{t_{n-1}}^{t_{n+1}} 1\cdot\|w_{tt}\|_{r+1}^2dt\big)^2+\|w(t_{n,\beta})\|_{r+1}^4\Big]\\
&\leq C(\theta)\Big(k_{\max}^7\int_{t_{n-1}}^{t_{n+1}}\|w_{tt}\|_{r+1}^4dt+\|w(t_{n,\beta})\|_{r+1}^4\Big),\\
\|\nabla w_{n,\beta}\|^4 \leq& C(\theta)\Big(k_{\max}^7\int_{t_{n-1}}^{t_{n+1}}\|\nabla w_{tt}\|^4dt+\|\nabla w(t_{n,\beta})\|^4\Big)
\end{aligned}
$$

Thus (204) becomes

$$
\begin{aligned}
&\widehat{k}_n b^*(e_{n,\beta},w_{n,\beta},\phi_{n,\beta}^h)\\
\leq&\frac{C(\theta)h^{2r}}{\nu}\Big(k_{\max}^8\int_{t_{n-1}}^{t_{n+1}}\|w_{tt}\|_{r+1}^4dt+k_{\max}^8\int_{t_{n-1}}^{t_{n+1}}\|\nabla w_{tt}\|^4dt\\
&\qquad+(k_n+k_{n-1})\|w(t_{n,\beta})\|_{r+1}^4+(k_n+k_{n-1})\|\nabla w(t_{n,\beta})\|^4\Big)\\
&+\frac{C\widehat{k}_n}{\nu^3}\|\nabla w_{n,\beta}\|^4\|\phi_{n,\beta}^h\|^2+\frac{\nu\widehat{k}_n}{32}\|\nabla\phi_{n,\beta}^h\|^2.
\end{aligned}
\tag{205}
$$

By (173) and approximation of Stokes projection in (180)

$$
\begin{aligned}
\widehat{k}_n b^*(w_{n,\beta}^h,e_{n,\beta},\phi_{n,\beta}^h)\leq&\frac{C\widehat{k}_n}{\nu}\|\nabla w_{n,\beta}^h\|^2\|\nabla\eta_{n,\beta}\|^2+\frac{\nu\widehat{k}_n}{32}\|\nabla\phi_{n,\beta}^h\|^2\\
\leq&\frac{Ch^r\widehat{k}_n}{\nu}\||w|\|_{\infty,r+1,2}^2\|\nabla w_{n,\beta}^h\|^2+\frac{\nu\widehat{k}_n}{32}\|\nabla\phi_{n,\beta}^h\|^2.
\end{aligned}
\tag{206}
$$

By Local Lipschitz continuity (176) in Lemma 64

$$
\begin{aligned}
&(C_s\delta)^2\widehat{k}_n\int_\Omega(|\nabla w_{n,\beta}|\nabla w_{n,\beta}-|\nabla W_{n,\beta}|\nabla W_{n,\beta}):(\nabla\phi_{n,\beta}^h)dx\\
\leq&(C_s\delta)^2\widehat{k}_nC_2\mathcal{R}_n\|\nabla\eta_{n,\beta}\|_{0,3}\|\nabla\phi_{n,\beta}^h\|_{0,3}\\
\leq&\frac{C(C_s\delta)^2C_2^{3/2}\widehat{k}_n}{\sqrt{C_1}}\mathcal{R}_n^{3/2}\|\nabla\eta_{n,\beta}\|_{0,3}^{3/2}+\frac{C_1(C_s\delta)^2\widehat{k}_n}{3}\|\nabla\phi_{n,\beta}^h\|_{0,3}^3,
\end{aligned}
\tag{207}
$$

where $\mathcal{R}_n=\max\{\|\nabla w_{n,\beta}\|_{0,3},\|\nabla W_{n,\beta}\|_{0,3}\}$. By triangle inequality,

$$
\mathcal{R}_n\leq\max\big\{\|\nabla w_{n,\beta}\|_{0,3},\big\|\nabla\big(W_{n,\beta}-w_{n,\beta}\big)\big\|_{0,3}+\|\nabla w_{n,\beta}\|_{0,3}\big\}=\|\nabla\eta_{n,\beta}\|_{0,3}+\|\nabla w_{n,\beta}\|_{0,3}.
$$

We use (178) in Theorem 65, triangle inequality and approximation theorem of interpolation in (177)

$$
\|\nabla\eta_{n,\beta}\|_{0,3}\leq Ch^{-d/6}\|\nabla\eta_{n,\beta}\|\leq Ch^{r-d/6}\|w_{n,\beta}\|_{r+1}
$$

By the fact: for any $a, b, c \in \mathbb{R}$ with $c > 1$,

$$(|a| + |b|)^c \leq 2^{c-1}(|a|^c + |b|^c), \tag{208}$$

we have

$$\begin{aligned}\mathcal{R}_n^{3/2}\|\nabla\eta_{n,\beta}\|_{0,3}^{3/2} \leq & C\big(\|\nabla\eta_{n,\beta}\|_{0,3}^3 + \|\nabla\eta_{n,\beta}\|_{0,3}^{3/2}\|\nabla w_{n,\beta}\|_{0,3}^{3/2}\big) \\ \leq & Ch^{3r-d/2}\|w_{n,\beta}\|_{r+1}^3 + Ch^{3/2r-d/4}\|w_{n,\beta}\|_{r+1}^{3/2}\|\nabla w_{n,\beta}\|_{0,3}^{3/2} \\ \leq & Ch^{3r-d/2}\|w_{n,\beta}\|_{r+1}^3 + Ch^{3/2r-d/4}\big(\|w_{n,\beta}\|_{r+1}^3 + \|\nabla w_{n,\beta}\|_{0,3}^3\big).\end{aligned} \tag{209}$$

By triangle inequality, the fact in (208), (186) in Lemma 69 and Hölder's inequality,

$$\begin{aligned}\|w_{n,\beta}\|_{r+1}^3 \leq & C\|w_{n,\beta} - w(t_{n,\beta})\|_{r+1}^3 + C\|w(t_{n,\beta})\|_{r+1}^3 \\ \leq & C\Big(k_{\max}^3\int_{t_{n-1}}^{t_{n+1}}\|w_{tt}\|_{r+1}^2 dt\Big)^{3/2} + C\|w(t_{n,\beta})\|_{r+1}^3 \\ \leq & Ck_{\max}^5\int_{t_{n-1}}^{t_{n+1}}\|w_{tt}\|_{r+1}^3 dt + C\|w(t_{n,\beta})\|_{r+1}^3.\end{aligned} \tag{210}$$

By (209) and (210), (207) becomes

$$\begin{aligned}&(C_s\delta)^2\widehat{k}_n\int_\Omega(|\nabla w_{n,\beta}|\nabla w_{n,\beta} - |\nabla W_{n,\beta}|\nabla W_{n,\beta}) : (\nabla\phi_{n,\beta}^h)dx \\ \leq & \frac{C(C_s\delta)^2C_2^{3/2}}{\sqrt{C_1}}\Big[(1 + h^{\frac{3r}{2}-\frac{d}{4}})h^{\frac{3r}{2}-\frac{d}{4}}\big(k_{\max}^6\int_{t_{n-1}}^{t_{n+1}}\|w_{tt}\|_{r+1}^3 dt + (k_n + k_{n-1})\|w(t_{n,\beta})\|_{r+1}^3\big) \\ & + h^{\frac{3r}{2}-\frac{d}{4}}\big(k_{\max}^6\int_{t_{n-1}}^{t_{n+1}}\|\nabla w_{tt}\|_{0,3}^3 dt + (k_n + k_{n-1})\|\nabla w(t_{n,\beta})\|_{0,3}^3\big)\Big].\end{aligned} \tag{211}$$

We choose p^h to be L^2-projection of $q(t_{n,\beta})$ onto Q^h, then

$$\widehat{k}_n\big(q(t_{n,\beta}), \nabla\cdot\phi_{n,\beta}^h\big) = \widehat{k}_n\big(q(t_{n,\beta}) - p^h, \nabla\cdot\phi_{n,\beta}^h\big) \leq \sqrt{d}\widehat{k}_n\|q(t_{n,\beta}) - p^h\|\|\nabla\phi_{n,\beta}^h\|. \tag{212}$$

By Young's inequality and approximation of pressure in (177), (212) becomes

$$\widehat{k}_n\big(q(t_{n,\beta}), \nabla\cdot\phi_{n,\beta}^h\big) \leq \frac{Ch^{2s+2}}{\nu}(k_n + k_{n-1})\|q(t_{n,\beta})\|_{s+1}^2 + \frac{\nu\widehat{k}_n}{32}\|\nabla\phi_{n,\beta}^h\|^2 \tag{213}$$

Now we deal $\widehat{k}_n\tau_n(\phi^h_{n,\beta})$: by Cauchy Schwarz inequality, Poincaré inequality and (186) in Lemma 69, the first three terms become

$$\begin{aligned}
&\widehat{k}_n\Big(\frac{\alpha_2 w_{n+1}+\alpha_1 w_n+\alpha_0 w_{n-1}}{\widehat{k}_n}-w_t(t_{n,\beta}),\phi^h_{n,\beta}\Big)\\
\leq& C\widehat{k}_n\Big\|\frac{\alpha_2 w_{n+1}+\alpha_1 w_n+\alpha_0 w_{n-1}}{\widehat{k}_n}-w_t(t_{n,\beta})\Big\|\|\nabla\phi^h_{n,\beta}\|\\
\leq&\frac{C\widehat{k}_n}{\nu}\Big\|\frac{\alpha_2 w_{n+1}+\alpha_1 w_n+\alpha_0 w_{n-1}}{\widehat{k}_n}-w_t(t_{n,\beta})\Big\|^2+\frac{\nu\widehat{k}_n}{32}\|\nabla\phi^h_{n,\beta}\|^2\\
\leq&\frac{C(\theta)k_{\max}^4}{\nu}\int_{t_{n-1}}^{t_{n+1}}\|w_{ttt}\|^2dt+\frac{\nu\widehat{k}_n}{32}\|\nabla\phi^h_{n,\beta}\|^2,
\end{aligned}\tag{214}$$

$$\begin{aligned}
\nu\widehat{k_n}\big(\nabla(w_{n,\beta}-w(t_{n,\beta})),\nabla\phi^h_{n,\beta}\big)\leq&\frac{C\widehat{k}_n}{\nu}\big\|\nabla w_{n,\beta}-\nabla w(t_{n,\beta})\big\|+\frac{\nu\widehat{k}_n}{32}\|\nabla\phi^h_{n,\beta}\|^2\\
\leq&\frac{Ck_{\max}^4}{\nu}\int_{t_{n-1}}^{t_{n+1}}\|\nabla w_{tt}\|^2dt+\frac{\nu\widehat{k}_n}{32}\|\nabla\phi^h_{n,\beta}\|^2,
\end{aligned}\tag{215}$$

and

$$\begin{aligned}
&\frac{C_s^4\delta^2\widehat{k}_n}{\mu^2}\Big(\frac{\alpha_2\nabla w_{n+1}+\alpha_1\nabla w_n+\alpha_0\nabla w_{n-1}}{\widehat{k}_n}-\nabla w_t(t_{n,\beta}),\nabla\phi^h_{n,\beta}\Big)\\
\leq&\frac{C\widehat{k}_n}{\nu}\Big(\frac{C_s^4\delta^2}{\mu^2}\Big)^2\Big\|\nabla\Big(\frac{\alpha_2 w_{n+1}+\alpha_1 w_n+\alpha_0 w_{n-1}}{\widehat{k}_n}-w_t(t_{n,\beta})\Big)\Big\|^2+\frac{\nu\widehat{k}_n}{32}\|\nabla\phi^h_{n,\beta}\|^2\\
\leq&\frac{C(\theta)k_{\max}^4}{\nu}\Big(\frac{C_s^4\delta^2}{\mu^2}\Big)^2\int_{t_{n-1}}^{t_{n+1}}\|\nabla w_{ttt}\|^2dt+\frac{\nu\widehat{k}_n}{32}\|\nabla\phi^h_{n,\beta}\|^2.
\end{aligned}\tag{216}$$

By (174) in Lemma 62 and triangle inequality, two non-linear terms become

$$\begin{aligned}
&\widehat{k}_n b^*\big(w_{n,\beta},w_{n,\beta},\phi^h_{n,\beta}\big)-\widehat{k}_n b^*\big(w(t_{n,\beta}),w(t_{n,\beta}),\phi^h_{n,\beta}\big)\\
=&\widehat{k}_n b^*\big(w_{n,\beta}-w(t_{n,\beta}),w_{n,\beta},\phi^h_{n,\beta}\big)+\widehat{k}_n b^*\big(w(t_{n,\beta}),w_{n,\beta}-w(t_{n,\beta}),\phi^h_{n,\beta}\big)\\
\leq&\frac{C\widehat{k}_n}{\nu}\big\|\nabla(w_{n,\beta}-w(t_{n,\beta}))\big\|^2\big(\|\nabla w_{n,\beta}\|^2+\|\nabla w(t_{n,\beta})\|^2\big)+\frac{\nu\widehat{k}_n}{32}\|\nabla\phi^h_{n,\beta}\|^2\\
\leq&\frac{C\widehat{k}_n}{\nu}\big\|\nabla(w_{n,\beta}-w(t_{n,\beta}))\big\|^2\big(\big\|\nabla(w_{n,\beta}-w(t_{n,\beta}))\big\|^2+2\|\nabla w(t_{n,\beta})\|^2\big)+\frac{\nu\widehat{k}_n}{32}\|\nabla\phi^h_{n,\beta}\|^2.
\end{aligned}$$

By (186) in Lemma 69 and Hölder's inequality,

$$\left\|\nabla(w_{n,\beta}-w(t_{n,\beta}))\right\|^4 \leq C(\theta)k_{\max}^7\int_{t_{n-1}}^{t_{n+1}}\|\nabla w_{tt}\|^4dt.$$

$$\begin{aligned}\left\|\nabla(w_{n,\beta}-w(t_{n,\beta}))\right\|^2\|\nabla w(t_{n,\beta})\|^2 \leq& C(\theta)k_{\max}^3\int_{t_{n-1}}^{t_{n+1}}\|\nabla w(t_{n,\beta})\|^2\|\nabla w_{tt}\|^2dt\\ \leq& C(\theta)k_{\max}^3\int_{t_{n-1}}^{t_{n+1}}\left(\|\nabla w(t_{n,\beta})\|^4+\|\nabla w_{tt}\|^4\right)dt\\ \leq& C(\theta)k_{\max}^3\int_{t_{n-1}}^{t_{n+1}}\|\nabla w_{tt}\|^4dt+C(\theta)k_{\max}^4\|\nabla w(t_{n,\beta})\|^4.\end{aligned}$$

$$\begin{aligned}&\widehat{k}_n b^*\left(w_{n,\beta},w_{n,\beta},\phi_{n,\beta}^h\right)-\widehat{k}_n b^*\left(w(t_{n,\beta}),w(t_{n,\beta}),\phi_{n,\beta}^h\right) \qquad (217)\\ \leq&\frac{C(\theta)k_{\max}^4}{\nu}\Big[\left(1+k_{\max}^4\right)\int_{t_{n-1}}^{t_{n+1}}\|\nabla w_{tt}\|^4dt+(k_n+k_{n-1})\|\nabla w(t_{n,\beta})\|^4\Big]+\frac{\nu\widehat{k}_n}{32}\|\nabla\phi_{n,\beta}^h\|^2.\end{aligned}$$

$$\begin{aligned}\widehat{k}_n\left(f(t_{n,\beta})-f_{n,\beta},\phi_{n,\beta}^h\right)\leq&\frac{C\widehat{k_n}}{\nu}\|f(t_{n,\beta})-f_{n,\beta}\|_{-1}^2+\frac{\nu\widehat{k}_n}{32}\|\nabla\phi_{n,\beta}^h\|^2\\ \leq&\frac{C\widehat{k_n}}{\nu}k_{\max}^3\int_{t_{n-1}}^{t_{n+1}}\|f_{tt}\|_{-1}^2dt+\frac{\nu\widehat{k}_n}{32}\|\nabla\phi_{n,\beta}^h\|^2. \qquad (218)\end{aligned}$$

By (176) in Lemma 64 and Young's inequality,

$$\begin{aligned}&\widehat{k}_n\Big((C_s\delta)^2(|\nabla w_{n,\beta}|\nabla w_{n,\beta}-|\nabla w(t_{n,\beta})|\nabla w(t_{n,\beta})),\nabla\phi_{n,\beta}^h\Big) \qquad (219)\\ \leq&\widehat{k}_n(C_s\delta)^2C_2\mathcal{S}_n\left\|\nabla(w_{n,\beta}-w(t_{n,\beta}))\right\|_{0,3}\|\nabla\phi_{n,\beta}^h\|_{0,3}\\ \leq&\frac{C(C_s\delta)^2C_2^{3/2}\widehat{k}_n}{\sqrt{C_1}}\mathcal{S}_n^{3/2}\left\|\nabla(w_{n,\beta}-w(t_{n,\beta}))\right\|_{0,3}^{3/2}+\frac{C_1(C_s\delta)^2\widehat{k}_n}{4}\|\nabla\phi_{n,\beta}^h\|_{0,3}^3,\end{aligned}$$

where $\mathcal{S}_n=\max\left\{\|\nabla w_{n,\beta}\|_{0,3},\|\nabla w(t_{n,\beta})\|_{0,3}\right\}$. By (186) in Lemma 69 and Young's inequality,

$$\begin{aligned}&\mathcal{S}_n^{3/2}\left\|\nabla\left(w(t_{n,\beta})-w_{n,\beta}\right)\right\|_{0,3}^{3/2} \qquad (220)\\ \leq&C\Big(\left\|\nabla\left(w(t_{n,\beta})-w_{n,\beta}\right)\right\|_{0,3}^3+\left\|\nabla\left(w(t_{n,\beta})-w_{n,\beta}\right)\right\|_{0,3}^{3/2}\|\nabla w_{n,\beta}\|_{0,3}^{3/2}\Big)\\ \leq&C(\theta)\Big(k_{\max}^3\int_{t_{n-1}}^{t_{n+1}}\|\nabla w_{tt}\|_{0,3}^2dt\Big)^{3/2}+C(\theta)\Big(k_{\max}^3\int_{t_{n-1}}^{t_{n+1}}\|\nabla w_{tt}\|_{0,3}^2dt\Big)^{3/4}\|\nabla w_{n,\beta}\|_{0,3}^{3/2}\end{aligned}$$

$$
\begin{aligned}
&\le C(\theta)k_{\max}^{9/2}\Big(\int_{t_{n-1}}^{t_{n+1}}\|\nabla w_{tt}\|_{0,3}^2dt\Big)^{3/2}+C(\theta)k_{\max}^{3/2}\Big(\int_{t_{n-1}}^{t_{n+1}}\|\nabla w_{tt}\|_{0,3}^2dt\Big)^{3/2}+C(\theta)k_{\max}^3\|\nabla w_{n,\beta}\|_{0,3}^3\\
&\le C(\theta)k_{\max}^{9/2}\Big(\int_{t_{n-1}}^{t_{n+1}}\|\nabla w_{tt}\|_{0,3}^2dt\Big)^{3/2}+C(\theta)k_{\max}^{3/2}\Big(\int_{t_{n-1}}^{t_{n+1}}\|\nabla w_{tt}\|_{0,3}^2dt\Big)^{3/2}\\
&\quad+C(\theta)k_{\max}^3\Big(\big\|\nabla\big(w(t_{n,\beta})-w_{n,\beta}\big)\big\|_{0,3}^3+\|\nabla w(t_{n,\beta})\|_{0,3}^3\Big).\\
&\le C(\theta)\big(k_{\max}^{15/2}+k_{\max}^{9/2}+k_{\max}^{3/2}\big)\Big(\int_{t_{n-1}}^{t_{n+1}}\|\nabla w_{tt}\|_{0,3}^2dt\Big)^{3/2}+C(\theta)k_{\max}^3\|\nabla w(t_{n,\beta})\|_{0,3}^3.
\end{aligned}
$$

By Hölder's inequality,

$$
\Big(\int_{t_{n-1}}^{t_{n+1}}\|\nabla w_{tt}\|_{0,3}^2dt\Big)^{3/2}\le Ck_{\max}^{1/2}\int_{t_{n-1}}^{t_{n+1}}\|\nabla w_{tt}\|_{0,3}^3dt. \tag{221}
$$

By (220) and (221), (219) becomes

$$
\begin{aligned}
&\widehat{k}_n\Big((C_s\delta)^2(|\nabla w_{n,\beta}|\nabla w_{n,\beta}-|\nabla w(t_{n,\beta})|\nabla w(t_{n,\beta})),\nabla\phi_{n,\beta}^h\Big) \qquad (222)\\
&\le\frac{C(\theta)k_{\max}^3(C_s\delta)^2C_2^{3/2}}{\sqrt{C_1}}\Big[\big(k_{\max}^6+k_{\max}^3+1\big)\int_{t_{n-1}}^{t_{n+1}}\|\nabla w_{tt}\|_{0,3}^3dt+(k_n+k_{n-1})\|\nabla w(t_{n,\beta})\|_{0,3}^3\Big].
\end{aligned}
$$

We combine (196), (199), (200), (203), (204), (206), (211), (213)-(218), (222) in (195) and then sum (195) over n from 1 to $N-1$ to obtain

$$
\begin{aligned}
&\left\|\begin{matrix}\phi_N^h\\ \phi_{N-1}^h\end{matrix}\right\|_{G(\theta)}^2+\frac{C_s^4\delta^2}{\mu^2}\left\|\begin{matrix}\nabla\phi_N^h\\ \nabla\phi_{N-1}^h\end{matrix}\right\|_{G(\theta)}^2+\sum_{n=1}^{N-1}\Big(\Big\|\sum_{\ell=0}^{2}\lambda_\ell^{(n)}\phi_{n-1+\ell}^h\Big\|^2+\Big\|\sum_{\ell=0}^{2}\lambda_\ell^{(n)}\nabla\phi_{n-1+\ell}^h\Big\|^2\Big)\\
&+\sum_{n=1}^{N-1}\frac{\nu}{2}\widehat{k}_n\|\nabla\phi_{n,\beta}^h\|^2+\sum_{n=1}^{N-1}\gamma\widehat{k}_n\|\nabla\cdot\phi_{n,\beta}^h\|^2+\sum_{n=1}^{N-1}C_1(C_s\delta)^2\widehat{k}_n\|\nabla\phi_{n,\beta}^h\|_{0,3}^3\\
&\le\sum_{n=1}^{N-1}\frac{C(\theta)\widehat{k}_n\|\nabla w_{n,\beta}\|^4}{\nu^3}\big(\|\phi_{n+1}^h\|^2+\|\phi_n^h\|^2+\|\phi_{n-1}^h\|^2\big)+\frac{Ch^r}{\nu^2}|||w|||_{\infty,r+1,2}^2\Big(\sum_{n=1}^{N-1}\nu\widehat{k}_n\|\nabla w_{n,\beta}^h\|^2\Big)\\
&\quad+F(\theta,k_{\max},h,\delta)+\left\|\begin{matrix}\phi_1^h\\ \phi_0^h\end{matrix}\right\|_{G(\theta)}^2+\frac{C_s^4\delta^2}{\mu^2}\left\|\begin{matrix}\nabla\phi_1^h\\ \nabla\phi_0^h\end{matrix}\right\|_{G(\theta)}^2,
\end{aligned}
\tag{223}
$$

where

$$
F(\theta,k_{\max},h,\delta)=C(\theta)h^{2r+2}\|w_t\|_{L^2(0,T;H^{r+1})}^2+C(\theta)\Big(\frac{C_s^4\delta^2}{\mu^2}\Big)^2h^{2r}\|w_t\|_{L^2(0,T;H^{r+1})}^2
$$

$$
\begin{aligned}
&+\frac{C\gamma^2h^{2r}}{\nu}\Big(k_{\max}^4\|w_{tt}\|^2_{L^2(0,T;H^{r+1})}+|||w|||^2_{2,r+1,2,\beta}\Big)\\
&+\frac{C(\theta)h^{2r}}{\nu}\Big(k_{\max}^8\|w_{tt}\|^4_{L^4(0,T;H^{r+1})}+k_{\max}^8\|\nabla w_{tt}\|^4_{L^4(0,T;L^2)}+|||w|||^4_{4,r+1,2,\beta}\\
&+|||\nabla w|||^4_{4,0,2,\beta}\Big)\\
&+\frac{C(C_s\delta)^2C_2^{3/2}}{\sqrt{C_1}}\Big[(1+h^{\frac{3r}{2}-\frac{d}{4}})h^{\frac{3r}{2}-\frac{d}{4}}\big(k_{\max}^6\|w_{tt}\|^3_{L^3(0,T;H^{r+1})}+|||w|||^3_{3,r+1,2,\beta}\big)\\
&\qquad\qquad+h^{\frac{3r}{2}-\frac{d}{4}}\big(k_{\max}^6\|\nabla w_{tt}\|^3_{L^3(0,T;L^3)}+|||\nabla w|||^3_{3,0,3,\beta}\big)\Big]\\
&+\frac{Ch^{2s+2}}{\nu}|||q|||^2_{2,s+1,2,\beta}+\frac{C(\theta)k_{\max}^4}{\nu}\|w_{ttt}\|^2_{L^2(0,T;L^2)}+\frac{Ck_{\max}^4}{\nu}\|\nabla w_{tt}\|^2_{L^2(0,T;L^2)}\\
&+\frac{C(\theta)k_{\max}^4}{\nu}\Big(\frac{C_s^4\delta^2}{\mu^2}\Big)^2\|\nabla w_{ttt}\|^2_{L^2(0,T;L^2)}\\
&+\frac{C(\theta)k_{\max}^4}{\nu}\Big[\big(1+k_{\max}^4\big)\|\nabla w_{tt}\|^4_{L^4(0,T;L^2)}+|||\nabla w|||^4_{4,0,2,\beta}\Big]+\frac{Ck_{\max}^4}{\nu}\|f_{tt}\|^2_{L^2(0,T;X')}\\
&+\frac{C(\theta)k_{\max}^3(C_s\delta)^2C_2^{3/2}}{\sqrt{C_1}}\Big[\big(k_{\max}^6+k_{\max}^3+1\big)\|\nabla w_{tt}\|^3_{L^3(0,T;L^3)}+|||\nabla w|||^3_{3,0,3,\beta}\Big].
\end{aligned}
$$

By (187) in Theorem 70,

$$
\sum_{n=1}^{N-1}\nu\widehat{k}_n\|\nabla w^h_{n,\beta}\|^2<C(\theta).
$$

We set

$$
D_n=\frac{C(\theta)\widehat{k}_n\|\nabla w_{n,\beta}\|^4}{k_{\max}\nu^3},\qquad 1\le n\le N-1,
$$

and

$$
d_n=\begin{cases}
D_1 & n=0\\
D_1+D_2 & n=1\\
D_{n-1}+D_n+D_{n+1} & 2\le n\le N-2\\
D_{N-2}+D_{N-1} & n=N-1\\
D_{N-1} & n=N
\end{cases}\cdot \tag{224}
$$

By the time step restriction in (190), we have $k_{\max}d_n < 1$ for all n. Then we use the definition of $G(\theta)$-norm in (184) and apply Grönwall's inequality in Lemma 63 to (223) (with d_n defined in (224) and $\Delta t = k_{\max}$)

$$\|\phi_N^h\|^2 + C(\theta)\sum_{n=1}^{N-1}\frac{\nu}{2}\widehat{k}_n\|\nabla\phi_{n,\beta}^h\|^2 \tag{225}$$
$$\leq \exp\Big(\sum_{n=1}^{N-1}\frac{k_{\max}d_n}{1-k_{\max}d_n}\Big)\Big[\frac{C(\theta)h^r}{\nu^2}|||w|||_{\infty,r+1,2}^2 + F(\theta,k_{\max},h,\delta)$$
$$+ C(\theta)\big(\|\phi_1^h\|^2 + \|\phi_0^h\|\big) + \frac{C(\theta)C_s^4\delta^2}{\mu^2}\big(\|\nabla\phi_1^h\|^2 + \|\nabla\phi_0^h\|\big)\Big].$$

By triangle inequality and approximation of Stokes projection in (177), we have (191). □

Remark 75. *The Semi-implicit DLN algorithm has been applied to the Navier Stokes equation [118] and outperforms the corresponding fully implicit algorithm in two aspects: removing the time step restriction like* (190) *as well as avoiding the non-linear solver at each time step. For error analysis of the semi-implicit DLN algorithm for CSM* (182)*, the SM* (175) *and LLC* (176) *conclusions should be adjusted and are left as open problems. To do so, one can follow the work in [75, 76] where a new linear extrapolation of the convecting velocity for CNLE is proposed that ensures energetic stability without a time-step restriction.*

4.5 Numerical Tests

In this section, we perform two numerical tests. In the first test, we show the numerical error and the rate of convergence of the DLN scheme. In the second test, we show whether DLN exhibits intermittent backscatter for both the constant time step and variable time step. In both tests, we consider the DLN algorithm with three particular values of the parameter $\theta = 2/3,\ 2/\sqrt{5},\ 1$. In order to minimize the error constant and maintain strong stability qualities, the value $\theta = 2/3$ was proposed in [47]. In [87, 88], the value $\theta = 2/\sqrt{5}$ was suggested to guarantee the best stability at infinity, i.e. for this value the scheme has

good performance in long-time simulation. In the case when $\theta = 1$, the DLN method reduces to the symplectic midpoint rule, having the smallest error constant [98] and conserving all quadratic Hamiltonians. For test 2, we also consider $\theta = \ 0.95,\ 0.98$ so that we can check how the DLN scheme behaves near $\theta = 1$.

4.5.1 A test with exact solution

(We choose the test problem from DeCaria, Layton, and McLaughlin [52]). The first experiment tests the accuracy of the DLN algorithm and convergence rate of (182) with constant time-step. It confirms the second-order convergence of the DLN method. The following test has an exact solution for the 2D Navier Stokes problem. Let the domain be $\Omega = (-1, 1) \times (-1, 1)$. The exact solution is as follows:

$$u(x, y, t) = \pi \sin t(\sin 2\pi y \sin^2 \pi x, -\sin 2\pi x \sin^2 \pi y).$$
$$p(x, y, t) = \sin t \cos \pi x \sin \pi y.$$

This is inserted into the CSM and the body force $f(x, t)$ is calculated. Taylor-Hood elements (P2-P1) were used in this test for the spatial discretization. We simulate the test up to $T = 10.$ and take $C_s = 0.1,\ \mu = 0.4,\ \delta$ is taken to be the shortest edge of all triangles. We test the constant step DLN with $\theta = 2/3$. We define the error for velocity and pressure to be

$$e_n^w = w(t_n) - w_n^h, \quad e_n^p = p(t_n) - p_n^h.$$

Let k be the constant time step. We define two discrete norms for the errors as follows

$$|||e^w|||_{\infty,0} := \max_{0\le n\le N} \|e_n^w\|_{L^2(\Omega)}, \quad |||e^w|||_{0,0} := \Big(\sum_{0\le n\le N} k\|e_n^w\|^2_{L^2(\Omega)} \Big)^{1/2},$$
$$|||e^p|||_{\infty,0} := \max_{0\le n\le N} \|e_n^p\|_{L^2(\Omega)}, \quad |||e^p|||_{0,0} := \Big(\sum_{0\le n\le N} k\|e_n^p\|^2_{L^2(\Omega)} \Big)^{1/2}.$$

Time step k	Mesh size h	$\|\|\|e^w\|\|\|_{\infty,0}$	Rate	$\|\|\|\nabla e^w\|\|\|_{\infty,0}$	Rate	$\|\|\|e^p\|\|\|_{\infty,0}$	Rate
0.08	0.08571	6.0302	-	56.8481	-	10.8576	-
0.04	0.04221	0.0498844	6.9175	1.35745	5.3881	0.079143	7.1000
0.02	0.02095	0.0119835	2.0575	0.399758	1.7637	0.0192928	2.0364
0.01	0.01048	0.00297779	2.0087	0.10394	1.9434	0.00490525	1.9757

Table 9: Errors by $\|\cdot\|_{\infty,0}$-norm and Convergence Rate for the constant DLN with $\theta = 2/3$.

Time step k	Mesh size h	$\|\|\|e^w\|\|\|_{0,0}$	Rate	$\|\|\|\nabla e^w\|\|\|_{0,0}$	Rate	$\|\|\|e^p\|\|\|_{0,0}$	Rate
0.08	0.08571	7.8961	-	79.3971	-	12.3373	-
0.04	0.04221	0.107395	6.2001	3.06024	4.6974	0.143315	6.4277
0.02	0.02095	0.024972	2.1045	0.900864	1.7643	0.0345612	2.0520
0.01	0.01048	0.00617647	2.0155	0.234349	1.9427	0.00877951	1.9769

Table 10: Errors by $\|\cdot\|_{0,0}$-norm and Convergence Rate for the constant DLN with $\theta = 2/3$.

In this test, Section 4.5.1 and Section 4.5.1 show that for a true solution, we get the predicted rate of convergence. We also see the same behavior for $\theta = 2/\sqrt{5},\ 1$ (See Appendix). This is also evident that the DLN allows larger time steps to get the desired accuracy.

4.5.2 Test2. Flow between offset cylinder

(We choose the test problem from Jiang and Layton [78, 2D Test Problem]). This flow problem is tested to show whether or not the transfer of energy from fluctuations back to means in the turbulent flow using the Corrected Smagorinksy Model (171) happens. The domain is a disk with a smaller off-center obstacle inside. Let $r_1 = 1, r_2 = 0.1, c = (c_1, c_2) =$

$(1/2, 0)$, then the domain is given by

$$\Omega = \{(x, y) : x^2 + y^2 < r_1^2 \text{ and } (x - c_1)^2 + (y - c_2)^2 > r_2^2\}.$$

The flow is driven by a counterclockwise rotational body force

$$f(x, y, t) = (-4y * (1 - x^2 - y^2), 4x * (1 - x^2 - y^2))^T,$$

with no-slip boundary conditions on both circles. We discretize in space using Taylor-Hood elements. There are 400 mesh points around the outer circle and 100 mesh points around the inner circle. The flow is driven by a counterclockwise force (f=0 on the outer circle). Thus, the flow rotates about the origin and interacts with the immersed circle. We start the initial condition by solving the Stokes problem. We compute up to the final time $T_{final} = 10$. Take $C_s = 0.1, \mu = 0.4, \delta$ is taken to be the shortest edge of all triangles ≈ 0.0112927, Re=10,000. For the DLN algorithm in (182), we compute the following quantities:

Model dissipation, $\mathcal{E}_N^{\texttt{MD}}$

$$= \int_\Omega \Big(\frac{C_s^4 \delta^2}{\mu^2} \frac{\alpha_2 \boldsymbol{\nabla} w_N^h + \alpha_1 \boldsymbol{\nabla} w_{N-1}^h + \alpha_0 \boldsymbol{\nabla} w_{N-2}^h}{\widehat{k_{N-1}}} \cdot \boldsymbol{\nabla} w_{N-1,\beta}^h + (C_s\delta)^2 |\widetilde{\boldsymbol{\nabla} w_{N-1,\beta}^h}| |\boldsymbol{\nabla} w_{N-1,\beta}^h|^2 \Big) dx.$$

Effect of new term from CSM, $\mathcal{E}_N^{\texttt{CSMD}}$

$$= \int_\Omega \left(\frac{C_s^4 \delta^2}{\mu^2} \frac{\alpha_2 \boldsymbol{\nabla} w_N^h + \alpha_1 \boldsymbol{\nabla} w_{N-1}^h + \alpha_0 \boldsymbol{\nabla} w_{N-2}^h}{\widehat{k_{N-1}}} \cdot \boldsymbol{\nabla} w_{N-1,\beta}^h \right) dx.$$

Numerical dissipation, $\mathcal{E}_N^{\texttt{ND}} = \left\| \frac{\sum_{l=0}^2 \lambda_l^{N-1} w_{N-2+l}^h}{\sqrt{\widehat{k_{N-1}}}} \right\|^2 + \frac{C_s^4 \delta^2}{\mu^2} \left\| \frac{\sum_{l=0}^2 \lambda_l^{N-1} \boldsymbol{\nabla} w_{N-2+l}^h}{\sqrt{\widehat{k_{N-1}}}} \right\|^2.$

Viscous dissipation, $\mathcal{E}_N^{\texttt{VD}} = \nu \| \boldsymbol{\nabla} w_{N-1,\beta}^h \|^2$.

Kinetic Energy, $KE = \frac{1}{2} \| w_N^h \|^2$.

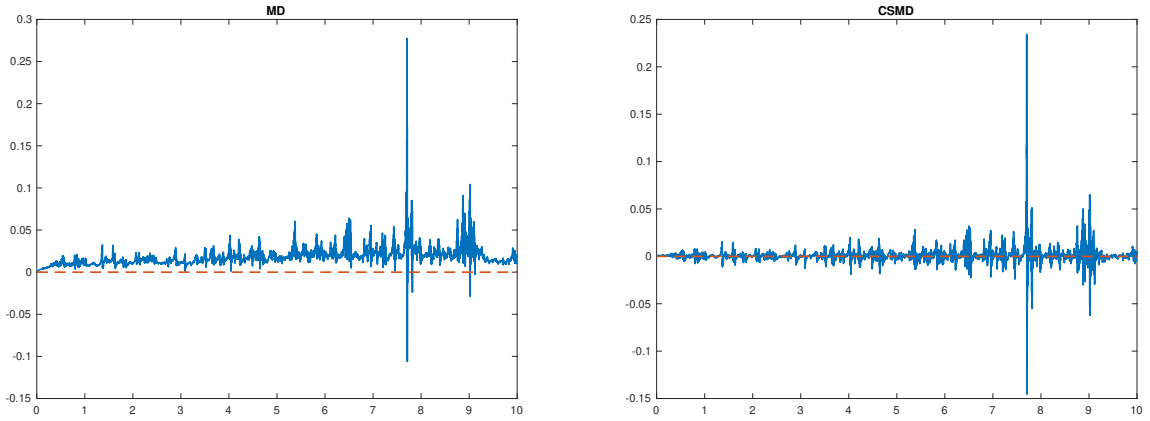

(a) $\mathcal{E}_N^{\texttt{MD}}$ (b) $\mathcal{E}_N^{\texttt{CSMD}}$

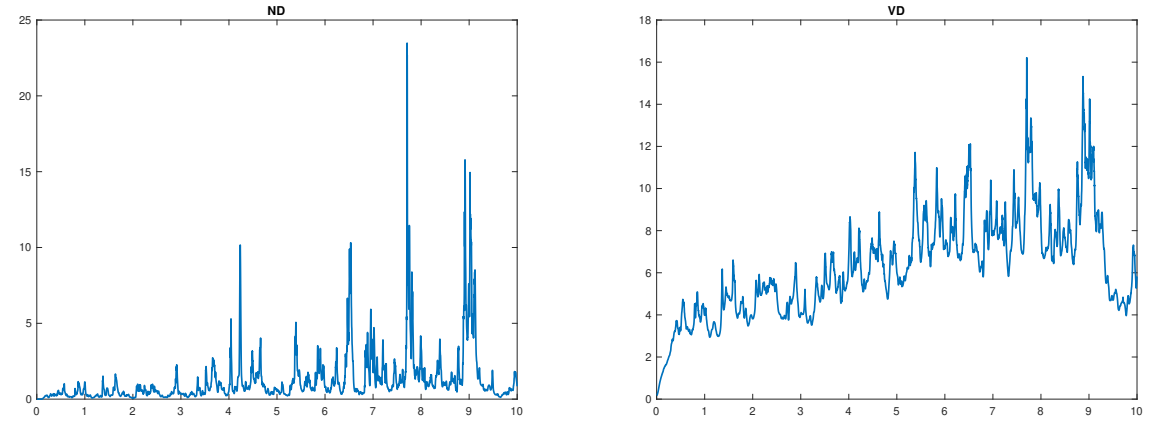

(c) $\mathcal{E}_N^{\texttt{ND}}$ (d) $\mathcal{E}_N^{\texttt{VD}}$

Figure 18: Constant time step DLN (182) with $k = 0.001,\ Re = 10,000,\ \theta = 0.98,\ C_s = 0.1,\ \mu = 0.4$. We do not see backscatter in $\mathcal{E}_N^{\texttt{MD}}$.

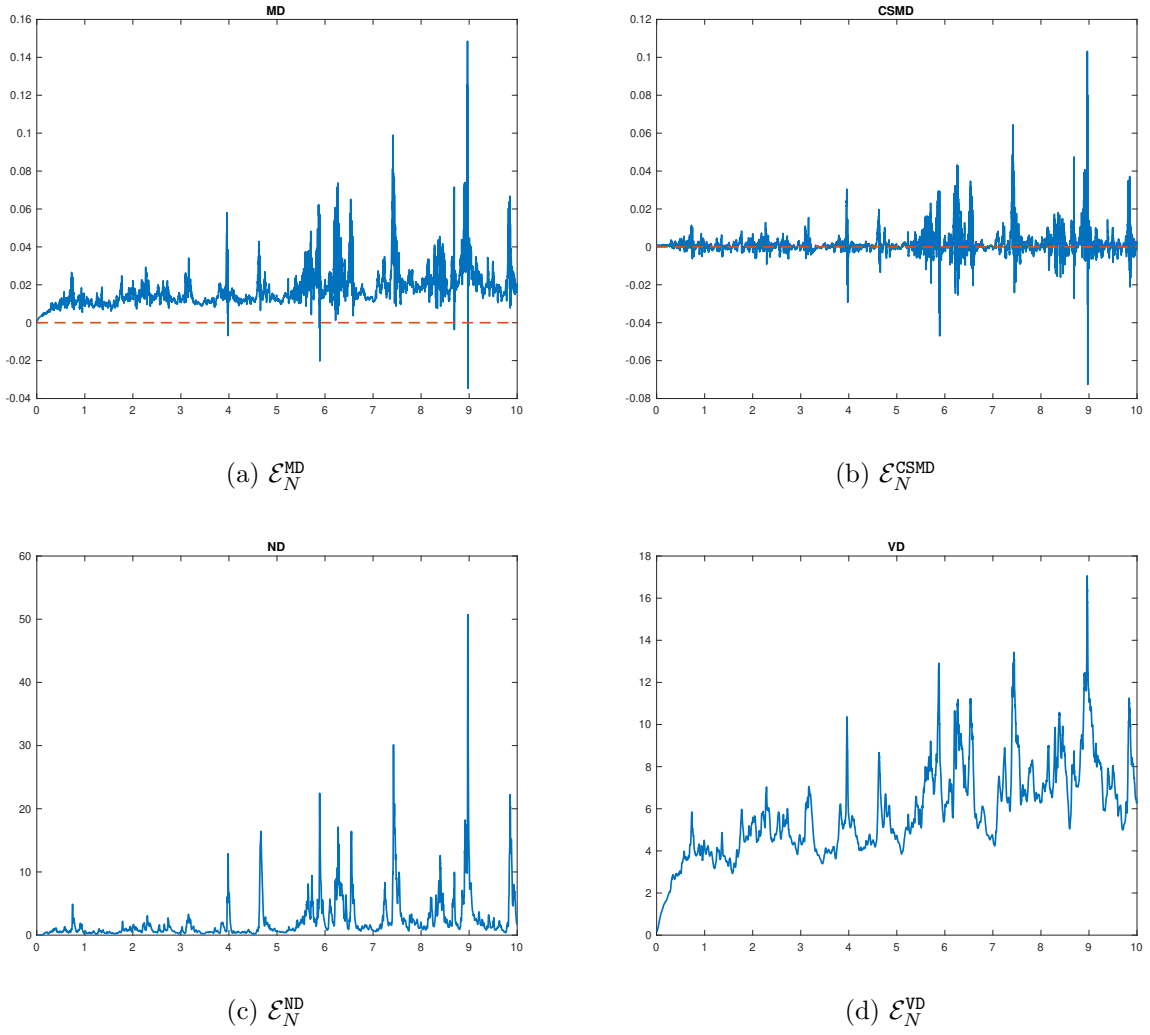

(a) $\mathcal{E}_N^{\texttt{MD}}$ (b) $\mathcal{E}_N^{\texttt{CSMD}}$

(c) $\mathcal{E}_N^{\texttt{ND}}$ (d) $\mathcal{E}_N^{\texttt{VD}}$

Figure 19: Constant time step DLN (182) with $k = 0.001,\ Re = 10,000,\ \theta = 0.95,\ C_s = 0.1,\ \mu = 0.4$. We do not see backscatter in $\mathcal{E}_N^{\texttt{MD}}$.

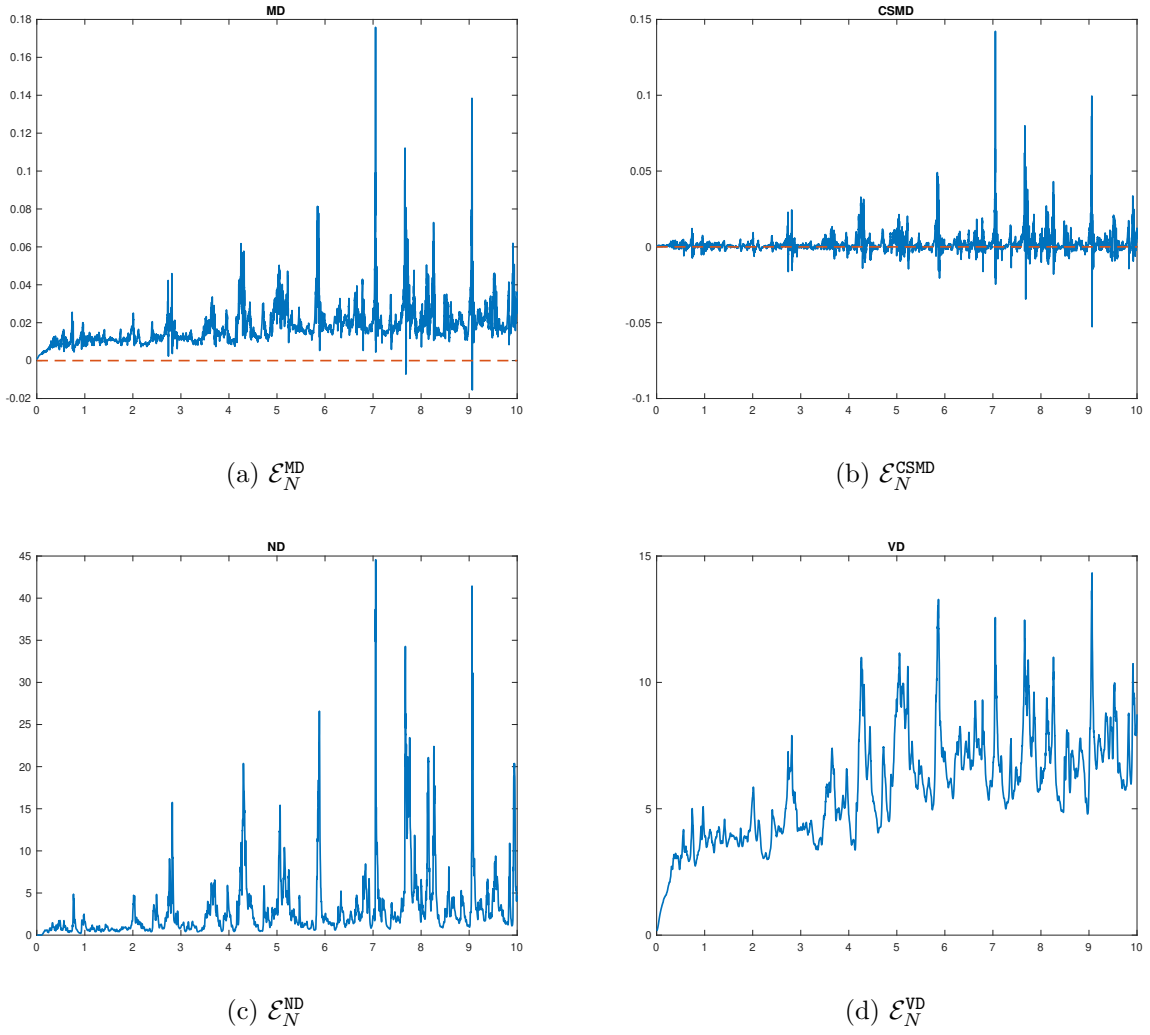

(a) $\mathcal{E}_N^{\texttt{MD}}$ (b) $\mathcal{E}_N^{\texttt{CSMD}}$

(c) $\mathcal{E}_N^{\texttt{ND}}$ (d) $\mathcal{E}_N^{\texttt{VD}}$

Figure 20: Constant time step DLN (182) with $k = 0.001,\ Re = 10,000,\ \theta = 2/\sqrt{5},\ C_s = 0.1,\ \mu = 0.4$. We do not see backscatter in $\mathcal{E}_N^{\texttt{MD}}$.

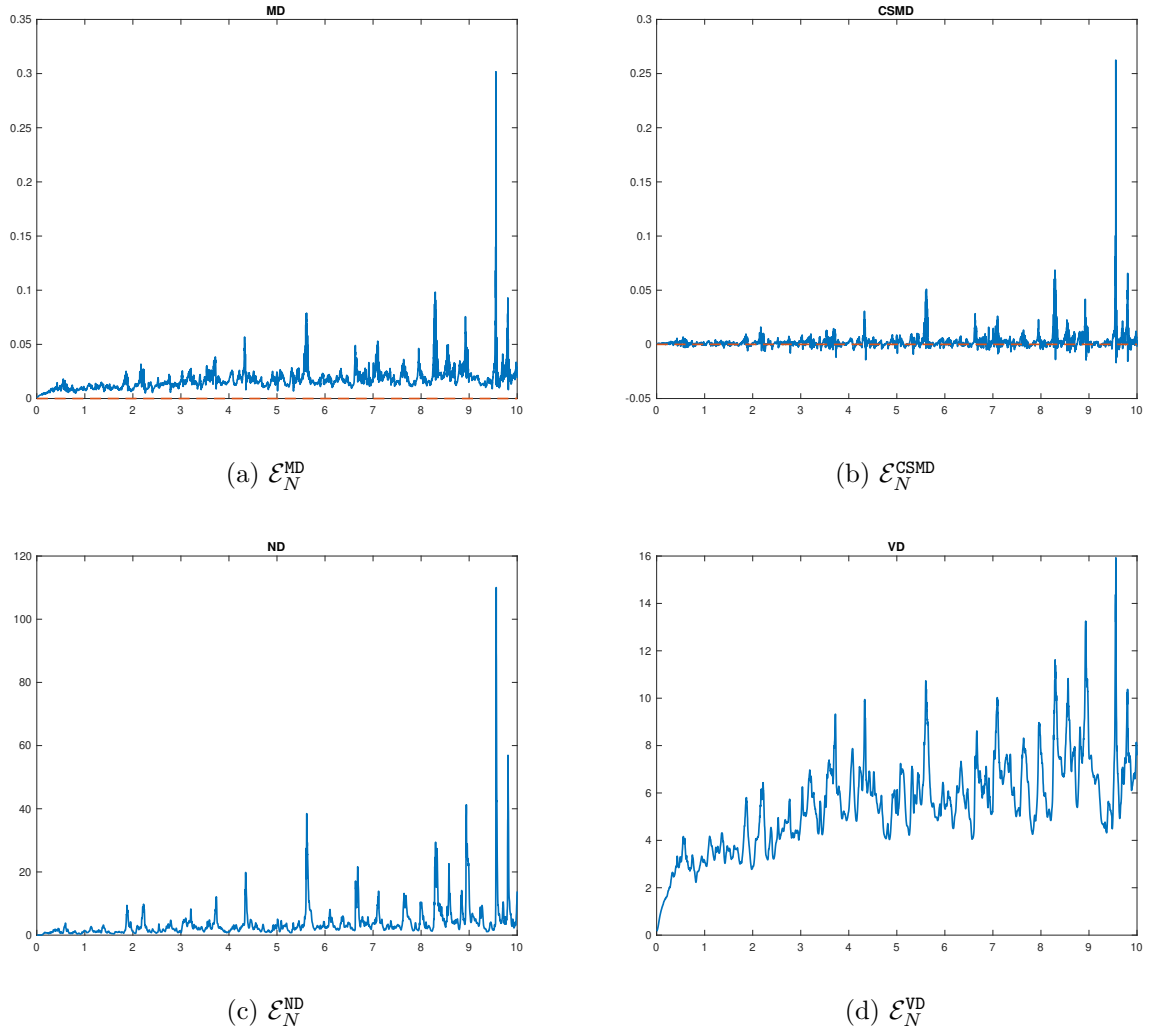

(a) $\mathcal{E}_N^{\texttt{MD}}$ (b) $\mathcal{E}_N^{\texttt{CSMD}}$

(c) $\mathcal{E}_N^{\texttt{ND}}$ (d) $\mathcal{E}_N^{\texttt{VD}}$

Figure 21: Constant time step DLN (182) with $k = 0.001,\ Re = 10,000,\ \theta = 2/3,\ C_s = 0.1,\ \mu = 0.4$. We do not see backscatter in $\mathcal{E}_N^{\texttt{MD}}$.

For constant time step

$$k = 0.001 \text{ and } \theta = 1,$$

we first run the test which reduces the method to a midpoint rule. We saw the results were very close to the results in [137] (See Appendix). This indicates the accuracy of our implementation. However, it is unclear that the oscillations in the model dissipation are the effect

of the new modeling term or normal ringing [28] which is seen in the standard Midpoint rule. Hence, we need to investigate further. This suggests that approximation would be improved with a bit of numerical dissipation in the method provided that numerical dissipation vanishes as k goes to 0 and it does not dominate the physical dissipation. Figure 18, Figure 19, and Figure 20 look plausible since the solution seems quasi-periodic even though there is very negligible backscatter in the model dissipation. We notice that numerical dissipation, $\mathcal{E}_N^{\texttt{ND}}$ is overwhelming the effect of new backscatter term, $\mathcal{E}_N^{\texttt{CSMD}}$. That's why we do not see much backscatter. In Figure 21, we see $\mathcal{E}_N^{\texttt{ND}}$ is still hiding the effect of small negative values in the $\mathcal{E}_N^{\texttt{CSMD}}$ from the model dissipation, $\mathcal{E}_N^{\texttt{MD}}$. Hence, there is no predicted backscatter which we believe is due to $\mathcal{E}_N^{\texttt{ND}}$ being too big. There is a substantial difference between the DLN algorithm for the Corrected Smagorinksy when $\theta = 1$ and other values of θ. The only way to tell which is correct is by adapting the time step to control the $\mathcal{E}_N^{\texttt{ND}}$. Since $\mathcal{E}_N^{\texttt{ND}}$ is overwhelming the effect of the new term, it emphasizes that the adaptivity based on dissipation criteria is important. The minimum dissipation criteria by F. Capuano, B. Sanderse, E. M. De Angelis, and G. Coppola [32] is to keep the ratio of numerical dissipation, $\mathcal{E}_N^{\texttt{ND}}$ and the viscous dissipation, $\mathcal{E}_N^{\texttt{VD}}$ less than some tolerance, Tol for adapting the time step. Thus adapt for

$$\chi = \left| \frac{\mathcal{E}_N^{\texttt{ND}}}{\mathcal{E}_N^{\texttt{VD}}} \right| < \text{Tol}.$$

The number of time steps to reach the final time is the indicator of how sensitive the DLN method is. We fix the final time, $T = 10$, and report the number of time steps to reach there in Section 4.5.2 for each value of θ. However, the code has maximum time step

$$k_{max} = 0.025$$

, minimum time step $k_{min} = 0.001$, and the initial time step $k_0 = 0.0001$. That means even if we use the adaptivity by doing dissipation criteria, there are very few times when the criteria is not satisfied and we see spiking which is visible in Figure 22, Figure 23, Figure 24,

Figure 25. This is the evidence of sensitivity of the CSM problem. To see the backscatter, we set the Tol $= 0.01$ for $\theta = 0.98$, we set the Tol $= 0.05$ for $\theta = 0.95$, we set the

$$\text{Tol} = 0.15$$

for $\theta = \frac{2}{\sqrt{5}}$. We started the test for all θ with Tol $= 0.01$ and gradually increased Tol when we failed to see the backscatter in $\mathcal{E}_N^{\texttt{MD}}$. By increasing Tol, we are allowing more $\mathcal{E}_N^{\texttt{ND}}$. Hence instead of seeing less backscatter, we see more backscatter. This is an anomaly for which we do not have an explanation. It could be because increased tolerance led to larger time steps, see Section 4.5.2. But in the case of $\theta = \frac{2}{3}$ for Tol $= 0.15$, Figure 25 looks plausible even though we fail to see backscatter in $\mathcal{E}_N^{\texttt{MD}}$. Hence, when θ is smaller, there is more $\mathcal{E}_N^{\texttt{ND}}$ and we see evidence of backscatter in $\mathcal{E}_N^{\texttt{CSMD}}$, but it's smaller than the $\mathcal{E}_N^{\texttt{ND}}$ in the method. Next, we check the effect of the new term in the model on Kinetic Energy (KE) in the flow for each case. Bigger KE means less energy dissipation. When backscatter is happening, we notice from Figure 26 that after a certain amount of time, the KE stabilizes or only varies within a small range. This new term may be highly fluctuating, but it has an impact on KE. Since we get one pattern for all the cases when backscatter in $\mathcal{E}_N^{\texttt{MD}}$ is happening and another pattern for all the cases when backscatter in $\mathcal{E}_N^{\texttt{MD}}$ is not happening, we show one example for

$$\theta = 0.95$$

in Figure 26.

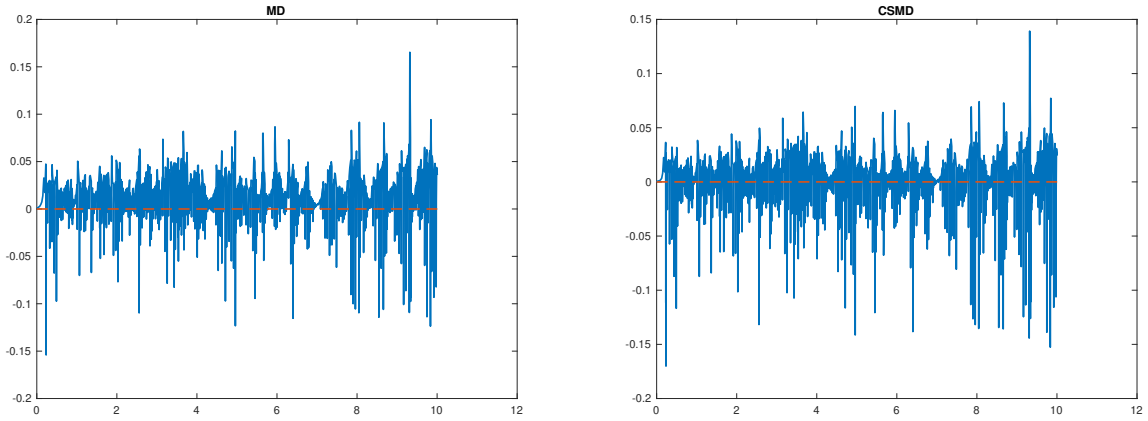

(a) $\mathcal{E}_N^{\texttt{MD}}$

(b) $\mathcal{E}_N^{\texttt{CSMD}}$

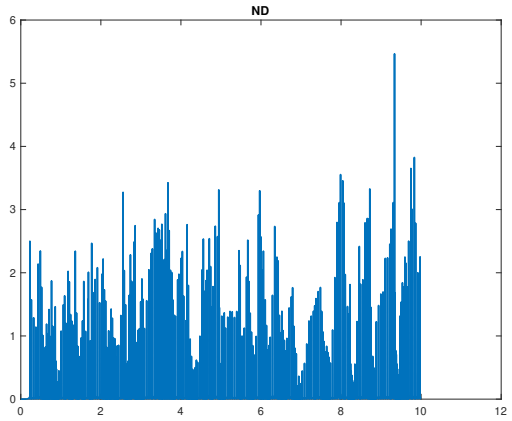

(c) $\mathcal{E}_N^{\texttt{ND}}$

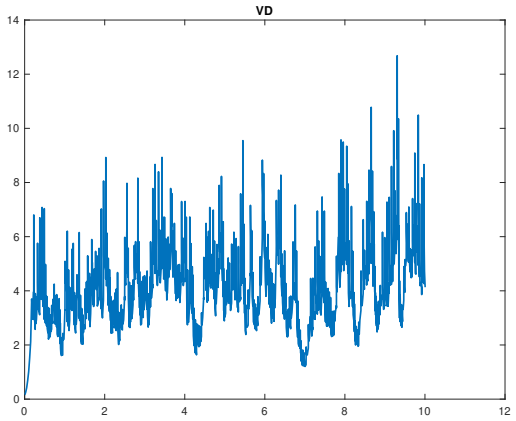

(d) $\mathcal{E}_N^{\texttt{VD}}$

Figure 22: Variable Step DLN (182) with $Tol = 0.01,\ Re = 10,000,\ \theta = 0.98,\ C_s = 0.1,\ \mu = 0.4$. We see backscatter in $\mathcal{E}_N^{\texttt{MD}}$.

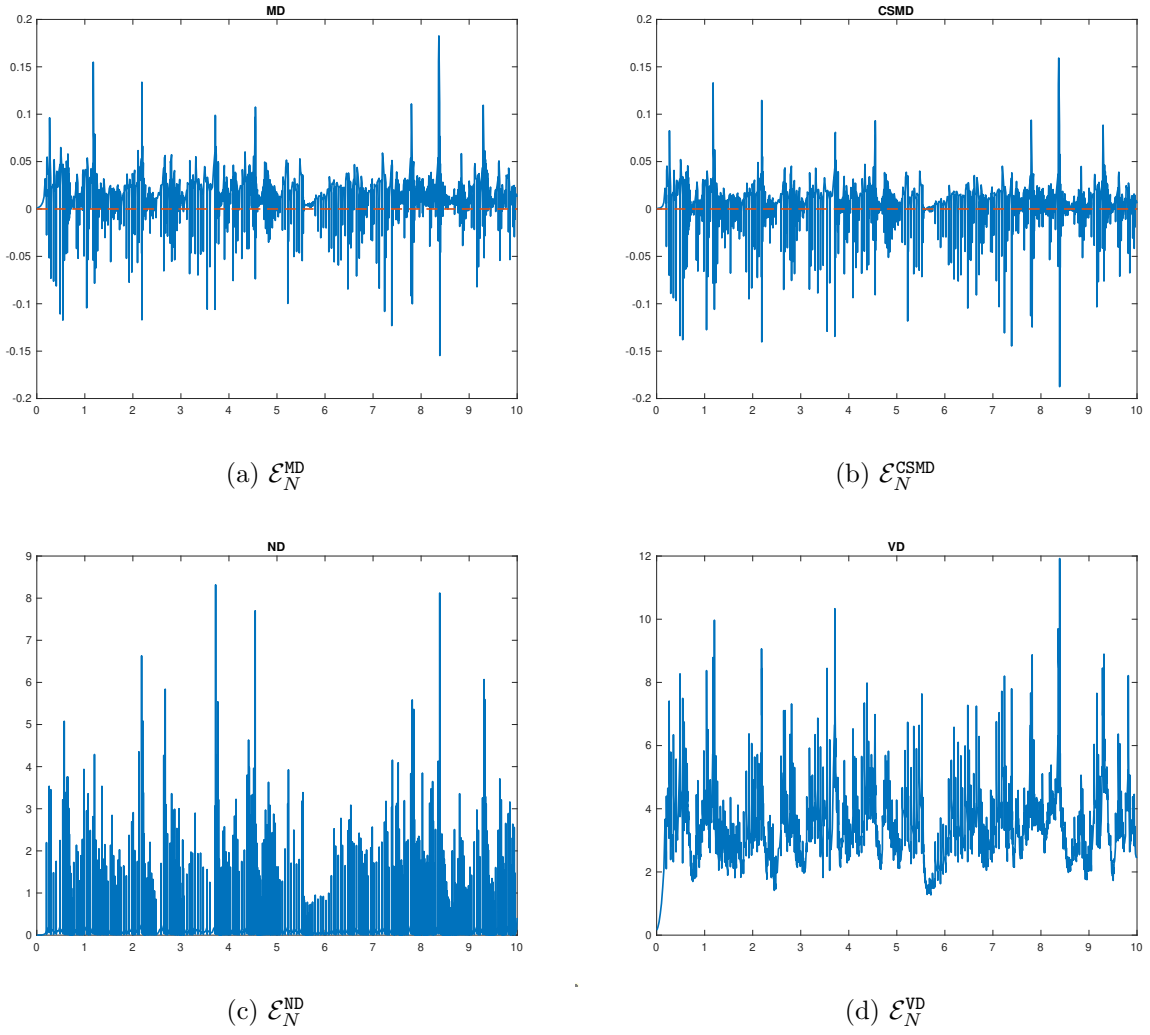

(a) $\mathcal{E}_N^{\texttt{MD}}$ (b) $\mathcal{E}_N^{\texttt{CSMD}}$

(c) $\mathcal{E}_N^{\texttt{ND}}$ (d) $\mathcal{E}_N^{\texttt{VD}}$

Figure 23: Variable Step DLN (182) with $Tol = 0.05,\ Re = 10,000,\ \theta = 0.95,\ C_s = 0.1,\ \mu = 0.4$. We see backscatter in $\mathcal{E}_N^{\texttt{MD}}$.

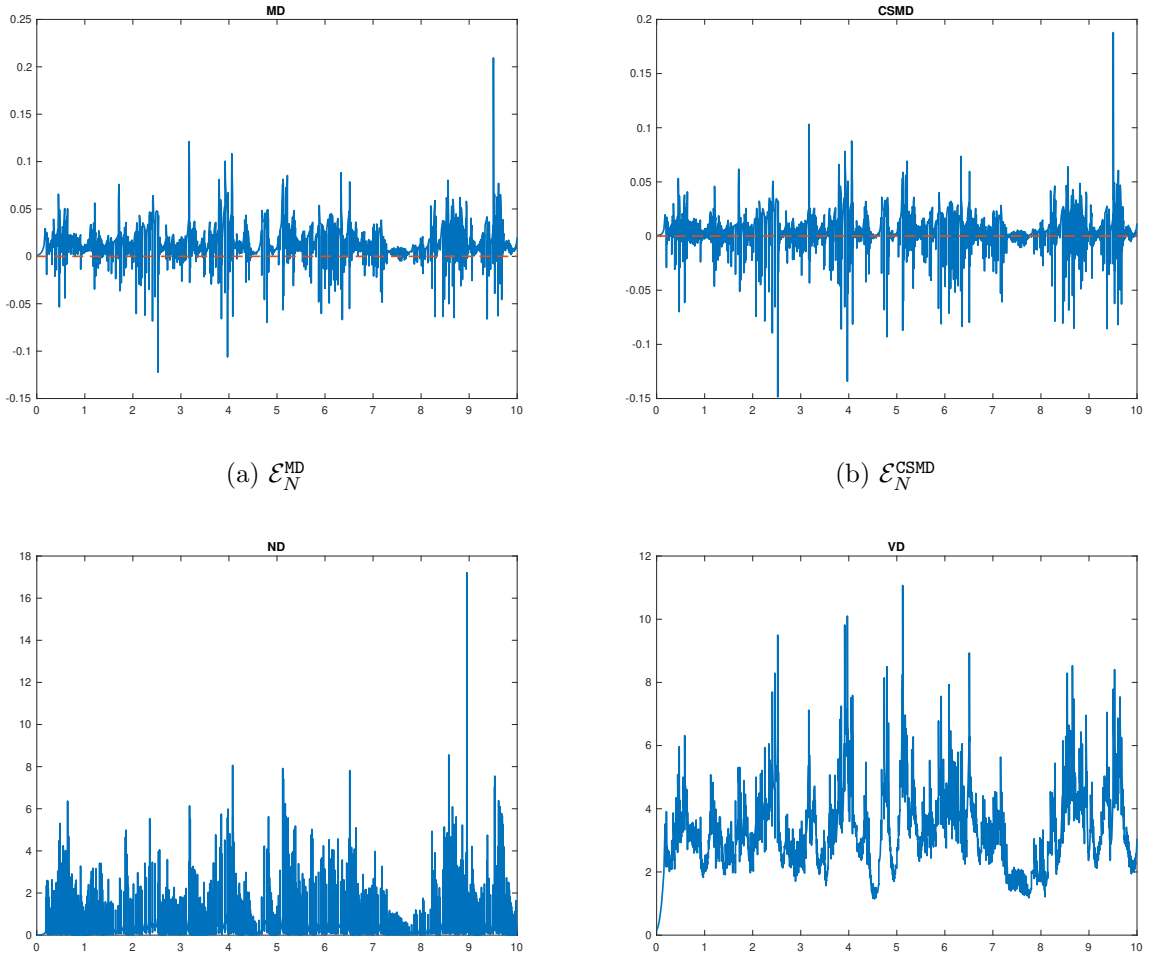

(a) $\mathcal{E}_N^{\texttt{MD}}$ (b) $\mathcal{E}_N^{\texttt{CSMD}}$

(c) $\mathcal{E}_N^{\texttt{ND}}$ (d) $\mathcal{E}_N^{\texttt{VD}}$

Figure 24: Variable Step DLN (182) with $Tol = 0.15,\ Re = 10,000,\ \theta = \frac{2}{\sqrt{5}},\ C_s = 0.1,\ \mu = 0.4$. We see backscatter in $\mathcal{E}_N^{\texttt{MD}}$.

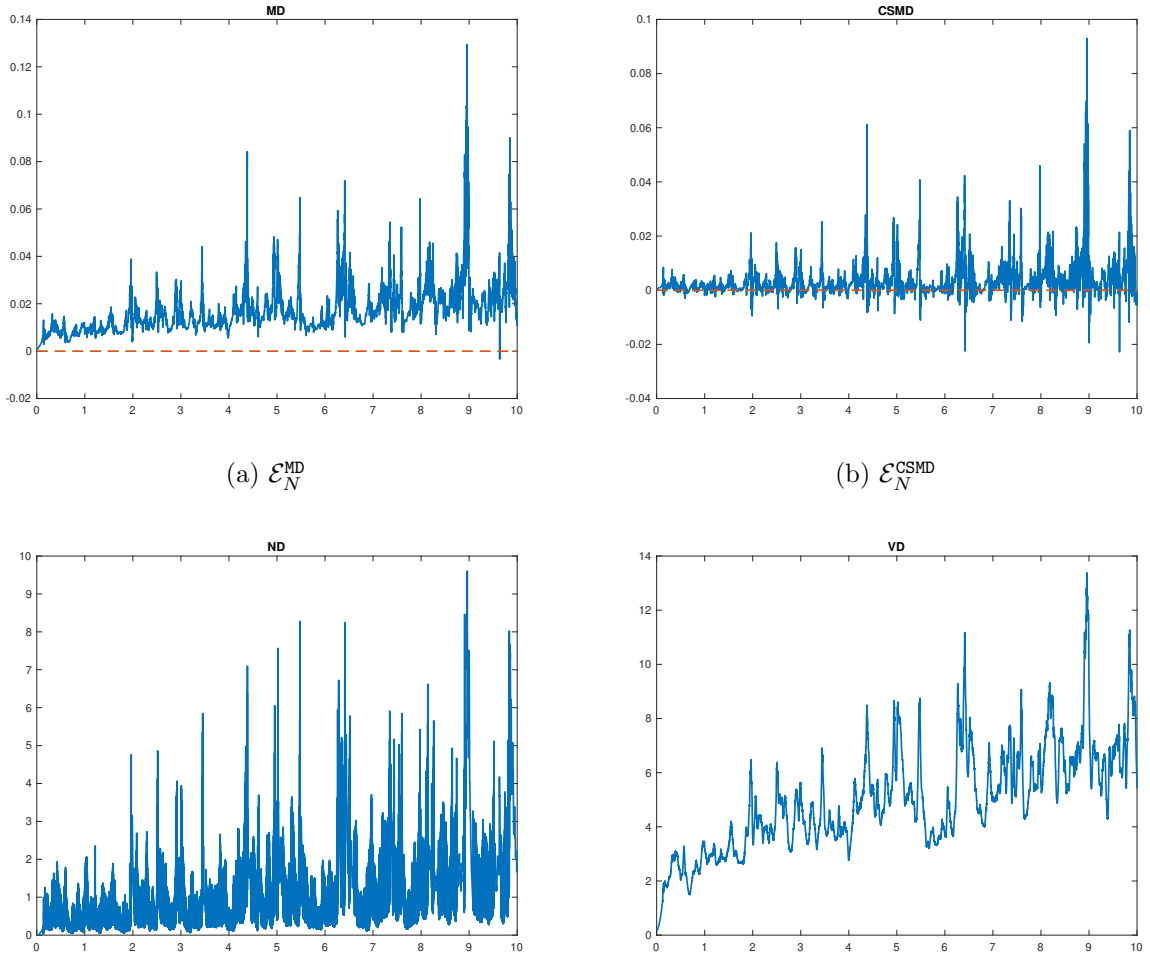

(a) $\mathcal{E}_N^{\texttt{MD}}$ (b) $\mathcal{E}_N^{\texttt{CSMD}}$

(c) $\mathcal{E}_N^{\texttt{ND}}$ (d) $\mathcal{E}_N^{\texttt{VD}}$

Figure 25: Variable Step DLN (182) with $Tol = 0.15,\ Re = 10,000,\ \theta = \frac{2}{3},\ C_s = 0.1,\ \mu = 0.4$. We do not see backscatter in $\mathcal{E}_N^{\texttt{MD}}$.

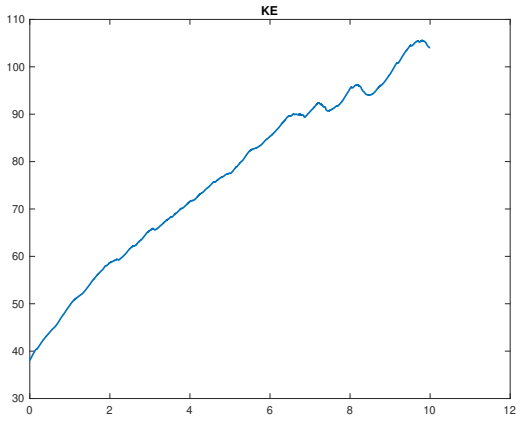

(a) KE, Tol=0.01

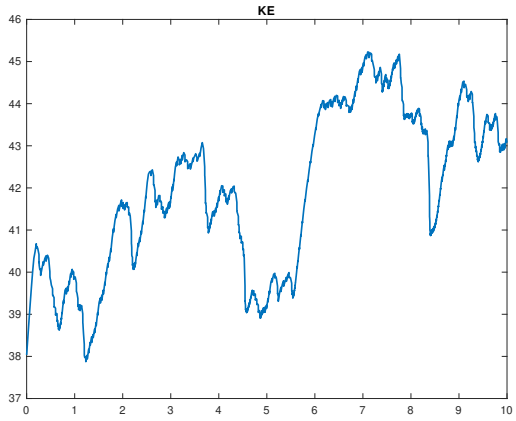

(b) KE, Tol=0.05

Figure 26: Variable Step DLN (182) with $Re = 10,000,\ \theta = 0.95,\ C_s = 0.1,\ \mu = 0.4$. The left picture is for no backscatter and right picture is for backscatter.

θ	Tol	Total time steps
0.98	**0.01**	**9575**
0.95	0.01	6505
0.95	**0.05**	**1604**
$2/\sqrt{5}$	0.01	8988
$2/\sqrt{5}$	0.05	5680
$\mathbf{2/\sqrt{5}}$	**0.15**	**1973**
$2/3$	0.01	9944
$2/3$	0.05	9575
$2/3$	0.15	7149

Table 11: Total time steps taken to reach $T = 10$ while using variable DLN for different values of θ.

In Section 4.5.2, for the highlighted values, we notice significant backscatter in MD.

5.0 Conclusions and future perspectives

The first project in Chapter 2 presents a complete stability and error analysis of a simulation tool for modeling the adsorption process for the constant and affine adsorption cases. For the nonlinear, explicit adsorption, we proved stability analysis for the continuous, semi-discrete, and fully discrete cases. For the nonlinear, explicit adsorption, we also proved the error estimate in the semi-discrete case and the existence of a solution for the fully discrete case. The error analysis for the nonlinear case in a fully discrete case is more involved and is currently an open problem. Numerically, we showed that the midpoint method gives second-order convergence for all adsorption cases. In the future, one can compare results from a numerical simulation to experimental data. Besides, the next most important step in developing this simulation tool is coupling the reactive transport problem with porous media flow Implementing the variable time step methods is another direction that will allow time adaptivity.

The second project in Chapter 3 demonstrates that the Smagorinsky Model could be extended to non-equilibrium turbulence. In addition, we showed the statistical backscatter without using negative turbulent viscosities. We analyze the stability of the model, uniqueness of the model's solution, modeling error, and numerical error. Since BE has numerical diffusion while CNLE does not, we can observe backscatter from CNLE in the second numerical test. We observe that the backscatter is sensitive to the time discretization scheme in the CSM model.

In the Chapter 4, we analyzed the variable time-stepping DLN algorithm for the CSM. We showed that the numerical solutions are unconditionally stable in energy over the long term. We proved that the numerical velocity converges with second-order accuracy under mild time step limits if the highest polynomial degrees satisfy $r = 2$ and $s = 1$, which is verified by the first numerical test problem in Subsection 4.5.1. It's clear that to get the backscattering phenomenon not from the ringing property of the method, we need some

dissipative methods and we need some control of numerical dissipation, $\mathcal{E}_N^{\mathtt{ND}}$. We therefore test in Subsection 4.5.2 by adapting the time step using minimum dissipation criteria. The closer $\theta = 1$, the closer the DLN method gets to be exactly conservative. If it is exactly conservative, we do not need tight control over $\mathcal{E}_N^{\mathtt{ND}}$. The further we go away from exactly conservative, the tighter control we need over $\mathcal{E}_N^{\mathtt{ND}}$ to see what seems to be true. In the future, error analysis for a semi-implicit DLN algorithm for CSM to avoid time restriction could be proven since it's an important open problem. Furthermore, in 3D, storage can be an issue and hence analysis of the reduced storage penalty method is also an interesting problem.

Appendix Additional tables and figures related to Chapter 4

In this appendix, we provide additional some additional tables and figures related to Chapter 4.

Time step k	Mesh size h	$\|\|\|e^w\|\|\|_{\infty,0}$	Rate	$\|\|\|\nabla e^w\|\|\|_{\infty,0}$	Rate	$\|\|\|e^p\|\|\|_{\infty,0}$	Rate
0.08	0.08571	6.1375	-	59.5951	-	10.2725	-
0.04	0.04221	0.0499412	6.9412	1.35769	5.4560	0.0803944	6.9975
0.02	0.02095	0.0119888	2.0585	0.399817	1.7637	0.0195956	2.0366
0.01	0.01048	0.00297839	2.0091	0.103952	1.9434	0.00502445	1.9635

Table 12: Errors by $\|\cdot\|_{\infty,0}$-norm and Convergence Rate for the constant DLN with $\theta = 2/\sqrt{5}$.

Time step k	Mesh size h	$\|\|\|e^w\|\|\|_{0,0}$	Rate	$\|\|\|\nabla e^w\|\|\|_{0,0}$	Rate	$\|\|\|e^p\|\|\|_{0,0}$	Rate
0.08	0.08571	8.05856	-	86.5876	-	11.9822	-
0.04	0.04221	0.107272	6.2312	3.05843	4.8233	0.143556	6.3831
0.02	0.02095	0.0249452	2.1044	0.900625	1.7638	0.0346417	2.0510
0.01	0.01048	0.00616932	2.0156	0.234285	1.9427	0.00880143	1.9767

Table 13: Errors by $\|\cdot\|_{0,0}$-norm and Convergence Rate for the constant DLN with $\theta = 2/\sqrt{5}$.

Time step k	Mesh size h	$\|\|\|e^w\|\|\|_{\infty,0}$	Rate	$\|\|\|\nabla e^w\|\|\|_{\infty,0}$	Rate	$\|\|\|e^p\|\|\|_{\infty,0}$	Rate
0.08	0.08571	6.03148	-	72.2845	-	14.0717	-
0.04	0.04221	0.0499902	6.9147	1.35784	5.7343	0.0831369	7.4031
0.02	0.02095	0.0120016	2.0584	0.399858	1.7638	0.0203057	2.0336
0.01	0.01048	0.00298191	2.0089	0.103961	1.9434	0.00512713	1.9857

Table 14: Errors by $\|\cdot\|_{\infty,0}$-norm and Convergence Rate for the constant DLN with $\theta = 1$.

Time step k	Mesh size h	$\|\|\|e^w\|\|\|_{0,0}$	Rate	$\|\|\|\nabla e^w\|\|\|_{0,0}$	Rate	$\|\|\|e^p\|\|\|_{0,0}$	Rate
0.08	0.08571	8.50684	-	105.23	-	14.0354	-
0.04	0.04221	0.107277	6.3092	3.05802	5.1048	0.14397	6.6072
0.02	0.02095	0.0249479	2.1044	0.90061	1.7636	0.0347625	2.0502
0.01	0.01048	0.0061698	2.0156	0.234279	1.9427	0.00883384	1.9764

Table 15: Errors by $\|\cdot\|_{0,0}$-norm and Convergence Rate for the constant DLN with $\theta = 1$.

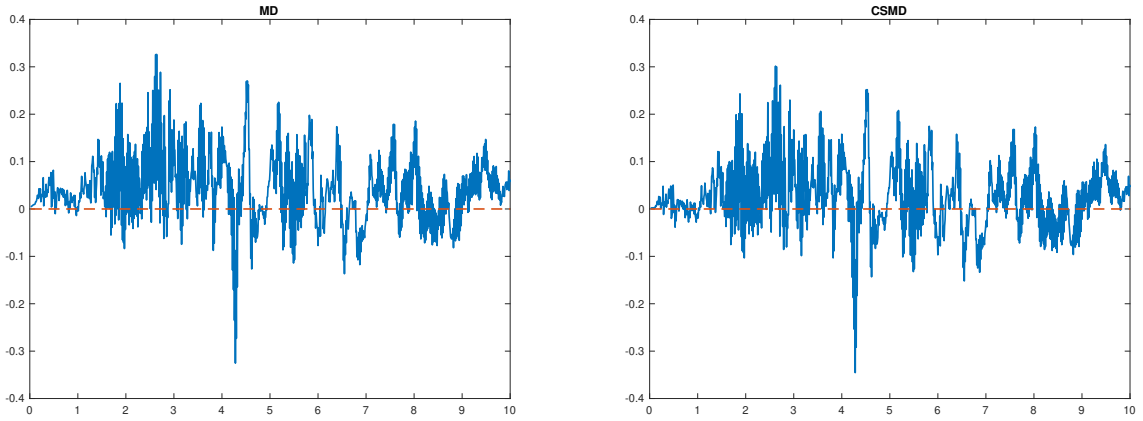

(a) $\mathcal{E}_N^{\texttt{MD}}$ (b) $\mathcal{E}_N^{\texttt{CSMD}}$

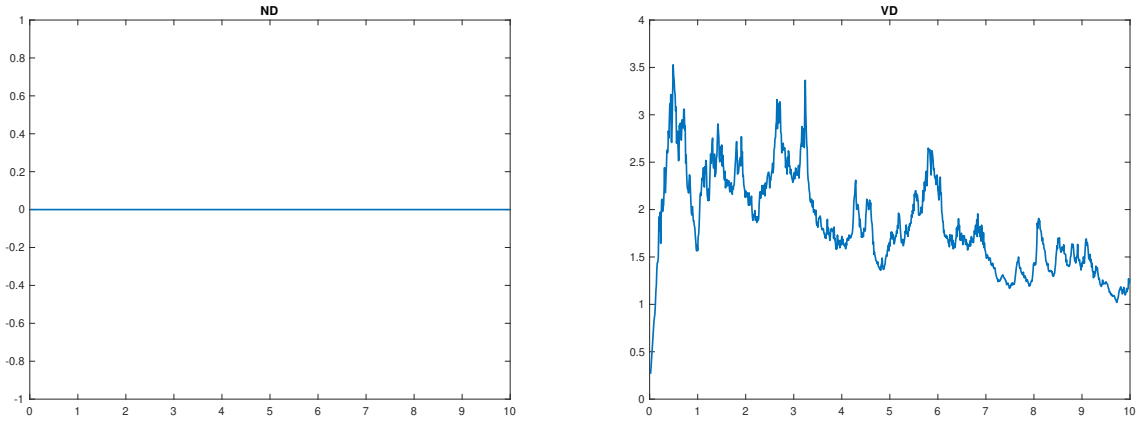

(c) $\mathcal{E}_N^{\texttt{ND}}$ (d) $\mathcal{E}_N^{\texttt{VD}}$

Figure 27: Constant time step DLN (182) with $k = 0.001$, $Re = 10,000$, $\theta = 1$, $C_s = 0.1$, $\mu = 0.4$.

Bibliography

[1] Anti-sars-cov-2 monoclonal antibodies. https://www.covid19treatmentguidelines.nih.gov/therapies/antivirals-including-antibody-products/anti-sars-cov-2-monoclonal-antibodies/, 2022. Accessed: 2022-08-18.

[2] Biopharmaceutical market size to hit us $856.1 billion by 2030. https://www.globenewswire.com/news-release/2021/12/22/2357003/0/en/Biopharmaceutical-Market-Size-to-Hit-US-856-1-Bn-by-2030.html, 2022. Precedence Research, Accessed: 2022-08-01.

[3] Coronavirus (covid-19) update: Fda authorizes new monoclonal antibody for treatment of covid-19 that retains activity against omicron variant. https://www.fda.gov/news-events/press-announcements/coronavirus-covid-19-update-fda-authorizes-new-monoclonal-antibody-treatment-covid-19-retains, 2022. Accessed: 2022-02-11.

[4] Covid-19 treatments and medications. https://www.cdc.gov/coronavirus/2019-ncov/your-health/treatments-for-severe-illness.html, 2022. Accessed: 2022-10-19.

[5] D. S. Abdi, F. X. Giraldo, E. M. Constantinescu, L. E. Carr, L. C. Wilcox, and T. C. Warburton. Acceleration of the Implicit–Eplicit nonhydrostatic unified model of the atmosphere on manycore processors. *The International Journal of High Performance Computing Applications*, 33(2):242–267, 2019.

[6] R. A. Adams and J. J. Fournier. *Sobolev spaces*. Elsevier, 2003.

[7] C. Amrouche, L. C. Berselli, R. Lewandowski, and D. D. Nguyen. Turbulent flows as generalized Kelvin–Voigt materials: Modeling and analysis. *Nonlinear Analysis*, 196:111790, 2020.

[8] T. Arbogast and M. F. Wheeler. A characteristics-mixed finite element method for advection-dominated transport problems. *SIAM Journal on Numerical analysis*, 32(2):404–424, 1995.

[9] T. Arbogast and M. F. Wheeler. A nonlinear mixed finite element method for a degenerate parabolic equation arising in flow in porous media. *SIAM Journal on Numerical Analysis*, 33(4):1669–1687, 1996.

[10] U. M. Ascher and L. R. Petzold. *Computer methods for ordinary differential equations and differential-algebraic equations*. Society for Industrial and Applied Mathematics (SIAM), Philadelphia, PA, 1998.

[11] B. Baldwin and H. Lomax. Thin-layer approximation and algebraic model for separated turbulentflows. In *16th aerospace sciences meeting*, page 257, 1978.

[12] R. E. Bank, J. F. Bürgler, W. Fichtner, and R. K. Smith. Some upwinding techniques for finite element approximations of convection-diffusion equations. *Numerische Mathematik*, 58(1):185–202, 1990.

[13] E. S. Baranovskii. Strong solutions of the incompressible Navier–Stokes–Voigt model. *Mathematics*, 8(2):181, 2020.

[14] J. Bardina, J. Ferziger, and W. C. Reynolds. Improved subgrid-scale models for large-eddy simulation. In *13th fluid and plasmadynamics conference*, page 1357, 1980.

[15] J. W. Barrett and P. Knabner. Finite element approximation of the transport of reactive solutes in porous media. part ii: Error estimates for equilibrium adsorption processes. *SIAM journal on numerical analysis*, 34(2):455–479, 1997.

[16] J. Bear. *Dynamics of fluids in porous media*. Courier Corporation, 1988.

[17] L. C. Berselli, R. Lewandowski, and D. D. Nguyen. Rotational forms of large eddy simulation turbulence models: Modeling and mathematical theory. *Chinese Annals of Mathematics, Series B*, 42(1):17–40, 2021.

[18] S. Bhattacharjee, J. Dong, Y. Ma, S. Hovde, J. H. Geiger, G. L. Baker, and M. L. Bruening. Formation of high-capacity protein-adsorbing membranes through simple adsorption of poly (acrylic acid)-containing films at low ph. *Langmuir*, 28(17):6885–6892, 2012.

[19] B. V. Bhut and S. M. Husson. Dramatic performance improvement of weak anion-exchange membranes for chromatographic bioseparations. *Journal of Membrane Science*, 337(1-2):215–223, 2009.

[20] B. V. Bhut, S. R. Wickramasinghe, and S. M. Husson. Preparation of high-capacity, weak anion-exchange membranes for protein separations using surface-initiated atom transfer radical polymerization. *Journal of Membrane Science*, 325(1):176–183, 2008.

[21] E. T. Bouloutas and M. A. Celia. An improved cubic Petrov-Galerkin method for simulation of transient advection-diffusion processes in rectangularly decomposable domains. *Computer methods in applied mechanics and engineering*, 92(3):289–308, 1991.

[22] J. Boussinesq. *"Essai sur la théorie des eaux courantes", Mémoires présentés par divers savants à l'Académie des Sciences 23 (1): 1-680.* Imprimerie Nationale, 1877.

[23] F. Boyer and P. Fabrie. *Mathematical Tools for the Study of the Incompressible Navier-Stokes Equations and Related Models*, volume 183. Springer Science & Business Media, 2012.

[24] S. C. Brenner and L. R. Scott. *The mathematical theory of finite element methods*, volume 15 of *Texts in Applied Mathematics*. Springer, New York, third edition, 2008.

[25] H. Brezis. *Functional analysis, Sobolev spaces and partial differential equations*. Universitext. Springer, New York, 2011.

[26] M. Bukač, A. Seboldt, and C. Trenchea. Refactorization of Cauchy's method: a second-order partitioned method for fluid-thick structure interaction problems. *J. Math. Fluid Mech.*, 23(3):Paper No. 64, 25, 2021.

[27] M. Bukač and C. Trenchea. Adaptive, second-order, unconditionally stable partitioned method for fluid-structure interaction. *Comput. Methods Appl. Mech. Engrg.*, 393:Paper No. 114847, 24, 2022.

[28] J. Burkardt, W. Pei, and C. Trenchea. A stress test for the midpoint time-stepping method. *International Journal of Numerical Analysis & Modeling*, 19, 2022.

[29] J. Burkardt and C. Trenchea. Refactorization of the midpoint rule. *Applied Mathematics Letters*, 107:106438, 2020.

[30] E. Burman, P. Hansbo, and M. G. Larson. Error estimates for the Smagorinsky turbulence model: enhanced stability through scale separation and numerical stabilization. *arXiv preprint arXiv:2102.00043*, 2021.

[31] F. Cadieux, G. Sun, and J. A. Domaradzki. Effects of numerical dissipation on the interpretation of simulation results in computational fluid dynamics. *Computers & Fluids*, 154:256–272, 2017.

[32] F. Capuano, B. Sanderse, E. M. D. Angelis, and G. Coppola. A minimum-dissipation time-integration strategy for large-eddy simulation of incompressible turbulent flows. 2017.

[33] M. A. Case, V. J. Ervin, A. Linke, and L. G. Rebholz. A connection between Scott-Vogelius and grad-div stabilized Taylor-Hood FE approximations of the Navier-Stokes equations. *SIAM J. Numer. Anal.*, 49(4):1461–1481, 2011.

[34] D. Caughey and E. Turkel. Effects of numerical dissipation on finite-volume solutions of compressible flow problems. In *26th Aerospace Sciences Meeting*, page 621, 1988.

[35] A. V. Chechkin, M. I. Kopp, V. V. Yanovsky, and A. V. Tur. Negative viscosity for Rossby wave and drift wave turbulence. *Journal of Experimental and Theoretical Physics*, 86:357–366, 1998.

[36] N. Chorfi, M. Abdelwahed, and L. C. Berselli. On the analysis of a geometrically selective turbulence model. *Advances in Nonlinear Analysis*, 9(1):1402–1419, 2020.

[37] J. C. Chrispell, V. J. Ervin, and E. W. Jenkins. A fractional step θ-method for convection–diffusion problems. *Journal of Mathematical Analysis and Applications*, 333(1):204–218, 2007.

[38] P. G. Ciarlet. *The finite element method for elliptic problems*. Studies in Mathematics and its Applications, Vol. 4. North-Holland Publishing Co., Amsterdam-New York-Oxford, 1978.

[39] K. G. Clarke. *Bioprocess engineering: an introductory engineering and life science approach*. Elsevier, 2013.

[40] R. Codina. Comparison of some finite element methods for solving the diffusion-convection-reaction equation. *Computer methods in applied mechanics and engineering*, 156(1-4):185–210, 1998.

[41] V. Coker. Biotherapeutics outpace conventional therapies. *BioPharm International*, 25(3):s20–s23, 2012.

[42] J. J. R. Conde, E. W. Jenkins, and S. Husson. Surrogate-based optimization for the techno-economic feasibility analysis of membrane capture chromatography platforms. In *2023 AIChE Annual Meeting*. AIChE, 2023.

[43] G. D. Marsily. Quantitative hydrogeology: Groundwater hydrology for engineers academic press. *Inc., Orlando, Florida*, 1986.

[44] G. G. Dahlquist. On the relation of G-stability to other stability concepts for linear multistep methods. *Dept. of Comp. Sci. Roy. Inst. of Technology*, Report TRITA-NA-7621, 1976.

[45] G. G. Dahlquist. G-stability is equivalent to A-stability. *BIT*, 18(4):384–401, 1978.

[46] G. G. Dahlquist. Positive functions and some applications to stability questions for numerical methods. In *Recent advances in numerical analysis (Proc. Sympos., Math. Res. Center, Univ. Wisconsin, Madison, Wis., 1978)*, volume 41 of *Publ. Math. Res. Center Univ. Wisconsin*, pages 1–29. Academic Press, New York-London, 1978.

[47] G. G. Dahlquist, W. Liniger, and O. Nevanlinna. Stability of two-step methods for variable integration steps. *SIAM J. Numer. Anal.*, 20(5):1071–1085, 1983.

[48] T. Dai, S. Liu, J. Liu, N. Jiang, and Q. Chen. Development of a new dynamic Smagorinsky model by an artificial neural network for prediction of outdoor airflow and pollutant dispersion. *Building and Environment*, page 110624, 2023.

[49] A. Dale, C. T. John, and H. P. Richard. *Computational Fluid Mechanics and Heat Transfer*. Series in Computational and Physical Processes in Mechanics and Thermal Sciences. Taylor & Francis, 3rd edition, 2012.

[50] M. Dauge. *Elliptic boundary value problems on corner domains: smoothness and asymptotics of solutions*, volume 1341. Springer, 2006.

[51] C. Dawson. Analysis of an upwind-mixed finite element method for nonlinear contaminant transport equations. *SIAM journal on numerical analysis*, 35(5):1709–1724, 1998.

[52] V. DeCaria, W. J. Layton, and M. McLaughlin. A conservative, second order, unconditionally stable artificial compression method. *Computer Methods in Applied Mechanics and Engineering*, 325:733–747, 2017.

[53] N. S. Dickey, A. Selamet, and K. V. Tallio. Effects of numerical dissipation and dispersion on acoustic predictions from a time-domain finite difference technique for non-linear wave dynamics. *Journal of sound and vibration*, 259(1):193–208, 2003.

[54] Q. Du and M. D. Gunzburger. Finite-element approximations of a Ladyzhenskaya model for stationary incompressible viscous flow. *SIAM journal on numerical analysis*, 27(1):1–19, 1990.

[55] Q. Du and M. D. Gunzburger. Analysis of a Ladyzhenskaya model for incompressible viscous flow. *Journal of Mathematical Analysis and Applications*, 155(1):21–45, 1991.

[56] T. Dupont and R. Scott. Polynomial approximation of functions in Sobolev spaces. *Mathematics of Computation*, 34(150):441–463, 1980.

[57] P. A. Durbin and B. A. Pettersson-Reif. *Statistical Theory and Modeling for Turbulent Flows, Second Edition*. Wiley, Chichester, 2011.

[58] V. J. Ervin, M. Kubacki, W. J. Layton, M. Moraiti, Z. Si, and C. Trenchea. On limiting behavior of contaminant transport models in coupled surface and groundwater flows. *Axioms*, 4(4):518–529, 2015.

[59] L. C. Evans. *Partial differential equations (graduate studies in mathematics, vol. 19)*, volume 67. American Mathematics Society (1998) Text# 2 (Required):, 2009.

[60] J. H. Ferziger and M. Perić. *Computational methods for fluid dynamics*. Springer-Verlag, Berlin, revised edition, 1999.

[61] G. J. Fix, M. D. Gunzburger, and J. S. Peterson. On finite element approximations of problems having inhomogeneous essential boundary conditions. *Computers & mathematics with applications*, 9(5):687–700, 1983.

[62] G.P. Galdi and W.J. Layton. Approximation of the larger eddies in fluid motions. II. A model for space-filtered flow. *Math. Models Methods Appl. Sci.*, 10(3):343–350, 2000.

[63] W. K. George. Lectures in turbulence for the 21st century. Chalmers University of Technology, available at `http://www.turbulence-online.com`, 2013.

[64] V. Girault and P. Raviart. *Finite element methods for Navier-Stokes equations*, volume 5 of *Springer Series in Computational Mathematics*. Springer-Verlag, Berlin, 1986. Theory and algorithms.

[65] V. Girault and P. A. Raviart. *Finite element approximation of the Navier-Stokes equations*, volume 749 of *Lecture Notes in Mathematics*. Springer-Verlag, Berlin, 1979.

[66] P. Grisvard. *Elliptic problems in nonsmooth domains*. SIAM, 2011.

[67] M. D. Gunzburger and S. L. Hou. Treating inhomogeneous essential boundary conditions in finite element methods and the calculation of boundary stresses. *SIAM journal on numerical analysis*, 29(2):390–424, 1992.

[68] E. Hairer, S. P. Nørsett, and G. Wanner. *Solving ordinary differential equations. I*, volume 8 of *Springer Series in Computational Mathematics*. Springer-Verlag, Berlin, second edition, 1993. Nonstiff problems.

[69] W. Heinrichs. Defect correction for convection-dominated flow. *SIAM Journal on Scientific Computing*, 17(5):1082–1091, 1996.

[70] J. S. Hesthaven and T. Warburton. *Nodal discontinuous Galerkin methods: algorithms, analysis, and applications*. Springer Science & Business Media, 2007.

[71] J. G. Heywood and R. Rannacher. Finite-element approximation of the nonstationary Navier–Stokes problem. Part IV: Error analysis for second-order time discretization. *SIAM Journal on Numerical Analysis*, 27(2):353–384, 1990.

[72] P. Houston, C. Schwab, and E. Süli. Stabilized hp-finite element methods for first-order hyperbolic problems. *SIAM Journal on Numerical Analysis*, 37(5):1618–1643, 2000.

[73] T. Iliescu, V. John, W. J. Layton, G. Matthies, and L. Tobiska. A numerical study of a class of LES models. *Int. J. Comput. Fluid Dyn.*, 17(1):75–85, 2003.

[74] T. Iliescu and W. J. Layton. Approximating the larger eddies in fluid motion. III. The Boussinesq model for turbulent fluctuations. *An. Ştiinţ. Univ. Al. I. Cuza Iaşi. Mat. (N.S.)*, 44(2):245–261 (2000), 1998. Dedicated to Professor C. Corduneanu on the occasion of his 70th birthday.

[75] R. Ingram. A new linearly extrapolated Crank-Nicolson time-stepping scheme for the Navier-Stokes equations. *Mathematics of Computation*, 82(284):1953–1973, 2013.

[76] R. Ingram. Unconditional convergence of high-order extrapolations of the Crank-Nicolson, finite element method for the Navier-Stokes equations. *Int. J. Numer. Anal. Model.*, 10(2):257–297, 2013.

[77] N. Jiang and W. Layton. An algorithm for fast calculation of flow ensembles. *Int. J. Uncertain. Quantif.*, 4(4):273–301, 2014.

[78] N. Jiang and W. J. Layton. Algorithms and models for turbulence not at statistical equilibrium. *Computers & Mathematics with Applications*, 71(11):2352–2372, 2016. Proceedings of the conference on Advances in Scientific Computing and Applied Mathematics. A special issue in honor of Max Gunzburger's 70th birthday.

[79] N. Jiang, W. J. Layton, M. McLaughlin, Y. Rong, and H. Zhao. On the foundations of eddy viscosity models of turbulence. *Fluids*, 5(4), 2020.

[80] V. John. *Finite element methods for incompressible flow problems*, volume 51 of *Springer Series in Computational Mathematics*. Springer, Cham, 2016.

[81] V. John and W. J. Layton. Analysis of numerical errors in large eddy simulation. *SIAM Journal on Numerical Analysis*, 40(3):995–1020, 2002.

[82] C. Johnson. *Numerical solution of partial differential equations by the finite element method*. Courier Corporation, 2012.

[83] G. Karniadakis and S. J. Sherwin. *Spectral/hp element methods for computational fluid dynamics*. Oxford University Press, USA, 2005.

[84] T. K. Kim. *A modified Smagorinsky subgrid scale model for the large eddy simulation of turbulent flow*. University of California, Davis, 2001.

[85] A. N. Kolmogorov. Equations of turbulent motion of an incompressible fluid, Izv. Acad. Sci., USSR. *Physics*, 6(1):2, 1942.

[86] P. Kuberry, A. Larios, L. G. Rebholz, and N. E. Wilson. Numerical approximation of the Voigt regularization for incompressible Navier–Stokes and magnetohydrodynamic flows. *Computers & Mathematics with Applications*, 64(8):2647–2662, 2012.

[87] G. Y. Kulikov and S. K. Shindin. On stable integration of stiff ordinary differential equations with global error control. In *International Conference on Computational Science (1)*, pages 42–49, 2005.

[88] G. Y. Kulikov and S. K. Shindin. One-leg integration of ordinary differential equations with global error control. *Computational Methods in Applied Mathematics*, 5(1):86–96, 2005.

[89] A. Labovsky, W. J. Layton, C. C. Manica, M. Neda, and L. G. Rebholz. The stabilized extrapolated trapezoidal finite-element method for the Navier-Stokes equations. *Comput. Methods Appl. Mech. Engrg.*, 198(9-12):958–974, 2009.

[90] O. A. Ladyzhenskaya. *The mathematical theory of viscous incompressible flow*, volume 2. Gordon and Breach New York, 1969.

[91] O. A. Ladyzhenskaya. Modification of the Navier–Stokes equations for large velocity gradients. In *Seminars in Mathematics VA Stheklov Mathematical Institute*, volume 7, 1970.

[92] A. Larios, M. R. Petersen, E. S. Titi, and B. Wingate. A computational investigation of the finite-time blow-up of the 3d incompressible Euler equations based on the Voigt regularization. *Theoretical and Computational Fluid Dynamics*, 32(1):23–34, 2018.

[93] A. Larios and E. S. Titi. Higher-order global regularity of an inviscid Voigt-regularization of the three-dimensional inviscid resistive magnetohydrodynamic equations. *Journal of Mathematical Fluid Mechanics*, 16(1):59–76, 2014.

[94] W. Layton. A connection between subgrid scale eddy viscosity and mixed methods. *Applied Mathematics and Computation*, 133(1):147–157, 2002.

[95] W. Layton and M. McLaughlin. Doubly-adaptive artificial compression methods for incompressible flow. *Journal of Numerical Mathematics*, 28(3):175–192, 2020.

[96] W. Layton, W. Pei, Y. Qin, and C. Trenchea. Analysis of the variable step method of Dahlquist, Liniger and Nevanlinna for fluid flow. *Numer. Methods Partial Differential Equations*, 38(6):1713–1737, 2022.

[97] W. Layton, W. Pei, and C. Trenchea. Refactorization of a variable step, unconditionally stable method of Dahlquist, Liniger and Nevanlinna. *Appl. Math. Lett.*, 125:Paper No. 107789, 7, 2022.

[98] W. Layton, W. Pei, and C. Trenchea. Time step adaptivity in the method of Dahlquist, Liniger and Nevanlinna. Technical report, University of Pittsburgh, 2022.

[99] W. J. Layton. A nonlinear, subgridscale model for incompressible viscous flow problems. *SIAM Journal on Scientific Computing*, 17(2):347–357, 1996.

[100] W. J. Layton. *Introduction to the Numerical Analysis of Incompressible Viscous Flows.* Society for Industrial and Applied Mathematics, Philadelphia, PA, 2008.

[101] W. J. Layton. Energy dissipation in the Smagorinsky model of turbulence. *Applied Mathematics Letters*, 59:56–59, 2016.

[102] B. Leader, Q. J. Baca, and D. E. Golan. Protein therapeutics: a summary and pharmacological classification. *Nature reviews Drug discovery*, 7(1):21–39, 2008.

[103] E. Lee and M. D. Gunzburger. A finite element, filtered eddy-viscosity method for the Navier–Stokes equations with large Reynolds number. *Journal of Mathematical Analysis and Applications*, 385(1):384–398, 2012.

[104] B. P. Leonard. The ULTIMATE conservative difference scheme applied to unsteady one-dimensional advection. *Computer methods in applied mechanics and engineering*, 88(1):17–74, 1991.

[105] R. J. LeVeque. *Finite volume methods for hyperbolic problems*, volume 31. Cambridge university press, 2002.

[106] J. Z. Li and R. T. Gandhi. Realizing the potential of anti–SARs-CoV-2 monoclonal antibodies for covid-19 management. *Jama*, 327(5):427–429, 2022.

[107] D. K. Lilly. The representation of small-scale turbulence in numerical simulation experiments. *IBM Form*, pages 195–210, 1967.

[108] J. Málek, J. Nečas, M. Rokyta, and M. Ružička. *Weak and measure-valued solutions to evolutionary PDEs*. Chapman and Hall/CRC, 2019.

[109] J. Mathieu and J. Scott. *An Introduction to Turbulent Flow*. Cambridge University Press, 2000.

[110] B. Mohammadi and O. Pironneau. *Analysis of the K-epsilon turbulence model*. France Editions: Masson, 1993.

[111] J. M. Mollerup. A review of the thermodynamics of protein association to ligands, protein adsorption, and adsorption isotherms. *Chemical Engineering & Technology: Industrial Chemistry-Plant Equipment-Process Engineering-Biotechnology*, 31(6):864–874, 2008.

[112] J. M. Mollerup, T. B. Hansen, S. Kidal, and A. Staby. Quality by design—thermodynamic modelling of chromatographic separation of proteins. *Journal of Chromatography A*, 1177(2):200–206, 2008.

[113] A. S. Monin and A. M. Yaglom. Statistical fluid mechanics: Mechanics of turbulence. volume 2/revised and enlarged edition. *Cambridge*, 1975.

[114] B. K. Nfor, M. Noverraz, S. Chilamkurthi, P. D. E. M. Verhaert, L. A. M. van der Wielen, and M. Ottens. High-throughput isotherm determination and thermodynamic modeling of protein adsorption on mixed mode adsorbents. *Journal of Chromatography A*, 1217(44):6829–6850, 2010.

[115] R. H. Nochetto and C. Verdi. Approximation of degenerate parabolic problems using numerical integration. *SIAM Journal on Numerical Analysis*, 25(4):784–814, 1988.

[116] A. Pakzad. Damping functions correct over-dissipation of the Smagorinsky model. *Mathematical Methods in the Applied Sciences*, 40(16):5933–5945, 2017.

[117] Stoycho Panchev. *Random Functions and Turbulence*, volume 32 of *International Series in Natural Philosophy*. Pergamon, 1971.

[118] W. Pei. The semi-implicit DLN algorithm for the Navier-Stokes equations. *Numerical Algorithms*, pages 1–41, 2024.

[119] L. Prandtl. *Über ein neues Formelsystem für die ausgebildete Turbulenz*. Nachrichten der Akademie der Wissenschaften zu Göttingen, Mathematisch-Physikalische Klasse. Vandenhoeck & Ruprecht, 1945.

[120] M. H. Protter and H. F. Weinberger. *Maximum principles in differential equations*. Springer Science & Business Media, 2012.

[121] Y. Qin, L. Chen, Y. Wang, Y. Li, and J. Li. An adaptive time-stepping DLN decoupled algorithm for the coupled Stokes-Darcy model. *Appl. Numer. Math.*, 188:106–128, 2023.

[122] Y. Qin, Y. Hou, W. Pei, and J. Li. A variable time-stepping algorithm for the unsteady Stokes/Darcy model. *J. Comput. Appl. Math.*, 394:Paper No. 113521, 14, 2021.

[123] D. A. Quinteros, J. M. Bermúdez, S. Ravetti, A. Cid, D. A. Allemandi, and S. D. Palma. Therapeutic use of monoclonal antibodies: general aspects and challenges for drug delivery. In *Nanostructures for Drug Delivery*, pages 807–833. Elsevier, 2017.

[124] F. A. Radu and I. S. Pop. Mixed finite element discretization and Newton iteration for a reactive contaminant transport model with nonequilibrium sorption: convergence analysis and error estimates. *Computational Geosciences*, 15(3):431–450, 2011.

[125] F. A. Radu, I. S. Pop, and S. Attinger. Analysis of an Euler implicit-mixed finite element scheme for reactive solute transport in porous media. *Numerical Methods for Partial Differential Equations: An International Journal*, 26(2):320–344, 2010.

[126] M. E. Rafei, L. Könözsy, and Z. Rana. Investigation of numerical dissipation in classical and implicit large eddy simulations. *Aerospace*, 4(4):59, 2017.

[127] P. L. Roe. Characteristic-based schemes for the Euler equations. *Annual review of fluid mechanics*, 18(1):337–365, 1986.

[128] R. S. Rogallo and P. Moin. Numerical simulation of turbulent flows. *Annual review of fluid mechanics*, 16(1):99–137, 1984.

[129] J. J. Romero, E. W. Jenkins, and S. M. Husson. Surrogate-based optimization of capture chromatography platforms for the improvement of computational efficiency. *Computers & Chemical Engineering*, 173:108225, 2023.

[130] J. J. Romero, E. W. Jenkins, J. Osuofa, and S. M. Husson. Computational framework for the techno-economic analysis of monoclonal antibody capture chromatography platforms. *Journal of Chromatography A*, 1689:463755, 2023.

[131] Y. Rong, W. J. Layton, and H. Zhao. Extension of a simplified Baldwin–Lomax model to nonequilibrium turbulence: Model, analysis and algorithms. *Numerical Methods for Partial Differential Equations*, 35(5):1821–1846, 2019.

[132] V. Saini, H. Xia, and G. Page. Numerical dissipation rate analysis of Finite-Volume and continuous Galerkin methods for LES of combustor flow field. *Flow, Turbulence and Combustion*, 111(1):81–113, 2023.

[133] E. Schneid, P. Knabner, and F. Radu. A priori error estimates for a mixed finite element discretization of the Richards' equation. *Numerische Mathematik*, 98(2):353–370, 2004.

[134] L. R. Scott and S. Zhang. Finite element interpolation of nonsmooth functions satisfying boundary conditions. *Mathematics of computation*, 54(190):483–493, 1990.

[135] F. Siddiqua and W. Pei. Variable time step method of Dahlquist, Liniger and Nevanlinna (DLN) for a corrected Smagorinsky model. *arXiv preprint arXiv:2309.01867*, 2023.

[136] F. Siddiqua and C. Trenchea. A second-order symplectic method for an advection-diffusion-reaction problem in bioseparation. Technical report, University of Pittsburgh, 2022.

[137] F. Siddiqua and X. Xie. Numerical analysis of a corrected Smagorinsky model. *Numerical Methods for Partial Differential Equations*, 39(1):356–382, 2023.

[138] N. Singh, J. Wang, M. Ulbricht, S. R. Wickramasinghe, and S. M. Husson. Surface-initiated atom transfer radical polymerization: A new method for preparation of polymeric membrane adsorbers. *Journal of Membrane Science*, 309(1-2):64–72, 2008.

[139] J. Smagorinsky. General circulation experiments with the primitive equations: I. the basic experiment. *Monthly weather review*, 91(3):99–164, 1963.

[140] J. Smagorinsky. Some historical remarks on the use of nonlinear viscosities. *Large eddy simulation of complex engineering and geophysical flows*, 1:69–106, 1993.

[141] M. Stieger. The rheology handbook-for users of rotational and oscillatory rheometers. *Applied Rheology*, 12(5):232–232, 2002.

[142] J. C. Strikwerda. *Finite difference schemes and partial differential equations*. SIAM, 2004.

[143] S. Y. Suen and M. R. Etzel. A mathematical analysis of affinity membrane bioseparations. *Chemical engineering science*, 47(6):1355–1364, 1992.

[144] R. C. Swanson, R. Radespiel, and E. Turkel. On some numerical dissipation schemes. *Journal of computational Physics*, 147(2):518–544, 1998.

[145] A. Tarafder. Modeling and multi-objective optimization of a chromatographic system. *Multi-Objective Optimization in Chemical Engineering: Developments and Applications*, pages 369–398, 2013.

[146] H. Tennekes and J. L. Lumley. *A first course in turbulence*. MIT Press, Cambridge, 1972.

[147] V. Thomée and L. Wahlbin. On the existence of maximum principles in parabolic finite element equations. *Mathematics of computation*, 77(261):11–19, 2008.

[148] P. Walsh and T. Pulliam. The effect of turbulence model solution on viscous flow problems. In *39th Aerospace Sciences Meeting and Exhibit*, page 1018.

[149] J. Wang. *Development of a New Multimodal Membrane Adsorber and Its Application in Chromatographic Bioseparations*. PhD thesis, Clemson University, 2016.

[150] J. Wang, E. W. Jenkins, J. R. Robinson, A. Wilson, and S. M. Husson. A new multimodal membrane adsorber for monoclonal antibody purifications. *Journal of membrane science*, 492:137–146, 2015.

[151] J. Wang, R. T. Sproul, L. S. Anderson, and S. M. Husson. Development of multimodal membrane adsorbers for antibody purification using atom transfer radical polymerization. *Polymer*, 55(6):1404–1411, 2014.

[152] D. C. Wilcox. *Turbulence modeling for CFD*. La Canada, CA : DCW industries, 1998.

[153] A. B. Wilson. Modeling, analysis, and simulation of adsorption in functionalized membranes. `https://tigerprints.clemson.edu/all_dissertations/1687`, 2016.

[154] A. B. Wilson and E. W. Jenkins. Analysis of a fully implicit SUPG scheme for a filtration and separation model. *Computational and Applied Mathematics*, 39(2):1–19, 2020.

[155] C. S. Woodward and C. N. Dawson. Analysis of expanded mixed finite element methods for a nonlinear parabolic equation modeling flow into variably saturated porous media. *SIAM Journal on Numerical Analysis*, 37(3):701–724, 2000.

[156] H. Wu, P. Fu, J. P. Morris, R. R. Settgast, and F. J. Ryerson. ICAT: A numerical scheme to minimize numerical diffusion in advection-dispersion modeling and its application in identifying flow channeling. *Advances in water resources*, 134:103434, 2019.

[157] H. Zia and G. Simpson. Anti-diffusive, non-oscillatory central difference scheme (adNOC) suitable for highly nonlinear advection-dominated problems. *arXiv preprint arXiv:1911.03931*, 2019.